Directed Morphogenesis of Smallpox Vaccine for Enhanced Immunogenicity and Decreased Side Effects

Thesis

UNRESTRICTED

Directed Morphogenesis of Smallpox Vaccine for Enhanced Immunogenicity and Decreased Side Effects

Rachel Elizabeth Dean BSc (Hons)

A thesis submitted in partial fulfilment of the requirements of the Open University for the degree of Doctor of Philosophy

February 2010

Dstl Porton Down, Salisbury, Wiltshire, SP4 0JQ.

Date of Submission: 12 February 2010
Date of Award: 6 July 2010.

ProQuest LLC.
789 East Eisenhower Parkway
P.O. Box 1346
Ann Arbor, MI 48106 – 1346

Abstract

Vaccinia virus (VACV) produces two morphologically distinct mature virions: enveloped virus (EV) and intracellular mature virus (IMV). EV is produced first in the replication cycle and is required for virus dissemination. IMV is thought to be produced by default, when the cellular membranes that wrap EV become exhausted and as the more robust particle, is involved in host-to-host transmission.

The aim of this study was to examine the hypothesis that IMV production is not a default, but is an active process mediated by the IMV-specific protein, A26. Two recombinant VACVs were constructed: vIdA26L and vIdA26L.neo, in which the A26L gene was deleted or inactivated. One-step growth curves demonstrated a reduction in virus yields for these viruses. Examination of the kinetics of EV and IMV production by the A26L deletion mutants did not demonstrate a reduction in IMV as expected, yet the production of single-membraned virus was perturbed when compared to wild-type VACV IHD-J and a revertant virus. Constitutive expression of A26 from a synthetic early/late promoter did not affect virus yields and did not result in increased production of IMV in favour of EV.

Treatment of virions with membrane perturbing agents demonstrated increased susceptibility of EV to inactivation when compared to IMV, suggesting that the EV pre-cursor and mature IMV are different particles. Mutant IMV from A26L$^-$ VACV cultures demonstrated increased sensitivity to the detergent Tween-20 when compared to wild-type IMV, behaving similarly to stripped EV. This suggests resistance might be attributable to the presence of IMV-specific proteins that are not found on stripped EV.

This study provides evidence that IMV is a true end-stage product of VACV morphogenesis, and that OPVs employ a mechanism to actively differentiate particles towards IMV, thus preventing maturation of a subset of virions as EV. This results in two non-interchangeable isoforms of mature infectious virions that are produced to perform their individual functions in the virus life-cycle.

Declaration

Unless stated otherwise, the results and data presented in this thesis is soley the work of Rachel Dean. This work has not been submitted anywhere else for a higher degree. Where other sources of information have been used they have been acknowledged. The recombination cassettes for the vIdA26L.rev, vIdA26L.neo and vIdA26L.EL were constructed by GeneArt AG (Germany). Virus preparations were embedded and sectioned for transmission electron microscopy by Dr Simon Smith. Dr Tom Laws and Dr David Ulaeto assisted with statistical analyses. Polyclonal sera were kindly provided by Dr David Ulaeto, Dr Amanda Gates and Amanda Phelps.

Acknowledgements

I would like to thank Dr David Ulaeto for his guidance, continued patience and support throughout this epic journey, even when I felt there was no way that I could complete this, and for finding the time to help in the lab and review this thesis. I would also like to thank Dr Amanda Gates and Dr Diane Williamson for their guidance and support, and much appreciated review and proof reading of this thesis!

There are several people that I would also like to thank who have helped throughout this project: Dr Tom Laws for statistical advice, Dr Amanda Gates, Amanda Phelps for the mouse sera and help with virus titrations, Lin Eastaugh for help with tissue culture. I would also like to thank Dr Michelle Nelson, Dr Matthew Jackson and Dr Tim Milne for giving up their time to buddy me in the lab at the weekends.

To all my friends in Salisbury – a massive thank you. I know you must all feel like this has taken me years – and it has! But thank you so much for keeping me going, taking me out for drinks and cheering me up when it was much needed!

Finally, thank you to Phil and my parents for believing in me – I would not have been able to do this without your support and encouragement through the dark times!

Publications

Data in this thesis has been presented as follows:

1. Rachel Dean and David Ulaeto. The Effect of Disruption of the Vaccinia Virus A26L Gene on Maturation of IMV Particles. Poster presented at the XVth International Poxvirus and Iridovirus conference, Oxford, 2004.

2. Rachel Dean and David Ulaeto. The Effect of Disruption of the Vaccinia Virus A26L Gene on Maturation of IMV Particles. Poster presented at International Union of Microbiological Societies conference, San Francisco, 2005.

3. Rachel Dean and David Ulaeto. The Effect of Disruption of the Vaccinia Virus A26L Gene on Maturation of IMV Particles. Poster presented at the Society for General Microbiology conference, Edinburgh, 2005.

4. Rachel Dean and David Ulaeto. The Effect of Disruption of the Vaccinia Virus A26L Gene on Maturation of IMV Particles. Poster presented at the XVIIth International Poxvirus and Iridovirus Conference, Grainau, Germany, 2008.

Contents

List of Figures

Chapter 1

Chapter 3

Chapter 4

Chapter 5

Chapter 6

Chapter 7

Chapter 8

Appendix

List of Tables

Chapter 2

Chapter 3

Chapter 4

Chapter 6

Abbreviations

%	percent
Δ	delta
°C	Degrees Celsius
3H	tritium
6-TG	6-thioguanine
A	absorbance
A.D.	anno domini
ABS	adult bovine serum
ANOVA	analysis of variance
ATI	A-type inclusion
B.C.	before Christ
BFA	Brefeldin A
bp	base pair
c	centi
CAM	chorioallantoic membrane
CD	cluster of differentiation
CEV	cell-associated enveloped virus
CMLV	camelpoxvirus
CPE	cytopathic effect
cpm	counts per million
CPXV	cowpoxvirus
CsCl	caesium chloride
Ct	cycle threshold
Da	Daltons
DF	downstream flank
DMEM	Dulbecco's minimal essential medium
DNA	deoxyribonucleic acid
dNTPs	deoxynucleotides
DstI	Defence Science and Technology Laboratory
ECL	enhanced chemiluminescence
*Eco*GPT	*Escherichia coli* guanosine phosphoribosyltransferase
ECTV	ectromelia virus
EDTA	ethylenediaminetetra acetic acid
EEV	extracellular enveloped virus
ELISA	enzyme-linked immunosorbent assay
EV	enveloped virus
FCS	fetal calf serum
FPXV	fowlpoxvirus
g	grams
GAG	glycosaminoglycans
h	hours
HAT	hypoxanthine, aminopterin and thymidine
HIV	human immunodeficiency virus
HRP	horseradish peroxidise
HSV	Herpes simplex virus
IEV	intracellular enveloped virus
IHD-J	International Health Department-J

IMV	intracellular mature virus
IND	investigational new drug
IV	immature virion
k	kilo
l	litres
M	molar
m	mili or metre
mAb	monoclonal antibody
MHC	major histocompatibility complex
MOI	multiplicity of infection
MPA	mycophenolic acid
MPXV	monkeypoxvirus
MRV	malignant rabbit fibroma virus
MT	microtubule
MVA	modified vaccinia Ankara
Mwt	molecular weight
n	nano
neo	neomycin/G418/Geneticin®
NV	nascent virus
NYCBH	New York City Board of Health
OD	optical density
OPV	orthopoxvirus
ORF	open reading frame
p	pico or probability or plasmid
p.i.	post-infection
PAGE	polyacrylamide gel electrophoresis
PCR	polymerase chain reaction
pfu	plaque-forming units
pH	potential of hydrogen-measure of hydrogen ions associated with acidity
R	resistance
RNA	ribonucleic acid
rpm	revolutions per minute
RT	reverse transcription/reverse transcriptase
SDS	sodium dodecyl sulphate
SEM	standard error of the mean
SFV	shope fibroma virus
SMP	skimmed milk powder
STE	surface tubule element
t	time
TCID	tissue-culture infectious dose
TE	trypsin EDTA
TEM	transmission electron microscopy
TGN	trans-Golgi network
TK	thymidine kinase
U	units
UF	upstream flank
UV	ultraviolet
V	volts

v	volume
VACV	vaccinia virus
VARV	variola virus
w	weight
WR	Western Reserve
wt	wild-type
www	world wide web
x g	x gravity
a	alpha or anti-
µ	micro

1 Introduction

1.1 Smallpox, a Historical Disease

Smallpox is now considered a historical disease by the World Health Organisation since its certified eradication in 1980. The first cases of smallpox are thought to have appeared around 10,000 BC in early agricultural settlers in Northeastern Africa (1), at a time when the population density was thought to have reached a minimum required for the disease to be maintained without re-introduction. The first evidence for the disease was in ancient Egypt approximately 1580 years BC on scarred mummified remains. Ramses V, who reigned for only 5 years from 1157 BC, is one of the most famous figures thought to have died of smallpox. The disease was likely to have been spread from Egypt and Northern Africa by Egyptian traders to India and the Far East, but it was not until 400 AD that the disease was first documented in China (2).

In the fifth and sixth centuries AD smallpox reached Europe, where several epidemics occurred during the Middle Ages. It was around this time that the term *variola,* derived from the Latin words *varius* (spotted), and *varus* (pimple), was first used by the Swiss Bishop Marius of Avenches (3). Henry VIII's fourth wife Anne of Cleves, Mary II, and Elizabeth I of England were all famous survivors of the disease. The word *poc* or *pocca*, of Anglo-Saxon origin, meaning bag or pouch, was used to describe the disease and in the fifteenth century writers began to refer to the disease as small *pockes*, to distinguish it from syphilis, the great *pockes* (3).

Smallpox was introduced to the Americas by the Spanish and Portuguese conquistadors in the early sixteenth century and was a major cause in the fall of

Aztec and Inca Empires. It is speculated that in 1763 Lord Jeffrey Amherst, General of the British forces during the French-Indian war, presented two blankets and a handkerchief seeded with smallpox scabs to the Native Americans as an attempt at biological warfare.

By the middle of the eighteenth century smallpox had become epidemic in Northern America and Europe, leading to 400,000 deaths annually in Europe, and was endemic in Africa and India (3).

1.1.1 Smallpox, the Disease

Smallpox is caused by variola virus (VARV), a member of the *Poxviridae* family. There are two species of VARV, variola major which causes classical smallpox and variola minor which results in a milder form of the disease. The case fatality rate of variola major infection was reported as 30-40 %, whereas that of variola minor was generally 1 % or less (3). Variola minor was first described by Korté in 1904 as a very mild smallpox-like disease that had occurred in South Africa, and subsequently was identified in North and South America, Europe and Australia. In the 1950s, virological studies confirmed that these milder outbreaks were in fact mild varieties of smallpox caused by VARV.

1.1.2 Clinical Manifestation of Disease

The incubation period of smallpox is approximately 12-14 days and during this time the patient will feel healthy and is non-infectious. Illness begins with sudden onset of flu-like symptoms such as fever, headaches, malaise, back pain,

and in some cases abdominal pain and vomiting. After 2-3 days these symptoms subside and the characteristic rash appears first on the oral mucosa, and then approximately 24 hours later on the skin. The distribution of the lesions is centrifugal, with more lesions occurring on the extremities such as the head and limbs, and less on the trunk. Lesions also appear on the palmar and plantar surfaces. The rash develops from macules to papules to vesicles to pustules, which in survivors eventually scab and fall off 8-14 days after the onset of symptoms, sometimes leaving depressed depigmented scars. Lesions may differ in size, however all are at the same developmental stage throughout the course of the disease. The distribution of the lesions, and the fact that they exhibit the same developmental stage, are the main clinical signs for differential diagnosis of smallpox compared to chickenpox.

1.1.3 Infectivity and Transmission

VARV is highly contagious, although an infected person is unable to infect others during the incubation period. Following onset of fever and during the first week of rash, the virus is released via the respiratory tract where face-to-face contact results in the highest frequency of infection. The disease can also be transmitted by contaminated clothes and bedding, although the risk of infection is much lower by this route. Patients infected with variola major were generally bedridden early, i.e. before they became infectious and so transmission was limited to those in close contact. Variola minor was less severe and sufferers frequently remained ambulatory throughout the course of disease, thus infection was more

frequently transmitted. Patients continued to be infectious until the final stages of disease where the remaining virus-containing scabs were shed. Additionally, vaccinees could still be infected but typically would manifest a modified, less severe disease. Vaccinees who contracted variola major were more likely to be ambulatory, and thus to spread infection more widely. However, the potency of the vaccine was such that *overt* smallpox was rare in vaccinees (3;4). There is no known animal reservoir and the virus is not known to have been transmitted by insect vectors.

1.2 Poxvirus Biology

1.2.1 Taxonomy

As the causative agent of smallpox, VARV is the most infamous of the *Poxviridae* family, however, since its eradication research has continued using other poxviruses to increase understanding of virus-host relationships. The *Poxviridae* are divided into 2 main subfamilies: *Chordopoxvirinae* and *Entomopoxvirinae*, which infect vertebrates and insects, respectively. The *Chordopoxvirinae* consist of 8 genera that infect a wide range of birds, mammals and reptiles, and the viruses are genetically, antigenically and morphologically similar. Four genera have members which infect humans: orthopox, parapox, yatapox and molluscipox, where molluscipox and some members of orthopox are obligate human pathogens. Only 3 genera have been identified in the *Entomopoxvirinae* subfamily, based on the insect host.

1.2.2 Vaccinia Virus (VACV)

Due its extensive use in research, VACV is the prototypic orthopoxvirus (OPV) used in laboratories to study poxviruses. It was the first animal virus to be seen microscopically, to be grown in tissue culture, accurately titred, physically purified and chemically analysed (5). VACV has no known natural host and its origin is not known, although there are several theories about its emergence: a) the virus evolved from variola virus as a result of continual passage through humans; b) the virus was derived from cowpox by continual passage through animals; c) or the natural host is now extinct (3). Indeed, the emergence of other OPVs such as buffalopox, are thought to be VACV that escaped during mass smallpox vaccinations, although there is a possibility that these are naturally occurring. It may also be that the virus causes a largely occult infection in their natural hosts, thereby limiting the opportunity for transmission to acutely susceptible hosts.

1.2.2.1 The Structure of VACV

VACV is the largest known DNA virus, measuring 310 x 240 x 140 nm with a smooth brick- or pillow-shaped particle (6-8). There is some uncertainty about the size of the virus particle as atomic force microscopy suggests a slightly flattened ellipsoidal shaped particle with dimensions of 350 x 300 x 265 nm (9), whereas cryo-electron tomography suggests a barrel-shaped particle of dimensions 360 x 270 x 250 nm (10). It would appear that the size of the particle is dependent on the method by which the virus is viewed and prepared, as demonstrated by Malkin *et al.* (2003) who found that air dried particles shrunk more than two-fold along the

shortest axis (9). The surface of the mature virion is smooth when negatively stained and viewed by cryo-electron microscopy (11;12). In contrast to this, virus preparations viewed by negative staining-, metal shadowing-, deep etch- or freeze etch- electron microscopy, or atomic force microscopy revealed randomly arranged surface ridges denoted "surface tubule elements" (STEs) (9;13-15). Dubochet *et al.* (1994) suggest that the STEs are artefacts, and are a result of osmotic stress during negative staining, however the biochemical evidence presented by Wilton *et al.* (1995), together with the reports of surface ridges by numerous research groups suggests that they are not artefactual, and it is more likely that the insensitivity of the cryo-electron microscopy fails to identify the fine surface detail of the virus particle (9;11;15).

Thin sections of non-enveloped mature virus particles reveal a membrane which surrounds the entire particle (note: at least one additional lipid membrane surrounds the enveloped forms), and a core wall which surrounds a homogenous core. The membrane consists of two layers approximately 1-20 nm thick: the outer domain is 3-9 nm thick, and the inner domain 5-6 nm thick. The outer core wall is estimated to be 8-17 nm thick, with a striated appearance and is referred to as the "palisade layer". The inner core wall is 5-8 nm thick, and is known as the "smooth layer". The inner membrane surface and outer core remain tightly apposed at the top and bottom of the particle however separation of the core wall and the membrane along the longer axis results in a characteristic dumb-bell shaped core. Two central bilateral concavities are formed between the core and membrane and within these reside two "lateral bodies". The core contains a tube-like structure

which is visualised when sectioned parallel to and bisecting the broadest plane of the virus (16).

1.2.2.2 Chemical Composition

The principal components of the mature virus particle are protein (90 %), lipid (5 %) and DNA (3.2 %) of the dry weight (17). The lipid components of mature virus are similar to that of the host cell with the exception of one third less phosphatidyl ethanolamine than the host cell and three to four times the amount of acyl bis(monoacylglycero)phosphate than found in host cells (18;19). Insignificant amounts of RNA have been reported, and trace amounts of spermine and spermidine may play a role in viral DNA core condensation (20).

1.2.2.3 The VACV Genome

Poxviruses have linear, double-stranded DNA genomes, which in the case of VACV is ~200 kb encoding approximately 200 genes. At each end of the DNA strand are identical but oppositely orientated inverted terminal repeats (ITRs); the lengths of ITRs can be variable even within a genus (5). These ITRs may contain coding regions, which results in two copies of some genes at each end of the genome. In OPVs, these regions are hypervariable resulting in terminal regions with transpositions and deletions (5). The central portion of the genome is highly conserved and contains genes that are essential for virus replication. The terminal regions are more variable, encoding non-essential genes required for virulence, host-range and modulation of the host immune response (5). The two strands of

DNA are connected by hairpin loops to form a covalently continuous polynucleotide chain. VACV mRNAs are not spliced, as replication occurs in the cytoplasm and therefore VACV DNA does not contain introns. Genes are closely spaced in the genome and appear to be expressed from their own promoter. The genome sequences of VACV and VARV are similar, and comparative analyses have demonstrated more than 90 % sequence identity (21-23).

It has been proposed that the viral genome exists in the core complexed with viral proteins in a helical structure: disruption of the core can release 30-40 nm diameter tubules that possess an apparently helical substructure (6;9). It is unclear if these tubules are the same as those described by Peters and Mueller in 1963 (16). Treatment of the core with detergents and denaturing agents resulted in the identification of DNA-protein complexes which were named "nucleoids" and "subnucleoids" (24-27).

1.2.2.4 VACV Gene Transcription

The mechanisms of VACV gene expression have been well documented (28), where transcription proceeds in three phases: early, intermediate and late. Each phase is controlled by distinct promoters and, in most cases, virally-encoded transcription factors. Approximately 25 virus-encoded factors have been identified, and each of these are encoded primarily by genes of the preceding gene class, thus gene regulation in poxviruses may be described as a "cascade." Viral RNA synthesis is carried out by a virus-encoded multi-sub-unit eukaryotic-like RNA polymerase that is encoded by at least 8 genes (5;29;30).

1.2.2.4.1 Early Phase

The early transcriptional phase occurs after virus entry and early class mRNA can be detected within minutes. The enzymes and other proteins required for this are packaged within the virion along with the genome. Approximately half of the VACV encoded genes are considered early class (31;32) and encode proteins participating in DNA replication (33-35), nucleotide synthesis (36;37) and intermediate gene transcription (34;38). In addition, some early genes encode virulence factors for modulation of host responses (39;40). Characteristically, early promoter sequences are defined by a critical core region from -13 to -27 that is A/T-rich with a G residue at -21 or -22 (41). Initiation of transcription occurs with a purine residue, usually 12-17 nucleotides downstream of the core region (41) and requires a single transcription factor, the vaccinia early transcription factor (VETF) (42) and RNA polymerase-associated early specificity factor RAP94 (43;44). VETF is a heterodimer of the D6R and A7L gene products (45;46) that interacts with two regions upstream and downstream of the transcriptional start site (45;47), and is thought to recruit the RNA polymerase to the transcriptional start site. Initiation also requires ATP hydrolysis to induce accelerated dissociation of the VETF-promoter complex (45). RAP94 is required for transcription initiation and formation of a stable complex with an early promoter template (48) and perhaps also for the targeting of the transcription complex of assembling virions (49). Termination of most early class genes occurs 20-50 bp downstream of the termination signal TTTTTNT, situated at the 3'-end of the gene on the non-template strand (50), and is thought to involve the capping enzyme (51) and nucleoside phosphohydrolase I

(NPH I) (52;53). It is proposed that as the mRNA is extruded from the RNA polymerase, it makes contact with the capping enzyme which signals NPH I to drive the release of the transcript through hydrolysis of ATP (53).

1.2.2.4.2 Intermediate Phase

Intermediate phase genes are expressed earlier than late phase genes and require the onset of DNA replication to occur prior to expression. In addition, their promoters lack the TAAATG motif characteristic of late promoters (54). Intermediate promoters have two important regions: a 14 bp A/T-rich core region situated 10-11 bp upstream of the initiator element, and the initiator element that has the minimal sequence of TAAAT/A at -1 to +4 relative to the first A in the motif (reviewed in (5);(55)).

Several proteins have been reported to be involved in intermediate transcription such as YinYang1 (YY1) that is thought to bind within the initiator element and facilitate RNA polymerase binding (56). The vaccinia intermediate transcription factors (VITF) have been identified by Vos and colleagues where VITF-A is thought to have promoter DNA-melting activity and VITF-B is the capping enzyme (57;58). Further studies have identified VITF-1, VITF-2 and VITF-3: VITF-1 is the 30 kDa subunit of the viral RNA polymerase (59); VITF-2 is a host nuclear protein that is thought to have a tethering role linking one of the other factors to the RNA polymerase (60); and VITF-3 has been identified as a heterodimer of A8L and A23R gene products (61).

Intermediate gene expression of VACV is also thought to require *de novo* synthesis of viral RNA polymerase (28), and as all characterised RNA polymerase sub-unit genes have early promoters, it is therefore likely that intermediate gene expression requires newly synthesised RNA polymerase.

1.2.2.4.3 Late Phase

Late gene expression occurs approximately 2 hours post-infection, where transcripts were detected after 140 minutes in synchronously infected HeLa cells, and continued for up to 48 hours (62). Late genes tend to produce structural proteins involved in virion morphogenesis, and enzymes and factors that are required for early gene expression in the subsequent round of infection, that will be packaged into the mature virion (42;46;63). As in intermediate promoters, late promoters have two important regions with an A/T-rich region upstream of a transcription initiator element (64). The initiator element contains the highly conserved TAAAT motif, usually followed by a G or A residue, where the G would form part of the ATG initiation codon; this would overlap the transcription initiation sequence. The core sequence is situated about -16 to -11 from the initiator element with consecutive T or A residues (28).

Late mRNAs have a 5'- capped heterogeneous-length poly(A) sequence that has been shown to be synthesised by RNA polymerase slippage. These poly(A) leader sequences are also found in those early and intermediate transcripts that contain the TAAAT initiator element, suggesting that strand slippage is an intrinsic feature of VACV RNA polymerase (65-67).

Up to five transcription factors have been described for late VACV gene expression. G8R (VLTF-1), A1L (VLTF-2) and A2L (VLTF-3) described by Keck *et al.* (1990), have been identified as the minimal gene set that are required for late promoter activity (68), however the functions of these gene products have yet to be assigned. A fourth transcription factor, encoded by H5R, belongs to an early class of genes and associates with the site of viral replication in the cytoplasm (69). More recent studies have demonstrated that the encoded proteins interact, and can further interact with the host cell factors A2/B1 or RBM3 (70). The fifth late transcription factor, VLTF-X, is host-derived (71) and thought to be responsible for targeting late VACV promoters as sites of initiation (28).

VACV RNA polymerase (RNAP) does not appear to respond to specific termination signals in intermediate and late genes, resulting in extremely heterogeneous 3'-terminal sequences (72). Yet, the gene products of G2R, J3R and A18R appear to affect transcript length (72-75) suggesting roles in promoting transcription elongation and termination.

Unusually for late genes, the A-type inclusion (ATI) protein transcript in cowpoxvirus (CPXV) terminates at a precise location after the ORF (76) by site-specific riboendonucleolytic cleavage; the 3'-end is then polyadenylated. This region is also found in the VACV orthologue, suggesting that this cleavage site is conserved in poxviruses (77). More recently, site-specific cleavage of VACV F17R transcripts has been reported, and the evidence suggests that cleavage is mediated by the same factor as for ATI transcripts (78). It is not known whether

RNA 3'-end processing is common in VACV however this indicates poxviruses employ at least two mechanisms to modify the 3'-ends of mRNA.

1.2.2.5 VACV DNA Replication

The onset of DNA replication during infection differs between poxviruses (79;80). DNA replication in VACV begins approximately 1-2 hours p.i., resulting in the synthesis of more than 10,000 genome copies per cell (81;82). Poxviruses exclusively replicate in the cytoplasm of infected cells which dictates that most, if not all, of the genes required for DNA replication must be virally-encoded (83). In support of this, virus replication has also been reported in enucleated cells (84;85).

Several poxvirus genes encode enzymes that are able to synthesise DNA pre-cursors, such as deoxyuridine 5'- triphosphatase (dUTPase) (86), thymidylate kinase (36), thymidine kinase (37;87;88) and ribonucleotide reductase (89;90). These pre-cursors may be at levels within the host cell that are sub-optimal for virus replication. Studies have shown that the virulence of poxviruses was reduced in animals when the thymidine kinase or ribonucleotide reductase genes were deleted, but these mutant strains were not attenuated when cultured *in vitro* (91;92).

The mechanism for DNA replication is largely undefined in poxviruses. Several proteins have been identified to be involved including a DNA polymerase (E9); (93), an essential and stoichiometric component of the processive polymerase (A20); (94), a single-strand DNA-binding protein (I3); (95), a type I topoisomerase (H6); (96;97), uracil DNA glycosylase (D4); (98), nucleic acid

independent nucleoside triphosphatase (D5); (99;100), serine/threonine kinase (B1); (101) and a bacterial-type Holliday junction resolvase (A22); (102). Unusually, an origin of replication has not yet been defined, although *cis*-acting sequences found within the telomeric 200 bp have been implicated as being necessary and sufficient for minichromosome replication (103). The existing model of poxvirus DNA replication suggests that DNA replication is initiated from a nick at either end of the hairpin termini to expose a 3'-OH group. The exposed 3' terminus serves as a site for the processive polymerase (A20) to perform strand-displacement primer extension. The nascent strand and the template are self-complementary and can isomerize to fold back on itself. Extension of the nascent strand occurs by copying the remainder of the genome resulting in the formation of concatemeric intermediates, where a concatemer junction forms by replication of the hairpin. The onset of late transcription (104;105), and the synthesis of Holliday junction resolvase (A22) and type 1 topoisomerase (H6) (106;107) are required for the resolution of concatemer structures to produce mature, monomeric genomes.

The ability of poxviruses to undergo recombination was first demonstrated over 50 years ago (108), occurring at high rates within infected cells. The process may be an important source of genetic variation among the *Poxviridae* and may occur as a result of DNA replication and concatemer resolution (109) but the proteins involved have yet to be elucidated. It is likely that many poxvirus genes, such as immunomodulatory proteins, have been acquired in this way, entering poxvirus genomes via genetic recombination from their host or possibly other viruses (110). There is strong evidence to suggest that recombination can occur

between poxvirus genomes during natural host transmission. For example, malignant rabbit fibroma virus (MRV) is derived from genetic recombination of the leporipoxviruses shope fibroma virus (SFV) and myxoma virus (111-113). Recombination also readily occurs between viral genomes and transfected DNA (114). This property, together with the large size of poxvirus genomes that are able to accept large portions of foreign DNA, has been exploited to try to further understand poxvirus biology by the construction of mutant viruses (115).

1.2.2.6 VACV Replicative Cycle

VACV infection yields two types of mature virion: enveloped virus (EV) and intracellular mature virus (IMV). EV is produced first in the replicative cycle (116), accounting for ~25 % of the total progeny and IMV is produced later (116) accumulating in the cell to make up the majority of progeny virions. The mechanism of both IMV and EV production has not been fully elucidated, however, the presence of proteins unique to each type of virion suggests that they are structurally, antigenically and functionally different. EV is thought to play a role in viral dissemination as viruses that cannot produce EV do not spread in tissue culture and are attenuated *in vivo* (117-120). This suggests that EV is required for dissemination within the host. In addition, EV is more resistant to neutralising antibody and complement as the membranes are host-derived, enabling long-range spread within a host. IMV is thought to be the more robust particle although is less resistant than EV to host defences, and is presumed to be involved in host-to-host spread.

1.2.2.6.1 VACV Entry into Host Cells

The mechanisms of entry for IMV and EV are thought to differ due to the different numbers of viral membranes and different surface proteins present (121). The fragility of the additional membrane has precluded extensive studies of EV binding, however, proteins present on the surface of non-enveloped single-membraned virions have been shown to be important for entry of both forms of the virus (122-124). Two models have been proposed: 1) direct fusion of a single-membraned virion with the plasma membrane allowing release of the core into the cytoplasm (125) and 2) endocytosis of a single-membraned virion into vesicles followed by fusion of the membrane with the vesicular membrane resulting in the release of the core into the cytoplasm (126). These mechanisms are not necessarily mutually exclusive but have been shown to require low pH (126;127) and may be influenced by the virus strain and cell-type used in the studies reported (128). How the EV additional membrane is lost during entry has only recently been demonstrated, where the EV membrane was shown to be disrupted at the point of cell contact after binding by a process that requires B5 and A34 (123). This resulted in a single-membraned virion that was able to enter the cell as described above. Recent studies by Mercer *et al.* (2008) have demonstrated that virions can also enter cells by macropinocytosis, where virions induce cell-surface blebbing that is characteristic of apoptosis (129).

Binding of single-membraned virions to the cell surface has been shown to involve the viral proteins H3, A27 and D8, which bind to glycosaminoglycans

(GAGs) (130-133), A26 which binds to the cellular matrix protein laminin (134) and L1 to an unknown cell surface receptor, independent of GAGs (135).

Binding of the EV particle, however, appears more complicated to delineate. Studies by Vanderplasschen and Smith (1997) demonstrate that non-enveloped and enveloped virus bind to different cell surface receptors (121), but no EV-specific proteins have been identified in EV attachment. It has been suggested that A34 may be involved as mutation of the A34R gene results in a reduction in infectivity of EV (136), however, this is likely due to the requirement for A34 for disruption of the EV membrane upon binding (123).

Unlike many other enveloped viruses that require only 1 protein, fusion of the VACV membrane and entry of the core into the cytoplasm is mediated by a complex of multiple proteins: A16, A21, A28, F9, G3, G9, H2, I2, J5, L1, L5 and O3 (122;124;137-146). Each of these proteins are essential for fusion but not binding, and have common features including membrane-anchored domains, situated at either their N- or C-terminus, and invariant cysteine residues. Many of these are conserved in all sequenced poxviruses (146;147) suggesting a common entry mechanism that is largely unchanged between species. The entry fusion complex (EFC) proteins have also been shown to be required for cell-to-cell fusion triggered by low pH or mutation of the A56 or K2 proteins (124;148;149).

1.2.2.6.2 VACV Morphogenesis

The synthesis of progeny virions begins in the cytoplasm of infected cells, in areas known as "virus factories". Few, if any, cellular organelles associate with

virus factories, although sometimes they are surrounded by endoplasmic reticulum (ER) derived cisternae (150). The onset of early viral transcription (151) and viral DNA replication (150) is followed by the appearance of viral crescents, the earliest evidence of virus assembly. These crescent structures are made up of lipid and protein and grow to form a closed, spherical structure that encases the viral DNA and core components to form an immature virion (IV). The structure of the crescent lipid bilayer is still under debate and several models have been proposed: 1) a single-membrane bilayer (152;153); 2) a double-membrane bilayer (154); and 3) folded cisternae (6;155). Although evidence has been provided for each of these models, there are several aspects of the VACV replication cycle that favour the single-membrane model. For example, two membranes would present problems with viral entry into cells compared to the more obvious single-membraned entry by simple fusion with the plasma membrane to release the viral core into the cytoplasm. In addition, clear images using freeze-fracture microscopy after treatment of cultures with rifampicin demonstrated a single lipid bilayer that was covered by a "spicule" layer composed of D13 scaffold protein (13;156). However, the origin of the lipid membrane is an enigma as it is believed, by some, that membranes are formed *de novo*, as they are dissimilar to intracellular membranes in structure and composition, although no plausible mechanism has been proposed for this (152).

Four viral proteins F10, H5, G5 and A11 are implicated in the formation of viral membranes as determined by mutagenesis experiments, as deletion of any one of these results in the disruption of virus assembly at the earliest stages of

morphogenesis (157-161). Of these, H5 is reported as the most abundant and has been implicated with additional roles in DNA replication due to its association with A20 and in late transcriptional regulation (69;162-164). F10, H5 and A11 are all phosphorylated, suggesting a role for phosphorylation in virus maturation (159;165-167) and F10 possesses intrinsic kinase activity (160;161;168).

The A14L and A17L gene products have been shown to be involved in membrane biogenesis and are critical for the diversion of ER membranes to virus factories and the formation of the viral membrane (169-171). Mutation of these genes results in the formation of crescents that do not make contact with the virus factories, however, it is not yet clear whether the absence of these proteins leads to stalling of the morphogenesis process or instability of viral membranes (172-177). Interactions between A14 and A17 have been reported to be mediated by the N-terminal region of A17 to form a lattice structure that is thought to sustain viral integrity and serves to anchor other viral proteins such as A27, to the membrane (170;178;179).

Following proteolytic cleavage of core proteins and condensation of DNA, the IVs transform into the characteristic brick-shaped single-membraned virion. A portion of these virions will become wrapped in host-derived membranes to form intracellular enveloped virus (IEV). These are exported to the cell surface to either remain bound as cell-associated enveloped virus (CEV), which are then moved towards neighbouring cells by polymerizing actin tails in the underlying cytoplasm, or are released from the surface into the extracellular milieu as extracellular enveloped virus (EEV). The proportion of enveloped virus that remains bound as

CEV or released as EEV varies between strains and is dependent on the host cell type (120;180;181). The formation of IEV using intracellular membranes and subsequent release of EEV appears to be unique to OPVs, however, there are reports of the budding of single-membraned virions through the plasma membrane to become EEV. This has been documented for the WR, IHD-J and MVA strains of VACV (182), and is analogous to the major route of release for fowlpoxvirus (FPXV) (183). It is unclear whether these membranes are similar in composition to EV produced as a result of intracellular wrapping. The majority of virions remain unwrapped within the cell until lysis, and there is much debate as to whether these particles are pre-cursors of EV that accumulate within the cell by default due to depletion of intracellular membranes, or are a true end-stage product of OPV maturation (116) (Figure 1.1).

In some poxviruses such as canarypoxvirus (CNPXV) and FPXV and in the OPVs ectromelia (ECTV) and CPXV, but not VACV or VARV, IMVs are occluded within A-type inclusion (ATI) bodies (184-187). It is thought that ATIs protect virions and increase their stability in the environment, aiding transmission. Occlusion of virions is not a passive process, requiring not only the ATI protein but also the 4c protein (A26) (188). Viruses with a truncated ATI, together with A26 are unable to occlude IMV within ATI bodies (188). This would suggest important additional roles for these proteins.

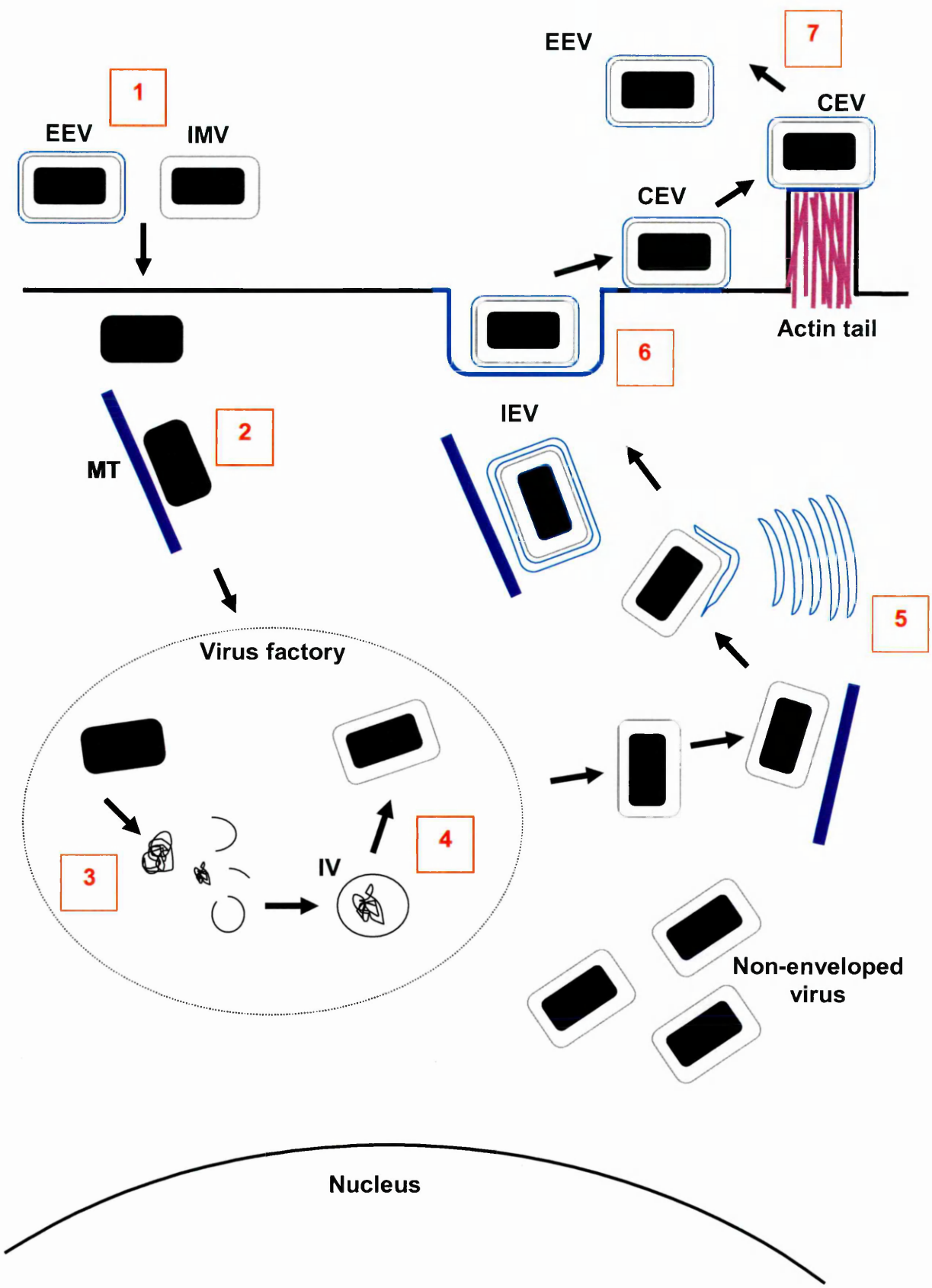
1
EEV
IMV
EEV
7
CEV
CEV
Actin tail
6
IEV
MT
2
5
Virus factory
3
IV
4
Non-enveloped
virus
Nucleus

Figure 1.1 VACV Morphogenesis

1 EEV or IMV bind to the cell and enter following the loss of one or more membranes. The naked viral core is released into the cytoplasm. **2** The core is transported via microtubules (MT) where the formation of viral factories occurs within the cell. **3** Transcription of the early mRNAs leads to core uncoating. DNA replication and viral crescent formation begins. **4** DNA is packaged and immature virions (IV) assemble. Concomitant with proteolytic cleavage of viral core proteins IV are processed to form single-membraned virions. **5** Some virions are transported via microtubules to intracellular membranes for envelopment. **6** Particles are wrapped by a Golgi- or trans-Golgi network (TGN)-derived double membrane to form triple-membraned IEV and are then transported to the cell surface via microtubules. **7** To exit the cell, the outer IEV membrane fuses with the cell membrane to expose a CEV at the cell surface. Actin polymerisation beneath the CEV forms an actin tail that drives the virus toward a neighbouring cell, or the virus is released as an EEV.

1.2.2.6.3 EV-specific Proteins

The wrapping of virions to become EV is a complex process and has been shown to require a multitude of virus-encoded proteins (reviewed in (189)). Up to 10 proteins are known to be unique to the EV membrane, with the first identified by Payne *et al.* (1978, 1979): A56 (89K/haemagglutinin), B5 (42K), F13 (37K), A33 and A34 (representing 5 proteins ranging from 20-23K, depending on the degree of glycosylation), and two proteins of 210K and 110K respectively that have yet to be identified but may be complexes of the other proteins (181;190-197). F12 and A36 have been more recently identified as unique to IEV, being absent from EEV and CEV, and are thought to be lost during fusion with the plasma membrane during exit from the cell (198-201).

All of these EV proteins are glycosylated, with the exception of A36, F12 and F13 which are acylated; the A33, A56, and B5 proteins are acylated in addition to being glycosylated (195;202). These modifications allow the proper folding of these proteins and may facilitate their association with or localisation in the lipid membranes.

Wrapping is dependent on F13 and B5, as deletion of these genes in VACV results in reduced IEV (117-119). The role of F13 is not fully understood: F13 has limited amino acid similarity to phospholipase D (PLD) (203;204) suggesting a role in signalling or membrane trafficking, however no PLD activity has been demonstrated for F13 when expressed in cell culture (205). Others have reported that F13 has broad lipase activity (206) and therefore suggest that F13 regulates vesicular budding (207;208). Studies by Husain and Moss (2001) provide evidence

for this by showing F13 localises to the Golgi and causes redistribution of B5 from the trans-Golgi network (TGN) to endosomal membranes (209). Overexpression of F13 causes a reduction in EEV, suggesting that the correct level of F13 production is critical (210). B5 is proteolytically processed to remove the N-terminal signal peptide (211) and exists as a viral membrane protein; it is also cleaved near the transmembrane domain to produce a 35 kDa secreted protein (212). This protein is highly acylated (195) and forms high molecular mass complexes (192) which are most likely due to B5-A34 (213), B5-F13 (195) and B5-A33 (214) interactions. It is suggested that the signals necessary for targeting to the Golgi reside in the transmembrane/cytoplasmic tails (215-217), and these may also be involved in retrieval of B5 from the plasma membrane (217). The amino acid sequence suggests 4 short consensus repeats (SCR) that are characteristic of complement activation, and which have been demonstrated to be important in wrapping (118;218). The SCR domain has also been shown to be a target for anti-VACV neutralising antibodies (219).

Deletion of other EV specific proteins does not appear to affect wrapping but has varying effects on plaque size and EEV production (189). It is therefore more likely that these proteins are involved in the transport of IEV to the cell surface and in facilitating egress. Deletion of F12L leads to a reduction in CEV/EEV as IEV accumulates within the cell, presumably by preventing IEV transport, implicating F12 in microtubule-mediated transport to the plasma membrane (198). In addition, the association of F12 with IEV has been shown to be via an interaction with A36, which is critical for the function of F12 during egress (220). More recently however,

Dodding *et al.* (2009) have reported that F12 is not essential for microtubule transport, but directly interacts with the viral protein E2 to form a complex that is involved in IEV wrapping (221). Thus the function of F12 remains unclear.

Deletion of A36 also results in a reduction in EEV, yet the levels of CEV remain normal. This suggests that A36 is involved in release of CEV from the cell surface and studies have demonstrated that actin tail formation requires A36 where the protein concentrates on the cytosolic face of the plasma membrane beneath CEV at the point of actin tail formation (222). It has been shown that recruitment of A36 requires A33 as a chaperone, to allow tyrosine phosphorylation of A36 thus inducing actin-tail formation. Deletion of A36 also results in the loss of kinesin-1 recruitment and therefore a loss in efficient transport of IEV to the cell periphery, suggesting a further role for A36 in microtubule-mediated transport (223).

The production of EEV was actually enhanced when A33R or A34R were deleted, although a reduction in infectivity was also observed in the case of the latter (136;191;224). Tyrosine phosphorylation of A36 is also reduced in the absence of A34 or F13, and inhibited in the absence of A33, suggesting a role in the control of modification of A36 to allow release of CEV (225).

Interestingly, the only EV-specific protein not to impact on EV morphogenesis and release is A56, although its deletion results in syncitial plaque formation (226). A56R encodes a haemagglutinin, which is found both on the surface of infected cells and on EEV (197;227). Not all strains of VACV express A56R, for example, the IHD-W strain does not. Its role appears to be to prevent cell-to-cell fusion (227) and reduce the entry of superinfecting virus, when

complexed with the virally-encoded K2 protein (228), through interaction with the EFC (229;230). Inhibition of synctial fusion may be required for the infection of uninfected neighbouring cells with CEV.

1.2.2.6.4 IMV-specific Proteins

It is assumed that the end-stage product of OPV morphogenesis is an enveloped virion, and it has been shown that enveloped virus is required for the dissemination of disease throughout the host: EV knockout viruses do not disseminate *in vitro* and are avirulent *in vivo* (reviewed in (189)). As previously described in this chapter, there are several proteins that are unique to the surface of EV that are necessary for its formation and function (section 1.2.2.6.3). This may also be the case for IMV as there are proteins that are unique to the surface of IMV that are produced late in the infectious cycle: A26 (4c) and A25 (ATI) (116). It has not yet been determined whether IMV is also a true end-stage product of morphogenesis, however its role in transmission between hosts has been considered. Both A26 and the ATI proteins have been shown to be necessary for the occlusion of virions within ATIs (188). The ancestral function of ATIs was thought to be to protect virions from environmental degradation during transmission between hosts, similar to occlusion bodies observed in entomopoxviruses (231) and baculoviruses (232). Comparative genomic analysis of sequenced OPV genomes demonstrates that both A26 and ATI gene sequences are highly conserved in most, if not all, OPVs yet the ATI gene is truncated in many of these for example in VACV and VARV (Figure 1.2B-E), and also in camelpoxvirus

(CMLV) and monkeypoxvirus (MPXV) (188;233). A truncated ATI renders the virus occlusion negative. The full length version of the ATI gene in CPXV and the atypically truncated version in ectromelia virus (ECTV) are approximately 60 % longer than the highly conserved truncate (233). Interestingly the approximate point of mutation is similar in all ATI truncate-OPVs, preserving the truncate COOH-terminal region which is immunodominant for antibody responses in mice (77). This would suggest an additional role in immunomodulation, perhaps to aid infection of phagocytic cells, such as a macrophage, that would be capable of ingesting the large ATI and degrading the ATI matrix, or perhaps the establishment of infection in an immune host (116). Interestingly, the ATI and A26L genes are completely absent in yatapoxviruses, leporipoxviruses, suipoxviruses and capripoxviruses (Figure 1.2F) (234;235).

The role of A26 is unlikely to be only as an occlusion factor as the truncated gene is retained in most OPVs and, as a result, additional roles for A26 have been suggested: Stern and Dales (1976) proposed that A26 was a component of the STEs that were visualised by electron microscopy (236;237), although viruses lacking A26 have also been shown to possess STEs (238;239). This is somewhat marred by the lack of confirmation of STEs by cryo-electron microscopy. More recently, Ulaeto *et al.* (1996) demonstrated a switch in production to IMV from EV late in the infectious cycle that was concomitant with detection of A26 in virus cultures (116). This has led to the suggestion that A26 is a differentiation switch, resulting in maturation of IMV instead of EV. This would be a unique mechanism by

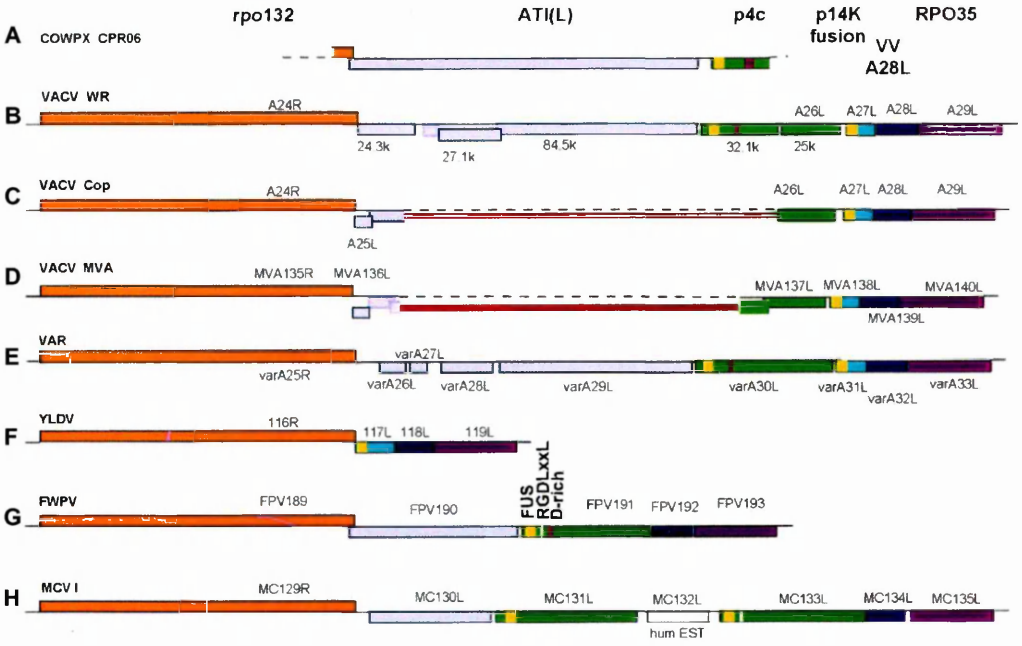

Figure 1.2 Organisation of the ATI Locus in Different Poxviruses

Genomes were examined for homologues of the A24R and A29L genes to locate the ATI locus for **A** CPX CPR06 (Accession no. D00319 and X06343); **B** VACV WR (Accession no. M37415 and M61187); **C** VACV Cop (Accession no. M35027); **D** VACV MVA (Accession no. U94848); **E** VARV Bangladesh-1975 (Accession no. L22579); **F** Yaba-like disease virus (YLDV) (Accession no. AJ293568); **G** FWPV (Accession no. AF198100); **H** MCV I (Accession no. U60315). YLDV is also representative of leporipoxvirus, suipoxvirus and capripox which do not contain homologues of the A25L or A26L genes.Genes are represented as blocks and are transcribed in a rightward direction when featured above the line or in a leftward direction when featured below the line. Filled blocks of the same colour represent equivalence where those bound by black lines have been described in the literature and those bound by coloured line have been identified from available sequence data. Disrupted genes are represented as smaller blocks and overlaps represent frameshifts. Red lines represent deletions in the genomes of VACV Cop and MVA and open-ended blocks represent gene fusions.

- rpo132 (A24R)
- ATI (A25L)
- p4c (A26L)
- p14K (A27L)
- VACV A28L
- RPO35 (A29L)
- Vac_fusion domain (FUS)
- aspartate-rich regions (D-rich)
- RGDLGSL motif
- deleted regions

(adapted from Boulanger *et al.* (2002))

which OPVs direct the differentiation of virions to produce two functionally distinct, non-interchangeable mature particles: EV in the earlier stages of infection to facilitate dissemination within the host and IMV later to facilitate host-to-host spread.

1.2.2.6.5 Host-Derived Proteins

Interestingly, several host cell proteins have been found associated with purified virions (240;241). All are present in low abundance and many of these have been reported as components of other viruses such as HIV-1 and human T-cell leukaemia/lymphoma virus (242-245).

Many of these are associated with EEV and are found on the outer envelope such as CD46, CD59, CD29, CD71, CD81 and MHC-1 (246;247), conferring resistance to complement. Advantageously, progeny virus will always carry complement regulators that are adapted to the complement of its most recent host, which may be important in OPVs that have a broad natural host-range.

Studies by Chung *et al.* (2006) have identified 23 host proteins associated with purified IMV particles that were present in low abundance (240). Many of these are not surprising as they are cytoskeleton proteins and protein transport/vesicular trafficking proteins that may be utilised during the virus life cycle. Several of these, such as cyclophilin A, ß-actin and ubiquitin have been previously found in IMV particles (241;248;249), and others such as 60S acidic ribosomal proteins, thioredoxin and peroxiredoxin 1 were uniquely identified in VACV (240), although their roles in VACV biology have not been established.

It is possible that some of these proteins are incorporated into the particle non-specifically or adhere to the particle during purification (250), however incorporation of cyclophilin A into viral cores, where inhibition of cyclophilin A by cyclosporine results in inhibition of VACV replication, may indicate that VACV requires this protein as part of the replicative cycle (248).

1.2.2.6.6 Immunomodulatory Proteins

Poxviruses encode proteins with immunomodulatory functions involving inhibition of apoptosis, production of cytokines and chemokines, the activity of immune cells such as NK (natural killer) cells and cytotoxic T cells, and the activity of complement and antibodies (reviewed in (251)). This enables them to elude detection and destruction by the host immune system. These proteins can be classified as virostealth, viromimicry and virotransduction.

Virostealth is a mechanism employed by many viruses to enable viral infections to remain undetected by subversion of discriminatory pathways by preventing presentation of viral antigens and/or downregulating recognition receptors (252;253). Viromimicry involves the production of virokines or viroreceptors that act as mimics of the host immune system to disrupt antiviral pathways. For example, viroreceptors resemble their cellular counterparts and act to sequester cytokines such as interferons (IFNs) and tumour necrosis factor (TNF) (254-257). The virokine vaccinia complement control protein (VCP) acts on C3 convertase, directly or indirectly causing its decay thus inhibiting the complement pathways (258). Virotransduction counteracts the deleterious effects of the pro-

inflammatory response thereby producing an environment that is conducive to viral replication. This is primarily by the production of anti-apoptotic proteins that interfere with caspases or disrupt intracellular signalling cascades (259;260).

The origins of poxvirus immunomodulatory proteins are unknown, however it is likely that some of these that are similar to their cellular counterparts may have originated from their host either by ancestral retrotranscription or acquired from other viruses via homologous recombination, and these viruses have co-evolved immunomodulatory strategies with their host.

1.3 Prevention and Treatment of Poxvirus Infections

Although smallpox was officially declared eradicated in 1980, the threat of a deliberate or accidental release of VARV, or a fully emergent human MPXV outbreak, has renewed interest in poxvirus research. The increasing knowledge of poxvirus biology has been used to provide further information about existing vaccines, identify ways in which poxviruses can be genetically manipulated to generate safer, more efficacious vaccines and develop novel drug therapies.

1.3.1 Vaccines

1.3.1.1 Live Vaccines

The traditional smallpox vaccine was VACV produced from the chorioallantoic membrane (CAM) of chicken embryos, or the exudates from the infected skin of domestic animals. During the smallpox eradication programme, Dryvax™ (New York City Board of Health (NYCBH) strain) was primarily used in

the USA and South America, and the Lister/Elstree strain was primarily used in Europe, Africa and Asia. The vaccine was administered by scarification using a bifurcated needle, and immunisation was deemed successful on the appearance of a 'take' (a vaccinial pustule or lesion) 7-9 days later (3).

1.3.1.2 Complications of Live Smallpox Vaccines

Although these vaccines were efficacious, as proven by the global eradication of smallpox, there was a high incidence of adverse events as a result of smallpox vaccination. These ranged from fever, myalgia, malaise and headaches, to more severe life-threatening effects such as generalised vaccinia, eczema vaccinatum, encephalitis and the almost always fatal progressive or necrotising vaccinia (3). Myopericarditis is a more recently described side-effect that may have occurred historically but has only been recognised in the past decade (261-263). Live smallpox vaccines cannot be administered to contraindicated individuals such as HIV patients, or patients undergoing immunosuppressive therapy or chemotherapy. In addition, complications can arise in patients who have skin disorders such as eczema, atopic dermatitis and psoriasis, in pregnant women, or anyone with these conditions who comes into contact with a recent vaccinee who is shedding virus. This is likely to represent a significant proportion of the UK population and as a result, efforts are being made to improve the safety of smallpox vaccines that could be used in a mass vaccination campaign.

1.3.1.3 Next Generation Smallpox Vaccines

Sometimes described as second generation smallpox vaccines, new smallpox vaccines have been developed that are produced in cell culture to generate safer, sterile vaccines that have reduced hazards from adventitious agents and transmissible spongiform encephalopathies. ACAM2000 (Acambis Plc) is based on Dryvax™ and is propagated in Vero cells. This vaccine has been demonstrated to induce similar cutaneous reactogenicity and immunogenicity to Dryvax™ in clinical trials (264;265). Other vaccines include Elstree-BN (Bavarian-Nordic) based on the Lister/Elstree strain and the cell-cultured smallpox vaccine (CCSV) developed by DynPort (a derivative of the NYCBH strain propagated in MRC-5 cells) all of which have similar reactogenic and immunogenic profiles to their parent strains (www.bavarian-nordic.com; (266)). However, the virulence of these live next generation vaccines remains similar to the parent strains with identical contra-indications (264;267), therefore new approaches are needed to try to produce vaccines that are not only safe for use but also maintain the efficacy of the original smallpox vaccines.

1.3.1.4 Attenuated, Replication Competent Vaccines

The generation of a live-attenuated replication-competent smallpox vaccine was achieved in Japan with LC16m8, produced by serial passage of the Lister strain in primary rabbit kidney cells at low temperature. The LC16m8 clone was selected for its ability to form small pocks on CAMs (268). This vaccine was shown to be safer than the Lister parent and was less neurovirulent, yet remained

immunogenic (269;270) as demonstrated by its protective efficacy in animals (271-273). Analysis of the genome sequence demonstrated a disruption of the B5R gene, necessary for the production of EV, suggesting the attenuation is due to reduced viral dissemination (270). Interestingly, B5 is a major target for EV-neutralising antibodies in poxvirus infection (274;275) and induces a robust immune response (275-277), which would suggest its importance in protection. LC16m8 however produces an 8 kDa truncate of B5, and yet is still able to confer protection and induce EV-neutralising antibodies (272). This vaccine is currently licensed for use in Japan and has investigational new drug (IND) status in the USA.

1.3.1.5 Attenuated, Replication-Defective Vaccines

Vaccine strains that are replication-defective are often referred to as third generation vaccines. The most successful example is the modified vaccinia Ankara (MVA) strain developed by Mayr *et al.* (1975) (278), subsequently developed for licensure by Acambis Plc (MVA3000) and Bavarian-Nordic (IMVA-MUNE). MVA was derived from the Ankara strain of VACV after >500 passages in chick embryo fibroblasts. The virus has lost ~15 % of the wild-type genome and is unable to replicate in most mammalian cells, including human cells (279). This has resulted in a safer vaccine that has been shown to have no serious adverse effects, but remains efficacious in animal models. Originally, this vaccine strain was considered for use only as a primary immunisation to protect against adverse events prior to vaccination with a traditional replicating vaccine strain. Studies have shown that

MVA can induce a protective immune response when administered alone, albeit with much higher doses than are required for traditional and next generation vaccines (280-284), but MVA was not able to protect mice against infection with VACV WR when administered post-exposure (285). The safety profile of MVA is promising (286) and currently this strain is in clinical trials for use as a stand alone smallpox vaccine candidate. In addition, recombinant MVA is being investigated as a vaccine vector against a variety of diseases (287;288). Studies have generated recombinant MVA as candidate vaccines against infectious diseases such as malaria (289;290), influenza A (291;292), tuberculosis (293) and HIV-1 (294-296). In addition, recombinant MVA viruses are being used as cancer vaccines (297-299).

1.3.1.6 Sub-unit Vaccines

Using recombinant proteins or using DNA vaccines encoding proteins that are abundant on either the IMV or EEV surface, or ideally both, has been the approach taken by many to create a smallpox sub-unit vaccine. Antigens such as L1, A27, B5 and A33 have been successfully used to protect against lethal disease in animal models (300-306). Although using a panel of antigens as a sub-unit vaccine is regarded as a safe alternative to a replicating smallpox vaccine, the limited repertoire of antigens that are displayed to the immune system could result in a less efficacious vaccine.

1.3.2 Antiviral Therapies

Currently there are no licensed therapies for smallpox, although some that showed efficacy *in vitro* were tested during the smallpox eradication programme in India, such as metisazone and thiosemicarbazone (3). However, nausea and vomiting were a common side-effect of treatment and as a result they were not considered further.

Novel drug therapies target parts of the poxvirus replicative process, or interfere with the release of virus thus preventing spread (reviewed in (307). A promising candidate is an acyclic nucleoside phosphonate, cidofovir (CDV), that is a potent inhibitor of poxvirus-encoded DNA polymerase (308;309). Its activity relies on several phosphorylation steps for conversion to 5'-nucleotides. Two adjacent incorporations of the active moiety into the elongating DNA strand are required to inhibit the viral DNA polymerase and induce chain termination thereby inhibiting viral replication. CDV, which is also a potent inhibitor of herpesvirus DNA polymerase (310), was first licensed for the treatment of cytomegalovirus retinitis in HIV patients, and has since been awarded IND status for emergency treatment of smallpox. However, the route of delivery may hinder its use; CDV is poorly absorbed when administered orally therefore administration is intravenous (i.v.) and probenecid, a competitive inhibitor of organic anion transport, must be co-administered to reduce nephrotoxicity. More recently a CDV derivative, CMX001 has been developed that incorporates a lipid group thereby increasing the antiviral activity by ~1000-fold and increasing the oral bioavailability to the extent that the drug can be administered orally (311;312). In addition, this derivative has been

shown to have a reduced nephrotoxic effect and is consequently much safer than the CDV parent. Once taken up into the cell, CMX001 is cleaved to yield free CDV, therefore the mechanism of action is the same. IND status has also been given to CMX001 and clinical trials have begun (reviewed in (313)). Resistance to CDV and its derivatives has arisen in viruses repeatedly passaged in the presence of the drug, and has been mapped to mutations in the virally encoded DNA polymerase (314).

Another anti-poxviral candidate drug is ST-246, a potent virus egress inhibitor developed by Siga Technologies Inc. (315). ST-246 targets the F13 protein, preventing wrapping of virions and subsequent egress from the infected cell (316). The exact mechanism of action is unclear, however, different OPVs demonstrate differing sensitivities to the drug; CPXV and CMLV are less sensitive than VACV, which may be due to their differing dependencies on the enveloped form for propagation (317). ST-246 has high oral bioavailability and does not appear to be toxic, although clinical trials are currently underway to investigate this.

Other antiviral therapies that have potential to be developed for the treatment of poxvirus infection include the nucleoside analogues ribavirin, adefovir and S-adenosylhomocysteine (SAH) hydrolase inhibitors, and kinase inhibitors such as Gleevac (318-322). Inhibitors of the virally-encoded topoisomerase 1B (vTOPO) enzyme such as novobiocin and coumermycin are effective at reducing replication and, interestingly, fluoroquinolones have been shown to have a similar effect. This suggests the possibility of a generic medical countermeasure that is effective against both bacteria and viruses (323-325).

1.4 Aims of the Project

The aim of this study is to investigate the role of the membrane protein A26 as a putative differentiation switch in IMV/EV maturation in VACV, the prototype OPV, by generating a defined A26L deletion mutant. This will provide insight into the complex process of OPV morphogenesis and examine the possibility that OPVs direct an active process of differentiation in progeny virions. In the event that the preliminary studies successfully generate the required mutants, the effects of modulation of A26L expression on the kinetics of IMV and EEV production by altering its attendant promoter will be investigated, with the overall aim of providing a rationale for developing a next generation live attenuated smallpox vaccine.

2 Materials and Methods

2.1 Materials

2.1.1 Oligonucleotide Primers

Oligonucleotide primers used in this study were synthesised by Eurogentec Inc. and Sigma-Genosys, UK.

2.1.2 Plasmid DNA

Plasmid DNA constructs used in this study were pCAP^{s} vector from the PCR cloning kit (blunt-end) supplied by Roche Diagnostics Ltd. (West Sussex, UK) and pCR®-XL-TOPO® supplied by Invitrogen Ltd. (Paisley, UK). The deletion plasmid p1107 was used to amplify the *Eco*GPT gene (326). Recombination cassettes described in Chapter 6 were synthesised by GeneArt AG (Germany).

2.1.3 General Reagents

Unless otherwise stated, chemicals were purchased from Sigma-Aldrich (Dorset, UK) and molecular biological reagents from Roche Diagnostics Ltd. Sterile H_2O and phosphate-buffered saline (PBS) were purchased from Gibco BRL, a division of Invitrogen Ltd.

2.2 Microbiological Methods

2.2.1 Preparation of Culture Media

Luria-Broth (L-broth) was prepared for the routine culture of *Escherichia coli* strains. 10 g of bacto-tryptone was added to 5 g of bacto-yeast extract and 10 g of

NaCl. The constituents were dissolved in 800 ml sterile H_2O and adjusted to pH 7 with NaOH. The final volume was corrected to 1 litre with sterile water and the medium was sterilised by autoclaving and stored at 4 °C.

Luria-agar (L-agar) was prepared for the routine culture of *E.coli* strains by the addition of 10 g of bacto-tryptone to 5 g bacto-yeast extract plus 15 g bacto-agar and 10 g NaCl. The constituents were dissolved in 800 ml sterile water and adjusted to pH 7 with NaOH. The final volume was corrected to 1 litre with sterile H_2O and the medium was sterilised by autoclaving and stored at 4 °C.

2.2.2 Media Supplements

Ampicillin or kanamycin (Sigma-Aldrich) were added to growth media where appropriate. To 200 ml L-broth or molten L-agar, 200 µl ampicillin (100 mg/ml) or 100 µl kanamycin (100 mg/ml) were added to give final concentrations of 100 µg/ml and 50 µg/ml respectively.

2.2.3 Maintenance of *E.coli* Strains

Strains were stored at -80 °C in L-broth containing the appropriate antibiotic supplemented with 30 % (v/v) glycerol, or streaked on L-agar plates containing the appropriate antibiotic and stored at 4 °C for approximately 1-2 weeks.

2.3 DNA Manipulation and Cloning

2.3.1 Agarose Gel Electrophoresis

Agarose gels were used to separate DNA following manipulation and cloning steps. In the first instance, 1 % agarose gels were prepared in 1 x TAE buffer with 0.5 µg/ml ethidium bromide. TAE buffer consists of 0.04 M Tris-acetate and 0.001 M EDTA at pH 8.0. After some time, the laboratory switched to use of pre-cast 1.2 % E-Gels® (Invitrogen Ltd.). These are bufferless self-contained agarose gels pre-equilibrated with ethidium bromide.

DNA samples were mixed with 4x sample loading buffer (300 µl glycerol, 700 µl distilled H_2O and 100 µg tartarazine) to a final volume of 20 µl and loaded onto the agarose gels alongside 20 µl of molecular weight marker at a concentration of 125 µg/ml. Poured agarose gels were electrophoresed for 30 minutes at 100 volts in 1x TAE buffer, and E-Gels® were electrophoresed for 30 minutes using a proprietary dedicated powerpack according to the manufacturer's instructions. DNA was visualised under ultraviolet (UV) light and photographed using a Syngene Gene Genius BioImaging System (Cambridge, UK).

2.3.2 Digestion of DNA

DNA was digested using restriction endonucleases supplied by Roche Diagnostics Ltd. (West Sussex, UK) according to the manufacturer's instructions. Briefly, a 20 µl reaction contained 1-2 µg DNA, 10 U enzyme, and 2 µl reaction buffer (10x) with the remaining volume made up to 20 µl with distilled H_2O.

Reactions were incubated for 2 hours at the manufacturer's recommended temperature.

2.3.3 Polymerase Chain Reaction (PCR)

PCR was used to amplify DNA using primers to target specific regions of the VACV genome (Table 2.1). Typically, each reaction contained 250 ng template DNA, 1 µl of each primer (10 pmol), 2.5 µl reaction buffer (10x), 1 µl dNTP mixture (10 mM each), 1 µl *Taq* polymerase (5 U) and made up to a final volume of 25 µl with distilled H_2O.

DNA was denatured for 3 minutes at 94 °C and then amplified during a reaction of 25 cycles (typically 1 minute at 94 °C for denaturing, 30 seconds at 55 °C for annealing, 1 minute at 72 °C for extension of the amplicon). Extension times were adjusted to give approximately 30 seconds/500 bp of predicted product. This was followed by a final period of extension at 72 °C for 10 minutes. Reactions were performed either in a GeneAmp 2400 (Applied Biosystems, UK) or a PTC-200 DNA Engine Thermal Cycler (MJ Research, USA).

2.3.4 Purification of DNA

Following a PCR or digestion, the DNA fragment of interest was purified to remove buffers, primers, nucleotides and enzymes. This was carried out either by excision of the DNA from an agarose gel, or directly from the reaction mix using a QIAquick PCR purification kit (Qiagen) or a MinElute PCR purification kit (Qiagen). These protocols are designed to purify single- or double-stranded DNA fragments

Primer Name	Primer Sequence 5' - 3'	Use	Annealing Temperature (°C)
GPT1	AAT TGG ATC AGC TTT TTT TTT TTT TTT TTT GGC ATA TAA ATA AGG TCG ACA AAA ATT GAA AAA CTA TTC TAA TTT ATT GCA CGG ATG AGC GAA AAA TAC ATC GTC ACC T	synthesis of *Eco*GPT gene plus synthetic early/late promoter (327)	70-77
GPT2	ATA TTG TCC CAA TGT TTC AAT GTG ATG TTC TAA CCT ATC AAC TGC CGC TGT ATC ACA ACA TTA GCG ACC GGA GAT TGG C	synthesis of *Eco*GPT gene plus downstream flank of A26L gene	70
GPT3	AGT AAC TTA ACT CTT TTG TTA ATT AAA AGT ATA TTC AAA AAA TGA GTT ATA TAA AAT TGG ATC AGC TTT TTT TTT TTT TTT TTT GGC	addition of upstream flank of A26L to synthetic early/late promoter	77
A	TTA ATT AAA AGT ATA TTC AAA AAA TGA GTT ATA TAA ATG GCG AAC ATT ATA AAT	addition of natural promoter to A26L gene	64
A2	CTC TGG CTA AAA AGA TTG ATG TTC AGA CTG GAC GGC GCC CAT ATG AGT AAC TTA ACT CTT TTG TTA ATT AAA AGT ATA TTC	addition of upstream flanking region to A26L gene plus native promoter	55
B	CAA AAA TTG AAA AAC TAT TCT AAT TTA TTG CAC GGA TGG CGA ACA TTA TAA AT	addition of synthetic early promoter to A26L gene (327)	57
B2	CTC TGG CTA AAA AGA TTG ATG TTC AGA CTG GAC GGC GCC CAT ATG AGT AAC TTA ACT CTT TTG TCA AAA ATT GAA AAA CTA	addition of upstream flanking region to A26L gene plus synthetic early promoter	55
C	AAT TGG ATC AGC TTT TTT TTT TTT TTT TTT GGC ATA TAA ATA ACG TCG ACA AAA ATT GAA AAA CTA TTC TAA TTT ATT GCA CGG ATG GCG AAC ATT ATA AAT	addition of synthetic early/late promoter to A26L gene (327)	51
C2	CTC TGG CTA AAA AGA TTG ATG TTC AGA CTG GAC GGC GCC CAT ATG AGT AAC TTA ACT CTT TTG AAT TGG ATC AGC TTT TTT	addition of upstream flanking region to A26L gene plus synthetic early/late promoter	55
D	AAT TGG ATC AGC TTT TTT TTT TTT TTT TTT GGC ATA TAA ATG GCG AAC ATT ATA AAT	addition of synthetic late promoter to A26L gene (327)	64

Primer Name	Primer Sequence 5' - 3'	Use	Annealing Temperature (°C)
D2	CTC TGG CTA AAA AGA TTG ATG TTC AGA CTG GAC GGC GCC CAT ATG AGT AAC TTA ACT CTT TTG ATT TGG ATC AGC TTT TTT	addition of upstream flanking region to A26L gene plus synthetic late promoter	55
F	GGA TGT ATA AGT TTT TAT GTT AAC TAA ATG GCG AAC ATT ATA AAT	addition of natural F13L promoter to A26L gene	57
F2	CTC TGG CTA AAA AGA TTG ATG TTC AGA CTG GAC GGC GCC CAT ATG AGT AAC TTA ACT CTT TTG GGA TGT ATA AGT TTT TAT	addition of upstream flanking region to A26L gene plus native F13L promoter	55
E4	TTT GGA GTG CTT GGT ACA TTT TTC AAT AAG GTT CGT GAC CTC CAT	re-designed A26L reverse primer - first 45 residues	51-64
FLA1	CTC TGG CTA AAA AGA TTG ATG TTC AGA CTG GAC GGC GCC CAT ATG AGT AAC TTA ACT CTT TTG TTA CCC GAT TGT AGT TAA GTT TTG AAT AAA ATT TTT TAT AAT AAA TGG AGG TCA CGA ACC	single stranded oligonucleotide containing upstream and downstream flanking sequences to A26L complementary to FLA2	55
FLA2	GAG ACC GAT TTT TCT AAC TAC AAG TCT GAC CTG CCG CGG GTA TAC TCA TTG AAT TGA GAA AAC AAT GGG CTA ACA TCA ATT CAA AAC TTA TTT TAA AAA ATA TTA TTT ACC TCC AGT GCT TGG	single stranded oligonucleotide containing upstream and downstream flanking sequences to A26L complementary to FLA1	55
FLA3	GAG ACC GAT TTT TCT	amplification of FLA1	55
FLA4	GGT TCG TGA CCT CCA	amplification of FLA2	55

Table 2.1 Oligonucleotide Primers Used Throughout This Study for Construction of Recombination Cassettes

Primers were purchased directly through Eurogentec Inc. and Sigma-Genosys, UK.

ranging from 100 bp to 10 kbp from enzymatic reactions by adsorption to a silica membrane in the presence of high salt followed by elution in low salt (328).

According to the manufacturer's instructions, 5 volumes of buffer PB were added to the PCR or digestion. This was mixed and placed in a QIAquick spin column. To bind the DNA, the column was centrifuged at 13,000 rpm for 1 minute and the flow through discarded. The column was washed with 750 µl buffer PE by centrifugation at 13,000 rpm for 1 minute. The flow through was discarded and the column was centrifuged for a further minute to dry. The column was placed into a fresh tube and 50 µl or 10 µl distilled H_2O for the QIAquick or MinElute protocol, respectively, was applied to the centre of the membrane and left to stand for 1 minute. The column was then centrifuged for 1 minute and the eluted DNA stored at -20 °C.

When necessary, DNA fragments were purified directly from an agarose gel to enable the selection of DNA fragments according to their size and separation on the gel. Purification of DNA was carried out using the QIAquick Gel Extraction kit (Qiagen) which is designed to extract and purify DNA of 70 bp to 10 kbp from standard or low-melting point agarose gels by adsorption to a silica membrane in the presence of high salt, followed by elution in low salt (328).

After excision of a DNA fragment, the gel slice was weighed and 3 volumes of buffer QG were added to 1 volume of gel. The sample was incubated at 50 °C for 10 minutes, or until the gel slice had completely dissolved. This was aided by vortexing the tube every 2 to 3 minutes. One gel volume of isopropanol was added to the sample and this was mixed and transferred to a QIAquick spin column. The

column was centrifuged for 1 minute at 13,000 rpm and the flow through discarded. The column was washed with 500 µl buffer QG by centrifugation for 1 minute at 13,000 rpm to completely remove all traces of agarose, and the flow through discarded. The sample was washed with 750 µl of buffer PE and centrifuged for 1 minute at 13,000 rpm. The flow through was discarded and the column was dried by centrifugation at 13,000 rpm for 1 minute. To elute the DNA, the spin column was placed in a fresh tube and 50 µl distilled H_2O was applied to the centre of the QIAquick membrane and left to stand for 1 minute. The column was then centrifuged for 1 minute and the eluted DNA stored at -20 °C.

2.3.5 Polishing of PCR Products

To achieve blunt ends for cloning into the pCAP^s vector, the PCR product was incubated with *PfuTurbo* DNA polymerase (Stratagene, California) to remove 3' overhangs which are produced during synthesis of the amplicon with *Taq* polymerase due to its terminal transferase activity. Briefly, to 20 µl of PCR product, 1 µl of *PfuTurbo* DNA polymerase (2.5 U), 1.5 µl dNTPs and 2.5 µl of 10x reaction buffer were added. Reactions were incubated at 72 °C for 30 minutes. DNA was purified as described for PCR products in section 2.3 4.

2.3.6 Estimation of Concentration of DNA

To estimate the DNA concentration of plasmid preparations and PCR products, dilutions of DNA samples were electrophoresed through agarose gels

and the intensity of ethidium bromide fluorescence under UV light compared by eye with a range of known standards (Roche Diagnostics Ltd.).

2.3.7 Ligation of DNA

Blunt-ended DNA fragments were sub-cloned into the pCAP^s vector, a specially designed suicide vector that contains the lethal mutant gene of the catabolite activator protein (CAP). There are several advantages of using this positive selection cloning system. The pCAP^s plasmid is linearised with the blunt-end cutting restriction enzyme *Mlu*N1 in the coding region of the lethal CAP gene. Blunt-ended DNA fragments can be ligated into the vector and disrupt the lethal CAP gene. Only clones that contain recombinant vectors will survive as *E.coli* that contain the re-ligated vectors without an insert will not survive the transformation because they contain the active CAP gene. In addition, the vector contains the *bla* (β-lactamase) gene which confers ampicillin resistance, allowing clones that contain the recombinant pCAP^s vector to grow on selective medium containing ampicillin (100 ug/ml).

Before ligation, the pCAP^s vector was linearised by digestion with *Mlu*N1. The reaction consisted of 2 µl of vector (10 ng), 1 µl SuRE/Cut buffer (10x), 1 µl of *Mlu*N1 (1 U) made up to 10 µl with 6 µl distilled H_2O, and was incubated for 1 hour at 37 °C followed by 65 °C for 15 minutes to inactivate the enzyme.

Purified blunt-ended PCR products were ligated into the pCAP^s vector as recommended by the manufacturer. Typically, reactions were set up containing 1 µl of linearised vector (1 ng), 10 µl ligation buffer (2x), up to 6 µl PCR product, 1 µl of

T4 DNA ligase (5 U), 2 µl T4 DNA dilution buffer (10x) made up to a final volume of 20 µl with distilled H_2O. Varying ratios of vector:insert were set up to optimise the efficiency of ligation. The reaction was incubated at room temperature for 15 minutes prior to transformation into XL1-Blue chemically competent cells (Stratagene) as described in section 2.3.8.

Alternatively, PCR products were sub-cloned directly into pCR®-XL-TOPO® (Invitrogen Ltd.). This vector is specifically designed for TA cloning of long PCR products (3-10 kb) and uses the lethal *ccd*B (control of cell death) gene to enable high efficiency cloning. This vector also has kanamycin and Zeocin™ resistance genes to aid the selection of transformants, and M13 forward and reverse priming sites for sequencing. The vector is supplied linearised, and has single overhanging 3' deoxythymidine residues. This allows ligation of PCR products synthesised by *Taq* polymerase which has terminal transferase activity to add a single deoxyadenosine residue to the 3' ends of PCR products. TOPO® cloning utilises the VACV DNA topoisomerase I, which acts as a restriction enzyme and as a ligase, cleaving and re-joining DNA during replication. The topoisomerase I specifically recognises the pentameric sequence 5'-CCCTT-3' and forms a covalent bond with the phosphate group of the 3' thymidine. It cleaves one DNA strand, enabling the DNA to unwind. The enzyme then re-ligates the ends of the cleaved strand and releases itself from the DNA (Invitrogen Ltd.).

Briefly, 4 µl of PCR product was added to 1 µl of linearised vector and incubated for 5 minutes at room temperature. Up to 5 µl of this reaction was used to transform TOP10 cells (Invitrogen Ltd.) as described in section 2.3.8.

2.3.8 Transformation of Recombinant Plasmids into *E. coli*

Plasmid DNA was transformed into chemically competent XL1-Blue cells (Stratagene) or TOP10 cells (Invitrogen Ltd.). According to the manufacturer's instructions, cells were thawed on ice and up to 5 µl of ligation reaction added to the cells. These were incubated for 30 minutes on ice to allow association of plasmid DNA with the cells. Cells were heat shocked by incubation at 42 °C for 30-45 seconds, which causes permeabilisation of the bacterial membrane to DNA. Following this, 250 µl of room temperature SOC growth medium (20 g of bacto-tryptone, 5 g of Bacto-yeast extract, 10 ml 1 M NaCl and 2.5 ml 1 M KCl per litre) was added to the cells and incubated at 37 °C shaking for 1 hour. A small sample of the transformed cells (usually 50 µl) was spread onto L-agar containing the appropriate antibiotic in a 9 cm Petri dish and cultures were incubated at 37 °C overnight.

Single colonies were used to inoculate 5 ml L-broth containing the appropriate selective antibiotic and incubated for approximately 16 hours with shaking at 37 °C. Plasmid minipreparation was carried out as described in section 2.3.9, and glycerol stocks prepared to maintain transformed *E.coli* strains at -80 °C as described in section 2.2.3.

2.3.9 Plasmid Minipreparation

Plasmid DNA from transformed *E.coli* strains was isolated using QIAprep Spin Plasmid Miniprep kit (Qiagen) according to the manufacturer's instructions.

The kit is designed to lyse bacterial cells by the alkaline lysis method of Birnboim and Doly (329) using the buffers provided.

Purification of plasmid DNA is by adsorption onto a silica membrane in the presence of high salt and elution in a low salt buffer. Briefly, transformed *E.coli* was cultured in 5 ml L-broth containing the appropriate antibiotic for approximately 16 hours with shaking at 37 °C. Bacterial cells were harvested via centrifugation at 13,000 rpm for 3 minutes in a microcentrifuge. The supernate was removed and bacterial cells were resuspended in 250 µl buffer P1. To this, 250 µl of buffer P2 was added and the tube was inverted to mix and incubated at room temperature for up to 5 minutes. After this time, 350 µl buffer N3 was added to precipitate cellular proteins, and the tube was inverted to mix immediately. The tube was centrifuged for 10 minutes at 13,000 rpm to remove the precipitate. The supernate was transferred to a QIAprep spin column and centrifuged for 1 minute at 13,000 rpm to bind the DNA. The column was washed with 750 µl of buffer PE by centrifugation at 13,000 rpm for 1 minute. The membrane was dried by centrifugation at 13,000 rpm for 1 minute. The column was placed into a fresh tube and 50 µl of distilled H_2O was applied to the centre of the QIAprep membrane and left to stand for 1 minute. The column was centrifuged for 1 minute and the eluted DNA stored at -20 °C.

2.3.10 Digestion of DNA Fragments with S1 Nuclease

The treatment of DNA fragments with S1 nuclease ensures that all single-stranded and mispaired fragments are degraded. A typical reaction consisted of 8

µl of DNA, 1 µl of S1 nuclease, 0.1 µl of NaCl (3 M) and 0.9 µl of reaction buffer (10x). Reactions were incubated for 1 hour at 37 °C. To check the integrity of the DNA, a small sample was examined using agarose gel electrophoresis.

2.3.11 Sequencing of DNA

Approximately 100 ng of DNA was required by Lark Technologies, Ltd. for single pass sequence reactions (up to 1 kbp). Inserts cloned into pCAP^{s} vector (Roche Diagnostics Ltd.) were sequenced using primers GPT2 and GPT3 (Table 2.1). Inserts cloned into the pCR®-XL-TOPO® vector were sequenced using universal primers M13F and M13R (Table 2.2) which anneal at either side of the cloning site and read into the insert from the opposite ends. Primers designed in house and synthesised by Lark Technologies, Ltd. were also used where specified to determine the sequence of larger inserts from a point of origin within the insert (Table 2.2). Sequences were analysed using DNASTAR Lasergene EditSeq and MegAlign programmes.

2.4 Cell Culture

2.4.1 Maintenance of Mammalian Cell Lines

RK13 (Rabbit kidney) and BSC40 (African Green Monkey kidney) cells kindly supplied by Dr D.O. Ulaeto (Dstl), and STO (mouse embryonic fibroblast) cells obtained from European Collection of Cell Cultures (ECACC, Porton Down, UK) were cultured in the growth medium D10 consisting of Dulbecco's minimal essential medium (DMEM) (Sigma-Aldrich) supplemented with 2 mM L-glutamine

Primer Name	Primer Sequence 5' - 3'	Used for	Annealing Temp (°C)
A27LF	AAA TGG ACG GAA CTC TTT TC	screen for A27L gene	45
A27LR	TTA CTC ATA TGG ACG CCG T	screen for A27L gene	45
GPTF	ATG AGC GAA AAA TAC ATC GTC ACC TGG GAC	re-designed screening *Eco*GPT primer	63
GPTR	TTA GCG ACC GGA CAT TGG CGG GAC GAA TAC	re-designed screening *Eco*GPT primer	63
neoF	CCG CCG AGA AGG TGT CC	screening for neo^R gene	48
neoR	AGC AGG CGG TAG AAG G	screening for neo^R gene	48
neo1	TAC GAC TGG GCC CAG CAG ACC ATC	re-designed for screening neo^R gene	55
neo2	TGC TTG GCC TGG TGG TCG AAG	re-designed for screening neo^R gene	55
UF	CTC TGG CTA AAA AGA TTG AT	Screening of vA26L-EL	55
RDA26LM	GAC ATA TAT GAT CGT AAT GCC	sequencing of A26L constructs	-
M13F	CAT TTT GCT GCC GGT C	universal primer used for sequencing	-
M13R	CAG GAA ACA GCT ATG AC	universal primer used for sequencing	-

Table 2.2 Oligonucleotide Primers Used Throughout This Study for Screening and Sequencing of Recombinant VACV

Primers were purchased directly through Eurogentec Inc. and Sigma-Genosys, UK, or synthesised in-house by Lark Technologies for sequencing purposes.

(Sigma-Aldrich), 100 U/ml penicillin (Sigma-Aldrich), 100 µg/ml streptomycin (Sigma-Aldrich) and 10 % (v/v) foetal calf serum (FCS) (Sigma-Aldrich), at 37 °C in a 5 % (v/v) CO_2 humidified atmosphere. Cultures were maintained as sub-confluent monolayers, and passaged twice weekly following trypsinisation to remove the monolayer with TE (0.1 % (w/v) trypsin, 0.01 % (w/v) EDTA in Hanks balanced salt solution with phenol red) (Sigma-Aldrich). Cells were seeded into new flasks at a concentration of approximately 5 x 10^4 cells/cm^2.

2.4.2 Transfection of Mammalian Cell Lines

Transfection of mammalian cell lines to deliver DNA into the cell was achieved using Lipofectamine™ Reagent (Invitrogen Ltd.), a 3:1 (w/w) liposome formulation of the polycationic lipid 2,3-dioleyloxy-N-[2(sperminecarboxamido)ethyl] -N,N-dimethyl-1-propanaminium trifluoroacetate (DOSPA) and the neutral lipid dioleoyl phosphatidylethanolamine (DOPE). DNA was combined with Lipofectamine™ Reagent to form a DNA-lipid complex which would fuse with the cell membrane and allow transport of DNA into the cell.

Cells were seeded into a 24-well tissue culture plate at a density of approximately 4 x 10^4 cells per well in 1 ml of growth media and incubated overnight at 37 °C in a humidified 5 % (v/v) CO_2 atmosphere. To increase transfection efficiency, cells were rinsed with 500 µl Opti-MEM® I Reduced Serum Medium (Invitrogen Ltd.) prior to transfection. Typically for each reaction, plasmid DNA was diluted to 0.2 - 0.4 µg in 25 µl Opti-MEM® I Reduced Serum Medium, and 5 µl of Lipofectamine™ Reagent was diluted into 25 µl of Opti-MEM® I Reduced

Serum Medium. These were combined and incubated for 45 minutes at room temperature to allow the DNA-lipid complexes to form. To each reaction, 150 µl of Opti-MEM® I Reduced Serum Medium was added and then the complexes were overlaid onto the cells. Cells were incubated for up to 5 hours then infected with 5 x 10^5 pfu of VACV, and incubated for a further 24-48 hours at 37 °C in a humidified 5 % (v/v) CO_2 atmosphere. In some cases, cultures were transfected then infected with VACV in selective medium (section 2.5.5).

2.5 Manipulation of VACV

2.5.1 Infection of Mammalian Cells with VACV

VACV was diluted to give the appropriate multiplicity of infection (MOI) in either PBS or D10. Cells were usually infected in a low volume and rocked slowly for 1 hour, prior to removal of the inoculum and replacement with tissue culture medium. Cells were incubated for up to 7 days at 37 °C in a humidified 5 % (v/v) CO_2 atmosphere.

In some experiments, cultures were supplemented with 10 µg/ml Blasticidin (Invitrogen Ltd.), 0.05 nM to 50 nM ST-246 (kindly provided by Dr D. Hruby, Oregon State University, USA) or 4 µg/ml Brefeldin A (BFA) (Sigma-Aldrich), or combinations thereof.

2.5.2 Purification of VACV

Virus was harvested from tissue culture vessels by carefully scraping the cells with a cell scraper or a pipette tip. Cells containing virus were then collected

by centrifugation at 2,500 rpm for 10 minutes (Jouan Centrifuge C3i, France). Cells were lysed by dounce homogenisation or freeze-thaw (x3 cycles) and cellular debris removed by further centrifugation at 2,500 rpm for 10 minutes. Virus in the supernate was concentrated by ultracentrifugation at 20,000 rpm for 60 minutes and purified through a 36 % (w/v) sucrose cushion at 13,500 rpm for 80 minutes (Beckman L8-70M, USA).

To purify VACV EV and IMV, virus cultures were separated on CsCl gradients. CsCl gradients were prepared with premixed solutions of densities 1.20, 1.25 and 1.30 g/ml, and virus purified through these gradients for approximately 18 hours at 28,000 rpm (Beckman L8-70M, USA), at 15 °C. For quantification of EV and IMV, each gradient was collected into a 96-well tissue culture plate by mechanical fractionation either from the top of the gradient under the control of a syringe drive (5 ml/minute) or from the bottom of the tube under the control of a peristaltic pump.

2.5.3 Quantification of Virus by Plaque Titration

The Reed-Muench limiting dilution method used in this study calculates the 50 % tissue culture infectious dose per ml ($TCID_{50}$/ml) (330). The number of virus positive wells in a titration plate was input to a spreadsheet (courtesy of Dr D.O. Ulaeto) to calculate the $TCID_{50}$/ml. The following calculation was used:

Where the proportionate distance (pd) is calculated (always a negative value) and the dilution interval is 1/3:

$$-pd = -\left[\frac{(\%\text{ well infected at dilution next above 50\%}) - 50\%}{(\%\text{ wells infected at dilution next above 50\% -}\ (\%\text{ wells infected at dilution next below 50\%})}\right] \times \log \text{ dilution interval}$$

$\log TCID_{50}$ = log dilution next to and above 50 % positives + (-pd)

$TCID_{50} = 10^{(\log TCID_{50})}$

$TCID_{50}/ml = (1/TCID_{50}) \times (1/\text{volume plated per well})$

The resulting $TCID_{50}$/ml can be used to estimate the number of plaque forming units per ml (pfu/ml) in a sample by applying the Poisson distribution. Where P(0) is the proportion of virus negative samples and *m* is the mean number of infectious units per unit volume (pfu/ml), therefore P(0) = e(-*m*). For any titre expressed as a $TCID_{50}$, P(0) = 0.5. Thus e(-m) = 0.5 and *m* = -ln 0.5 which is ~ 0.7 (courtesy of ATCC). Therefore, in this study the conversion of $TCID_{50}$/ml into pfu/ml is achieved by a simple multiplication of 0.7. This has been validated for VACV by direct comparison of $TCID_{50}$ titres with standard pfu titres (Dr. D.O. Ulaeto, personal communication).

Cells were seeded at a density of 5×10^4 per ml, in 100 µl volumes per well in a 96-well tissue culture plate and incubated overnight at 37 °C in a humidified 5 % (v/v) CO_2 atmosphere. Virus was diluted as appropriate in tissue culture medium prior to transferring 100 µl into each well of the first column of a 96-well tissue culture plate containing 200 µl tissue culture medium. Virus was diluted across the plate 1:3 to give a total of 8 wells per dilution. Fifty microlitres of each well was plated onto the corresponding wells of the 96-well tissue culture plate seeded with cells. Alternatively when large numbers of samples were to be quantified, a

variation of this method was used. Briefly, up to 300 µl of sample was transferred to one well of the first column of a 96-well tissue culture plate. This was diluted across the plate 1:3 by transferring 95 µl of sample into wells pre-loaded with 190 µl tissue culture medium. This would allow up to 8 samples to be diluted across a plate in parallel. Using a multi-stepper pipette, 15 µl of each dilution was plated per well down a column of a 96-well plate seeded with cells. In some cases, cultures were supplemented with selective agents to allow growth of recombinant virus, or in the presence of rabbit IMV-neutralising antibodies (1:800 dilution of neat sera) to quantify EEV in culture supernates. Plates were incubated for 5-7 days at 37 °C and 5 % (v/v) CO_2 then fixed with formaldehyde (final concentration 1 % v/v) or 75 % (v/v) ethanol. Monolayers were stained with crystal violet (1 % w/v) in 30 % or 75 % ethanol and excess crystal violet rinsed off with tap water. The number of growth positive wells was determined visually and the $TCID_{50}$/ml calculated.

To estimate the number of infectious units present in CsCl gradient fractions, a modified plaque titration method was used. Briefly, samples were diluted 1:100 in tissue culture medium. Then, 60 µl was transferred in triplicate to the first well of a column of a 96-well tissue culture plate containing 240 µl tissue culture medium per well. Samples were diluted 1:5 down the plate by transferring 60 µl to the next row. This allowed the dilution of 4 samples in parallel per plate. Fifty microlitres of each dilution was transferred to the corresponding well of a 96-well plate seeded with RK13 cells. Plates were incubated for 7 days then fixed and stained as described previously. To calculate the virus titre, the mean absorbance at 570 nm was calculated using a Titretek Multiskan Plus spectrophotometer and

Ascent software 2.4.2 (Thermolab systems, UK). The presence of virus in each sample was indicated by a low absorbance reading and the absence of virus by a high absorbance. When the absorbance was plotted versus the dilution factor, the dilution at which 50 % of the wells were infected was determined using the regression analysis function in Microsoft Excel®. The reciprocal of this dilution allowed conversion to a virus titre, 50 $\%_{max}$.

2.5.4 Quantification of Virus by Metabolic Labelling

As an alternative method to quantify virions, in particular particles separated through a CsCl gradient, viruses were cultured in the presence of tritiated thymidine (^{3}H thymidine) to metabolically label viral genomes, which can thus be quantitated using a scintillation counter.

BSC40 or RK13 cells were seeded at a density of 5 x 10^4 cells per well in a 24-well tissue culture plate and incubated overnight at 37 °C in a humidified 5 % (v/v) CO_2 atmosphere. Cells were infected at MOI 10 as described in section 2.5.1 and culture medium supplemented with 10 µCi ^{3}H thymidine (Amersham) and returned to incubation at 37 °C in a humidified 5 % (v/v) CO_2 atmosphere. Virus replication was halted by freezing at -80 °C and virus liberated from the cells by freeze-thaw (x1 cycle) followed by dounce homogenisation with a steel homogeniser (x10 passes). Cultures were clarified by centrifugation at 13,000 rpm for 30 seconds or 2,100 rpm for 5 minutes. The supernates were layered onto CsCl gradients as described in section 2.5.2, and fractions collected from the bottom of the tube into a 96-well tissue culture plate. Virus was inactivated with formaldehyde

(final concentration 1 % v/v) for 1 hour. In some cases, the density of each fraction was determined by weighing 100 µl on a fine balance (HR-120, A and D Instruments). Virus particles were captured onto 96-well glass fibre GF/C Unifilter microplates (Perkin Elmer) using a Packard Filtermate 196 cell harvester (Perkin Elmer) and left to dry at room temperature overnight. When dry, 20 µl of MicroScint O scintillation fluid (Perkin Elmer) was applied to each well and plates were subjected to counting on a TopCount liquid scintillation counter (Perkin Elmer).

2.5.5 Extraction of Viral DNA

Viruses were cultured in the appropriate cell line with or without selective agents for a minimum of 18 hours at 37 °C in a humidified 5 % (v/v) CO_2 atmosphere. Virus-containing cells were scraped from the bottom of the tissue culture flask or plate and 500 µl of the crude suspension transferred to a screw-capped Eppendorf tube. The sample was subjected to freeze-thaw (x3 cycles) to liberate intracellular virus, and cell debris removed by centrifugation at 2,100 rpm for 5 minutes. The supernate was transferred to a clean tube and 100 µl of lysis buffer (50 mM Tris-HCl, 10 mM EDTA, 1 % (v/v) SDS, 10 µg Proteinase K) added. Samples were heated at 80 °C for 1 hour. DNA was extracted by adding an equal volume of phenol:chloroform:isoamyl alcohol (25:24:1) (Sigma-Aldrich). After mixing, the sample was centrifuged at 13,000 rpm for 10 minutes. The DNA-containing top layer of the sample was transferred to a clean tube and the extraction repeated, twice. DNA was precipitated in 0.1 volume of ice-cold 100 % ethanol and incubated for 1 hour at -80 °C or overnight at -20 °C, and then pelleted

by centrifugation at 13,000 rpm for 30 minutes. The DNA pellet was washed with 200 µl 70 % (v/v) ice-cold ethanol and allowed to air dry. The pellet was resuspended in up to 1 ml nuclease-free H_2O and stored in 100 µl aliquots at -20 °C.

Alternatively, the QIAamp DNA blood mini kit (Qiagen) was used to purify viral DNA from the sample according to the manufacturer's instructions for purification from blood and body fluids. The kit allows the purification of multiple DNA samples of up to 50 kb and removes PCR inhibitors such a divalent cations and proteins, using the same principles as the QIAprep spin kit and QIAquick DNA extraction kit (Qiagen). To lyse cells, 20 µl Triton X-100 (Sigma-Aldrich) was added and cultures incubated for 10 minutes at 37 °C. Each sample was pre-digested with 1 mg DNase-free RNase A (Sigma-Aldrich) for 10 minutes at 37 °C to prevent co-purification of RNA. To lyse viral particles, 2 µg of Proteinase K (Sigma-Aldrich) and 500 µl of buffer AL were added and the samples were heated at 80 °C for a minimum of 10 minutes. To bind the DNA to the silica-gel column, 525 µl of 100 % ethanol was added and the solutions run through the QIAamp column at 8,000 rpm for 1 minute. The columns were sequentially washed twice with 500 µl of buffer AW1 and AW2 by centrifugation at 8,000 rpm. Residual buffer was removed from the column by centrifugation at 13,000 rpm for 3 minutes. To elute the DNA, 200 µl of nuclease-free H_2O pre-heated to 70 °C was added to each column and incubated for 5 minutes to increase efficiency of the elution. The columns were centrifuged at 13,000 rpm for 1 minute and the DNA collected in a microcentrifuge tube. DNA was stored at -20 °C until use.

2.5.6 Inhibition of EEV Production in Recombinant VACV Cultures

RK13 cells were seeded at approximately 5 x 10^4 cells per well in 24-well tissue culture plates and incubated overnight at 37 °C in a humidified 5 % (v/v) CO_2 atmosphere. Cells were infected at MOI 10 with the appropriate virus and incubated for 30 minutes to allow virus adsorption. The inoculum was removed and the cells rinsed with 1 ml PBS and the medium replaced with 0.5 ml tissue culture medium. For BFA experiments, a concentration of 4 µg/ml BFA (Sigma-Aldrich) was used and the medium was supplemented with 10 mM HEPES buffer (Sigma-Aldrich) to prevent changes in the pH that may affect the activity of BFA (331). Cultures were incubated for various times p.i. after which the culture supernate was removed and the cells rinsed twice with 1 ml PBS. Fresh tissue culture medium was applied to each culture with or without BFA (4 µg/ml) as appropriate and cultures incubated further to allow recovery of EEV. Cultures were sampled repeatedly over time by removing the culture supernate and replacing with fresh tissue culture medium. To quantify the amounts of secreted virus in each culture, the $TCID_{50}$/ml was obtained for each sample using the Reed-Muench limiting dilution method as described in section 2.5.3.

2.5.7 Effect of Antimicrobial Peptides (AMPs) on VACV Particles

EEV was prepared fresh for each experiment to avoid damage to the lipid envelope by the freeze-thaw process. Briefly, RK13 cells were seeded at a density of approximately 5 x 10^4 cells per well of a 24-well tissue culture plate and incubated for a minimum of 6 hours at 37 °C in 5 % (v/v) CO_2. Cells were infected

at an approximate MOI 10 of VACV IHD-J and cultures rocked slowly for 30 minutes. The inoculum was removed and the cells rinsed with 1 ml PBS. To each well, 0.5 ml tissue culture medium was added supplemented with 10 µCi ^{3}H thymidine as appropriate. Cultures were incubated for 15-20 hours at 37 °C in a humidified 5 % (v/v) CO_2 atmosphere. The EEV-enriched culture supernate was harvested from each culture and clarified by centrifugation at 2,100 rpm for 5 minutes to remove cellular debris.

IMV was prepared in RK13 cells as described above in tissue culture medium supplemented with 10 µCi ^{3}H thymidine. Cultures were incubated for 24 hours at 37 °C in 5 % (v/v) CO_2. To isolate IMV, the EEV-enriched culture supernate was discarded and the cells rinsed twice with 1 ml PBS. To remove CEV attached to the cell surface, cells were treated with 1 ml TE for 45 minutes at 37 °C in a humidified 5 % (v/v) CO_2 atmosphere. Cells were washed twice with 1 ml tissue culture medium with 10 % (v/v) FCS to inactivate the trypsin and collected by centrifugation at 2,100 rpm for 5 minutes to remove CEV. The pelleted cells were resuspended in 0.5 ml tissue culture medium and subjected to 2x freeze-thaw cycles to liberate IMV. IMV-enriched cultures were clarified by centrifugation at 2,100 rpm for 5 minutes and diluted to 600 µl with tissue culture medium. Cultures were freshly prepared for each experiment however the remainder was stored at -20 °C or -80 °C for future use if necessary.

The effect of AMPs on EEV and IMV was examined by incubating 45 µl of EEV- or IMV-enriched culture prepared as described above. To each culture, 5 µl of LL-37 (final 100 µg/ml), Magainin II (final 100 µg/ml) or Tween-20 (final 0.5 %

(v/v)) was added and vortexed briefly. Cultures were incubated for 1.5 and 3 hours at 37 °C.

Experiments consisted of three replicates allowing for the quantitation of one sample by Reed-Muench limiting dilution analysis as described in section 2.5.3. For EEV-enriched cultures, samples were treated with 1:100 dilution of rabbit IMV-neutralising antibody (courtesy of Dr D.O. Ulaeto and Dr A. Gates) for 15 minutes at room temperature prior to titration on RK13 cells, to give a final dilution of 1:800 of neutralising antibody. The remaining two replicates were subjected to ultracentrifugation at 28,000 rpm through CsCl gradients as described in sections 2.5.2 and 2.5.4 to separate virus particles by buoyant density. Gradients were fractionated and 100 µl of each fraction weighed prior to filtration onto glass fibre filter plates and scintillation counting.

2.5.8 Preparation of Virus for Transmission Electron Microscopy (TEM)

RK13 cells in a 24-well tissue culture plate were infected at MOI 10 with VACV and incubated for 24 hours at 37 °C in a humidified 5 % (v/v) CO_2 atmosphere. The culture supernate was removed and the cells rinsed twice, with 1 ml ice-cold PBS. The cells were scraped into 0.5 ml of 0.1 M cacodylate buffer and transferred to a screw-capped Eppendorf tube. Infected cells were collected by centrifugation at 2,100 rpm for 5 minutes, resuspended in 500 µl Karnovski fixative (2 % paraformaldehyde, 3 % glutaraldehyde in 0.1 M cacodylate buffer) and incubated for a minimum of 18 hours at 4 °C. Fixed cells were collected by centrifugation at 13,000 rpm for 30 seconds and post-fixed with osmium tetroxide

(2 % v/v) in 0.1 M cacodylate buffer for 1-2 hours. Cells were washed in 0.1 M cacodylate buffer, then 70 % (v/v) ethanol and collected by centrifugation at 13,000 rpm for 30 seconds. Samples were dehydrated in a graded ethanol series (30 minutes per wash) of 70 %, 90 % and 95 % concluding with 3 final washes of 100 % (v/v) ethanol for 30 minutes. After the final 100 % wash, cells were collected by centrifugation at 13,000 rpm for 30 seconds. Samples were infiltrated with LR White Resin (Agar Scientific, UK) and the resin polymerised by baking at 60 °C for 18 hours in a gelatin capsule. Ultrathin (gold) sections were cut using a diamond knife on a LKB Ultramicrotome and sections were collected onto copper grids. Sections were stained with 2 % aqueous uranyl acetate (w/v) and 1 % lead citrate (w/v) for 20 and 5 minutes, respectively. Samples were viewed using a Philips CM12 TEM operating at 80kV. Images were acquired using a SIS Keenview 1 mega-pixel digital camera and were adjusted for brightness and contrast only.

2.6. Generation of Recombinant VACV

2.6.1 Selection of Recombinant VACV

Following transfection and subsequent infection of cells with VACV, progeny recombinant VACV was selected using the appropriate selective medium. For recombinant viruses engineered with the *E. coli* guanine phosphoribosyl transferase (*Eco*GPT) gene for resistance to mycophenolic acid, recombinant viruses were grown in RK13 or BSC40 cells with mycophenolic acid (25 µg/ml) added to the tissue culture medium, supplemented with xanthine (250 µg/ml) and hypoxanthine (15 µg/ml). For reverse selection of *Eco*GPT recombinant viruses, non-*Eco*GPT expressing viruses were selected in STO cells in the presence of 0.1

mM 6-thioguanine (6-TG) (Sigma-Aldrich). Recombinant viruses engineered to contain the $G418^R$ gene for resistance to Geneticin®, were cultured in RK13 or BSC40 cells in the presence of 2 mg/ml Geneticin® (Invitrogen Ltd.)

All viruses were cultured for a minimum of 5 rounds of selection to enrich for recombinant virus and minimise the numbers of parental VACV prior to plaque purification.

2.6.2 Plaque Purification of Recombinant VACV

To isolate recombinant VACV such that a clonal population was achieved, virus was plaque purified either by limiting dilution or by plaque picking using agarose overlay. Using the agarose overlay method, BSC40 cells were seeded into 6-well tissue culture plates at a density of 5×10^4 cells per ml in a volume of 5 ml, and incubated overnight at 37 °C in a humidified 5 % (v/v) CO_2 atmosphere. Putative recombinant virus was dounce homogenised using a steel homogeniser and briefly treated in a sonicating water bath to disaggregate virus particles, prior to dilution to low MOI (approximately 10 pfu/well). Cells were infected in 500 µl of tissue culture medium and slowly rocked for 1 hour, before the inoculum was removed and replaced with 2 ml of low melting point agarose (final w/v 1 %) dissolved in DMEM supplemented with 2 mM L-glutamine plus 10 % FCS containing the appropriate selective agent and maintained molten at 37 °C until use. Once poured onto the cells, the agarose was allowed to set at room temperature before incubating for 24-72 hours at 37 °C in a humidified 5 % (v/v)

CO_2 atmosphere. Plaques were picked using a 1000 µl pipette tip and resuspended in 200 µl PBS. This process was generally repeated at least 3 times in succession.

Plaque purification by limiting dilution uses the Poisson distribution to calculate the number of growth positive wells that should ensure no more than 1 pfu per well. For this method, a 96-well tissue culture plate was seeded with RK13 cells at a density of 5 x 10^4 cells per ml in 100 µl volumes per well and incubated overnight at 37 °C in a humidified 5 % (v/v) CO_2 atmosphere. Putative recombinant virus was dounce homogenised using a steel homogeniser and briefly treated in a sonicating water bath to disaggregate virus particles. Where the $TCID_{50}$/ml had been calculated, virus was diluted in 5 ml tissue culture medium to give 0.3 and 3 $TCID_{50}$ per well, which should result in ~30 % and ~100 % virus positive wells per plate, respectively, according to the Poisson distribution. Fifty microlitres of each dilution was added to each well of RK13 cells and incubated for 5-7 days at 37 °C in a humidified 5 % (v/v) CO_2 atmosphere. At each round of purification, the numbers of growth positive wells were monitored where no more than 30 virus positive wells indicated that less than 1 pfu was present per well. Where the $TCID_{50}$/ml has not been calculated, virus was repeatedly diluted 3-fold into 1400 µl tissue culture medium and 100 µl of each dilution plated per well across a row of a 96-well tissue culture plate of RK13 cells. Plates were incubated for 5-7 days at 37 °C in a humidified 5 % (v/v) CO_2 atmosphere. Using the Poisson distribution, 3 or less virus positive wells in a row indicates that the virus-positive wells in that row are likely to have arisen from no more than 1 pfu and the wells from this row were harvested for the next round of plaque purification. Plaque purification by limiting

dilution was repeated for a minimum of 3 rounds. In some cases, a combination of agarose overlay and limiting dilution was used to plaque purify recombinant VACVs so as to utilise the advantages of both methods.

2.7 Reverse Transcription Polymerase Chain Reaction (RT-PCR)

The TaqMan® Gene Expression Assay contains forward and reverse sequence-specific primers and a dual-labelled probe that is specific to an internal region of the target sequence. This probe is labelled with a reporter fluorophore at the 5'- end and a quencher fluorophore at the 3'- end. During the amplification reaction, the probe anneals to the target sequence. In this state, the reporter and quencher fluorophore are in close proximity and the fluorescence intensity of the reaction is low. As the polymerase carries out extension of the forward and reverse primers and replicates the template to which the probe is bound, the 5'-exonuclease activity of the polymerase cleaves the probe. This releases the reporter away from the quencher and as a result the fluorescence intensity increases. Therefore, the increasing fluorescence correlates with the accumulation of PCR product in each cycle.

2.7.1 Isolation of Messenger Ribonucleic Acid (mRNA) from Virus Cultures

Viruses were cultured in RK13 cells at MOI 10 as described in section 2.5.1 and incubated until various times p.i. The RNAqueous® kit (Ambion) was used for RNA extraction. The kit uses phenol-free, filter based technology to rapidly isolate RNA from tissues. Briefly, cells are disrupted using a high concentration

guanidinium salt solution that also inactivates endogenous RNases (332). The sample is then passed through a glass fibre filter that binds the RNA and allows cellular components to run through (328;333;334). The RNA is washed several times before elution in a low ionic strength solution.

At the appropriate time p.i., the culture supernate was removed and 700 µl of lysis buffer was added to each well. Cells were gently pipetted up and down to lyse infected cells and liberate RNAs. Samples were transferred to nuclease-free tubes and stored at -80 °C until processing. To extract RNA, 700 µl of 64 % ethanol was added and each sample was gently mixed by inversion. The lysate was applied to a spin-filter column and was then centrifuged at 13,000 rpm for 1 minute. The filtrate was discarded and the filter was washed with 700 µl wash solution #1 containing guanidinium salt solution to denature residual RNases. The filtrate was discarded and the column was washed twice with 500 µl of wash solution #2/3. The filtrate was discarded and the filter dried by centrifugation at 13,000 rpm for 1 minute. The filter was transferred to a fresh nuclease-free tube and the RNA eluted by centrifugation at 13,000 rpm for 30 seconds in 40 µl nuclease-free H_2O (Ambion) pre-heated to 70 °C. To maximise RNA recovery, a second elution step of 10 µl pre-heated nuclease-free H_2O was included. Extracted RNA was stored at -80 °C.

2.7.2 Removal of Genomic DNA from Extracted RNA

Prior to reverse transcription of mRNA to complementary DNA, (cDNA) contaminating genomic DNA (gDNA) was degraded using DNA-*free* TURBO

DNase™ (Ambion); this removes trace amounts of genomic DNA in RNA samples more efficiently than wild-type DNase I. Removal of the TURBO DNase™ uses an Inactivation Reagent therefore avoiding organic extraction or heating that may result in degradation of RNA or interfere with downstream reactions. Briefly, 5 µl reaction buffer (10x) and 1 µl TURBO DNase™ was added to a 50 µl sample. This was mixed gently and incubated for up to 30 minutes at 37 °C. To inactivate the nuclease, 5 µl Inactivation Reagent was added and incubated for 2 minutes at room temperature with occasional mixing. The sample was then centrifuged at 13,000 rpm for 1.5 minutes and the RNA-containing supernate transferred to a fresh nuclease-free tube.

2.7.3 Quantification of RNA

RNA was quantified using a NanoDrop® ND-1000 spectrophotometer (ThermoScientific). Briefly, 1.5 µl was applied to the NanoDrop electrode and the UV absorbance at 260 nm (A_{260}) and 280 nm (A_{280}) was recorded. The concentration of single-stranded RNA was calculated in µg/ml by:

$$A_{260} \text{ x dilution factor x } 40 = \mu g \text{ RNA/ml}$$

To determine the purity of each sample the ratio of A_{260}:A_{280} was calculated, where a value outside the range of 1.8 to 2.1 was indicative of protein contamination.

2.7.4 One-step Real-Time PCR

For gene expression analysis, TaqMan® RNA-to-C_t 1-*Step* kit (Applied Biosystems, UK) was used. This kit allows the addition of RNA directly to the reaction where reverse transcription and real-time PCR are performed in one tube. A hot-start enzyme is included to prevent priming during reaction set up, an RNase inhibitor to prevent degradation of RNA template and the formula of enzymes provide high levels of sensitivity and quantitative discrimination (Applied Biosystems, UK). Typically reactions were performed in 20 µl volumes of 0.5 µl TaqMan® RT-Enzyme Mix (40x), 10 µl TaqMan® RT-PCR Mix (2x), 1 µl TaqMan® Gene Expression Assay (20x) and 8.5 µl template (~100 ng) in nuclease-free water (Ambion), using Applied Biosystems 7000 Real-Time PCR System. Reactions were dispensed into MicroAmp™ Optical 96-well reaction plates (Applied Biosystems) and the plate sealed with adhesive film. The cycling conditions used were 48 °C for 15 minutes; 95 °C for 10 minutes; followed by 40 cycles of 95 °C for 15 seconds then 60 °C for 1 minute. At the end of the run, the cycle threshold (Ct) was determined for each gene using the ABI 7000 sequence detection system software (Applied Biosystems).

To determine the fold change, the delta delta cycle threshold (ΔΔCt) method of Livak and Schmittgen was used (335). For each sample, the average Ct value of triplicate wells was calculated. This was normalised using the 18s ribosomal RNA (rRNA) endogenous control gene to give the ΔCt (average Ct target gene - average Ct endogenous control). All ΔCt values throughout the infectious cycle were compared to the ΔCt value at t=0 for each gene tested to give the ΔΔCt (ΔCt target

gene - ΔCt at t=0). The fold change was calculated as $2^{-\Delta\Delta Ct}$. This analysis was performed for the A26L, A27L and F13L genes at several time points.

2.8 Protein Techniques

2.8.1 SDS-PAGE

Viral proteins were separated by polyacrylamide gel electrophoresis (PAGE) on Novex® 10 % Tricine gels (Invitrogen Ltd.) using an Xcell *SureLock*® Mini-Cell apparatus (Invitrogen Ltd.) according to the manufacturer's instructions. Briefly, 8 µl of purified virus (~10^7 pfu) was heated to 80 °C with 2 µl NuPage® Reducing agent and 10 µl Novex® Tricine SDS running buffer, all from Invitrogen Ltd. Samples were loaded onto the gel and separated for up to 1.5 hours at 125 volts in Tricine running buffer (Invitrogen Ltd). Gels were stained using SimpyBlue™ SafeStain (Invitrogen Ltd.) for 1 hour with agitation and washed three times in distilled H_2O for up to 3 hours. Where required protein bands were excised from the gel with a sterile scalpel and stored at 4 °C until use.

2.8.2 Western blot Analysis

Protein from the SDS-PAGE gel was transferred to a nitrocellulose membrane by electroblotting using an XCell II® blot module at 25 volts for 2 hours in TrisGlycine transfer buffer plus 20 % methanol (all Invitrogen Ltd). All membranes, filter sponges and filter papers were pre-soaked in transfer buffer and, once assembled, air bubbles were removed from the transfer stack. After electroblotting, the membrane was incubated overnight at 4 °C in 5 % (w/v)

skimmed milk powder in PBS (SMP). The membrane was washed three times in PBS, and incubated with a primary antibody probe diluted in SMP with 0.1 % Tween-20 as appropriate for 2 hours at room temperature with agitation. The membrane was washed three times in PBS and incubated with a secondary antibody conjugated to Horseradish peroxidise (HRP) (goat anti-mouse or goat anti-rabbit) (BioRad) diluted 1:1000 in SMP with 0.1 % Tween-20 for 1 hour. The membrane was washed three times and developed using 3,3'-diaminobenzidine tetrahydrochloride (DAB) (Sigma-Aldrich) according to the manufacturer's instructions. Alternatively, for increased sensitivity, enhanced chemiluminescence (ECL) Western blotting detection reagents (Amersham Biosciences) were mixed at a ratio of 1:1 and applied to the membrane for 1 minute. An X-ray film was placed on the blot in the dark for ~1 minute and the film developed with Kodak solutions (Sigma-Aldrich).

2.9 Statistical Analyses

Statistical analyses were performed in consultation with Dr D.O. Ulaeto and Dr T. Laws using either Microsoft Excel® or GraphPad Prism version 5.0 (GraphPad software). One-phase exponential non-linear regression analyses using the F-test statistic and/or two-way ANOVA with Bonferroni's post tests were performed on one-step growth curve data. Repeated measures one-way ANOVA test was used to analyse the proportion of IMV produced in cultures. One-way ANOVA tests were used to analyse the recovery of EEV in BFA-treated cultures

and antimicrobial peptide experiments. Two-way ANOVA tests with Bonferroni's post tests were used to analyse quantitative RT-PCR data.

3 Construction of an A26L Gene Deletion Mutant Vaccinia Virus

3.1 Introduction

OPVs produce two types of mature virion: enveloped virus (EV) and intracellular mature virus (IMV). They are both fully infectious, yet differ in their structure and site of accumulation (222;336;337). EV is produced first in the replicative cycle (116) and is thought to be involved in dissemination of virus throughout the infected host to establish disease (120;338). The additional membrane serves to protect the virion from neutralisation by antibody and evade complement (247;339;340). IMV is produced later (116), presumably by default as a result of exhaustion of intracellular membranes, and as the more robust particle it is assumed to be involved in host-to-host spread. IMV is released from the cytoplasm upon cell lysis, and represents the majority of progeny virions. It is generally accepted that IMVs are pre-cursors of EVs, and may be an artefact produced in tissue culture systems, in which intracellular membranes are limiting compared to *in vivo* environments.

The A26 and A25 proteins have been identified as unique to the surface of IMV (116). A26 is thought to be the same protein described as 4c by Sarov and Joklik (341), and has been reported to have more than one role (15;134;188). These include A26 as a component of surface microtubules (15;236), acting on cell attachment by binding IMV to cell surface laminin (134), suppression of GAG-mediated cell fusion (342) and trafficking of IMVs to ATIs (188). Occlusion of virions occurs in some poxviruses such as CPXV, FPXV and ECTV, where both full-length ATI protein and A26 protein are produced, enabling virus particles to

become embedded in inclusion bodies. Interestingly, a portion of the A26L gene is conserved in some viruses that produce a full-length ATI protein, but these viruses are occlusion negative, suggesting additional roles for A26 may exist.

Studies by Ulaeto *et al.* identified A26 (4c) as unique to the surface of IMV and reported that synthesis of A26 occurred at late times during the infectious cycle concurrent with maturation of IMV (116). It has been speculated that A26 acts as a differentiation switch, resulting in maturation of particles to IMV instead of EV. This suggests that IMV may not be a pre-cursor of EV, and poxviruses have evolved mechanisms to control EV and IMV maturation enabling them to undertake their assumed roles in the poxvirus life-cycle.

3.1.1 Aims of this study

In order to examine the function of A26 in OPVs, an A26L gene deletion mutant was generated in VACV IHD-J. The intention was to use this particular strain of virus for its ability to produce elevated amounts of EEV in tissue culture (120;181), which would be useful in future experiments where a reduction in EEV may be assessed. It was anticipated that analysis of the production of the different particles produced *in vitro* would help to determine the function of this protein, in the event that deletion of A26L prevents maturation of particles as IMV.

3.2 Results

3.2.1 Design of the A26L Gene Deletion Cassette

The A26L gene is flanked upstream by A27L (also a late gene) which has been shown to play a role in virus penetration, cell fusion and envelopment of virions (170;343-346). The A25L gene (ATI gene) flanks A26L downstream, is truncated in VACV and is apparently non-functional. It was necessary to ensure the promoter and coding sequences of these genes were not disrupted as a result of genetic manipulation.

The VACV-WR A26L sequence (GenBank accession number YP_233031) was used to design the recombination cassette in this study as the genome sequence of the IHD-J strain was not available. To generate an A26L mutant, 1320 bp out of the predicted 1503 bp sequence of A26L was deleted, replacing the deleted region with the *E. coli* xanthine guanine phosphoribosyl-transferase (*Eco*GPT) selection marker gene (GenBank accession number: X00222) (347;348) expressed from a synthetic early/late promoter (327) (Figure 3.1). The *Eco*GPT gene allowed for positive selection in the presence of mycophenolic acid (MPA) to increase the proportion of recombinant virus over the wild-type parent.

3.2.2 Construction of the Deletion Cassette by PCR

Using the primers GPT1, GPT2 and GPT3 (Table 2.1), the coding sequence of the *Eco*GPT gene was amplified by PCR utilising p1107 (326) as template in two stages, adding the appropriate sequences as tails to the 5'- end of each primer.

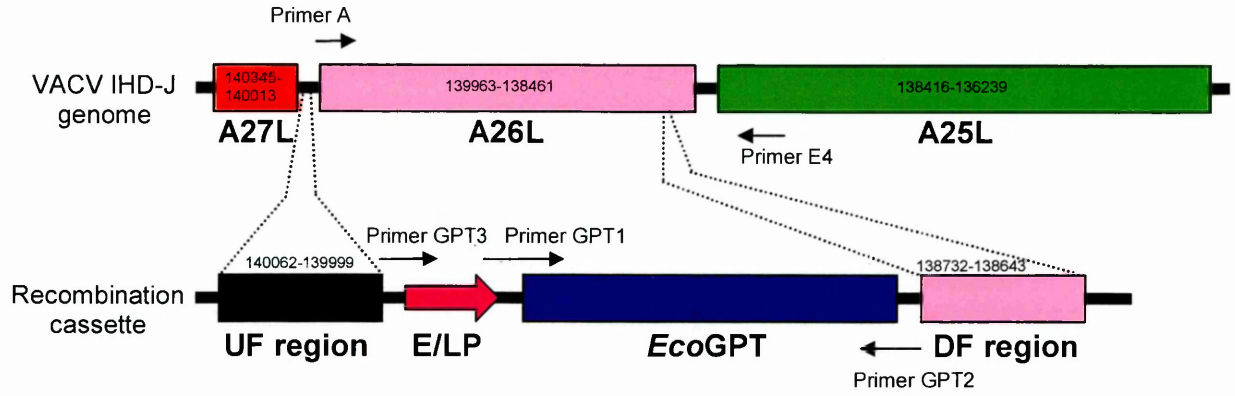

Figure 3.1 Schematic of VACV Recombination Cassette for Deleting the A26L Gene

The construct was synthesised by PCR and cloned into the pCAP^{s} vector, a commercially available vector (Roche Diagnostics Ltd.) as described in section 3.2.3. Positions of primer binding sites used for PCR amplification and screening purposes are indictated.

The first stage amplified the *Eco*GPT gene adding a synthetic early/late promoter (327) upstream of the initiation codon and VACV A26L downstream flanking sequence to the 3'- end. The second stage added VACV A26L upstream flanking sequence to the 5'- end of the early/late promoter sequence.

PCRs were optimised using Opti-Prime™ PCR Optimisation Kit (Stratagene) which contains a selection of buffers with varying $MgCl_2$ and KCl concentrations. PCR amplification of product 1 using buffers #3, #4 and #10 resulted in a product of 603 bp in each reaction. Using buffer #10 (product 1C) appeared to result in a single product whereas buffers #3 (product 1A) and #4 (product 1B) resulted in a secondary product of ~1200 bp (Figure 3.2A). Prior to the second stage PCR, the 603 bp products were extracted from the agarose gel and purified using a QIAquick gel extraction kit (QIAGEN) to remove secondary PCR products and remaining primers, buffers and enzymes from the reaction. This prevented carry over of primer GPT1, which could have resulted in a repeat of reaction 1, preventing the addition of the upstream flank to the final product.

PCR amplification of product 2, using product 1 as template with primers GPT3 and GPT2 with buffers #2, #6, #10 and #12 resulted in a product of 657 bp in most of the reactions (Figure 3.2B). Product 2 was pooled from each reaction using buffers #2 and #12 (lanes 2, 5, 6, 9 and 13) except the reaction using template 1C (lane 10), and purified using a QIAquick gel extraction kit (QIAGEN). The DNA concentration was estimated as 50 ng/µl by comparing the band intensity to that of a known standard on an agarose gel (section 2.3.6).

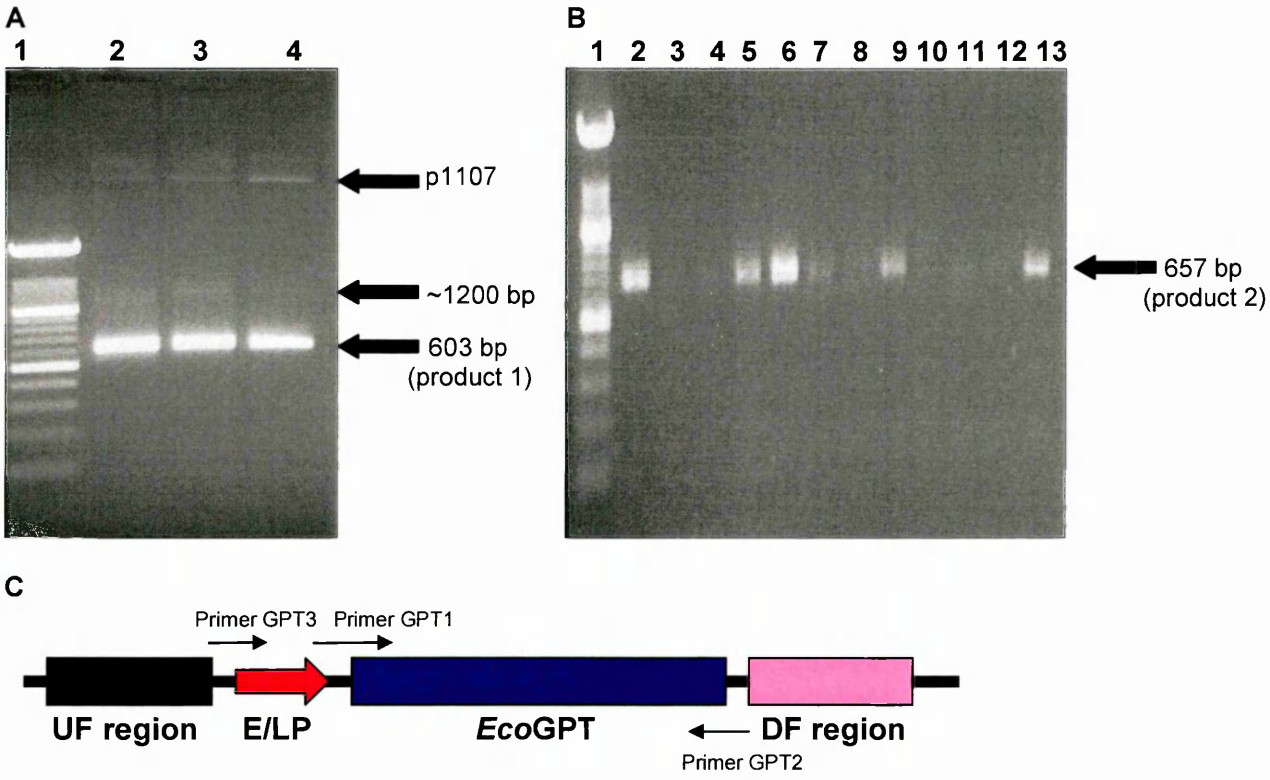

Figure 3.2 PCR Amplification of A26L Gene Deletion Cassette

A Agarose (1 %) gel electrophoresis of PCR products using primers GPT1 and GPT2 with a selection of buffers from the Stratagene Opti-Prime™ PCR optimisation kit. Lane 1 – 100 bp ladder; lane 2 – Stratagene buffer #3 (product 1A); lane 3 – Stratagene buffer #4 (product 1B); lane 4 – Stratagene buffer #10 (product 1C).

B Agarose (1 %) gel electrophoresis of PCR using products 1A, 1B and 1C as templates and primers GPT3 and GPT2 with a selection of buffers from the Stratagene Opti-Prime™ PCR optimisation kit. Lane 1 – 100 bp ladder; lane 2 – Stratagene buffer #2 (product 2A.2); lane 3 – Stratagene buffer #6 (product 2A.6); lane 4 – Stratagene buffer #10 (product 2A.10); lane 5 – Stratagene buffer #12 (product 2A.12); lane 6 – Stratagene buffer #2 (product 2B.2); lane 7 – Stratagene buffer #6 (product 2B.6); lane 8 – Stratagene buffer #10 (product 2B.10); lane 9 – Stratagene buffer #12 (product 2B.12); lane 10 – Stratagene buffer #2 (product 2C.2); lane 11 – Stratagene buffer #6 (product 2C.6); lane 12 – Stratagene buffer #10 (product 2C.10); lane 13 – Stratagene buffer #12 (product 2C.12).

C Schematic of recombination cassette. Arrows indicate primers.

3.2.3 Cloning of the Deletion Cassette into pCAP^{s} Plasmid Vector

The PCR Cloning Kit (Blunt-end) supplied by Roche Diagnostics Ltd. was used to sub-clone purified product 2 so that the recombination cassette could be easily synthesised for future experiments. This cloning kit requires blunt-ended DNA fragments for the ligation reaction, therefore the ends of product 2 were polished to remove 3' overhangs produced by *Taq* polymerase during the PCR reaction as described in section 2.3.5. The DNA fragment was purified using a QIAquick PCR purification kit (QIAGEN) to remove enzymes and buffers, and quantitated by comparing the band intensity to that of a known standard on an agarose gel (section 2.3.6). The concentration for each sample was estimated at 32 ng/µl.

Blunt-ended ligation was carried out as described in section 2.3.7 where the recommended molar ratio of vector:insert is 1:100 to 1:500. The ligation was performed using ratios of 1:100, 1:300 and 1:500 to increase the probability of success. A positive control reaction using the PCR control supplied with the kit and a negative control reaction using H_2O were also performed. Each ligation reaction was transformed into XL-1 Blue chemically competent cells (Stratagene, California) as described in section 2.3.8. Transformants were selected for ampicillin resistance and inactivation of the CAP lethality gene.

To investigate the presence of the recombinant plasmid in transformants, plasmid DNA was isolated using a QIAprep Spin Plasmid Miniprep kit (QIAGEN) as described in section 2.3.9. Presence of pDNA was confirmed on an agarose gel (Figure 3.3A). Transformants 1, 2 and 3 all gave a band of similar mobility,

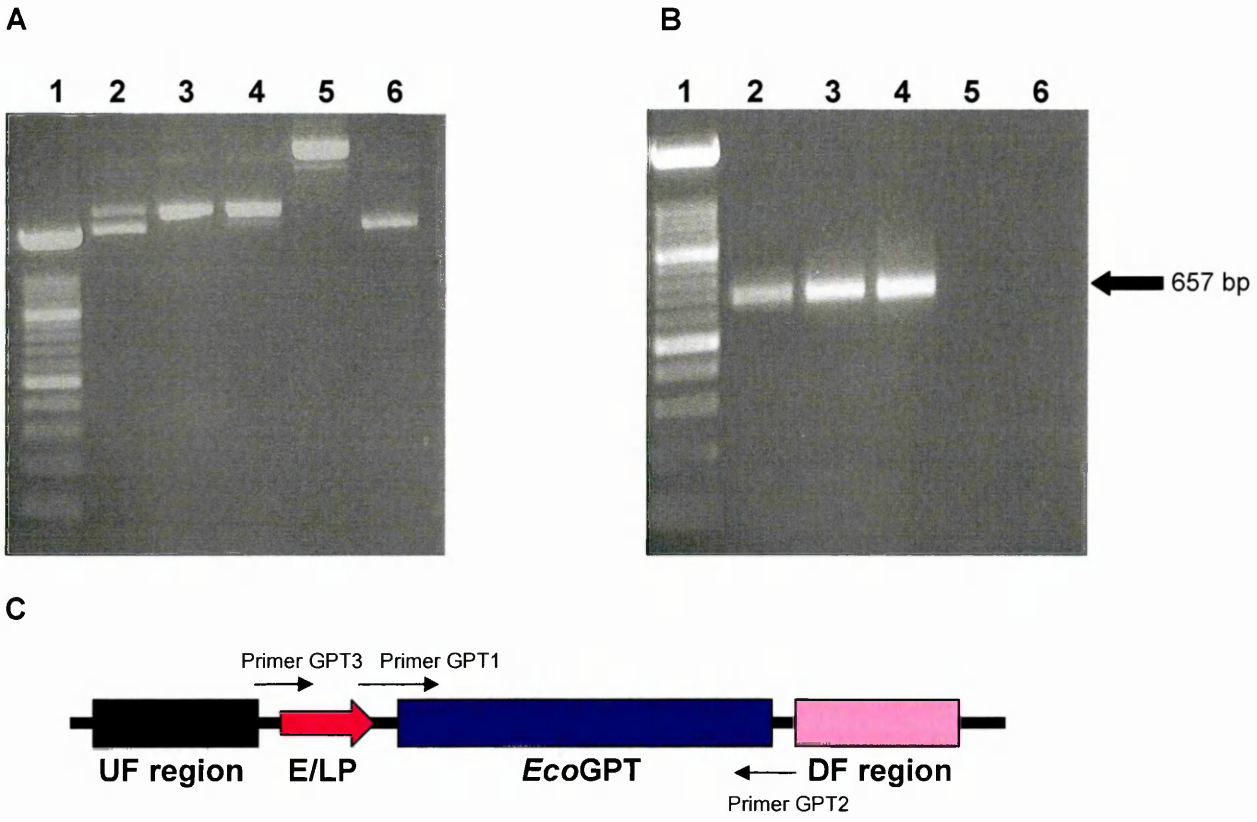

Figure 3.3 Screening for the *Eco*GPT Gene in pCAP^{s} Constructs

A 5 µl of purified plasmid DNA was separated on a 1 % agarose gel. Lane 1 – 100 bp ladder; lane 2 – transformant 1; lane 3 – transformant 2; lane 4 – transformant 3; lane 5 – transformant 4; lane 6 – transformant 5.

B PCR for the *Eco*GPT gene (657 bp) in transformants 1-5 using primers GPT 3 and GPT 2. Lane 1 – 100 bp ladder; lane 2 – transformant 1; lane 3 – transformant 2; lane 4 – transformant 3; lane 5 – transformant 4; lane 6 – transformant 5.

C Schematic of recombination cassette. Arrows indicate primers.

although clone 1 also had a slightly brighter band of apparent lower molecular weight. Transformant 4 also gave a single band of much higher molecular weight than the others, indicating that this transformant may contain multiple copies of the insert, or possibly is a concatemer of 2 or more plasmid molecules. Transformant 5 gave a single band corresponding to the low molecular weight band in transformant 1, suggesting that this band may represent re-ligated plasmid with no insert. This also suggests that transformant 1 may be a mixed "clone", containing both a plasmid with insert and one without.

To screen for the presence of product 2 in the transformants, a PCR was undertaken using primers GPT3 and GPT2 (Figure 3.3B). Transformants 1, 2 and 3 contained an insert of the correct size (657 bp) whereas the insert was not detected by PCR in transformants 4 and 5. Plasmid DNA from transformants 1, 2 and 3 was sent to Lark Technologies, Ltd. for sequencing to check the sequence integrity. The sequencing results demonstrated that pDNA from transformants 1 and 2 had several base substitutions within the *Eco*GPT gene, whereas the sequence from transformant 3 was correct. To obtain a high concentration stock of the deletion cassette, pDNA was isolated from a 250 ml culture of transformant 3 using a QIAGEN plasmid maxi preparation kit (QIAGEN). The presence of the plasmid was confirmed on an agarose gel and the concentration of pDNA estimated at 7.6 µg/µl (Figure 3.4A) as described in section 2.3.6. A PCR using GPT 3 and GPT 2 confirmed the presence of the insert (Figure 3.4B). In addition to this, pDNA was sent to Lark Technologies, Ltd. to re-confirm the sequence integrity.

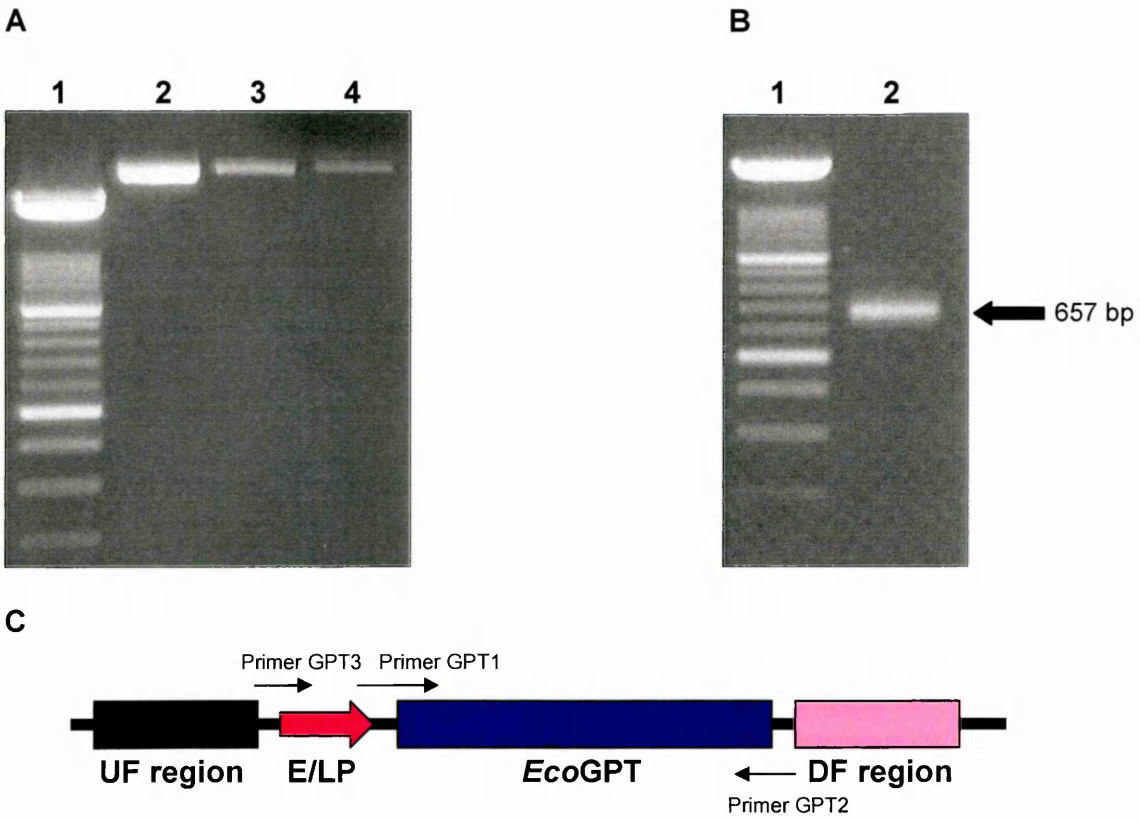

Figure 3.4 Screening for the *Eco*GPT Gene in pCAP^s Construct Transformant 3 from Large Scale Isolation

A Purified transformant 3 plasmid DNA was separated on a 1 % agarose gel. Lane 1 – 100 bp ladder; lane 2 – 1:20 dilution; lane 3 – 1:80 dilution; lane 4 – 1:320 dilution.

B PCR for the *Eco*GPT gene (657 bp) in transformant 3 using primers GPT3 and GPT2. Lane 1 – 100 bp ladder; lane 2 – transformant 3.

C Schematic of recombination cassette. Arrows indicate primers.

3.2.4 Construction of an A26L Deletion VACV by Homologous Recombination

The recombination cassette was introduced into the parental VAVC IHD-J genome via the upstream and downstream flanking regions that are homologous to the upstream and downstream regions of the A26L gene. This allows homologous recombination to take place, where the majority of the coding sequence of A26L was deleted and replaced by *Eco*GPT under the control of a synthetic early/late promoter. The resulting virus was amplified under positive selection conditions described in the next section.

3.2.5 Selection of Recombinant Virus for Mycophenolic Acid (MPA) Resistance

Following transfection of RK13 cells with pDNA from transformant 3, and subsequent infection with VACV IHD-J, newly generated recombinant virus was selected using MPA selective medium supplemented with xanthine and hypoxanthine in RK13 cells (sections 2.4.2 and 2.6.1). MPA inhibits the enzyme inosine monophosphate dehydrogenase preventing the formation of xanthine monophosphate (XMP) and in turn preventing the formation of guanine monophosphate (GMP) (347;348). This results in the intracellular depletion of purine nucleotides and an inhibition of cell growth, therefore inhibiting virus growth. In the presence of MPA, the GPT enzyme utilises the pre-cursors xanthine and hypoxanthine to synthesise purines via the salvage pathway. The mammalian hypoxanthine-guanine phosphoribosyl-transferase (HPRT) enzyme lacks the ability

to utilise xanthine, therefore the salvage pathway, and ultimately progeny recombinant virus, can only be produced in those cells infected with recombinant virus expressing *Eco*GPT.

Transfections were carried out using a range of DNA concentrations (0.2, 0.6, 2, 10 and 25 µg) to try to optimise the DNA:liposome ratios to increase the efficiency of delivering DNA into the cells (section 2.4.2). After 24 hours incubation, progeny virus was harvested and propagated in RK13 cells in MPA selection medium for 72 hours. A large plaque was found in the culture originating from the 10 µg transfection. The putative recombinant virus was serially passaged 7 times in RK13 cells in the selection medium to enrich for recombinant virus and decrease wild-type virus. A small stock of putative recombinant virus from passage 7 was prepared by infecting a T25 tissue culture flask of RK13 cells in selection medium at low MOI, and 1 ml of this culture was used to prepare viral DNA.

3.2.6 Genotypic Analysis of Recombinant Virus

The putative recombinant was able to replicate in the presence of MPA indicating expression of *Eco*GPT, however to confirm the presence of the *Eco*GPT gene and absence of the A26L gene, a PCR was undertaken using extracted viral DNA, using dH_2O as a negative control and either transformant 3 pDNA (for *Eco*GPT) or wild-type viral DNA (for A26L) as positive controls (Figure 3.5). The results demonstrated the presence of *Eco*GPT in the recombinant viral genome indicating a recombinant virus had been generated, however detection of the A26L gene indicated that wild-type virus was also present.

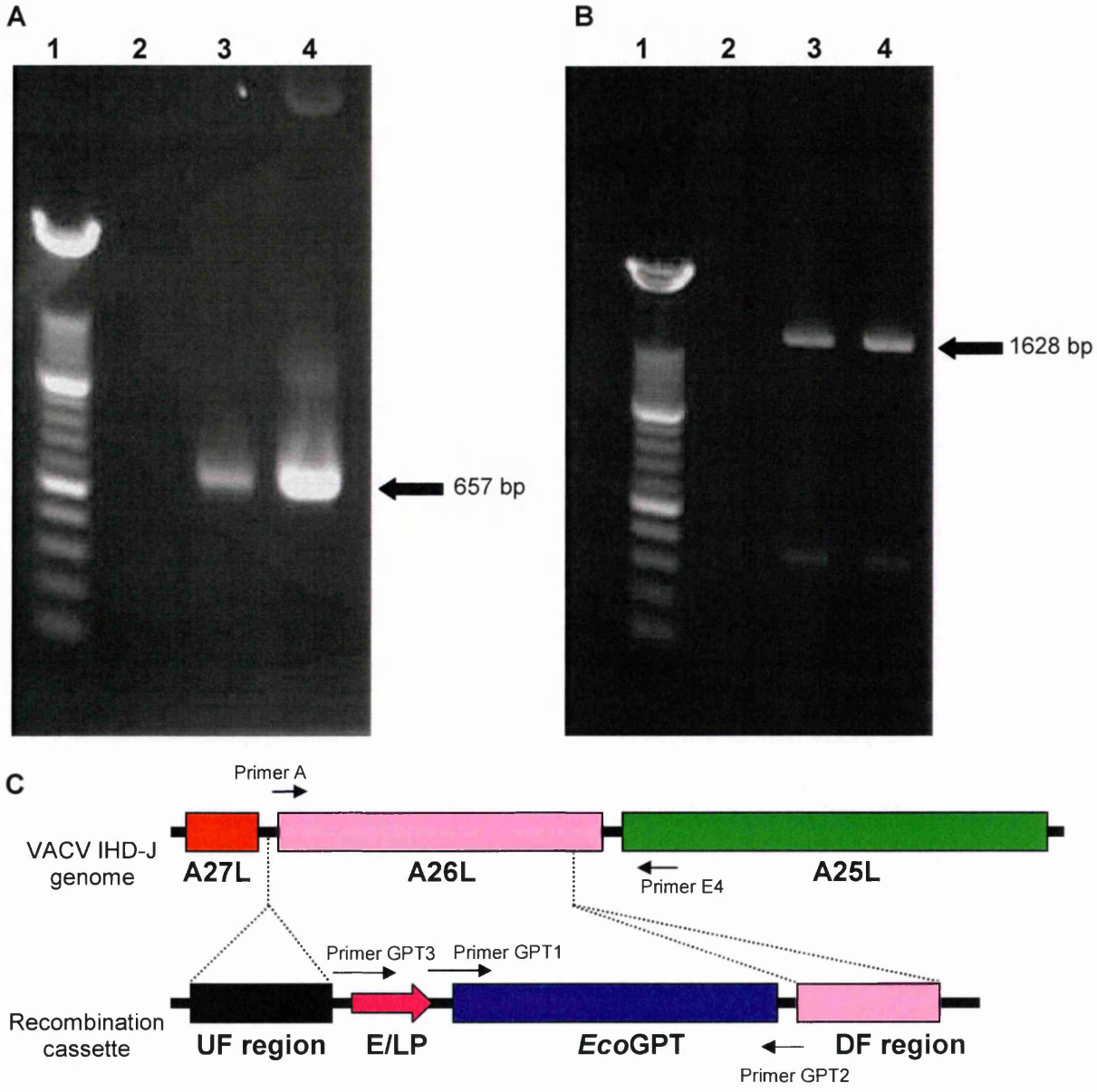

Figure 3.5 Genotypic Analysis of Recombinant Virus Following Serial Passage in Selection Medium

PCRs were performed **A** for the *Eco*GPT gene (657 bp) using primers GPT 3 and GPT 2 and **B** for the A26L gene (1628 bp) using primers A and E4 Lane 1 – 100 bp ladder; lane 2 – negative control; ane 3 – recombinant virus; lane 4 – positive control. **C** Schematic demonstrating primer binding sites.

3.2.7 Plaque Purification of Recombinant Virus

To obtain pure clones, recombinant virus was plaque purified by limiting dilution as described in section 2.4.8. Virus was purified for a total of 5 rounds in the presence of MPA selection medium. At each round, differential titres were obtained in the presence and absence of MPA to monitor residual wild-type virus (Table 3.1). After the first round of purification for both vIδA26L1 and vIδA26L2, the virus titre was reduced by a third and by a half, respectively, in the presence of MPA medium. Both clones were subjected to a second round of purification which resulted in 3 more clones, one of which (vIδA26L1.1) replicated equally well in the presence and absence of MPA, indicating high purity. The other 2 clones (vIδA26L1.2 and vIδA26L2.1) did not replicate well in the presence of MPA and passage of these viruses was discontinued.

Following the third round of purification, vIδA26L1.1.1 was quantitated in RK13 cells in the presence or absence of MPA medium, but also in STO cells in the presence or absence of 6-thioguanine (6-TG) (section 2.6.1). STO cells cultured in medium containing 6-TG are used in negative selection to inhibit the replication of virus expressing the *Eco*GPT gene (349), and are described in more detail in Chapter 4. Lack of replication in these culture conditions, compared to no selection, would indicate high purity of the clone. The titre of vIδA26L1.1.1 in STO cells in the presence of 6-TG was $6.0x10^2$ $TCID_{50}$/ml compared to $2.37x10^4$ $TCID_{50}$/ml with no selection, and $3.9x10^4$ $TCID_{50}$/ml in MPA medium. This is a 2-log reduction under negative selection conditions indicating the majority of the virus is recombinant virus expressing *Eco*GPT. To increase the probability that the clone

	MPA ($TCID_{50}$/ml)	No selection ($TCID_{50}$/ml)	Differential (%)
Round 1			
vIδA26L1	1.69×10^6	2.46×10^6	68.70
vIδA26L2	5.90×10^5	1.06×10^6	55.66
Round 2			
vIδA26L1.1	6.68×10^5	6.45×10^5	103.57
vIδA26L1.2	3.93×10^3	6.30×10^4	6.24
vIδA26L2.1	6.24×10^3	3.53×10^4	17.68
Round 3			
vIδA26L1.1.1	5.51×10^4	7.98×10^4	69.05
Round 4			
vIδA26L1.1.1.1	1.86×10^5	1.65×10^5	112.73
Round 5			
vIδA26L1.1.1.1.1	2.83×10^6	1.27×10^6	222.83
vIδA26L1.1.1.1.2	2.73×10^6	1.82×10^6	150.00

Table 3.1 Differential Titres of Recombinant Virus from Each Round of Plaque Purification

Virus was quantitated by Reed-Muench limiting dilution analysis in RK13 cells in the presence and absence of MPA selection. The differential is the titre in selection medium as a percentage of the titre in non-selective medium.

represented a pure clone of recombinant virus, the plaque purification was repeated. The resulting clone from round 4, vIδA26L1.1.1.1, was quantitated in RK13 cells in the presence and absence of MPA medium, and in STO cells in the presence and absence of 6-TG. Differential titres in RK13 cells indicated that virus was able to replicate equally well in the presence and absence of MPA. In addition to this, recombinant virus was unable to replicate in STO cells in the presence of 6-TG indicating the absence of wild-type virus in this culture. To confirm replication of a non-*Eco*GPT expressing virus was not inhibited by 6-TG in STO cells, cells were infected with VACV IHD-J. The titres obtained for wild-type virus in the presence and absence of 6-TG were similar.

A final round of purification resulted in 2 clones vIδA26L1.1.1.1.1 and vIδA26L1.1.1.1.2. When quantified in RK13 cells in the presence and absence of MPA, the titres in the presence of MPA exceeded that in the absence of drug. A small stock of each cloned recombinant virus was prepared by infecting a T25 tissue culture flask of RK13 cells in selection medium at low MOI and 1 ml of this culture was used to prepare viral DNA. The presence of *Eco*GPT gene and the absence of A26L in the 2 putative recombinant clones were confirmed by PCR (Figure 3.6). This demonstrated that the 5 rounds of plaque purification had reduced parental wild-type virus to undetectable levels.

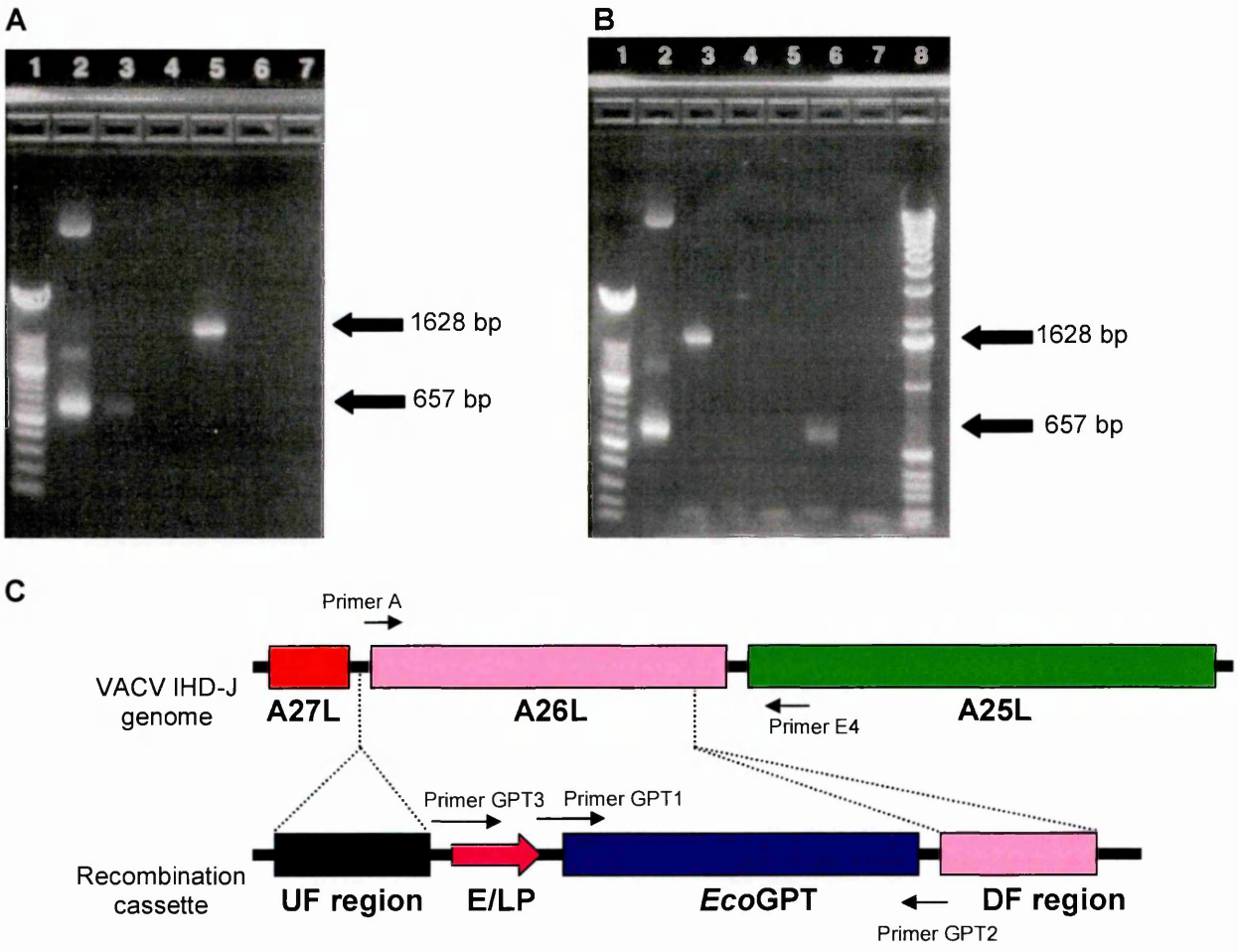

Figure 3.6 PCR Screening of Viral DNA Extracted from Recombinant VACV Clones from Round 5 of Purification

A PCR to detect *Eco*GPT (657 bp) using primers GPT3 and GPT2 (lanes 2-4) and A26L (1628 bp) using primers A and E4 (lanes 5-7) in vIδA26L1.1.1.1.1. Lane 1 – 100 bp ladder; lane 2 – p1107; lane 3 – recombinant vDNA; lane 4 – wt vDNA; lane 5 – wt vDNA; lane 6 – recombinant vDNA; lane 7 – dH_2O.

B PCR to detect *Eco*GPT (657 bp) using primers GPT3 and GPT2 (lanes 2, 4 and 6) and A26L (1628 bp) using primers A and E4 (lane 3, 5 and 7) in vIδA26L1.1.1.1.2. Lane 1 – 100 bp ladder; lane 2 – p1107; lane 3 – wt vDNA; lane 4 – wt vDNA; lane 5 – dH_2O; lane 6 – recombinant vDNA; lane 7 – recombinant vDNA; lane 8 – marker X (Roche Diagnostics, Ltd).

C Schematic demonstrating primers binding sites.

3.2.8 Propagation of vIδA26L

For all future experiments, vIδA26L1.1.1.1.1 was used and future use of the name vIδA26L refers to this clone. A purified high titre stock of this was produced by infecting multiple T150 tissue culture flasks of RK13 cells in the presence of MPA medium at low MOI (section 2.5.2). The virus titre was quantified as $2.77x10^8$ $TCID_{50}$/ml. This yield was lower than expected and this may have been due to a negative effect of the MPA medium on the cells.

Using virus from this stock, a Western blot was performed under reducing conditions to confirm the absence of A26 protein in vIδA26L (section 2.8). In VACV IHD-J, A26 resolved at approximately 60 kDa, however this band was absent in vIδA26L confirming the absence of the protein in the recombinant virus (Figure 3.7).

3.2.9 Characterisation of vIδA26L

3.2.9.1 Comparative Growth Kinetics of vIδA26L and VACV IHD-J *in vitro*

To investigate the effects of deletion of A26L on the growth rate and virus yields, one-step growth curves were performed in RK13 cells. The experiment was performed in triplicate in 24-well tissue culture plates, infecting at high MOI to give a synchronous infection. Cultures were harvested at 6, 17, 24, 30 and 48 hours p.i. and virus quantitated by Reed-Muench limiting dilution analysis (Figure 3.8A). The results demonstrated that vIδA26L had a similar growth rate to the IHD-J parent, however the overall yield was reduced by approximately 0.5 log.

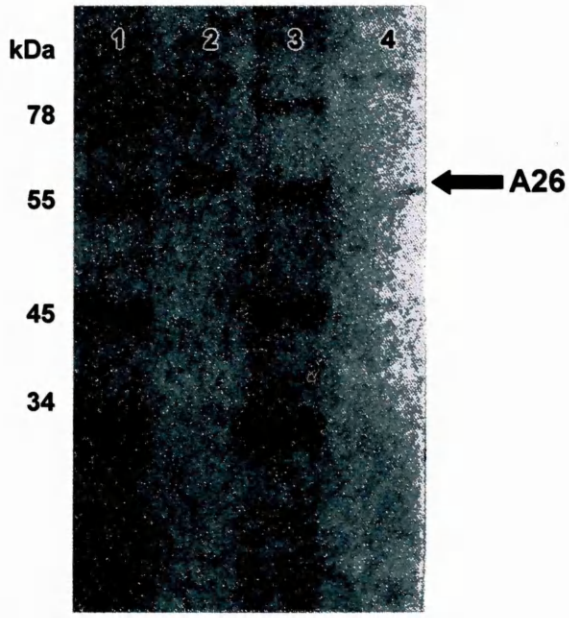

Figure 3.7 Western Blot Analysis of Purified VACV IHD-J and vIδA26L

Virus particles were heated to 85 °C for 2 minutes in Novex® Tricine SDS Sample Buffer with NuPAGE® Sample Reducing Agent and resolved in a Novex® 10 % Tricine Gel (Invitrogen Ltd). Proteins were then electroblotted onto nitrocellulose membrane and incubated with mono-specific rabbit antiserum for A26 protein. Lane 1 - SeeBlue®Plus2 Pre-stained standard; lane 2 - VACV IHD-J (~10^7 pfu); lane 3 - SeeBlue®Plus2 Pre-stained standard; lane 4 - vIδA26L (~10^7 pfu).

A

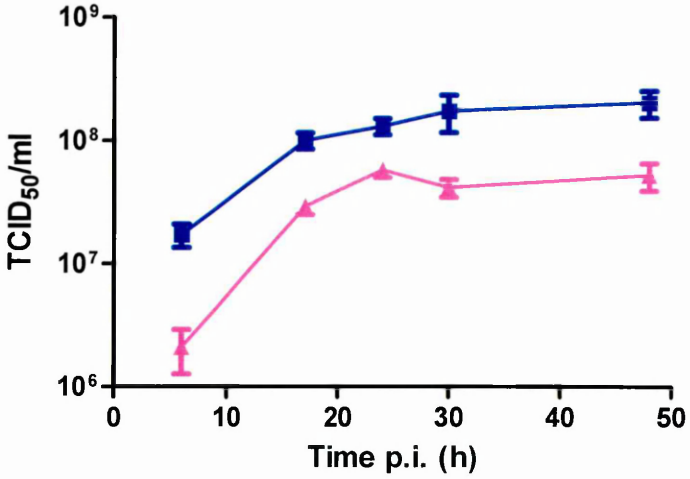

B

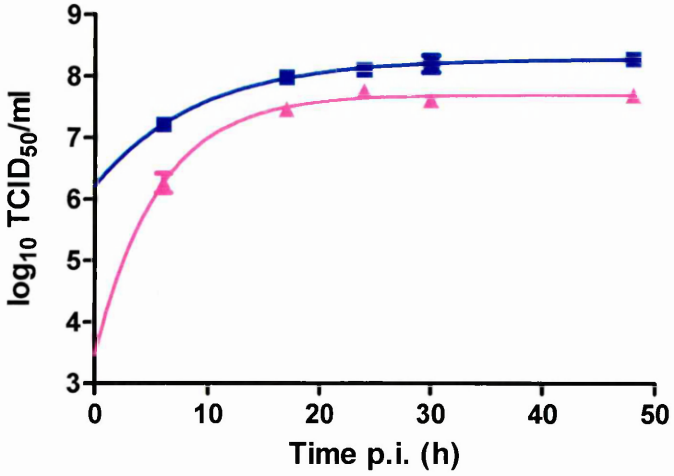

Figure 3.8 One-step Growth Curves for VACV IHD-J and vIδA26L

Freshly confluent monolayers of RK13 cells in 24-well tissue culture plates were infected at MOI 20 with wt VACV IHD-J (■) or vIδA26L (▲). Cultures were maintained at 37 °C in a 5 % CO_2 humidified atmosphere until the time of harvest. At the appropriate time p.i., replication was halted by freezing the cultures at -80 °C. Virus was liberated by three rounds of freeze-thaw followed by dounce homogenisation, prior to titration by Reed-Muench limiting dilution analysis. **A** Data is presented as mean $TCID_{50}$/ml and SEM of triplicate wells. **B** To allow statistical analyses, data was log_{10} transformed and fitted to a one-phase exponential association model.

To allow statistical analysis, the data was log_{10} transformed and fitted to a one phase exponential association model (Y=Ymax(1-exp(-KX))) where Ymax and K are changing variables (Figure 3.8B). Using an F-test to compare the total yield (Ymax), the wild-type virus was significantly different from vIδA26L ($p<0.05$), and there was no significant difference between the growth rates (K) of each virus.

The results of this experiment indicated deletion of A26L may affect the ability of VACV to replicate to high titres *in vitro,* which may be due to an effect on the recombinant virus ability to produce IMV. This issue was investigated further in this chapter. A second possible explanation may be due to a negative effect of the *Eco*GPT selection gene on the host cell or the virus. Importantly, the kinetics of growth for these viruses were similar and they reached their plateaux at similar times p.i. This was beneficial for subsequent work as viruses growing at different rates would have been problematic for kinetic experiments.

3.2.9.2 Analysis of IMV and EV Produced *in vitro* by Plaque Titration

Previous data have demonstrated detectable A26 protein from 9 hours p.i., and production of IMV after 15 hours p.i. (116). To investigate the production of IMV and EV throughout the replicative cycle and the hypothesis that A26 mediates IMV maturation, vIδA26L and wild-type virus were grown in RK13 cells infected at MOI 10 and the cultures harvested at 6, 8, 12, 17 and 22 hours p.i. A replicate culture was set up for the 22 hour timepoint, to control for the 17 hour culture which had to be initiated separately from the other time points for logistical reasons. At the earlier time points, it was anticipated that the majority of the progeny virus

would be EV, followed by IMV after 8 hours p.i as A26 begins to be synthesised. These time points were chosen to facilitate observation of the predicted switch of particle maturation from EV to IMV in wild-type virus, and any differences that might be observed in vIδA26L.

Total progeny virions were subjected to ultracentrifugation through CsCl gradients to separate enveloped and non-enveloped particles due to their difference in buoyant densities. Approximately 80 fractions were collected mechanically from the top of the gradient into a 96-well microtitre plate in ~200 µl volumes.

To determine the quantities of EV and IMV in each culture, plaque titrations of each fraction were undertaken. In an attempt to scale down the number of fractions to be tested, 10 µl of each fraction was diluted into 1 ml DMEM (to dilute the CsCl) and 50 µl of this used to infect corresponding wells of RK13 cells in a 96-well microtitre plate. This was used to indicate those fractions containing infectious virus simply by positive/negative screening for plaque formation. Plates were incubated for 4 days, then fixed and stained with crystal violet. The cell monolayers did not stain in any of the fractions tested, indicating cell death. This was unexpected but may indicate that infectious virus was present in each fraction or alternatively, may indicate cellular toxicity from residual CsCl.

To reduce the number of fractions to be tested, fractions were pooled into groups of 6 and the quantities of virus determined by a modified plaque titration method (section 2.5.3). Briefly, fractions were titrated in triplicate in a 96-well microtitre plate seeded with RK13 cells and incubated for up to 7 days. Following

staining of the cell monolayers with crystal violet, the absorbance at 570 nm (A_{570}) was determined. A high A_{570} indicated the absence of virus as the cell monolayer was still intact, and a low A_{570} indicated the presence of virus. The mean A_{570} for each fraction was plotted against the dilution factor in Microsoft Excel™ to give a curve, as shown in Figures 3.9 and 3.10 for 6 hours p.i. Using a regression analysis, these curves were used to calculate the dilution at which 50 % of the wells showed signs of infection (i.e. 50 % of the maximum A_{570} for the sample), in a manner analogous to calculation of $TCID_{50}$. For each time point, this was used to estimate the virus titre of each fraction where the greater the dilution factor, the greater number of infectious units present. Therefore to obtain a virus titre, the reciprocal of the dilution factor was calculated for each fraction (Figure 3.11).

Titration of pooled fractions in this fashion demonstrated an apparent decrease in the ratio of IMV to EV particles at 8 hours p.i. (Figure 3.11B), although the EV and IMV 'peaks' were less distinguishable in these gradients. This may be due to the pooling of fractions masking the trough between the EV and IMV 'peaks'. To try to mitigate this, the titrations were repeated for the 8 hour fractions pooling only 4 fractions which would increase the chances of detecting a trough (Figure 3.12). Again, there was a decrease in the ratio of IMV to EV particles, although the EV and IMV 'peaks' were distinguishable only in vIδA26L. No differences in the ratio of IMV to EV were seen at the other time points (Figures 3.11A, 3.11C, 3.11D, 3.11E and 3.11F).

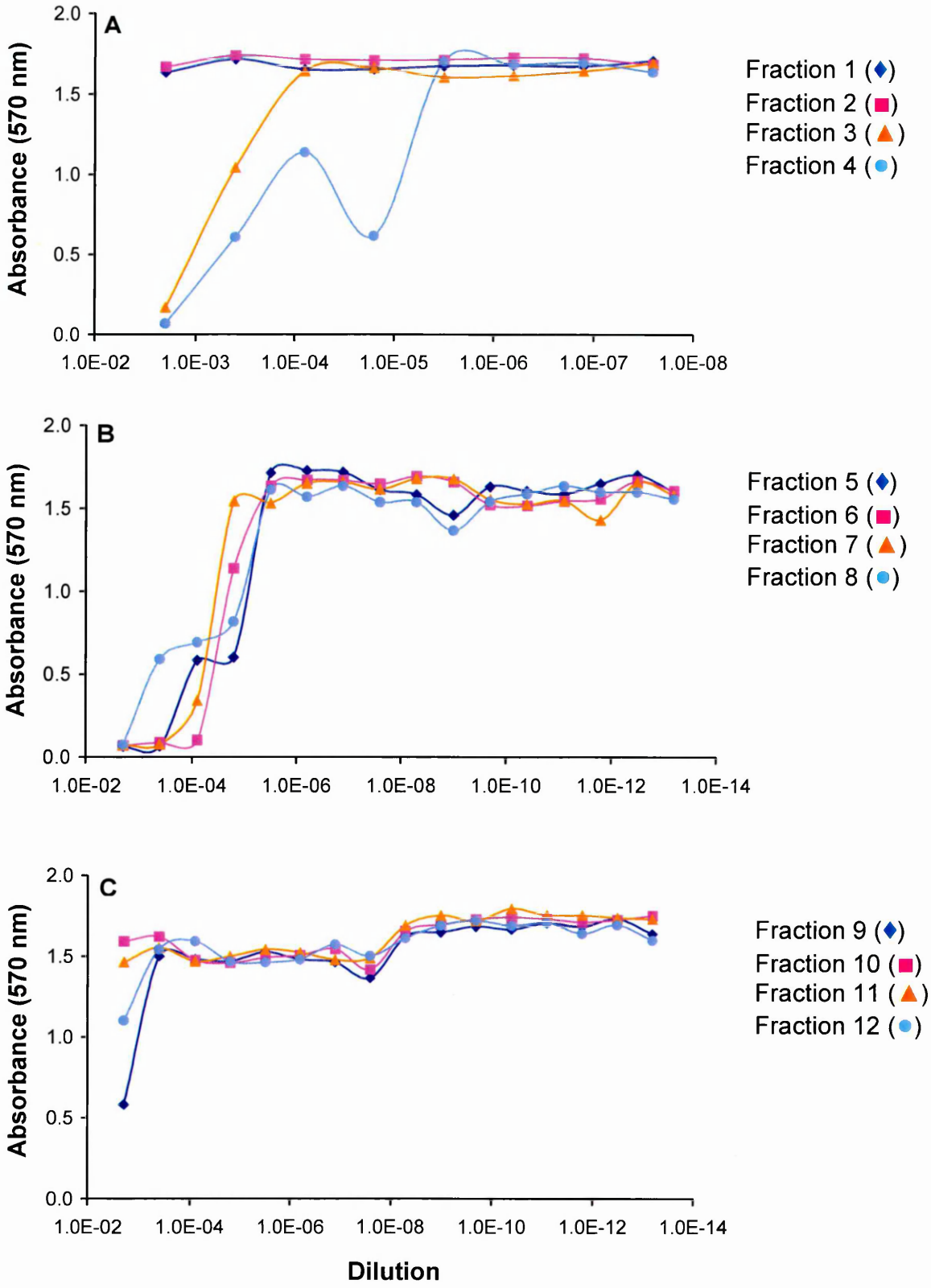
A
Absorbance (570 nm)
2.0
1.5
1.0
0.5
0.0
1.0E-02
1.0E-03
1.0E-04
1.0E-05
1.0E-06
1.0E-07
1.0E-08
Fraction 1 (♦)
Fraction 2 (■)
Fraction 3 (▲)
Fraction 4 (●)
B
Absorbance (570 nm)
2.0
1.5
1.0
0.5
0.0
1.0E-02
1.0E-04
1.0E-06
1.0E-08
1.0E-10
1.0E-12
1.0E-14
Fraction 5 (♦)
Fraction 6 (■)
Fraction 7 (▲)
Fraction 8 (●)
C
Absorbance (570 nm)
2.0
1.5
1.0
0.5
0.0
1.0E-02
1.0E-04
1.0E-06
1.0E-08
1.0E-10
1.0E-12
1.0E-14
Dilution
Fraction 9 (♦)
Fraction 10 (■)
Fraction 11 (▲)
Fraction 12 (●)

Figure 3.9 Mean Absorbance at 570 nm of RK13 Cell Monolayers Infected with CsCl Gradient Fractions of vlδA26L at 6 Hours p.i.

CsCl gradient fractions of vlδA26L cultures at 6 hours p.i. were titrated on RK13 cells for up to 7 days and stained with crystal violet. The absorbance at 570 nm (A_{570}) was determined for each well. A high A_{570} indicates the absence of virus, whereas a low absorbance indicates the presence of virus.

A Fractions 1 (♦), 2 (□), 3 (Δ) and 4 (○). **B** Fractions 5 (♦), 6 (□), 7 (Δ) and 8 (○). **C** Fractions 9 (♦), 10 (□), 11 (Δ) and 12 (○). Data is presented as means of triplicate wells.

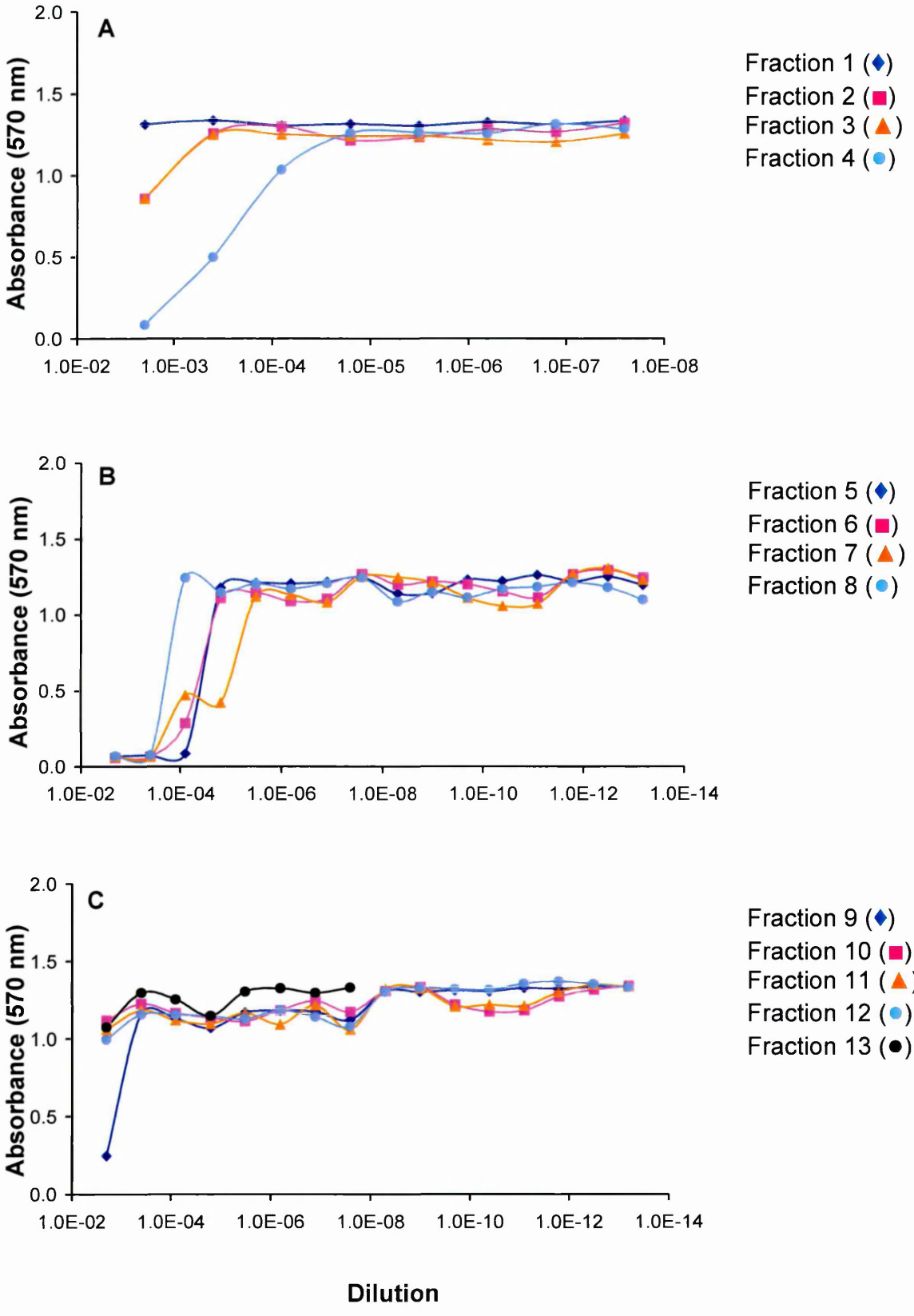
A
Absorbance (570 nm)
2.0
1.5
1.0
0.5
0.0
1.0E-02
1.0E-03
1.0E-04
1.0E-05
1.0E-06
1.0E-07
1.0E-08
Fraction 1 (♦)
Fraction 2 (■)
Fraction 3 (▲)
Fraction 4 (●)
B
Absorbance (570 nm)
2.0
1.5
1.0
0.5
0.0
1.0E-02
1.0E-04
1.0E-06
1.0E-08
1.0E-10
1.0E-12
1.0E-14
Fraction 5 (♦)
Fraction 6 (■)
Fraction 7 (▲)
Fraction 8 (●)
C
Absorbance (570 nm)
2.0
1.5
1.0
0.5
0.0
1.0E-02
1.0E-04
1.0E-06
1.0E-08
1.0E-10
1.0E-12
1.0E-14
Fraction 9 (♦)
Fraction 10 (■)
Fraction 11 (▲)
Fraction 12 (●)
Fraction 13 (●)
Dilution

Figure 3.10 Mean Absorbance at 570 nm of RK13 Cell Monolayers Infected with CsCl Gradient Fractions of VACV IHD-J at 6 Hours p.i.

CsCl gradient fractions of VACV IHD-J cultures at 6 hours p.i. were titrated on RK13 cells for up to 7 days and stained with crystal violet. The absorbance at 570 nm (A_{570}) was determined for each well. A high A_{570} indicates the absence of virus, whereas a low absorbance indicates the presence of virus. **A** Fractions 1 (♦), 2 (□), 3 (Δ) and 4 (○). **B** Fractions 5 (♦), 6 (□), 7 (Δ) and 8 (○). **C** Fractions 9 (♦), 10 (□), 11 (Δ), 12 (○) and 13 (●). Data is presented as means of triplicate wells.

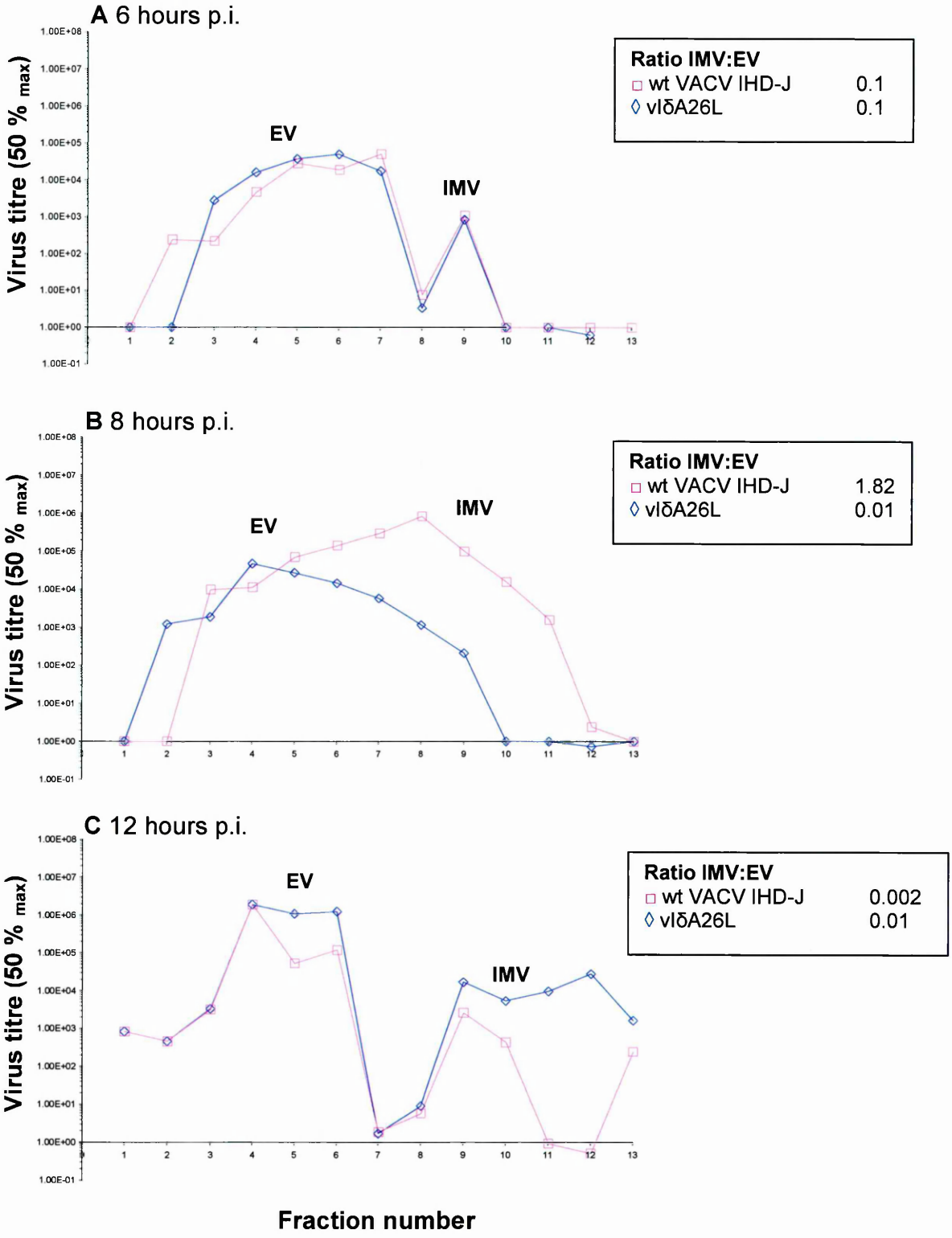
A 6 hours p.i.
Virus titre (50 % max)
EV
IMV
Ratio IMV:EV
wt VACV IHD-J 0.1
vIδA26L 0.1
B 8 hours p.i.
Virus titre (50 % max)
EV
IMV
Ratio IMV:EV
wt VACV IHD-J 1.82
vIδA26L 0.01
C 12 hours p.i.
Virus titre (50 % max)
EV
IMV
Ratio IMV:EV
wt VACV IHD-J 0.002
vIδA26L 0.01
Fraction number

D 17 hours p.i.

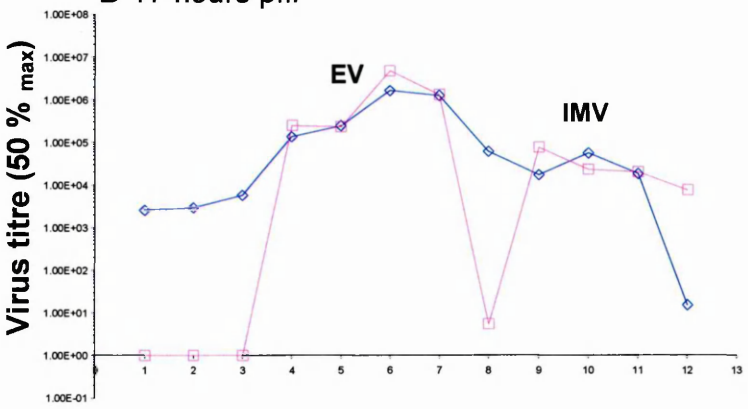

Ratio IMV:EV	
□ wt VACV IHD-J	0.02
◊ vIδA26L	0.03

E 22 hours p.i.

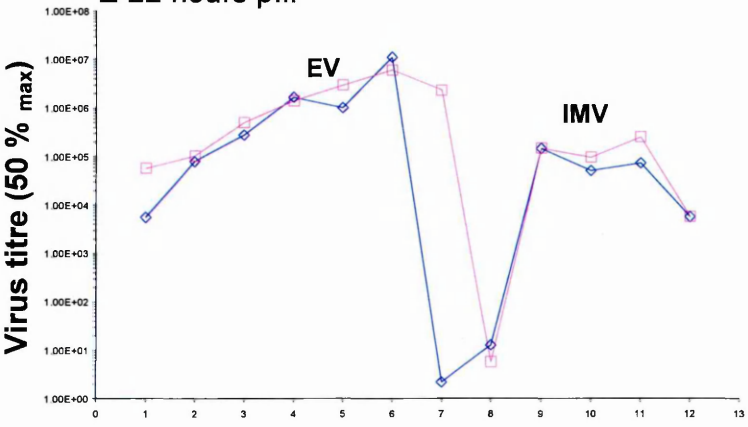

Ratio IMV:EV	
□ wt VACV IHD-J	0.04
◊ vIδA26L	0.02

F 22 hours p.i.

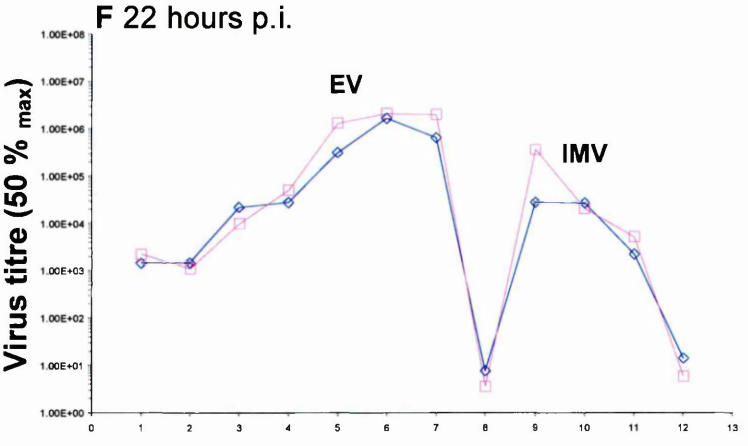

Ratio IMV:EV	
□ wt VACV IHD-J	0.07
◊ vIδA26L	0.02

Figure 3.11 Titres of CsCl Fractions of VACV IHD-J and vIδA26L Cultures at Various Times p.i.

RK13 cells were infected at MOI 10 with wt VACV IHD-J (□) or vIδA26L (◊) and cultured for 6 (**A**), 8 (**B**), 12 (**C**), 17 (**D**), 22i (**E**) and 22ii (**F**) hours. Progeny virus was separated through CsCl gradients and fractionated from the top. Fractions were pooled in groups of 6, and virus in each pool was quantified in RK13 cells (section 2.5.3). Fractions 1-7 and 8-13 were assumed to represent EV and IMV, respectively.

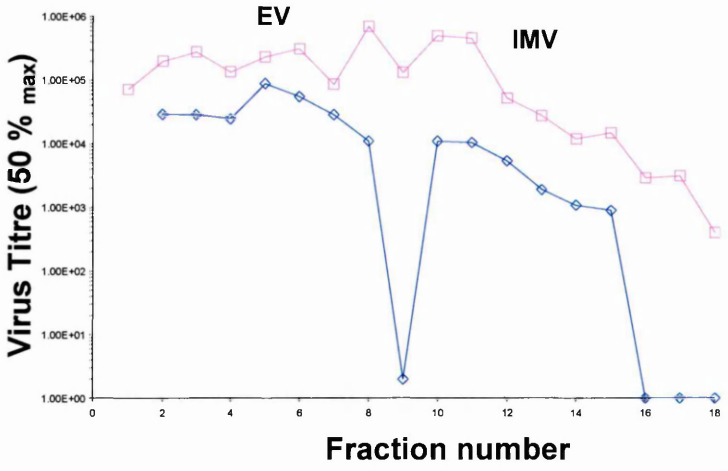

Ratio of IMV:EV	
□ wt VACV IHD-J	0.52
◊ vIδA26L	0.12

Figure 3.12 Repeat Titration of CsCl Fractions of VACV IHD-J and vIδA26L Cultures at 8 Hours p.i.

RK13 cells were infected at MOI 10 with wt VACV IHD-J (□) or vIδA26L (◊) and cultured for 8 hours. Progeny virus was separated through CsCl gradients and fractionated from the top of the gradient. Fractions were pooled in groups of 4, and virus in each pool was quantified in RK13 cells (section 2.5.3). Fractions 1-9 and 10-18 were assumed to represent EV and IMV, respectively.

Measuring the presence of virus in this way resulted in a high throughput assay where the quantities of virus in hundreds of samples could be determined. One of the clear limitations of this experiment is the crude nature of the output data. The quantity of fractions precludes removal of CsCl by washing and centrifugation of each fraction, and even if removal of CsCl by dilution in a standard virus titration assay is possible, the number of fractions to titrate is prohibitive. Pooling of the fractions leads to a reduction in the sensitivity of the assay by failing to adequately separate IMV and EV 'peaks'. Additionally, the effect of the absence of A26 protein on the characteristics and behaviour of IMV is unknown. Conceivably, its absence might cause IMV particles to be more (or less) likely to aggregate, confusing comparative analyses that are based on plaque forming units, which will quantify infectious units irrespective of the number of particles aggregated. This methodology may lead to an underestimate of the quantity of IMV in wild-type relative to recombinant virus. Consequently, it was decided to discontinue using this method for IMV and EV quantification, and to explore using tritiated thymidine to metabolically label virus particles.

3.2.9.3 Analysis of IMV and EV Produced *in vitro* by Radioactive Labelling of Virions in Lipid-Enriched Cultures

To address the limitations with the assay described in section 3.2.9.2, experiments were performed in which virus particles were metabolically labelled with a radioisotope (section 2.5.4). Viruses were cultured in medium containing tritiated thymidine (^{3}H thymidine) to metabolically label viral DNA. This method

enables estimation of relative numbers of viral genomes where it is assumed the ^{3}H thymidine is distributed evenly throughout the viral DNA. In addition, as cultures are separated through CsCl gradients, only ^{3}H-labelled DNA that has been packaged into intact virus particles will be counted. Therefore, the amount of radiolabel in each given fraction will relate directly to the number of virions present irrespective of the particle/pfu ratio.

The quantities of lipids available for incorporation into intracellular membranes are assumed to be much less in an *in vitro* tissue culture system than *in vivo*, and therefore may be artefactually limiting for EV production in experimental systems. In an attempt to increase the intracellular lipids available for envelopment, cultures were supplemented with cholesterol-enriched adult bovine serum (ABS) (Sigma-Aldrich, UK). This may mimic *in vivo* conditions more closely than standard tissue culture conditions, where it is thought EV production is limited by the lack of intracellular membranes available. Preliminary experiments were performed to observe the effects of addition of the lipids at various timepoints on cells and virus replication.

RK13 cells were infected with wild-type or vIδA26L at MOI 5 in a 6-well tissue culture plate. Following 1 hour incubation, the medium was replaced with either DMEM + 10 % FCS or DMEM + 10 % ABS. Increased CPE and cell lysis was observed in wild-type and vIδA26L cultures supplemented with ABS after 24 hours incubation suggesting that virus was able to replicate at a greater rate, than in FCS supplemented cultures. To speculate, an increased supply of lipids to the cells may have enhanced replication and envelopment of virions, which in turn

could lead to increased cell-to-cell spread. This may account for the increased CPE observed after 24 hours.

To investigate this further, the production of EV in cultures supplemented with ABS, RK13 cells were infected at MOI 10 with wild-type or vIδA26L where the cells were supplemented with 10 % ABS 20 hours prior to infection (t=-20), with 10 % ABS at the time of infection (t=0) or supplemented with 10 % FCS only, as described in standard protocols. To each culture, 10 µCi ^{3}H thymidine was added at the time of infection and cultures were incubated for a further 24 hours. Total progeny virions were subjected to ultracentrifugation through CsCl gradients to separate the different particles due to their difference in buoyant densities. Approximately 60 fractions were collected mechanically from the bottom of the gradient into a 96-well microtitre plate in ~300 µl volumes. Virus particles were collected onto a UniFilter-96 GF/C glass fibre filter microplate (Perkin Elmer) using a Filtermate 196 cell harvester (Packard) and subjected to liquid scintillation counting on a TopCount 9904 liquid scintillation counter (Packard). This experiment was repeated in triplicate and the results are shown in Figures 3.13, 3.14 and 3.15. In each culture condition there was a dramatic reduction in IMV production in vIδA26L compared to wild-type virus. To obtain a ratio of IMV:EV, the sum of CPM per peak was calculated, demonstrating a reduction in the ratio of IMV:EV. Unexpectedly, a concomitant increase in EV was not observed where the numbers of IMV had reduced. This may be due to the limitations of an *in vitro* tissue culture system where the supply of intracellular membranes is inadequate. Interestingly, the production of both types of virus particle in cultures supplemented

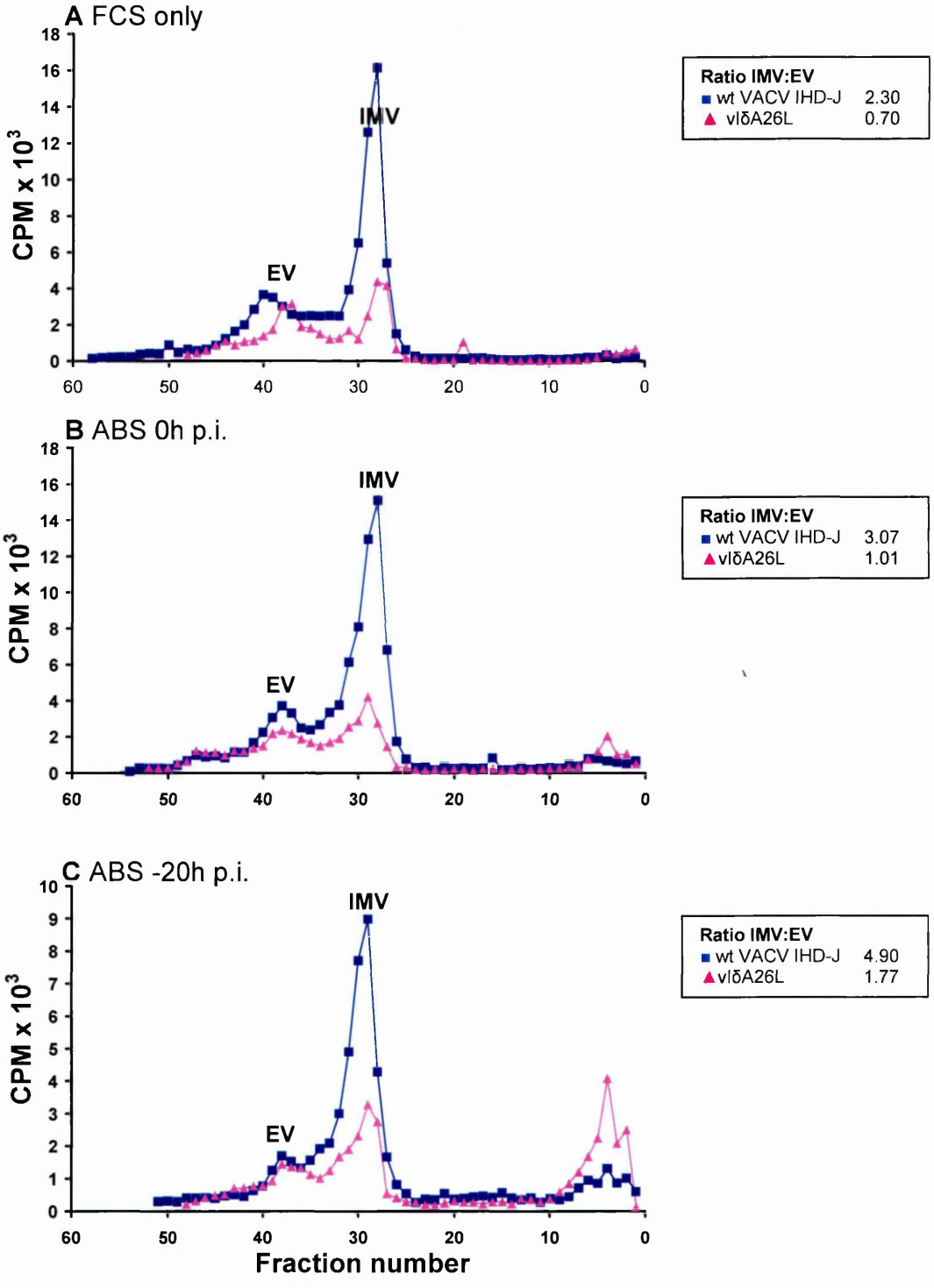
A FCS only
CPM x 10^3
IMV
EV
Ratio IMV:EV
wt VACV IHD-J 2.30
vIδA26L 0.70
B ABS 0h p.i.
CPM x 10^3
IMV
EV
Ratio IMV:EV
wt VACV IHD-J 3.07
vIδA26L 1.01
C ABS -20h p.i.
CPM x 10^3
IMV
EV
Ratio IMV:EV
wt VACV IHD-J 4.90
vIδA26L 1.77
Fraction number

Figure 3.13 Analysis of IMV and EV by Radioactive Labelling of Virions in VACV IHD-J and vIδA26L Cultures

Liquid scintillation counting of CsCl fractions of ^{3}H thymidine labelled progeny virions from wt (■) and vIδA26L (Δ) virus grown in cultures supplemented with 10 % FCS (**A**), or 10 % ABS added at t=0 (**B**) or t=-20 h (**C**). Progeny virus was harvested at 24 hours p.i. and subjected to ultracentrifugation through CsCl gradients. Gradients were mechanically fractionated from the bottom of the gradient and individual fractions subjected to liquid scintillation counting.

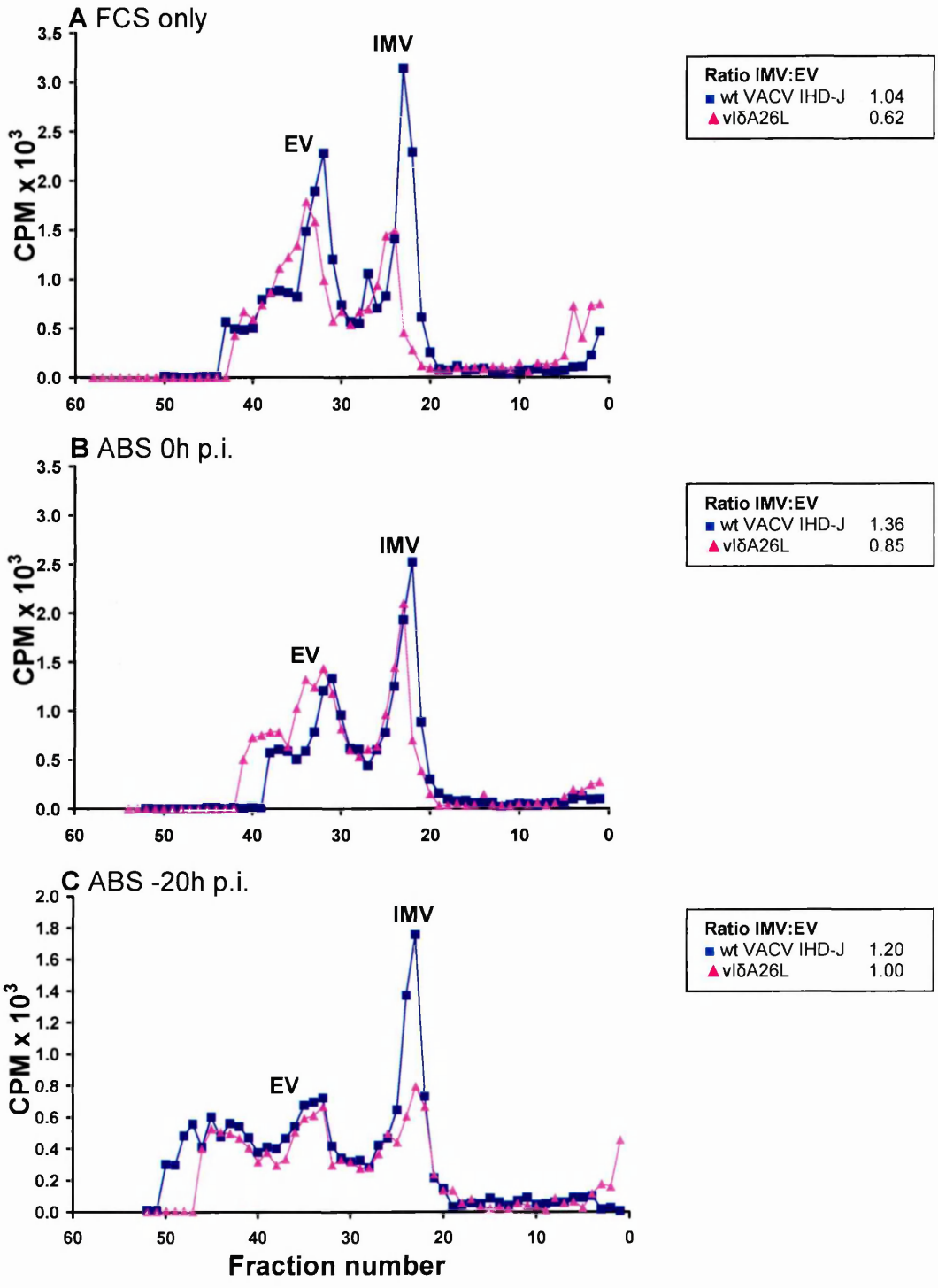
A FCS only
IMV
EV
CPM x 10^3
Ratio IMV:EV
wt VACV IHD-J 1.04
vIδA26L 0.62
B ABS 0h p.i.
IMV
EV
CPM x 10^3
Ratio IMV:EV
wt VACV IHD-J 1.36
vIδA26L 0.85
C ABS -20h p.i.
IMV
EV
CPM x 10^3
Ratio IMV:EV
wt VACV IHD-J 1.20
vIδA26L 1.00
Fraction number

Figure 3.14 Analysis of IMV and EV by Radioactive Labelling of Virions in VACV IHD-J and vIδA26L Cultures

Liquid scintillation counting of CsCl fractions of ^{3}H thymidine labelled progeny virions from wt (■) and vIδA26L (Δ) virus grown in cultures supplemented with 10 % FCS (**A**), or 10 % ABS added at t=0 (**B**) or t=-20 h (**C**). Progeny virus was harvested at 24 hours p.i. and subjected to ultracentrifugation through CsCl gradients. Gradients were mechanically fractionated from the bottom of the gradient and individual fractions subjected to liquid scintillation counting.

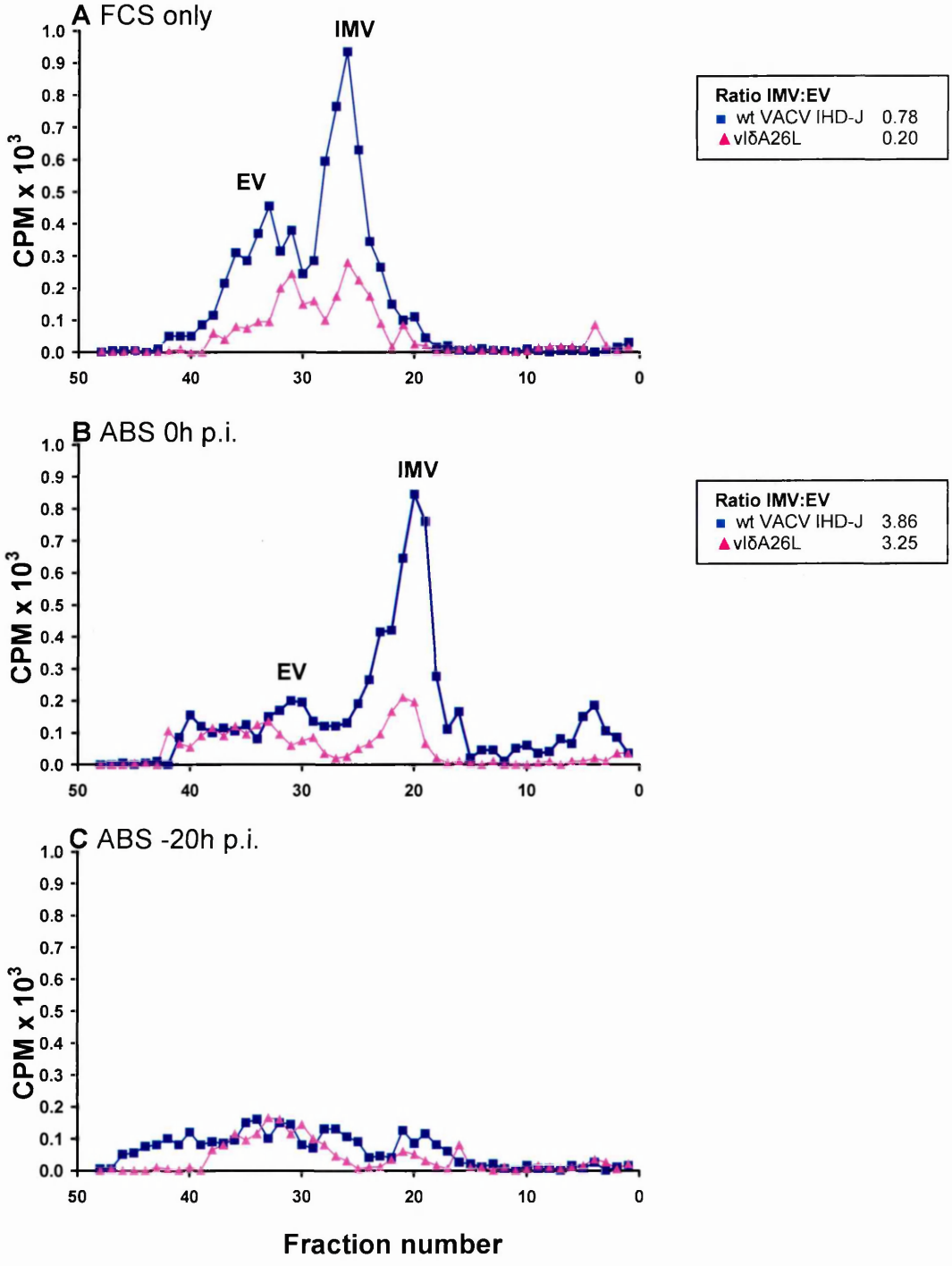
A FCS only
IMV
EV
CPM x 10^3
Ratio IMV:EV
wt VACV IHD-J 0.78
vIδA26L 0.20
B ABS 0h p.i.
IMV
EV
CPM x 10^3
Ratio IMV:EV
wt VACV IHD-J 3.86
vIδA26L 3.25
C ABS -20h p.i.
CPM x 10^3
Fraction number

Figure 3.15 Analysis of IMV and EV by Radioactive Labelling of Virions in VACV IHD-J and vIδA26L Cultures

Liquid scintillation counting of CsCl fractions of ^{3}H thymidine labelled progeny virions from wt (■) and vIδA26L (Δ) virus grown in cultures supplemented with 10 % FCS (**A**), or 10 % ABS added at t=0 (**B**) or t=-20 h (**C**). Progeny virus was harvested at 24 hours p.i. and subjected to ultracentrifugation through CsCl gradients. Gradients were mechanically fractionated from the bottom of the gradient and individual fractions subjected to liquid scintillation counting. IMV:EV ratios were not calculated for samples where ABS was added at t=-20 h, because the counts were too low to reliably identify peaks.

with ABS 20 hours prior to infection was particularly reduced compared to the other culture conditions indicating that extended incubation in cholesterol-enriched medium may be toxic to the cells. Possibly, several different fatty acids as opposed to cholesterol alone may be required for EV production to continue, or the timing and quantity of cholesterol requires optimisation.

These data suggest that deletion of the A26L gene in VACV IHD-J results in disruption of IMV production, therefore reducing the ratio of IMV:EV. Further investigation into the kinetics of virus maturation of vIδA26L, and restoration of the wild-type phenotype in a revertant virus will be described later in this study in Chapters 5 and 6.

3.2.9.4 Production of EEV in Brefeldin A-treated Cultures

The results in section 3.2.9.3 suggest that the A26L gene product is required for virus particles to mature as IMV. It may also be that once virions have acquired this marker they can no longer mature as EV, serving to negatively regulate wrapping. To investigate this further, EEV production in BFA-treated cultures was examined.

Incubation of infected cells with BFA specifically inhibits EV maturation, and removal of the drug results in the rapid recovery of EV (331). Previous studies have suggested that when removal of the drug is delayed beyond a certain point (i.e. after virions have had the opportunity to acquire IMV specific markers), EV recovery is reduced or abrogated (Dr D.O. Ulaeto, personal communication).

In the absence of A26L, it was predicted that increased EEV would be recovered at later times p.i. in vIδA26L cultures than in wild-type cultures once BFA is washed out. Consequently, RK13 cells were infected at MOI 10 with wild-type virus or vIδA26L in the presence or absence of 4 μg/ml BFA (section 2.5.6). Cultures were incubated for 10, 20 and 24 hours after which time the BFA was washed out and replaced with tissue culture medium. Culture supernatants were harvested at 20, 24 and 28 hours and the secreted virus, assumed to be EEV, in each culture determined by Reed-Muench limiting dilution analysis. The recovery of EEV in BFA-treated cultures was calculated as a percentage of EEV recovered in untreated cultures (Figure 3.16). At each timepoint, the recovery of EEV was substantially greater in vIδA26L than wild-type virus indicating that vIδA26L has a greater ability to recover EEV following removal of the drug even at late times p.i. when compared to wild-type. This suggests that the absence of A26L allows EEV production even at late times p.i. in vIδA26L, suggesting that maturation to IMV had been disrupted.

3.3 Discussion

It has been known for some time that the EV particle of OPVs is an end-stage of virus maturation. However, this has not been clear for IMV particles and the possibility that IMV is not a structural pre-cursor of EV has not previously been excluded. One hypothesis for the formation of IMV is that it is virus left over when the supply of Golgi-derived membranes that are used to wrap EV becomes exhausted. This study was designed to investigate whether IMV is in fact produced

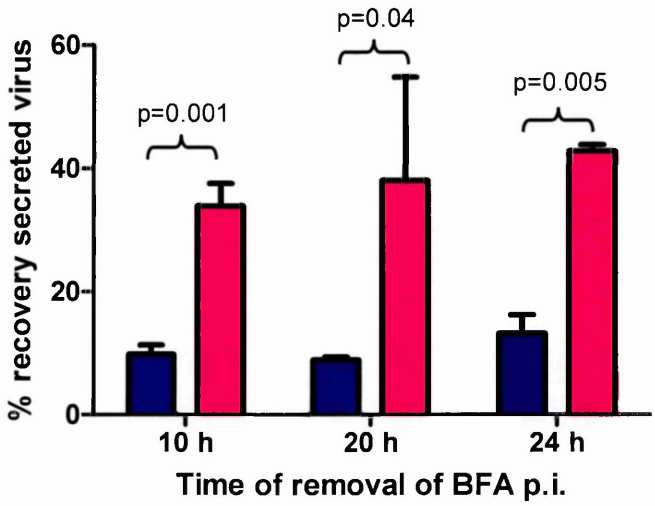

Figure 3.16 Effect of BFA on EEV Production in VACV IHD-J and vIδA26L Cultures

RK13 cells were infected at MOI 10 with VACV IHD-J (■) or vIδA26L (■) and incubated in the presence or absence of 4 µg/ml BFA. BFA was washed out of the cultures and replaced with tissue culture medium at 10, 20 and 24 hours p.i. and the culture supernatant harvested at 20, 24 and 28 hours p.i., respectively. Secreted virus was quantitated by Reed-Muench limiting dilution analysis. Data is presented as means and SEM of triplicate experiments. p-values were calculated using a one-way ANOVA.

by a distinct maturation pathway resulting in a switch from EV to IMV formation, mediated by the IMV-specific protein A26.

To investigate the role of A26 in VACV morphogenesis, the A26L gene was successfully deleted from the IHD-J genome and replaced with the *Eco*GPT selection marker gene. This allowed selection of a pure, clonal recombinant virus in the presence of MPA as demonstrated by differential titrations in the presence and absence of selection. To further confirm the absence of wild-type virus in cultures, growth of recombinant virus was shown to be inhibited in STO cells in the presence of 6-TG, conditions previously described to inhibit growth of *Eco*GPT-expressing viruses (349). The use of differential titres may be a useful tool in future experiments to screen cultures for the presence of recombinant virus, and indicate their purity. In addition to this, the presence of the *Eco*GPT gene and absence of the A26L gene were demonstrated by PCR, and the absence of A26 protein was confirmed by Western blot.

One-step growth curves were performed to examine growth rates of vIδA26L *in vitro*. Although the growth rates of vIδA26L and wild-type virus were similar, there was a reduction in the overall yield of virus. There are two plausible explanations for this reduction: deletion of A26L has an effect on virus yields, or the expression of *Eco*GPT may have a negative effect on the host cell or the virus, resulting in a reduction in virus production. In future studies, it is necessary to determine whether the wild-type phenotype can be restored by re-introducing the A26L gene, therefore attributing the reduction in yields to the absence of A26L or by removing the selection marker gene to determine if the phenotype observed is

due to the presence of *Eco*GPT. There was a slight delay in the onset of replication in vIδA26L cultures which may be attributed to a decrease in the rate of infectivity of this virus. It has been reported that VACV binds to host cells via an interaction with laminin mediated by A26 (134), by binding to GAGs via H3, A27 and D8 (130-133), and via L1 to an unknown receptor (135). It is possible that disruption of any one of these interactions may reduce the ability of the virus to enter cells, leading to a delay in the onset of replication as seen in cultures infected with the A26L deletion mutant.

Separation of virus particles through CsCl gradients and quantitation by plaque titration was used to examine the production of IMV and EV in vIδA26L. As expected at 6 hours p.i., where F13 is detectable and A26 is not (116), the quantities of EV exceeded that of IMV in both wild-type and vIδA26L cultures. At 8 hours p.i., when A26 production begins (116) the ratio of IMV:EV increased in wild-type but not in vIδA26L, indicating that A26 may be necessary for maturation of IMV. Unexpectedly, a continuing reduction in the ratio of IMV:EV in vIδA26L compared to wild-type was not observed at the later time points. The reasons for this are unclear, although the limitations of the assay with respect to the logistics of directly quantitating the number of infectious particles have the effect of reducing its sensitivity, and the uncertainty over the possible phenotypic effect of the deletion of A26L on particle/pfu ratios for IMV are causes for concern.

Using ^{3}H thymidine to metabolically label viral genomes was a more accurate method to enumerate virus particles following separation of virions through CsCl gradients. The results demonstrated a profound decrease in IMV in

vIδA26L cultures. Interestingly, the data did not show a rise in the quantity of EV produced by vIδA26L concomitant with the apparent reduction in IMV. This suggests that failure to acquire the A26 protein by maturing virions does not automatically result in these virions undergoing envelopment. It may be that, just as IMV production appears to be controlled independently of EV production, so too EV production may be limited by a mechanism independent of IMV production. It has been previously suggested that EV production is limited by the availability of intracellular membranes for wrapping (350); and the presumed reduced pools of lipids in tissue culture systems may thus be artefactually limiting for EV production in this system. Supplementation of cultures with cholesterol-enriched serum to increase the pool of available lipids did not increase the production of EV, and in some cultures had an adverse effect on virus production. It is likely that this was a toxicity effect, and optimisation of concentrations and periods of incubation might improve EV yields. It may also be possible to increase the amounts of intracellular membranes available for wrapping by using an alternative cell line such as an adipocyte cell line that may have greater quantities of intracellular lipids.

There is no obvious explanation for the absence of large quantities of "undifferentiated" virions that would presumably sediment with the same density as IMV in CsCl gradients from vIδA26L cultures, however this may help to explain the reduction in overall progeny virus observed in one-step growth curves. Perhaps virus that is unable to differentiate as either IMV, due to the absence of A26, or EV due to lack of membranes, is unstable and does not withstand the purification process.

Previous studies suggest that following the production of A26 at around 8 hour p.i. the recovery of EV is reduced or abrogated when envelopment is delayed by treating cultures with BFA (Dr D.O. Ulaeto, personal communication). This suggests that an increasing proportion of non-enveloped particles that would normally have become EV may instead have matured as IMV. It is possible that these particles are no longer available for envelopment because they have already acquired the IMV-specific marker, A26. Further experiments with vIδA26L cultures treated with BFA demonstrate a greater recovery of EEV compared to VACV IHD-J. This suggests that the absence of A26L allows EEV production to continue at elevated levels at relatively late times p.i. in vIδA26L because differentiation to IMV does not occur.

The other functions for A26, previously discussed, do not explain why this gene, or at least a segment of it, is conserved in many OPVs such as VARV, MPXV and CPXV, most of which do not produce ATIs. More recent studies have demonstrated that A26 forms a complex with A27, anchored to the surface of the virion by association with A17 (351). A27 is required for EV formation (170), therefore binding of A26 may act to prevent wrapping of virions, leading them down a distinct maturation pathway.

During this study, attempts were made to generate hybridoma cell lines to produce monoclonal antibodies (mAbs) to A26, to use in place of polyclonal serum. Polyclonal sera contain a mixture of immunoglobulin molecules that recognise different epitopes of the same antigen and other non-target antigens. The specificity is therefore reduced and the polyclonal serum used in this study has

been shown to cross-react with the 4b core protein (D.O. Ulaeto, personal communication); generation of mAbs specific to A26 was thus desirable. These mAbs would be a useful tool for the detection of A26 on the surface of IMV particles produced by the various recombinant VACVs generated during this project. The resulting hybridoma cultures produced antibodies that reacted with proteins of various sizes, yet none of these were of the size expected for A26. Therefore, the polyclonal serum was used for future experiments, as the specificity had been demonstrated for A26 with minimal cross-reactivity to 4b.

In conclusion, the data provide evidence that IMV particles are an end-stage product of OPV maturation that has lost the ability to become EV by acquiring the A26 protein, and that the A26L gene operates as a switch controlling the differentiation of developing virions into IMV. Formal proof of this requires analysis of a revertant virus constructed by re-insertion of the A26L gene into the original locus in vIδA26L. The hypotheses that EV production is limited by the supply of Golgi-derived membranes for envelopment, and that IMV and EV are both independent end-stages of maturation, are not mutually exclusive.

4 Construction of Secondary Recombinant VACV using Reverse Guanine Phosphoribosyl Transferase (GPT) Selection

4.1 Introduction

Following the construction of the A26L deletion mutant vIδA26L1.1.1.1.1, it was necessary to construct a revertant recombinant VACV by re-inserting A26L under the control of its native promoter, and hence restore function. This was required to validate the phenotype observed in the deletion mutant. In parallel with this, a panel of recombinants were designed using a variety of promoters to modulate A26L expression. Characterisation of such recombinants has the potential to further inform our understanding of the relationship between IMV and EV.

An approach described by Isaacs *et al.*, (1990) describes reverse GPT selection used to negatively select against a recombinant VACV containing the *Eco*GPT gene (349). This allows growth of secondary recombinant virus where *Eco*GPT has been deleted by homologous recombination and replaced by a gene of interest. This method circumvents many of the problems inherent in other selection systems, such as insertional inactivation of the thymidine kinase (TK) gene, and allows the construction of a recombinant VACV that does not contain heterologous selection marker genes.

Six recombination cassettes for the construction of six secondary recombinant viruses were designed (Figure 4.1). Four of these recombinants were designed to examine the effects of altered expression kinetics for A26L, using promoters that will initiate transcription at different phases of the virus replicative

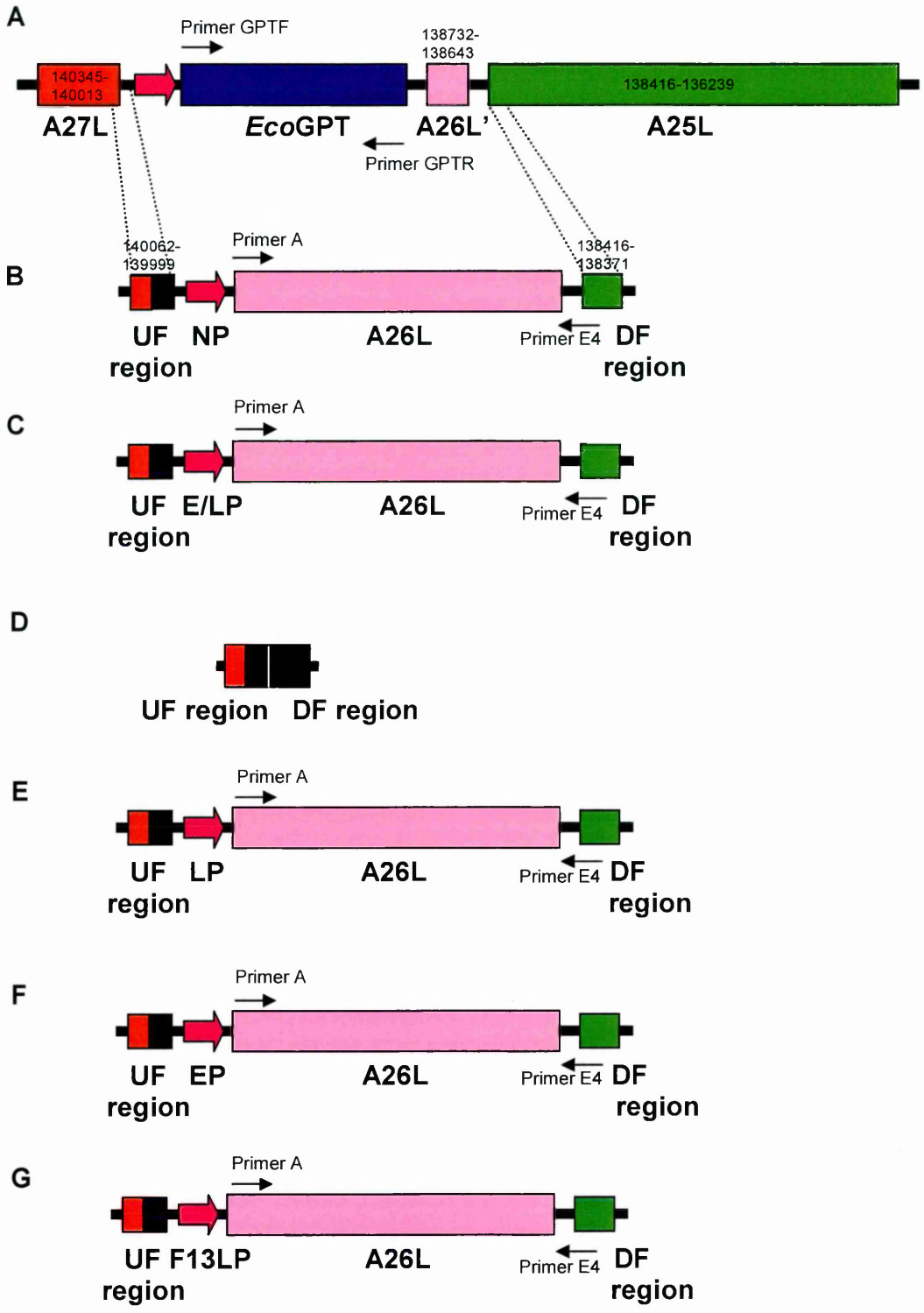
A
Primer GPTF
138732-
138643
140345-
140013
138416-136239
A27L
EcoGPT
A26L'
A25L
Primer GPTR
B
140062-
139999
Primer A
138416-
138371
UF
region
NP
A26L
Primer E4
DF
region
C
Primer A
UF
region
E/LP
A26L
Primer E4
DF
region
D
UF region
DF region
E
Primer A
UF
region
LP
A26L
Primer E4
DF
region
F
Primer A
UF
region
EP
A26L
Primer E4
DF
region
G
Primer A
UF
region
F13LP
A26L
Primer E4
DF
region

Figure 4.1 Schematic of Secondary VACV Recombination Cassettes for Modulating Expression of A26L

Each construct was synthesised by PCR and cloned into pCR®-XL-TOPO® vector, a commercially available vector (Invitrogen, Ltd) as described in section 4.2. **A** represents the region of the parental vIδA26L1.1.1.1.1 genome; **B** the revertant construct; **C** the early/late construct; **D** null construct; **E** late construct; **F** early construct; **G** F13L construct. Nucleotide sequences can be found in Appendix Figures A2-A7.

process. The remaining two include revertant and null recombinants. All the constructs utilised VACV genomic regions immediately upstream and downstream of the A26L gene and its promoter, to facilitate homologous recombination in vIδA26L1.1.1.1.1. The recombination event will result in deletion of the entire coding sequence of the *Eco*GPT gene and its attendant synthetic early/late promoter. This would generate a panel of secondary recombinant viruses with the minimum of non-native sequence.

The revertant recombinant VACV was designed to facilitate re-insertion of A26L under the control of the native promoter (NP), regenerating the wild-type phenotype and controlling for possible artefacts in the phenotype of the other recombinant viruses (Figure 4.1B). This should demonstrate that the phenotype observed in vIδA26L1.1.1.1.1 is due to the deletion of A26L. This recombinant will be genetically and phenotypically identical to the wild-type.

The second recombinant VACV was designed to re-insert A26L into its original locus but under the control of a synthetic early/late promoter (E/LP) described by Hammond *et al.* (1997) (Figure 4.1C) (327). It is predicted that this will result in constitutive expression of A26L and direct morphogenesis towards IMV maturation immediately upon virion assembly in late stages of replication, thus increasing IMV and reducing EV formation. This virus is a potential candidate for a live recombinant vaccine against smallpox, and possibly as a vector for vaccines against heterologous viruses and diseases.

The third recombinant VACV was designed to delete *Eco*GPT but not replace it (Figure 4.1D). This null recombinant was designed as a control, to

ensure that any observed phenotypic effects in the primary recombinant are not due to a previously undescribed effect of *Eco*GPT expression, or a positional effect of insertion of the *Eco*GPT gene. This recombinant was also designed to act as an internal control for reverse GPT selection. Reverse GPT selection allows the replication of non-*Eco*GPT-expressing viruses, including wild-type VACV. As described earlier, the revertant and wild-type strains are genetically and phenotypically identical and therefore cannot be distinguished. To address this, the null recombinant can be used to screen for both A26L and *Eco*GPT, where their absence is indicative of a true secondary recombinant. In this case, it is possible to extend the assumption that if the null recombinant has been constructed as a result of homologous recombination then the revertant is likely to be a true secondary recombinant, and not wild-type VACV, that may have been carried through the MPA selection process. This recombinant would also be useful for future studies as an alternative to vIδA26L1.1.1.1.1, in particular those in animals, where foreign genes may complicate the interpretation of results.

The additional secondary recombinants were designed to examine the effects of altered expression kinetics for A26L, using promoters that will initiate transcription at different phases of the virus replicative process. The fourth and fifth recombinants will contain a synthetic early promoter (EP) or a synthetic late promoter (LP) respectively, using the early and late elements of the synthetic E/LP described by Hammond *et al.* (1997) controlling the expression of A26L (Figures 4.1E and 4.1F) (327). It is predicted that when A26L is expressed from an EP, maturation of particles will favour IMV production in the early stages of maturation

as an abundance of A26 will be present upon virion assembly, however at late times expression will cease and due to lack of available A26 maturation of EV may thus become dominant. Late expression of A26L will have a similar phenotype to wild-type, however expression of A26L may occur at an earlier time than in wild-type causing a switch from EV to IMV production at an earlier time in the infectious cycle. The final recombinant was designed to express A26L under the control of the F13L promoter (F13LP) (Figure 4.1G). F13L is an EV-specific protein that is required for IEV formation (117) and in the context set here, may be regarded as directing virus differentiation towards EV in the initial stages of virus late gene expression. Precisely co-ordinated expression of A26L and F13L may indicate which, if either, is the dominant controller of virus differentiation as IMV or EV.

4.1.1 Aims of This Study

The aim of this study was to replace the *Eco*GPT gene in vlδA26L1.1.1.1.1 with a recombination cassette containing A26L under the control of a variety of promoters, to create a panel of six recombinants with potentially differing phenotypes. It was anticipated that modulation of A26L expression, so that it is constitutively expressed, would increase the ratio of IMV:EV by reducing the absolute quantity of virions that are available for envelopment. Such a reduction in EV has the potential to be attenuating giving rise to an improved smallpox vaccine and/or vaccine vector candidate.

4.2 Results

4.2.1 Design and Construction of VACV Secondary Recombination Cassettes

The recombination cassettes (Figure 4.1) were constructed using PCR to synthesise the coding sequence of A26L gene utilising VACV IHD-J DNA as template, adding the appropriate promoter and upstream and downstream flanks as tails at the 5' end of the primers. The constructs were made in two stages: the first to amplify A26L and the downstream flanking region, adding the appropriate promoter upstream of the initiation codon; the second to add the upstream flank to the 5' end of the newly inserted promoter sequence.

4.2.1.1 Null Recombination Cassette

A null recombination cassette was designed to delete *Eco*GPT from the primary recombinant virus vIδA26L1.1.1.1.1 and not replace it with A26L therefore deleting the entire locus. This required a very small recombination cassette containing only upstream and downstream flanking regions of A26L, therefore construction of this cassette differs from the others described previously.

The oligonucleotides FLA3 and FLA4 were designed to amplify the oligonucleotides FLA1 and FLA2, respectively, which were complimentary sequences of the 63 bp region upstream of A26L gene immediately followed by the 63 bp region downstream of A26L gene (Table 2.1). Care was taken when designing this construct to ensure that the coding sequences of both adjacent genes A27L and A25L were maintained. The resulting product of 126 bp was confirmed on an agarose gel (Figure 4.2A) and the construct was cloned into

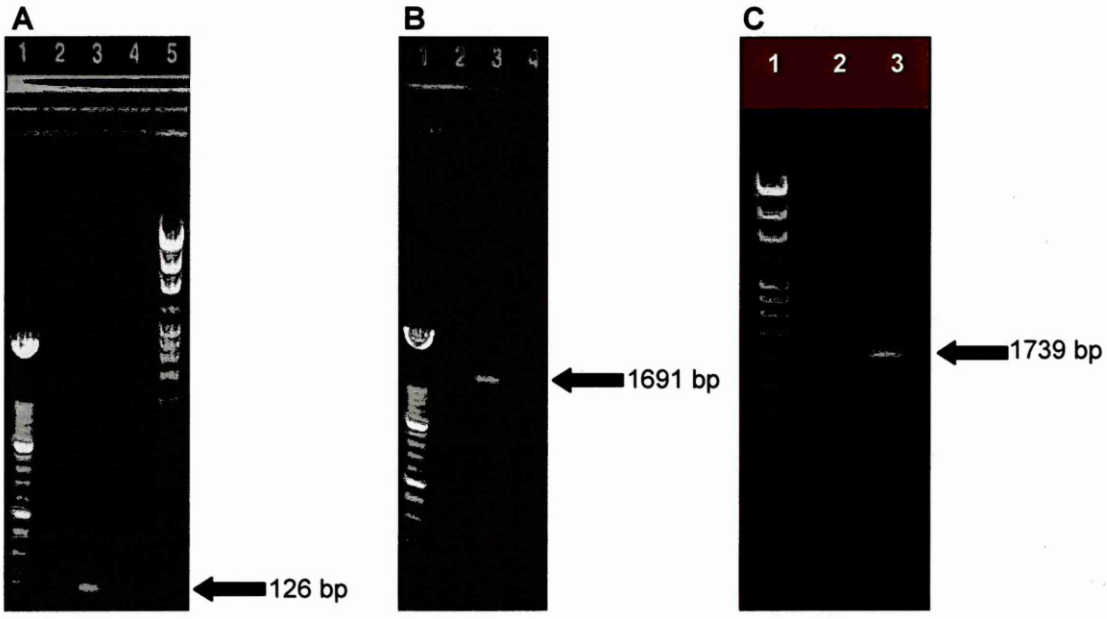

Figure 4.2 Synthesis of Secondary Recombination Cassettes

A PCR using primers FLA3 and FLA4 to synthesise the null recombination cassette (126 bp). Lane 1 – 100 bp ladder; 2 – empty; 3 – null cassette; 4 – empty; 5 – Mwt marker IV.

B PCR using primers A2 and E4 to synthesise revertant recombination cassette (1691 bp). Lane 1 – 100 bp ladder; 2 – empty; 3 – revertant cassette.

C PCR using primers C2 and E4 to synthesise early/late recombination cassette (1739 bp). Lane 1 – Mwt marker IV; lane 2 – empty; lane 3 – early/late cassette.

pCR®-XL-TOPO® (Invitrogen). DNA sequencing confirmed the sequence integrity of the null construct.

4.2.1.2 Revertant Recombination Cassette

The revertant virus was required to have A26L re-inserted into its original locus in vIδA26L1.1.1.1.1 under the control of the NP. The genomic sequence upstream of A26L (VACV WR sequence) was studied for traits of late VACV promoters and a region of 36 bp that was predicted to contain the promoter and 63 nucleotides of upstream flanking sequence was selected (Figure A2). Using primers A and E4, and then A2 and E4 (Table 2.1), the recombination cassette of 1691 bp was constructed by PCR (Figure 4.2B) and cloned into pCR®-XL-TOPO® (Invitrogen). DNA sequencing confirmed the sequence integrity except for the upstream flanking region was absent. It was decided however, that the promoter sequence of the A26L gene should be sufficient for homologous recombination and therefore transfection experiments should begin with this construct.

4.2.1.3 Early/Late Recombination Cassette

In addition to a revertant virus, a further recombinant virus was to be constructed in which A26L was re-inserted into its original locus in vIδA26L1.1.1.1.1 under the control of a synthetic E/LP (327). The cassette was constructed in two stages using primers C and E4 in the first stage and primers C2 and E4 in the second stage (Table 2.1). The second stage construct proved to be more problematic to synthesise as the PCR to add the upstream flank was

inefficient and produced only a small amount of product of the correct size (1739 bp), even though several attempts were made to try to optimise the reaction (Figure 4.2C). Cloning of this second stage construct was unsuccessful and as a result, it was decided to use the gel purified PCR product in the transfection. To conserve DNA, it was decided to delay sequencing and to wait until the recombinant virus had been isolated so that viral DNA could be used to check the final sequence.

4.2.1.4 Early, Late and F13L Recombination Cassettes

Recombination cassettes were designed so that the *Eco*GPT gene would be replaced by A26L under the control of either a synthetic EP, a synthetic LP or the F13LP (Figures A5-A7). The F13LP sequence was predicted by studying the region upstream of the F13L gene (GenBank Accession number AA089331) in the VACV WR genome sequence for traits of poxvirus promoters identifying a region of 27 bp. This region has a characteristic TAAATG initiation sequence that is common in poxvirus late promoters. The inserts were constructed by PCR using primers B, D and F for EP, LP and F13LP respectively, and the reverse primer E4 to synthesise the A26L gene from VACV IHD-J DNA, adding the appropriate promoter and a downstream flank (Table 2.1). The second stage added the upstream flanking region to the 5'-end of the promoter sequence using the corresponding primers B2, D2 and F2, and the reverse primer E4 (Table 2.1).

Construction of EP, LP and F13LP secondary recombinant viruses was delayed until the revertant, E/LP and null recombinant viruses had been isolated,

because it was felt it was not practical to attempt to isolate more than three recombinant viruses in parallel.

4.2.2 Construction and Selection of Secondary Recombinant *Eco*GPT-negative VACV by Homologous Recombination

Reverse *Eco*GPT selection enables the selection of secondary recombinants that have had their *Eco*GPT gene replaced by another gene of interest. This method takes advantage of the ability of *Eco*GPT to convert purine analogues into products that prevent *Eco*GPT-expressing viruses from replicating. The purine analogue used in this study was 6-thioguanine (6-TG) which has been shown to prevent the growth of *Eco*GPT-expressing viruses at a concentration of 0.1-1 mM in tissue culture medium (349). The cell line for this had to be carefully chosen as those cell lines that contain the mammalian hypoxanthine-guanine phosphoribosyltransferase (HPRT) enzyme will incorporate 6-TG into DNA, a toxic event for both *Eco*GPT and non-*Eco*GPT-expressing virus. In this study STO cells, an HPRT-negative mouse embryonic fibroblast cell line, was used for selection of secondary recombinants in the presence of 0.1 mM 6-TG (349). The resulting *Eco*GPT-negative virus present can be easily amplified with each round of selection, and by comparing growth in the presence and absence of drug, it is possible to monitor the reduction of residual *Eco*GPT-expressing virus with each round of 6-TG selection, until it is eliminated.

The null, revertant and early/late constructs described above were introduced into the parental vIδA26L1.1.1.1.1 genome using upstream and

downstream flanking regions that were homologous to regions upstream and downstream of the *Eco*GPT locus (formerly A26L locus in VACV IHD-J), as previously used in Chapter 3. The resulting viruses were amplified under reverse *Eco*GPT selection conditions.

4.2.2.1 Isolation of Secondary Recombinant VACV

Progeny virus was harvested and cultured in STO cells under 6-TG selection for 5 passages. A small stock of each putative recombinant virus was produced by culture in STO cells in the presence of 6-TG at low MOI for 24 hours, and 1 ml was used to prepare viral DNA.

4.2.2.2 Screening of Secondary Recombinant VACV DNA by PCR

The null recombinant virus acts as a control for the 6-TG selection method, as absence of the A26L in this virus would strongly suggest that the other recombinant VACVs are true secondary recombinants, and the A26L signal observed in their DNA is not due to contaminating wild-type VACV. PCRs were carried out to confirm the genotype of the putative null recombinant (Figure 4.3). The *Eco*GPT gene was not detected, however there was a strong signal for A26L of ~1628 bp. This indicates that the virus isolated during the selection was A26L positive and this was therefore most likely to be wild-type virus that has been carried over in the vIδA26L1.1.1.1.1 stock used in the transfections. It is possible that a secondary recombinant was indeed produced as a result of homologous recombination during the transfection. However, if contaminating wild-type virus

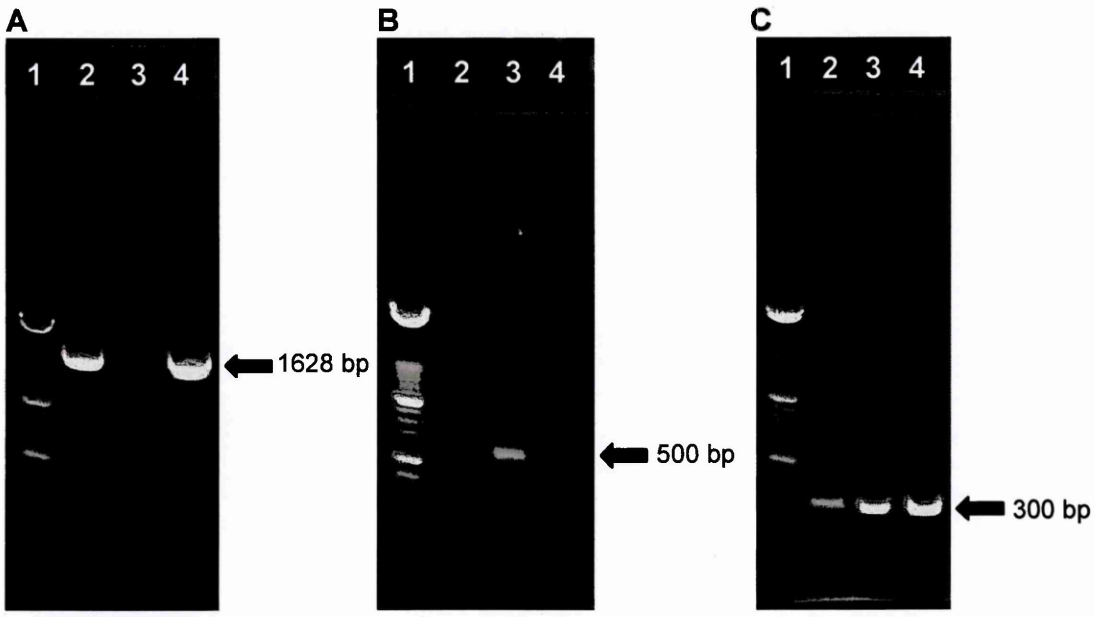

Figure 4.3 Screening of the Null Secondary Recombinant by PCR

A PCR for A26L (1628 bp) using primers A and E4. Lane 1 – 100 bp ladder; lane 2 – wt VACV IHD-J; lane 3 – vIδA26L1.1.1.1.1; lane 4 – null recombinant.

B PCR for EcoGPT (500 bp) using primers GPT1 and GPT2. Lane 1 – 100 bp ladder; lane 2 – wt VACV IHD-J; lane 3 – vIδA26L1.1.1.1.1; lane 4 – null recombinant.

C PCR for A27L (300 bp) using primers A27LF and A27LR. Lane 1 – 100 bp ladder; lane 2 – wt VACV IHD-J; lane 3 – vIδA26L1.1.1.1.1; lane 4 – null recombinant.

was present, this would be likely to rapidly amplify during the reverse selection against *Eco*GPT expression, and this would explain the data in Figure 4.3A.

This data casts doubt upon the validity of the other secondary recombinants, and suggests the very real possibility that they may in fact be contaminating wild-type virus that has survived below the level of PCR detection in parental vIδA26L1.1.1.1.1 cultures. It would be difficult to determine whether the isolated viruses were true secondary recombinants, in particular a revertant, which was designed to be genetically identical to wild-type VACV IHD-J.

Although vIδA26L1.1.1.1.1 used in the transfections had undergone 5 rounds of plaque purification by limiting dilution, PCRs to detect A26L were negative and A26 could not be detected by Western blotting, it must nevertheless be concluded that wild-type virus had survived as a vanishingly small population in the vIδA26L1.1.1.1.1 stock. To examine this possibility, viral DNA was extracted from the vIδA26L1.1.1.1.1 stock used in the transfections, and the PCRs repeated for A26L, A27L and *Eco*GPT (Figure 4.4). This confirmed the apparent absence of A26L in the virus stock, and so the quantity of contaminating wild-type VACV IHD-J must be below the level of sensitivity of the PCR.

At this point it was decided to carry out a further round of plaque purification of vIδA26L1.1.1.1.1 to try to eliminate the remaining wild-type VACV IHD-J and to repeat the transfection experiments for each construct using this virus.

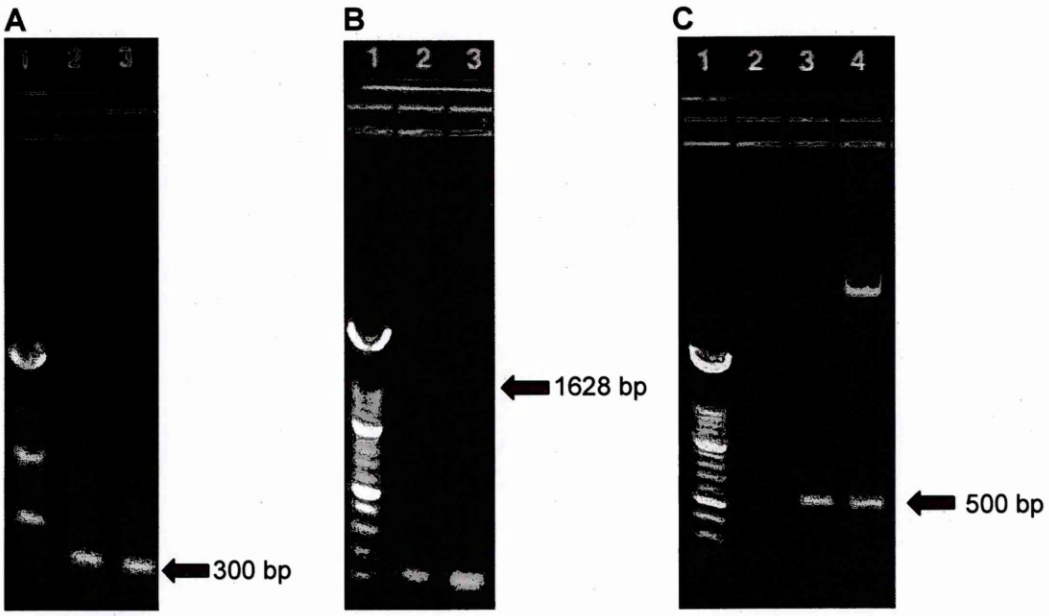

Figure 4.4 Screening of Extracted DNA from vIδA26L1.1.1.1.1 Stock by PCR

A PCR for A27L (300 bp) using primers A27LF and A27LR. Lane 1 – 100 bp ladder; 2 – wt VACV IHD-J; 3 – vIδA26L1.1.1.1.1.

B PCR for A26L (1628 bp) using primers A and E4. Lane 1 – 100 bp ladder; 2 – wt VACV IHD-J; 3 – vIδA26L1.1.1.1.1.

C PCR for *Eco*GPT (500 bp) using primers GPT1 and GPT2. Lane 1 – 100 bp ladder; 2 – wt VACV IHD-J; 3 – vIδA26L1.1.1.1.1; 4 – p1107.

4.2.3 Repeat Plaque Purification of vIδA26L1.1.1.1.1

Quantification of the parental clone vIδA26L1.1.1.1.1 used in the transfections in this chapter was repeated and a further round of plaque purification by limiting dilution performed, to try to remove final traces of wild-type VACV IHD-J. This was done as previously described in section 2.6.2, and resulted in the isolation of 5 clones. Viral DNA was extracted and PCRs to confirm the absence of the A26L gene and the presence of the *Eco*GPT gene were carried out (Figure 4.5).

The absence of the A26 protein was also confirmed in each clone by Western blot using polyclonal rabbit antisera raised against A26 protein (courtesy of Dr D.O. Ulaeto) (Figure 4.6A). The Western blot in Figure 4.6B demonstrates that similar concentrations of viral proteins were loaded per sample by probing with mouse antisera from raised against the Lister strain of VACV (courtesy of Amanda Phelps).

4.2.3.1 MPA Inhibits Replication of wt VACV-IHD-J

To investigate the inhibition of replication provided by culturing viruses in reduced concentrations of MPA medium, ~1 x 10^5 pfu per ml of vIδA26L1.1.1.1.1 or VACV IHD-J was titrated in RK13 cells in the presence of 1 x MPA medium, 0.1x MPA medium or in the absence of drug. Replication of vIδA26L1.1.1.1.1 in cultures appeared to be similar in both the presence and absence of drug as expected, although with a slight inhibition when cultured in 1x MPA medium (Figure 4.7).

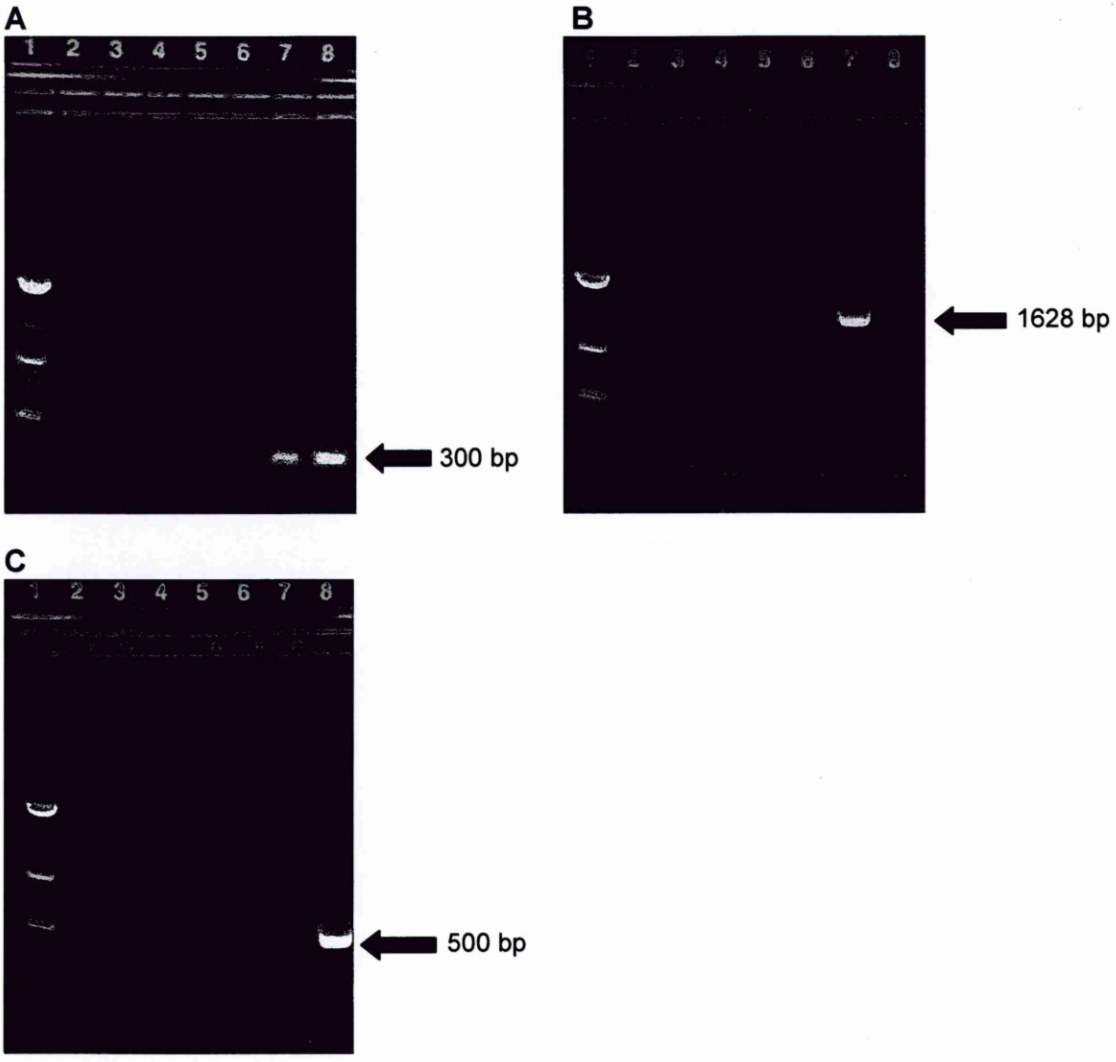

Figure 4.5 Screening by PCR of Extracted Viral DNA from Repeat Plaque Purified Clones Derived from vIδA26L1.1.1.1.1

A PCR for A27L (~300 bp) using primers A27LF and A27LR. Lane 1 – 100 bp ladder; 2 – clone vIδA26L1.1.1.1.1.1; 3 – clone vIδA26L1.1.1.1.1.2; 4 – clone vIδA26L1.1.1.1.1.3; 5 – clone vIδA26L1.1.1.1.1.4; 6 – clone vIδA26L1.1.1.1.1.5; 7 – wt VACV IHD-J; 8 – vIδA26L1.1.1.1.1.

B PCR for A26L (~1628 bp) using primers A and E4. Lane 1 – 100 bp ladder; 2 – clone vIδA26L1.1.1.1.1.1; 3 – clone vIδA26L1.1.1.1.1.2; 4 – clone vIδA26L1.1.1.1.1.3; 5 – clone vIδA26L1.1.1.1.1.4; 6 – clone vIδA26L1.1.1.1.1.5; 7 – wt VACV IHD-J; 8 – vIδA26L1.1.1.1.1.

C PCR for *Eco*GPT (~500 bp) using primers GPTF and GPTR. Lane 1 – 100 bp ladder; 2 – clone vlδA26L1.1.1.1.1.1; 3 – clone vlδA26L1.1.1.1.1.2; 4 – clone vlδA26L1.1.1.1.1.3; 5 – clone vlδA26L1.1.1.1.1.4; 6 – clone vlδA26L1.1.1.1.1.5; 7 – wt VACV IHD-J; 8 – vlδA26L1.1.1.1.1.

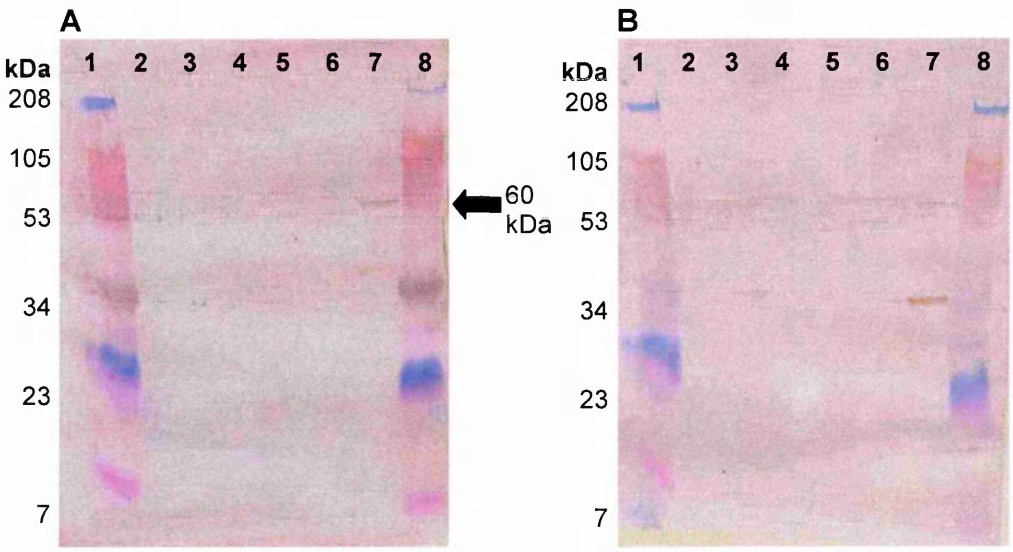

Figure 4.6 Detection of A26 by Immunoblotting in Repeat Plaque Purified Clones Derived from vIδA26L1.1.1.1.1

A A26 was detected by Western blotting analysis of clones using α-4c rabbit sera. Lane 1 – marker; 2 – clone vIδA26L1.1.1.1.1.1; 3 – clone vIδA26L1.1.1.1.1.2; 4 – clone vIδA26L1.1.1.1.1.3; 5 – clone vIδA26L1.1.1.1.1.4; 6 – clone vIδA26L1.1.1.1.1.5; 7 – wild-type VACV IHD-J; 8 – marker.

B VACV proteins were detected by Western blotting analysis of clones using α-Lister mouse sera to demonstrate equal loading. Lane 1 – marker; 2 – clone vIδA26L1.1.1.1.1.1; 3 – clone vIδA26L1.1.1.1.1.2; 4 – clone vIδA26L1.1.1.1.1.3; 5 – clone vIδA26L1.1.1.1.1.4; 6 – clone vIδA26L1.1.1.1.1.5; 7 – wild-type VACV IHD-J; 8 – marker.

A vIδA26L1.1.1.1.1.1 no drug

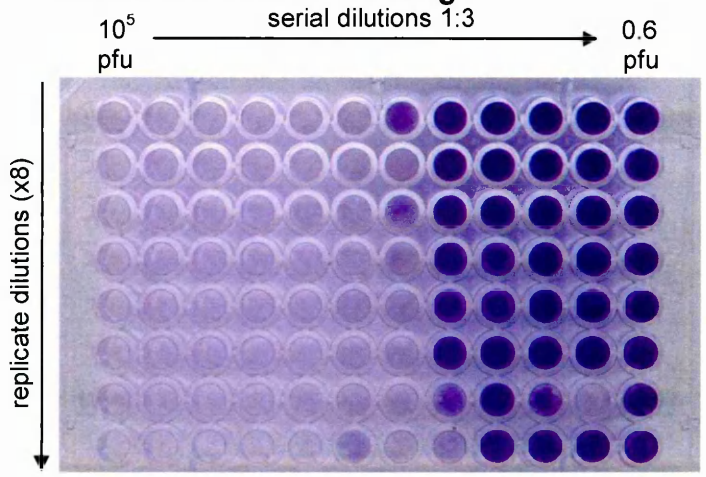

B vIδA26L1.1.1.1.1.1 1x MPA medium

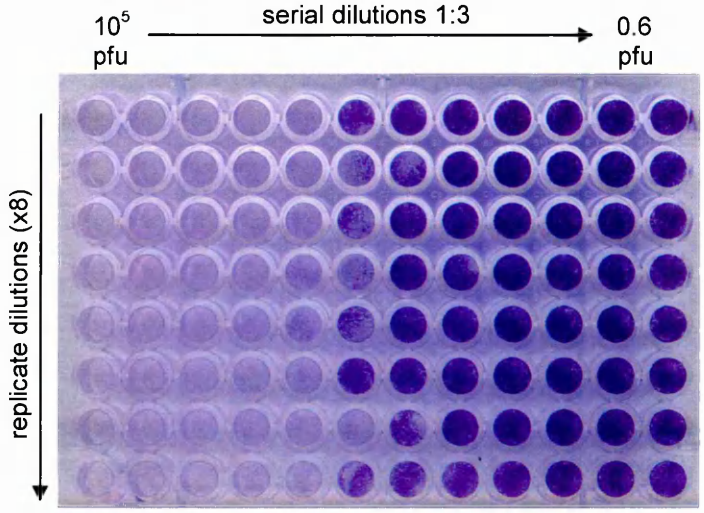

C vIδA26L1.1.1.1.1.1 0.1x MPA medium

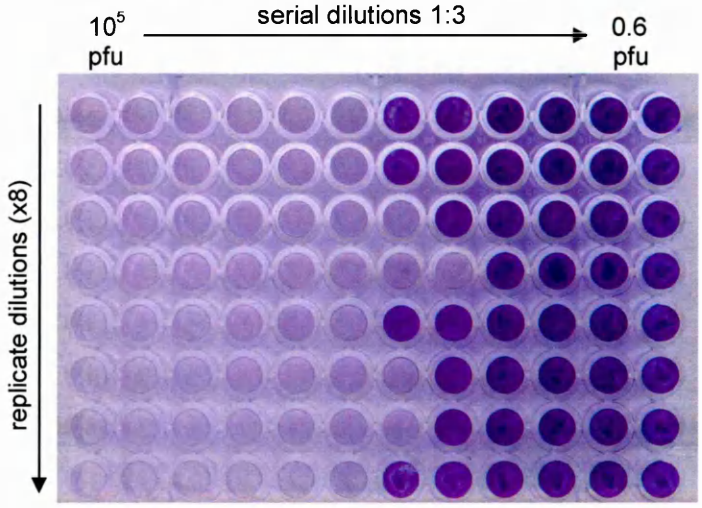

Figure 4.7 Titration of vIδA26L1.1.1.1.1 in the Presence of MPA in RK13 cells

~10^5 pfu vIδA26L1.1.1.1.1 was serially diluted 1:3 across a 96-well tissue culture plate. 50µl was transferred to corresponding wells seeded with RK13 cells. Wells were topped up with 50µl DMEM (**A**); 50µl MPA medium to give final concentrations of 1x (**B**) and 0.1x (**C**) and incubated for 5 days at 37 °C, 5 % CO_2 before fixing to final concentration (v/v) 1 % formalin and staining with 1 % crystal violet.

Cell death was apparent in the presence of 1x MPA around the edges of the wells indicating the toxic effect of the drug at this concentration. Conversely, replication of VACV IHD-J appeared to be dramatically inhibited in both 1x and 0.1x MPA compared to growth in the absence of drug (Figure 4.8). At the higher concentrations of VACV IHD-J, there is evidence of viral replication and this was confirmed using a light microscope to inspect the monolayers more closely. There did appear to be more replication occurring in the presence of 0.1x MPA compared to 1x MPA. To quantify this, plates were scanned on a 96-well plate reader at an absorbance of 570 nm (Figure 4.9A). In vIδA26L1.1.1.1.1 there was approximately 0.5 log reduction in virus replication in the presence of 1x MPA compared to in 0.1x MPA and no drug. Interestingly, there is approximately 1 log reduction in replication of VACV IHD-J in the presence of 1x MPA and 0.5 log reduction in the presence of 0.1x MPA, compared to in the absence of drug (Figure 4.9B). The experiments were repeated to confirm these findings and again replication of VACV IHD-J was inhibited in the presence of MPA as seen in the first experiments. This demonstrated that MPA was able to inhibit replication of wild-type VACV IHD-J at concentrations of approximately 10^2-10^3 pfu or less, and there was little difference between the inhibitory effect of 1x and 0.1x MPA.

4.2.3.2 Culture of New Clones Derived from vIδA26L1.1.1.1.1 in MPA and 6-TG

Differential titres of these clones in the presence and absence of 0.1x MPA demonstrated that MPA resistant viruses represented the majority of the viruses in culture (Table 4.1A). The slight reduction in titre in the presence of MPA may be

A wt VACV IHD-J no drug

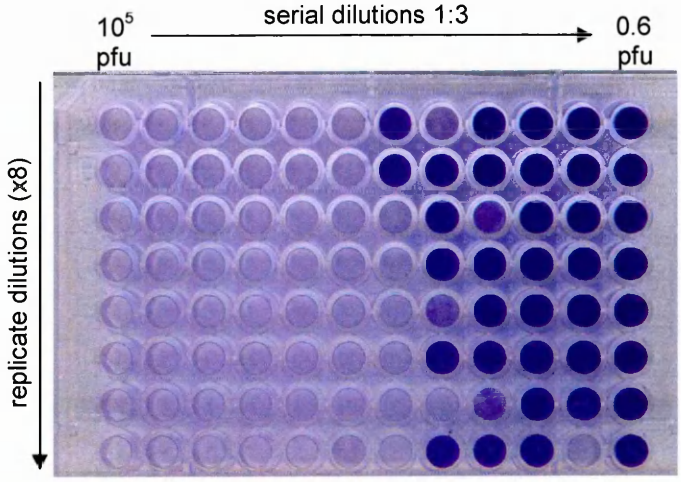

B wt VACV IHD-J 1x MPA medium

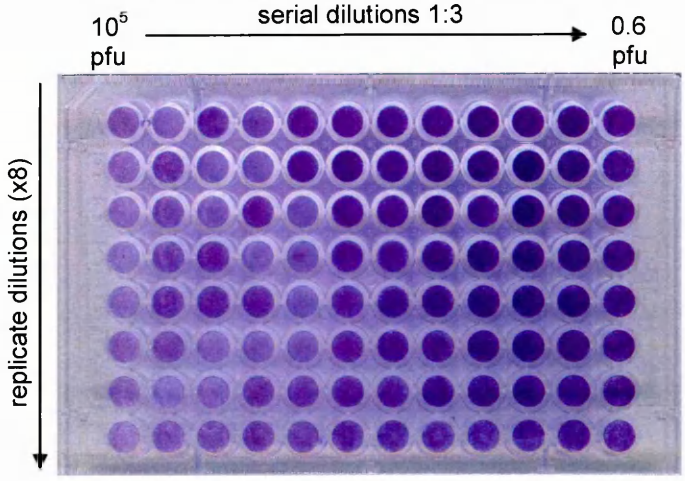

C wt VACV IHD-J 0.1x MPA medium

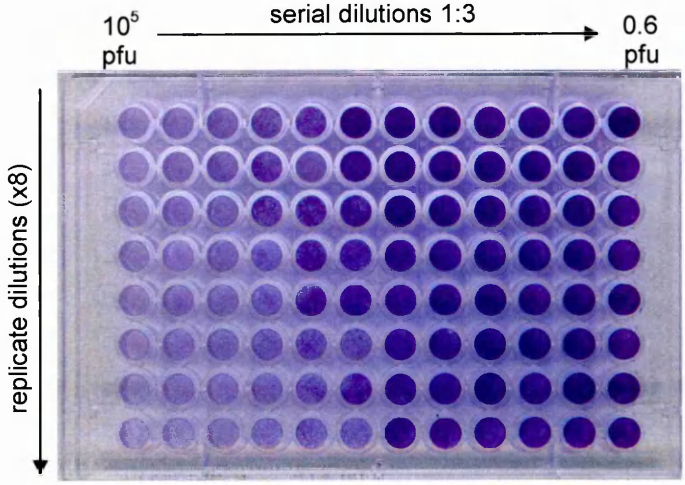

Figure 4.8 Titration of VACV IHD-J in the Presence of MPA in RK13 cells

~10^5 pfu VACV IHD-J was serially diluted 1:3 across a 96-well tissue culture plate. 50 µl was transferred to corresponding wells seeded with RK13 cells. Wells were topped up with 50 µl DMEM (**A**); 50 µl MPA medium to give final concentrations of 1x (**B**) and 0.1x (**C**) and incubated for 5 days at 37 °C, 5 % CO_2 before fixing to final concentration (v/v) 1 % formalin and staining with 1 % crystal violet.

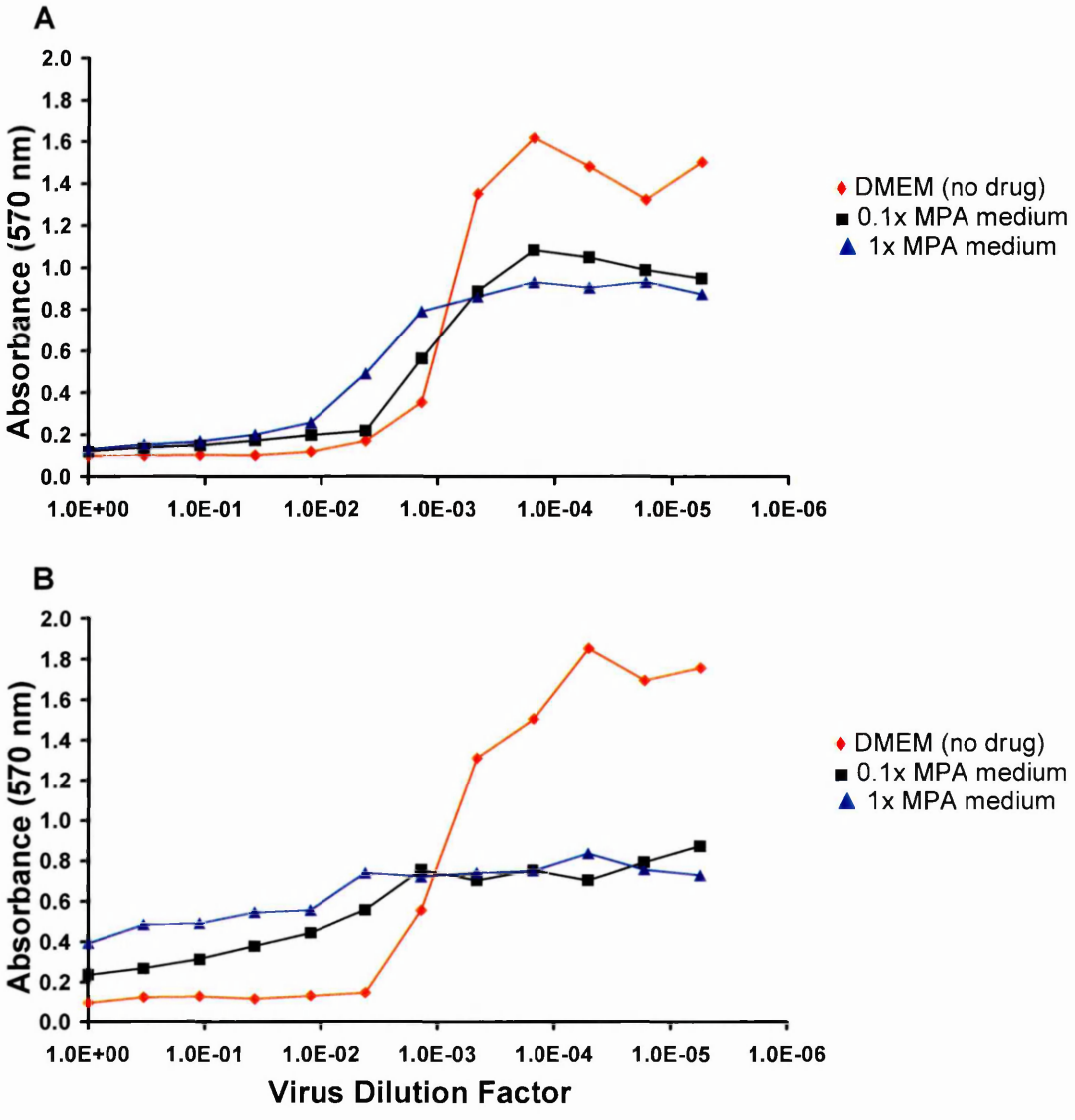

Figure 4.9 Absorbance (570 nm) of Differential Titrations of vIδA26L1.1.1.1.1 and VACV IHD-J

~10^5 pfu vIδA26L1.1.1.1.1 (**A**) and ~10^5 pfu VACV IHD-J (**B**) was serially diluted 1:3 across a 96-well tissue culture plate. 50 µl was transferred to corresponding wells seeded with RK13 cells. Wells were topped up with 50 µl DMEM (♦), or 50 µl MPA medium to give final concentrations of 0.1x (■) and 1x (▲) and incubated for 5 days at 37 °C, 5 % CO_2 before fixing to final concentration (v/v) 1 % formalin and staining with 1 % crystal violet. Plates were scanned on a Titretek multiskan plus MKII plate reader and the absorbance at 570 nm recorded.

A No selection

Clone	No selection ($TCID_{50}$/ml)	MPA ($TCID_{50}$/ml)	Differential (%)
vIδA26L1.1.1.1.1.1	$2.62x10^6$	$1.47x10^6$	56
vIδA26L1.1.1.1.1.2	$4.92x10^6$	$2.43x10^6$	49
vIδA26L1.1.1.1.1.3	$3.98x10^6$	$1.5x10^6$	38
vIδA26L1.1.1.1.1.4	$3.97x10^6$	$4.46x10^6$	112
vIδA26L1.1.1.1.1.5	$5.64x10^6$	$3.31x10^6$	59

B 6-TG Selection Passage 1

Clone	No selection ($TCID_{50}$/ml)	MPA ($TCID_{50}$/ml)	Differential (%)
vIδA26L1.1.1.1.1.1	$2.1x10^6$	$1.48x10^5$	7
vIδA26L1.1.1.1.1.2	$1.66x10^6$	$2.73x10^5$	16
vIδA26L1.1.1.1.1.3	$1.79x10^6$	$3.1x10^5$	17
vIδA26L1.1.1.1.1.4	$1.33x10^6$	$1.84x10^5$	14
vIδA26L1.1.1.1.1.5	$1.18x10^6$	$1.02x10^5$	9

C 6-TG Selection Passage 2

Clone	No selection ($TCID_{50}$/ml)	MPA ($TCID_{50}$/ml)	Differential (%)
vIδA26L1.1.1.1.1.1	$2.51x10^7$	$9.55x10^6$	38
vIδA26L1.1.1.1.1.2	$6.68x10^6$	$2.99x10^6$	45
vIδA26L1.1.1.1.1.3	$2.46x10^7$	$6.25x10^6$	25
vIδA26L1.1.1.1.1.4	$8.19x10^6$	$2.1x10^6$	26
vIδA26L1.1.1.1.1.5	$6.08x10^6$	$2.29x10^6$	38

D 6-TG Selection Passage 3

Clone	No selection ($TCID_{50}$/ml)	MPA ($TCID_{50}$/ml)	Differential (%)
vIδA26L1.1.1.1.1.1	$1.29x10^6$	$1.95x10^5$	15
vIδA26L1.1.1.1.1.2	$7.39x10^5$	$7.42x10^4$	10
vIδA26L1.1.1.1.1.3	$5.97x10^6$	$2.63x10^5$	4
vIδA26L1.1.1.1.1.4	$2.46x10^6$	$2.59x10^5$	10
vIδA26L1.1.1.1.1.5	$3.17x10^6$	$3.04x10^5$	10

Table 4.1 Virus Titres of Repeat Plaque Purified Clones Derived from vIδA26L1.1.1.1.1

Virus was quantitated by Reed-Muench limiting dilution analysis in RK13 cells in the presence and absence of MPA selection. The differential is the titre in selection medium as a percentage of the titre in non-selective medium. **A** Virus titres of clones from plaque purification cultures. **B** Virus titres of clones from 1st passage in 0.1 mM 6-TG in STO cells. **C** Virus titres of clones from 2nd passage in 0.1 mM 6-TG in STO cells. **D** Virus titres of clones from 3rd passage in 0.1 mM 6-TG in STO cells.

due to the toxic effects of MPA on the cells that may impact on the efficiency of replication of virus and perhaps the burden of expression of *Eco*GPT leading to a decrease in viral yield.

To confirm the absence of VACV IHD-J in these stocks, clones were cultured in STO cells in the presence of 0.1 mM 6-TG and differential titres obtained in the presence of 0.1 x MPA medium. If the clones could undergo sequential passage where virus was unable to grow in the presence of 6-TG they would be likely to be free from wild-type VACV IHD-J. STO cells were infected at low MOI and incubated for 48 or 72 hours as described in section 2.6.1.

In the first passage, no growth was observed in the presence of drug, compared to 100 % CPE observed in the absence of drug. The differential titres showed between only 7-17 % of virus was MPA-resistant following 1 round of negative selection in 6-TG: much lower than anticipated (Table 4.1B). In the second and third passages of 6-TG selection, 100 % CPE was observed for each clone in the presence and absence of 6-TG. The differential titres demonstrated a reduction in MPA resistant virus in each clone (Table 4.1C and D). This suggested that 6-TG was effectively inhibiting the replication of *Eco*GPT-expressing recombinants represented by reduced quantities of virus when titrated in MPA medium, yet in the absence of MPA medium overall numbers of virus were not reduced. It is possible that the replicating virus maybe contaminating wild-type virus that increased when MPA selection was removed, or perhaps 6-TG selection was overcome by *Eco*GPT positive virus, although there was no evidence of this in the first passage.

PCRs of extracted viral DNA from the third round of passage in 6-TG demonstrated that 2 out of the 5 clones contained the A26L gene and therefore were contaminated with wild-type virus, and all clones were found to have the *Eco*GPT gene (Figure 4.10). This suggests that clones vIδA26L1.1.1.1.1.3 and vIδA26L1.1.1.1.1.4 are mixed species, although the levels of wild-type virus in these clones may be considered low, as weak signals for the A26L gene could only be detected following 3 rounds of reverse selection. This does not explain why clones absent of wild-type virus were also able to replicate in these cultures. It is possible that selective pressure has caused a mutation in the *Eco*GPT gene in these clones which results in an inactive gene product, allowing replication in the presence of 6-TG. To confirm this, the *Eco*GPT region from each clone could be sequenced to look for mutations in the DNA sequence.

4.3 Discussion

The construction and isolation of a panel of secondary recombinant VACVs was attempted using reverse *Eco*GPT selection in this study as it has several advantages over other selection methods. Positive selection is an effective selective strategy to obtain recombinant viruses however, construction of these viruses that contain selection marker genes to enable their isolation from wild-type or parental viruses is not ideal, and these selection marker genes may affect the phenotype in the resulting recombinant virus. Generation of secondary recombinant viruses without selection marker genes using reverse *Eco*GPT selection would be advantageous for potential vaccine candidates, and would

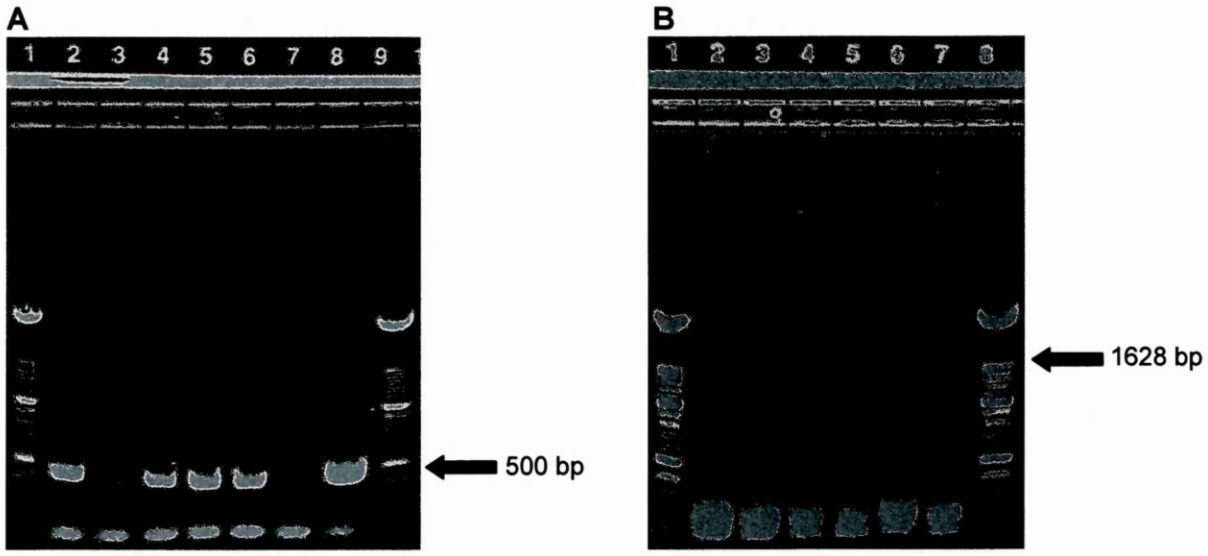

Figure 4.10 Screening by PCR of Repeat Plaque Purified Clones Derived from vIδA26L1.1.1.1.1 Following 3 Rounds of Reverse *Eco*GPT Selection in STO cells + 0.1 mM 6-TG

A PCR for EcoGPT (500 bp) using primers GPT1F and GPTR. Lane 1 – 100 bp ladder; 2 – clone vIδA26L1.1.1.1.1.1; 3 – clone vIδA26L1.1.1.1.1.2; 4 – clone vIδA26L1.1.1.1.1.3; 5 – clone vIδA26L1.1.1.1.1.4; 6 – clone vIδA26L1.1.1.1.1.5; 7 – wt VACV IHD-J; 8 – vIδA26L1.1.1.1.1; 9 – 100 bp ladder.

B PCR for A26L (1628 bp) using primers A and E4. Lane 1 – 100 bp ladder; 2 – clone vIδA26L1.1.1.1.1.1; 3 – clone vIδA26L1.1.1.1.1.2; 4 – clone vIδA26L1.1.1.1.1.3; 5 – clone vIδA26L1.1.1.1.1.4; 6 – clone vIδA26L1.1.1.1.1.5; 7 – wt VACV IHD-J; 8 – 100 bp ladder.

eliminate the possibility that these genes may have phenotypic effects. Other selection methods such as insertional inactivation of the TK gene allows isolation of TK-negative viruses in the presence of bromodeoxyuridine (BrdU), however, spontaneous TK-negative mutants can occur and inactivation of the TK gene results in attenuation *in vivo* (92;352;353).

Alternative methods that allow initiation of expression of genes using inducible promoters such as the TET- and lac- repressor/operator systems were considered for use in this study (173;354;355). These would result in the construction of a secondary recombinant virus where A26L is re-inserted into it original locus under the control of an inducible promoter. The phenotype of the proposed recombinants in this study could have been studied by inducing expression of A26L at various points in the replicative cycle to try to understand the relationship between IMV and EV maturation. These systems are notoriously leaky, and complete repression of a gene of interest is virtually impossible. Due to this, the use of inducible promoter systems was not considered further.

As demonstrated in this study, the reverse *Eco*GPT selection method also appears to have limitations. This method allows the growth of all non-*Eco*GPT-expressing virus, including wild-type VACV. Following serial rounds of propagation of virus in 6-TG treated cultures, the isolated viruses, including the null mutant, were found to contain the A26L gene when the DNA was assessed by PCR. This strongly suggested that these viruses were not *bona fide* recombinants but were contaminating wild-type virus. It is likely that the undetectable residual wild-type virus present in the vIδA26L1.1.1.1.1 stock, used as the parent strain in this study,

was able to propagate during the rounds of 6-TG selection, thus resulting in a population of VACV that contained the A26L gene. Even after a further round of plaque purification, the new clones derived from vIδA26L1.1.1.1.1 still contained traces of wild-type virus. This may be due to the particle/pfu ratio (reported as between 12.7 to 64.6 virions) (121), where a plaque undoubtedly will arise from more than one virus particle, and so conceivably a truly pure population of recombinant VACV is unobtainable. If this is the case, purification by either the plaque picking or by the limiting dilution method is unlikely to be more favourable than the other, as both rely on plaque formation. In addition, the methodology reported by Isaacs *et al.* (1990) has been adapted in this study to first enrich for putative secondary recombinant VACV thus reducing the quantities of parental virus prior to plaque purification. In Isaacs and colleagues study, plaque purification by plaque picking in STO cells in the presence of 6-TG commenced immediately following the transfection and infection event. It is unlikely that these changes would negatively affect the success of this method, as the enrichment step used in this study was intended as an enhancement to the reported method.

Interestingly in the study, repeated passage of *Eco*GPT-expressing VACV resulted in 6-TG resistant VACV. Some of these viruses were proven to be a mixture of vIδA26L1.1.1.1.1 and wild-type VACV as they contained both the *Eco*GPT and A26L genes, however some of these viruses contained the *Eco*GPT only. It is possible that the *Eco*GPT gene was mutated in these viruses due to selective pressure, thus enabling replication in 6-TG treated cultures. Spontaneous deletion of or random mutations in positive selection marker genes such as

*Eco*GPT in VACV, to our knowledge, has not been reported prior to or during the course of this study. This may be due the fact that reverse *Eco*GPT selection is not widely utilised for the construction of recombinant VACV, and although mutations are likely to occur quite frequently, they may only be highlighted during reverse *Eco*GPT selection in instances such as these. Definitive proof of this would require DNA sequencing of the *Eco*GPT gene in each of these viruses to determine mutations of the coding sequence.

In conclusion, success of the reverse *Eco*GPT method for generation of secondary recombinant VACV has been shown to be dependent on the purity of the stocks of the parent strain as all non-*Eco*GPT-expressing viruses will propagate using this method. The possibility of mutation of the *Eco*GPT gene due to selective pressure should also be considered. It is likely that secondary recombinant viruses were generated throughout this study, however, due to the low frequency of a recombination event, recombinant viruses were unable to compete with the residual wild-type virus that propagated from vIδA26L1.1.1.1.1 parent strain stocks in the presence of 6-TG.

5 Generation of Secondary Recombinant Viruses using a Positive Selection Method: neomycin resistance

5.1 Introduction

Deletion of the A26L gene in VACV has provided insight into the mechanisms by which IMV is produced during the infectious cycle. However, formal proof of this requires the construction of a revertant virus and a secondary A26L deletion mutant, replacing the *Eco*GPT gene with an alternative dominant selectable marker gene. In addition to this, a third recombinant VACV was designed to express the A26L gene constitutively where overexpression of A26 may result in increased production of IMV, reducing the numbers of virions available for wrapping, thus reducing EV formation.

In this study, the $G418^R$ gene was introduced into vIδA26L1.1.1.1.1.1 (section 4.2.3) to create a panel of secondary recombinant VACVs. $G418^R$ confers resistance to Geneticin® (G418, neomycin), an aminoglycoside antibiotic that inhibits eukaryotic protein synthesis by interfering with 80s ribosome function (356). VACV replication is essentially blocked and visible plaque formation is inhibited in cultures supplemented with 2 mg/ml Geneticin®, where the extent of inhibition can be increased by pre-treating cells with Geneticin® prior to infection (357). This is likely due to a reduction in the expression of a subset of late viral genes, however it is unclear whether the effect is at the translational or post-translational level (357). No equivalent enzymatic activity exists in eukaryotic systems therefore spontaneous G418-resistant mutants are highly unlikely to occur. Inhibition can only be overcome by introducing the $G418^R$ gene into the VACV genome, therefore

this dominant selectable marker can be used to isolate recombinant virus and rapidly reduce the quantities of parental virus. This positive selection method introduces another foreign gene ($G418^R$) for which the experimental control is its presence in all secondary recombinant VACVs in this study, and precludes problems associated with negative selection such as reverse GPT selection (349) and insertion into non-essential genes such as the TK gene (358).

All constructs were designed to utilise the *Eco*GPT gene as flanking regions to facilitate homologous recombination into the original A26L locus in vIδA26L1.1.1.1.1.1. Recombination events will result in a deletion of a 350 bp internal region of the *Eco*GPT gene, replacing it with the $G418^R$ gene expressed from a synthetic early/late promoter (327), linked to the A26L gene and its engineered attendant promoter sequence.

5.1.1 Aims of This Study

To design and construct a panel of secondary recombinant VACVs to a) re-insert the A26L gene into its original locus thus creating a revertant; b) replace the *Eco*GPT gene with a different selection marker gene, $G418^R$ and c) constitutively express the A26L gene from a synthetic early/late promoter. These recombinants will be used to confirm the earlier findings in this study, and may provide further insight into the formation and function of IMV, where modulation of A26 may result in an attenuated VACV strain that could be used to develop a safer alternative to current smallpox vaccines.

5.2 Results

5.2.1 Design of Recombination Cassettes

A construct was designed to re-insert the A26L gene expressed from its native promoter (using WR sequence as described in Chapter 4) into the original locus in vIδA26L1.1.1.1.1.1, where the *Eco*GPT gene had been previously inserted, and thus create a revertant recombination cassette (Figure 5.1A). The recombination cassette was designed so that recombination was facilitated by upstream flanking (UF) and downstream flanking (DF) regions homologous to the first and last 50 residues of the *Eco*GPT gene situated at the 5'- and the 3'- ends of the construct; this would insertionally inactivate *Eco*GPT. The construct also contained the $G418^R$ gene expressed from a synthetic early/late promoter (327) that confers resistance to Geneticin® allowing for positive selection (357). Expression of A26L should occur at late times during the infectious cycle to restore the wild-type phenotype.

To generate the secondary A26L deletion mutant, a construct was designed to re-insert a disrupted A26L gene (disrupted by introducing a frameshift mutation at position 4, and stop codons throughout the sequence at positions 226, 484, 832, 1069 and 1324), where a promoter sequence upstream of the gene was absent (Figure 5.1B). As in the revertant, this construct was designed to be inserted into the original A26L locus in vIδA26L1.1.1.1.1.1, facilitated by UF and DF regions homologous to the *Eco*GPT gene, and contained the $G418^R$ gene. A26L should not be expressed in this recombinant and the phenotype should reproduce that of the

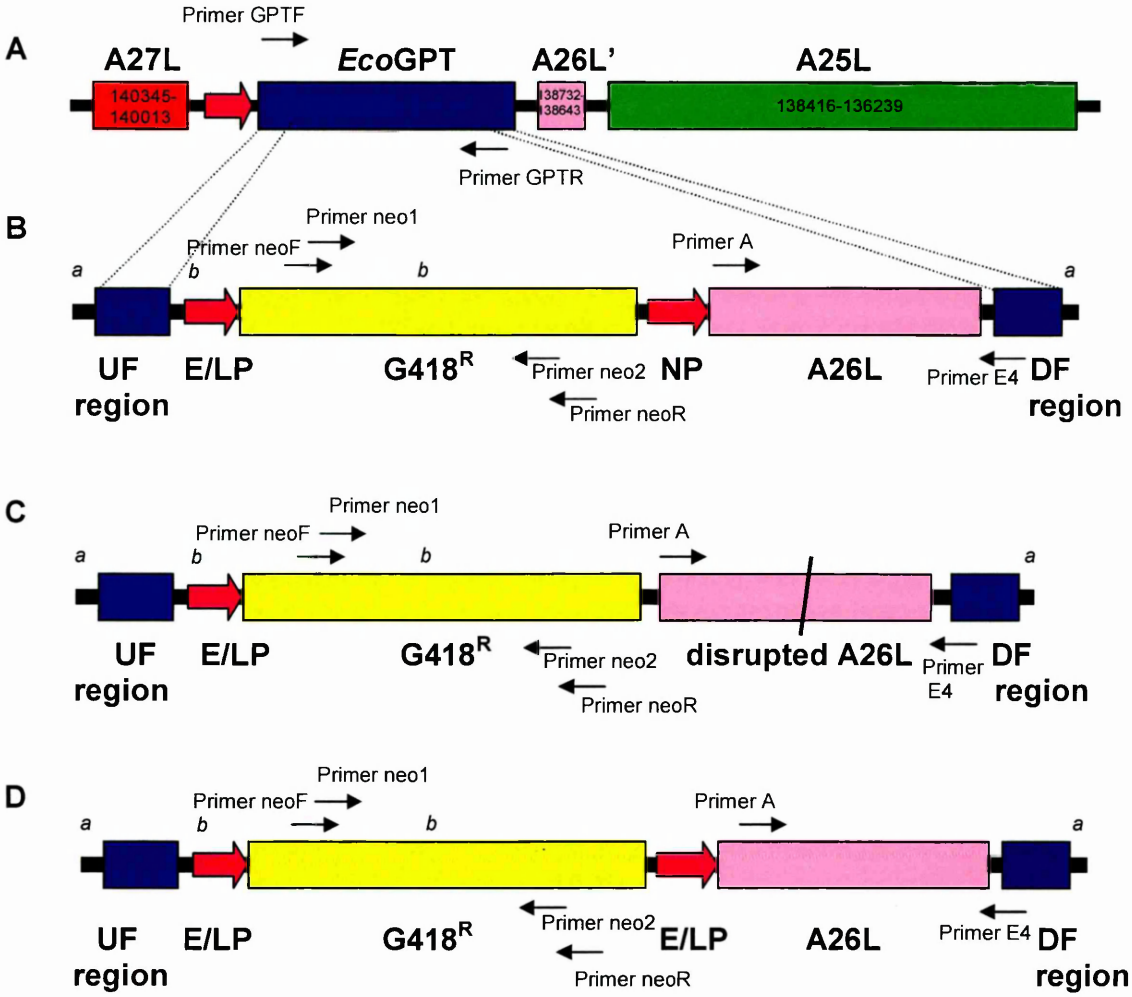

Figure 5.1 Schematic of Secondary VACV Recombination Cassettes for Modulating Expression of A26L

Each construct was synthesised by GeneArt AG (Germany). Upstream flanking (UF) and downstream flanking (DF) regions correspond to the first and last 50 nucleotides of the *Eco*GPT gene respectively, to facilitate homologous recombination with vIδA26L1.1.1.1.1.1 DNA (A). The G418^R gene expressed from a synthetic early/late promoter (E/LP) confers resistance to Geneticin®, allowing positive selection of recombinant viruses (327;357). Constructs B and D were designed to express A26L from its native promoter (NP) for a revertant virus or from a synthetic E/LP (327) for a recombinant VACV that overexpresses A26, respectively. Construct C was designed with no promoter sequence for A26L and a disrupted A26L sequence with engineered stop codons and a

frameshift mutation for a secondary A26L deletion mutant. DNA sequences can be found in Figures A8-10. Positions of primers used for PCR screening purposes are indicated by arrows.

[a] *SmaI* sites were engineered at each end of the construct to facilitate excision of the construct from the plasmid vector if necessary.

[b] *NotI* sites were engineered to facilitate inactivation of $G418^R$ if necessary.

primary deletion mutant, vIδA26L1.1.1.1.1.1. This mutant would act as an internal control to observe the effect, if any, of the presence of selection marker genes.

The final construct was designed to re-insert A26L into the original locus, constitutively expressed from a synthetic early/late promoter (327) to overexpress A26L (Figure 5.1C). As in the revertant and secondary deletion mutant, homologous recombination was facilitated by UF and DF regions homologous to the *Eco*GPT gene, and the construct contained the $G418^R$ gene. It was anticipated that expression of A26L throughout the replicative cycle would result in an abundance of A26 protein and thus increase the proportion of virions maturing as IMV. This would likely result in a concomitant decrease in EV production, and may provide a method to achieve an attenuated VACV with reduced dissemination due to decreased EV production, yet maintained immunogenicity as the two distinct forms of virions are still produced.

These constructs were designed with *Sma*I restriction sites at the 5'- and 3'-ends to facilitate excision of the construct from the plasmid vector, and *Not*I restriction sites upstream of the synthetic early/late promoter of the $G418^R$ gene and within the $G418^R$ gene to allow inactivation of this gene if required.

5.2.2 Construction of Recombination Cassettes

Constructs were synthesised by GeneArt AG (Germany) and supplied as cloned sequences in plasmid vectors conferring ampicillin resistance (Amp^R). Obtaining DNA sequences in this way should guarantee sequence integrity, and

due to the similarity of these sequences, the constructs were 'built' in parallel with relative efficiency and reduced cost.

Plasmids were transformed into TOP10 chemically competent cells (Invitrogen, Ltd) as described in section 2.3.8, and transformants selected for ampicillin resistance encoded by the Amp^R gene. The presence of plasmid was confirmed following extraction from 1 ml bacterial cells (section 2.3.9).

5.2.3 Construction and Selection of Secondary Recombinant Viruses

Purified preparations of each plasmid were transfected into RK13 cells as described in section 2.4.5, and subsequently infected at MOI 0.1 with vIδA26L1.1.1.1.1.1. Putative recombinant virus was enriched and selected for in the presence of Geneticin® (2 mg/ml) (Invitrogen, Ltd), as described in section 3.2.5. for a total of 6 passages. To increase the effect of inhibition, RK13 cells were pre-incubated in Geneticin® (2 mg/ml) for 2 hours prior to infection to allow the drug to penetrate the cells and inhibit protein synthesis (357). A crude stock of each putative recombinant virus was prepared by infecting RK13 cells in a T25 tissue culture flask cultured in Geneticin® (2 mg/ml) for 24 hours.

The inhibitory effect of Geneticin® on G418-negative virus was confirmed using the parental strain vIδA26L1.1.1.1.1.1. RK13 cells were infected at a range of MOIs in the presence and absence of Geneticin®. Replication of virus was reduced in the presence of Geneticin® at low MOI, and following a further 2 passages virus replication was undetected demonstrating the quantity of virus was substantially reduced following serial passage in the presence of 2 mg/ml Geneticin®.

5.2.4 Plaque Purification of a Revertant VACV

Putative revertant virus from passage 6 was plaque purified by limiting dilution analysis (section 2.6.2) in RK13 cells to obtain a pure clonal population of virus. Three rounds of purification by limiting dilution were carried out, followed by a fourth round using a modified plaque titration method by limiting dilution was performed as described in section 2.6.2 (Figure 5.2). This resulted in 3 clones, of which only vIδA26L.rev2.2.3.2 was confirmed as a *bona fide* revertant virus where the *Eco*GPT gene had been replaced by the A26L and $G418^R$ genes (Figure 5.3). A purified stock was prepared of vIδA26L.rev2.2.3.2 cultured in RK13 cells in the presence of Geneticin® as described in section 2.5.2 and virus was quantitated as 3.69×10^9 $TCID_{50}$/ml by Reed-Muench limiting dilution analysis (section 2.5.3).

5.2.5 Plaque Purification of the Secondary A26L Mutant

Putative recombinant virus from passage 6 was plaque purified as for the revertant virus (section 5.2.4), using 4 sequential rounds. To improve the probability of isolating recombinant virus, individual plaques were picked from virus cultures under an agarose overlay for the first 3 rounds (section 2.6.2), followed by a final round using the limiting dilution method (Figure 5.4). This resulted in 5 clones and PCR analysis demonstrated that vIδA26L.neo3.3.3.3 was a *bona fide* recombinant virus where the *Eco*GPT gene had been replaced by a disrupted A26L gene and the $G418^R$ gene (Figure 5.5). A purified stock was prepared of clone 3 cultured in RK13 cells in the presence of Geneticin® as described in

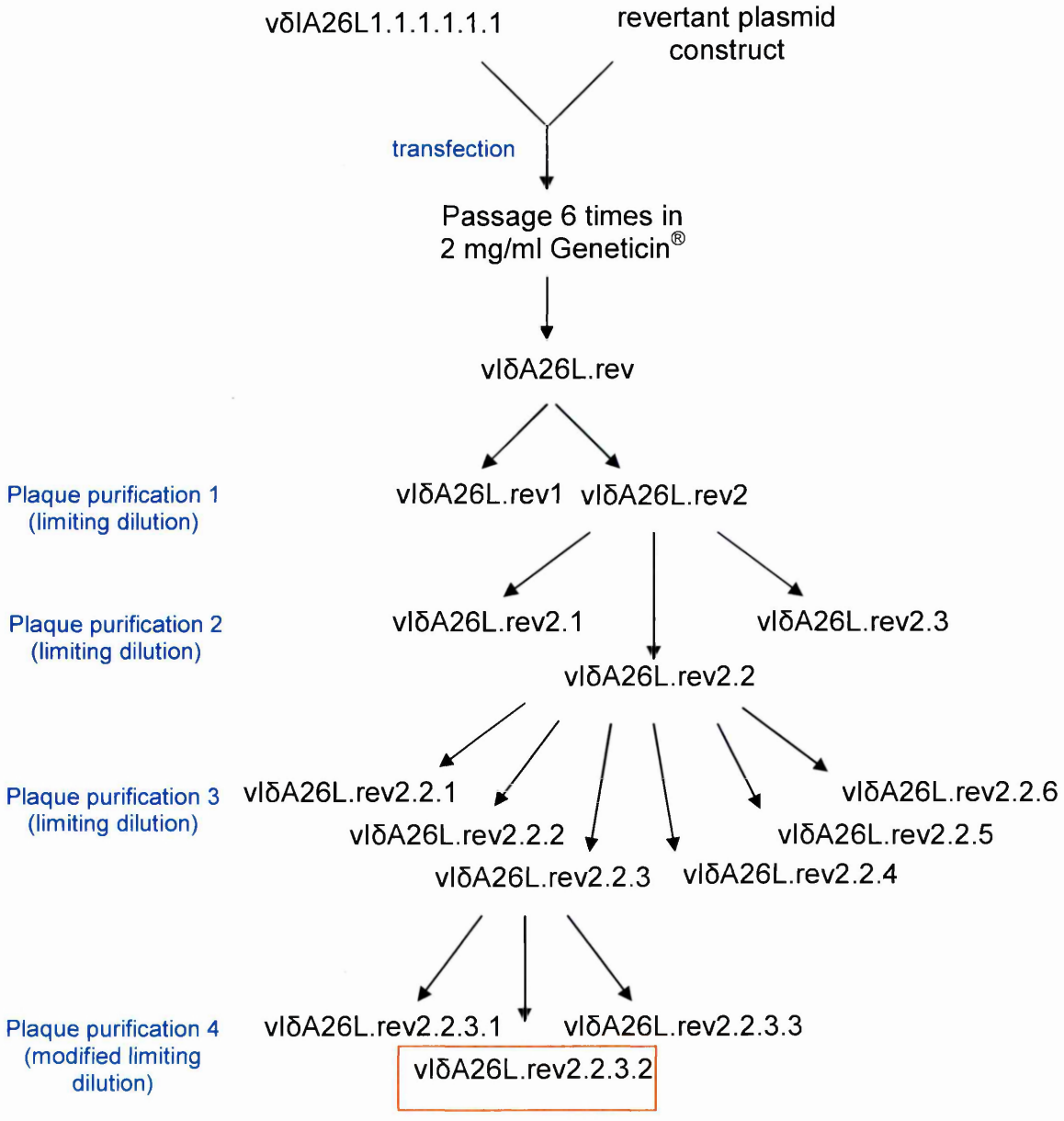

Figure 5.2 Flow Diagram Representing Process of Isolation of Revertant VACV

The revertant virus, denoted here a vIδA26L.rev2.2.3.2, was derived from the parental strain vIδA26L1.1.1.1.1.1 following transfection of cells with the revertant construct (section 5.2.2 and 5.2.3). Putative recombinant virus was isolated following 6 passages in 2 mg/ml Geneticin® and 4 rounds of plaque purification.

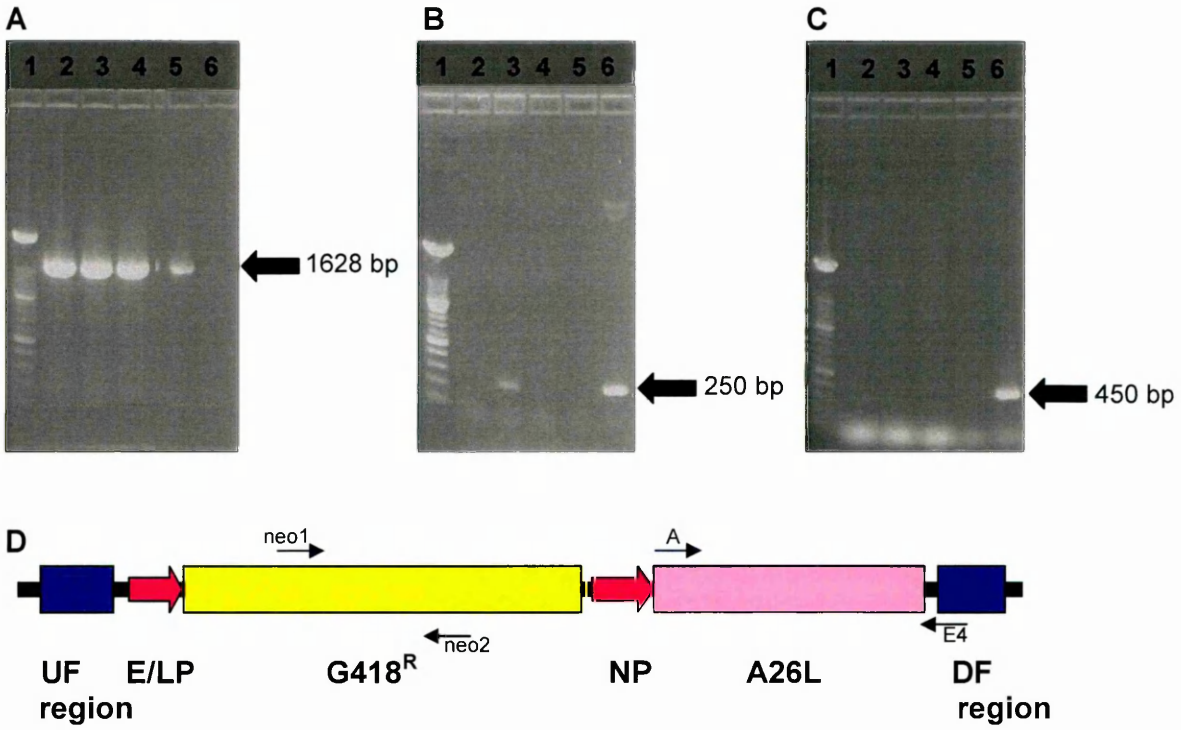

Figure 5.3 Screening of Revertant Clones vIδA26L.rev2.2.3.1, vIδA26L.rev2.2.3.2 and vIδA26L.rev2.2.3.3 by PCR

PCRs were performed for the A26L gene (1628 bp) using primers A and E4 (A), for a region of the G418^R gene (~250 bp) using primers neo1 and neo2 (B) and the *Eco*GPT gene (~450 bp) using GPTF and GPTR (C) on viral DNA extracted of putative revertant clones from plaque purification 4.

A Lane 1 – 100 bp marker; lane 2 – vIδA26L.rev2.2.3.1; lane 3 – vIδA26L.rev2.2.3.2; lane 4 – vIδA26L.rev2.2.3.3; lane 5 – VACV IHD-J DNA; lane 6 – vIδA26L1.1.1.1.1.1 DNA.

B Lane 1 – 100 bp marker; lane 2 – vIδA26L.rev2.2.3.1; lane 3 – vIδA26L.rev2.2.3.2; lane 4 – vIδA26L.rev2.2.3.3; lane 5 – VACV IHD-J DNA; lane 6 – revertant construct (GeneArt plasmid).

C Lane 1 – 100 bp marker; lane 2 – vIδA26L.rev2.2.3.1; lane 3 – vIδA26L.rev2.2.3.2; lane 4 – vIδA26L.rev2.2.3.3; lane 5 – VACV IHD-J DNA; lane 6 – vIδA26L1.1.1.1.1.1 DNA.

D Schematic of the revertant construct. Positions of primers are indicated by arrows.

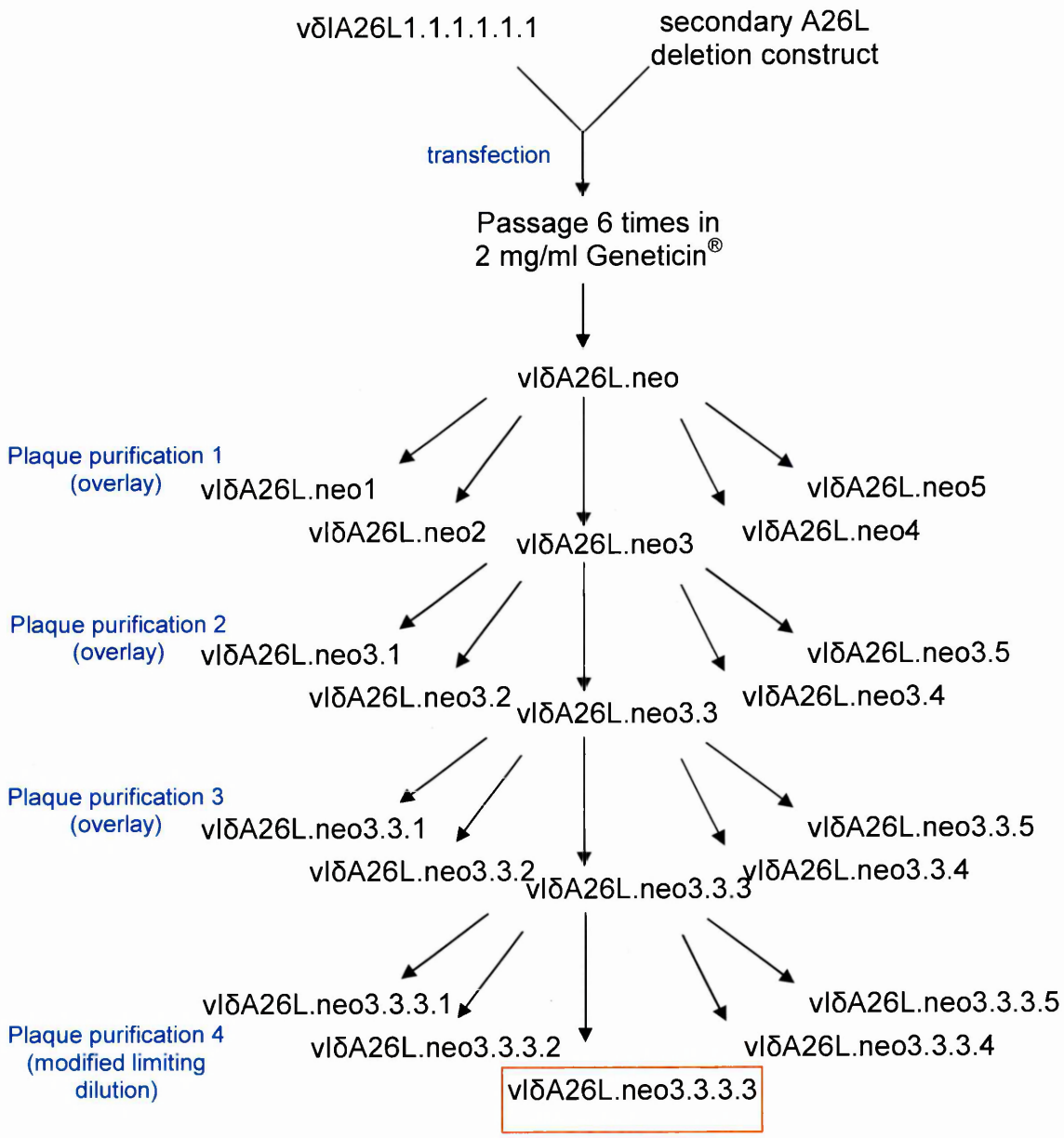

Figure 5.4 Flow Diagram Representing Process of Isolation of Secondary A26L Deletion VACV

The secondary A26L deletion virus, denoted here a vIδA26L.neo3.3.3.3, was derived from the parental strain vIδA26L1.1.1.1.1.1 following transfection of cells with the secondary A26L deletion construct (section 5.2.2 and 5.2.3). Putative recombinant virus was isolated following 6 passages in 2 mg/ml Geneticin® and 4 rounds of plaque purification.

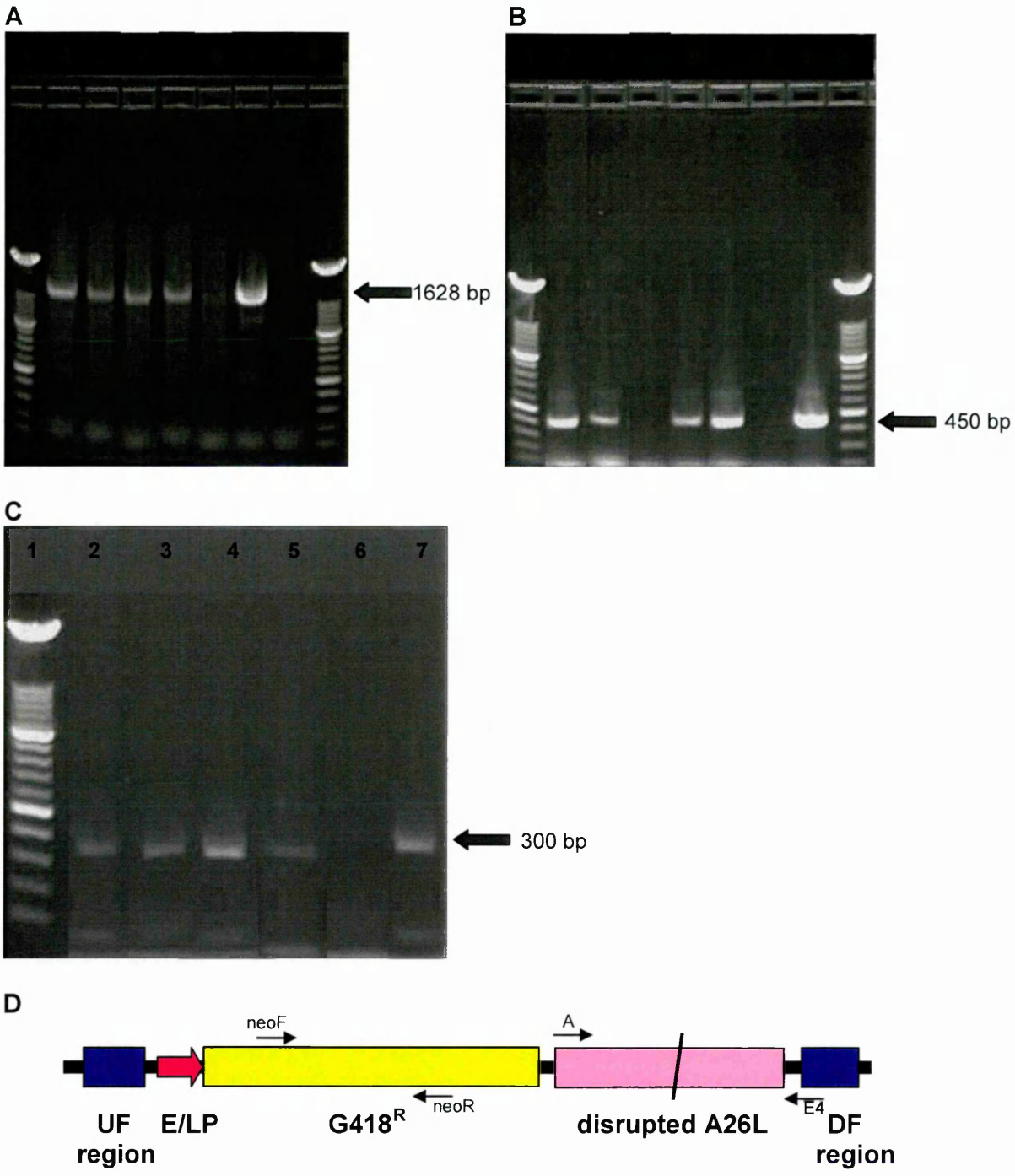

Figure 5.5 Screening of Putative vIδA26L.neo Clones by PCR

PCRs were performed for the A26L gene (1628 bp) using primers A and E4 (**A**), the *Eco*GPT gene (~450 bp) using GPTF and GPTR (**B**) and for a region of the G418^R gene (~300 bp) using primers

neoF and neoR (**C**) on viral DNA extracted from putative secondary A26L deletion virus from plaque purification 4.

A Lane 1 – 100 bp marker; lane 2 – vIδA26L.neo3.3.3.1; lane 3 – vIδA26L.neo3.3.3.2; lane 4 – vIδA26L.neo3.3.3.3; lane 5 – vIδA26L.neo3.3.3.4; lane 6 – vIδA26L.neo3.3.3.5; lane 7 – VACV IHD-J DNA; lane 8 – vIδA26L1.1.1.1.1.1 DNA; lane 9 – 100 bp marker.

B Lane 1 – 100 bp marker; lane 2 – vIδA26L.neo3.3.3.1; lane 3 – vIδA26L.neo3.3.3.2; lane 4 – vIδA26L.neo3.3.3.3; lane 5 – vIδA26L.neo3.3.3.4; lane 6 – vIδA26L.neo3.3.3.5; lane 7 – VACV IHD-J DNA; lane 8 – vIδA26L1.1.1.1.1.1 DNA; lane 9 – 100 bp marker.

C Lane 1 – 100 bp marker; lane 2 – vIδA26L.neo3.3.3.1; lane 3 – vIδA26L.neo3.3.3.2; lane 4 – vIδA26L.neo3.3.3.3; lane 5 – vIδA26L.neo3.3.3.4; lane 6 – vIδA26L.neo3.3.3.5; lane 7 – secondary A26L deletion construct.

D Schematic of secondary deletion construct. Positions of primers are indicated by arrows.

section 2.5.2 and virus was quantitated as 1.09 x 10^9 $TCID_{50}$/ml by Reed-Muench limiting dilution analysis (section 2.5.3).

5.2.6 Plaque Purification of vIδA26L.EL

Putative recombinant virus from passage 6 was plaque purified as for the revertant virus (section 5.2.4), using 3 sequential rounds by limiting dilution. The resulting clones were examined for their ability to replicate in the presence of Geneticin® with each round of plaque purification suggesting that the proportion of $G418^{R+}$ virus was diminishing, questioning the ability of virus overexpressing A26L to form plaques. It was plausible that the increased production of A26 would not only lead to increased IMV, but also a dramatic reduction in EEV that would render the virus unable to form plaques. If this were the case, using a method to clone a virus that is reliant on plaque formation is virtually useless as the recombinant virus is unable to produce plaques and thus cannot be plaque purified. Plaquing observed in the earlier rounds of amplification in Geneticin® may be a result of a mixed population containing both parental (plaque forming) and secondary recombinant (non-plaque forming) viruses.

5.2.6.1 Growth of Putative vIδA26L.EL in Different Cell Lines to Increase Virus Replication

Two approaches were used to attempt to increase the proportion of $G418^{R+}$ virus and reduce parental virus. The first approach was to harvest virus from the culture supernates of infected RK13 cells in the presence of Geneticin®, to maximise the proportion of EEV in the sample (181). EEV is reported to have a

lower particle/pfu ratio than IMV (121), therefore this approach reduces the probability of using a mixed population of viruses to infect subsequent cultures. This should reduce carry-over of parental virus. Alternatively, putative recombinant virus was cultured in BSC40 cells, as the increased rate of replication in BSC40 cells relative to RK13 cells may counteract possible deleterious effects of early production of A26. This should enrich cultures for the secondary recombinant and reduce parental virus. In both cell lines, plaque formation diminished over 3 sequential passages, suggesting that this virus was unable to produce EEV, or that the virus was unable to replicate in the presence of Geneticin®.

To determine the presence of virus in each of the cultures, DNA was extracted and PCRs for the A27L gene were carried out (Figure 5.6). The A27L gene was detected in passage 1 and 2 in RK13 cultures, but not in passage 3; and in passage 1, 2 and 3 in BSC40 cultures, but not at the highest dilutions in passage 3, confirming the presence of virus in cultures as demonstrated when grown in tissue culture. Overall, this indicated that the isolated virus was unable to replicate in the presence of Geneticin®, resulting in a reduction in progeny virus as opposed to the enrichment in culture expected from a $G418^{R+}$ recombinant.

5.2.7 Plaque Purification of vIδA26L.EL from a Repeat Transfection

The transfection was repeated as described in section 2.4.5, and progeny recombinant virus amplified in Geneticin®-treated cultures for a total of 6 passages. On consideration of previous attempts to plaque purify recombinant viruses by limiting dilution, a combination of the agarose overlay method to pick individual

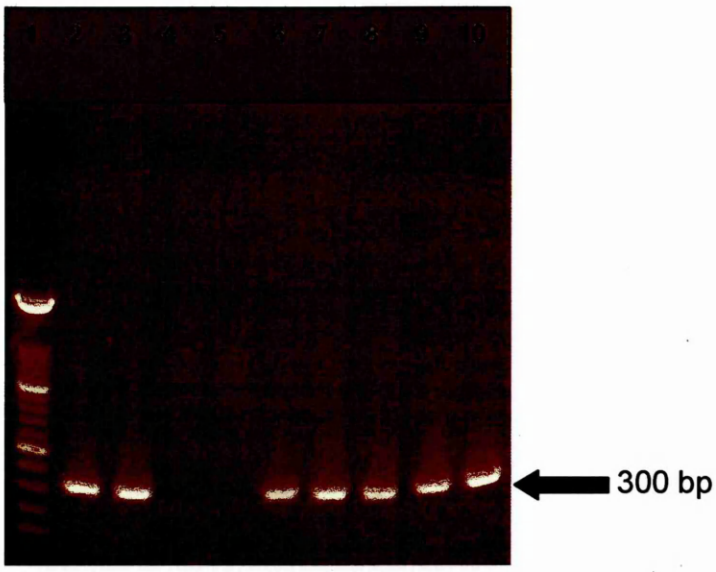

Figure 5.6 Screening of Putative vIδA26L.EL Cultured in RK13 Cells and BSC40 Cells by PCR

PCRs were performed for A27L (~300 bp) using A27LF and A27LR on DNA extracted from virus cultured in RK13 cells or BSC40 cells for 3 passages. Wt VACV IHD-J and vIδA26L1.1.1.1.1.1 DNA were used as positive controls. Lane 1 – 100 bp marker; lane 2 – virus from RK13 passage 1; lane 3 – virus from RK13 passage 2; lane 4 – virus from RK13 passage 3; lane 5 – empty; lane 6 – virus from BSC40 passage 1; lane 7 – virus from BSC40 passage 2; lane 8 – virus from BSC40 passage 3; lane 9 – wt VACV IHD-J DNA; lane 10 – vIδA26L1.1.1.1.1.1 DNA.

plaques, followed by 3 rounds of purification by limiting dilution was carried out (Figure 5.7) (section 2.6.2). PCR analysis of the 2 resulting viruses demonstrated that only clone vIδA26L.EL2.2.1.2 was a *bona fide* recombinant where the *Eco*GPT gene had been replaced by the A26L and $G418^R$ genes (Figure 5.8).

A purified stock was prepared of vIδA26L.EL2.2.1.2 cultured in RK13 cells in the presence of Geneticin® as described in section 2.5.2 and virus was quantitated as 1.67×10^9 $TCID_{50}$/ml by Reed-Muench limiting dilution analysis (section 2.5.3).

5.2.8 Confirming the Isolation of Recombinant VACVs

Using DNA extracted from RK13 cells infected with vIδA26L.rev2.2.3.2, vIδA26L.EL2.2.1.2 and vIδA26L.neo3.3.3.3, PCRs were performed to amplify the upstream flanking regions of the A26L gene. Resulting PCR products were isolated from gels and the sequence integrity confirmed by Lark Technologies. Sequence data confirmed the presence of the native promoter in vIδA26L.rev2.2.3.2 and the synthetic early/late promoter in vIδA26L.EL2.2.1.2, and the absence of a promoter in vIδA26L.neo3.3.3.3 upstream of the engineered A26L gene. The engineered frameshift mutation at position 4 was also confirmed in vIδA26L.neo3.3.3.3.

Following propagation and purification of vIδA26L.rev2.2.3.2, vIδA26L.EL2.2.1.2 and vIδA26L.neo3.3.3.3, the presence of A26 protein in each virus was assessed by Western blot (Figure 5.9). The presence of a band of the same molecular weight of A26 (~60 kDa) was observed in wild-type VACV IHD-J,

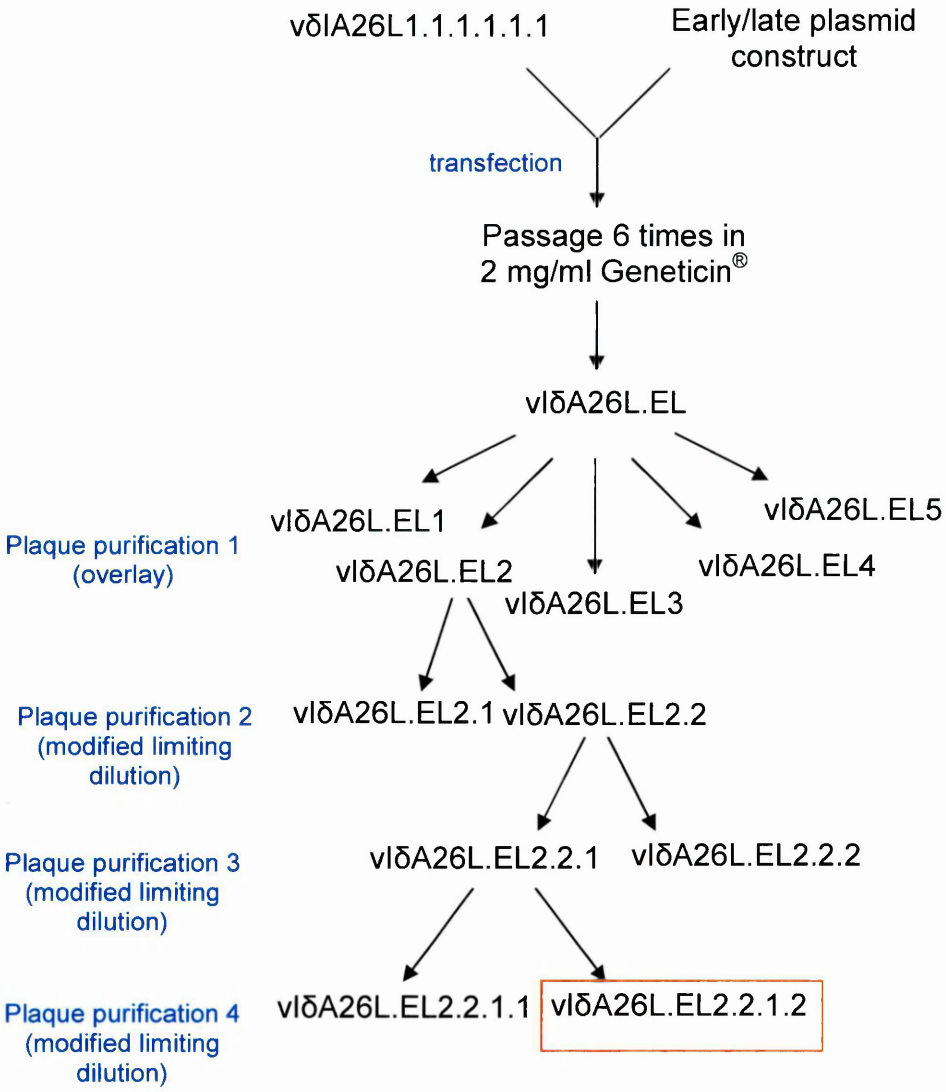

Figure 5.7 Flow Diagram Representing Process of Isolation of vIδA26L.EL

The recombinant VACV to overexpress A26 from a synthetic early/late promoter, denoted here a vIδA26L.EL2.2.1.2, was derived from the parental strain vIδA26L1.1.1.1.1.1 following transfection of cells with the early/late construct (section 5.2.2 and 5.2.3). Putative recombinant virus was isolated following 6 passages in 2 mg/ml Geneticin® and 4 rounds of plaque purification.

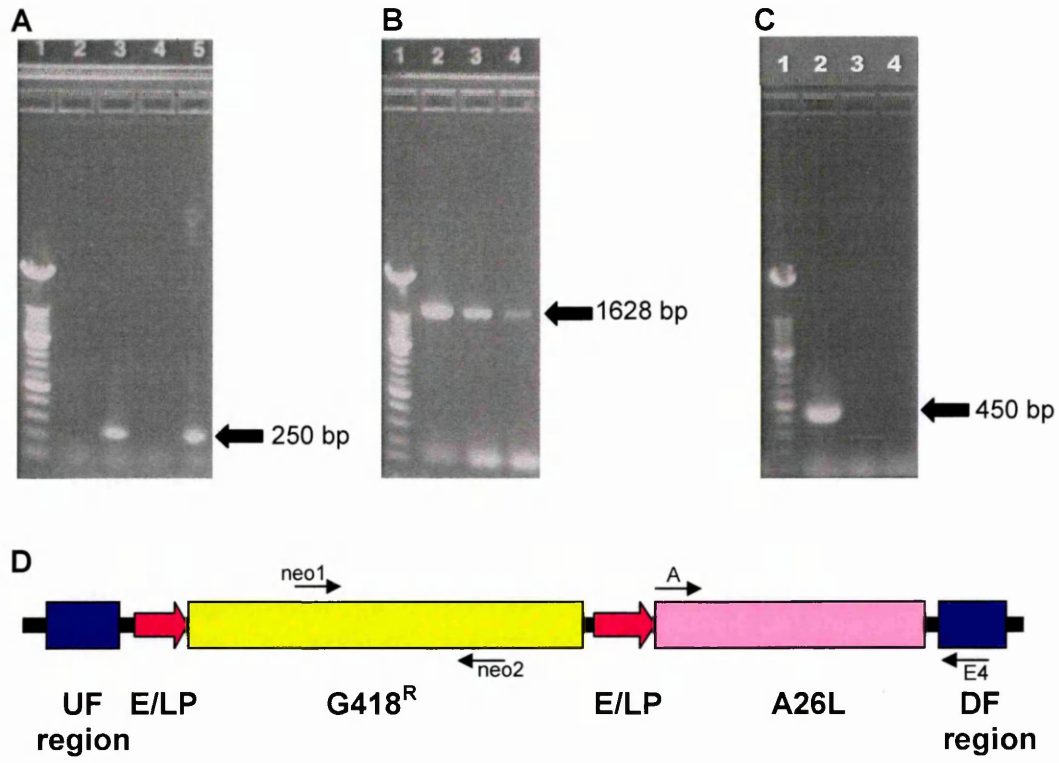

Figure 5.8 Screening of Putative vIδA26L.EL Clones from Plaque Purification 4 by PCR

PCRs were performed on extracted DNA for the, for a region of the G418^R gene (~250 bp) using primers neo1 and neo2 (**A**), for the A26L gene (1628 bp) using primers A and E4 (**B**) and for the *Eco*GPT gene (~450 bp) using primers GPTF and GPTR (**C**).

A Lane 1 – 100 bp marker; lane 2 – clone vIδA26L.EL2.2.1.1; lane 3 – clone vIδA26L.EL2.2.1.2; lane 4 – wt VACV IHD-J DNA; lane 5 – GeneArt early/late construct.

B Lane 1 – 100 bp marker; lane 2 – clone vIδA26L.EL2.2.1.1; lane 3 – clone vIδA26L.EL2.2.1.2; lane 4 – wt VACV IHD-J DNA.

C Lane 1 – 100 bp marker; lane 2 – clone vIδA26L.EL2.2.1.1; lane 3 – clone vIδA26L.EL2.2.1.2; lane 4 – wt VACV IHD-J DNA.

D Schematic of early/late construct. Primers positions are indicated by arrows.

vIδA26L.rev2.2.3.2 and vIδA26L.EL2.2.1.2, whereas this band was absent in both vIδA26L.neo3.3.3.3 and vIδA26L1.1.1.1.1.1. A secondary non-specific band of approximately 35 kDa was observed in all viruses, and the similar band intensities were indicative of equivalent amounts of protein loaded onto the gel. Interestingly, the band intensity of A26 in vIδA26L.EL2.2.1.2 appeared to be more intense than with wild-type and vIδA26L.rev2.2.3.2 suggesting that this virus contains more A26 protein and was indicative of increased synthesis of A26.

5.3 Discussion

In this study, a panel of secondary recombinant VACVs were successfully engineered to a) restore the A26L gene expressed from its own promoter thus restoring the wild-type phenotype; b) replace the *Eco*GPT selection marker gene with the $G418^R$ gene and a disrupted copy of the A26L gene to produce a secondary A26L deletion mutant; and c) restore the A26L gene expressed from a synthetic early/late promoter to result in overexpression of A26.

Exploiting the ability of these viruses to replicate in the presence of Geneticin® (afforded by the engineered $G418^R$ gene) allowed selection and amplification of secondary recombinant virus at the expense of parental primary recombinant virus. Previous reports suggest 2 mg/ml of Geneticin® results in up to84 % inhibition of growth of wild-type virus at MOI 5 without the pre-treatment of cells (357), therefore to ensure maximum inhibition, selection was carried out using MOI < 1, and cells were pre-treated with Geneticin® for 2 hours prior to infection. For each recombinant virus, at least 6 rounds of amplification under selective

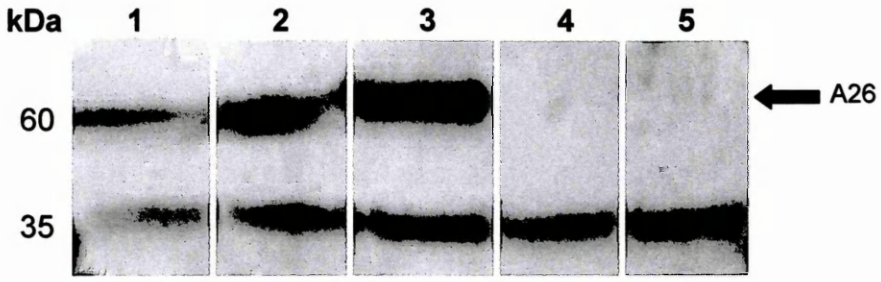

Figure 5.9 Immunoblotting for A26 Protein

Approximately 10^7 pfu of purified virus was run on a tricine gel under reducing conditions to separate viral proteins. Proteins were transferred onto a nitrocellulose membrane and probed with polyclonal antisera to A26 raised in New Zealand White rabbits. Lane 1 – wt VACV IHD-J; lane 2 – vIδA26L.rev2.2.3.2; lane 3 – vIδA26L.EL2.2.1.2; lane 4 – vIδA26L.neo3.3.3.3; lane 5 – vIδA26L1.1.1.1.1.1.

conditions and 4 rounds of plaque purification were required to remove traces of parental virus. To achieve pure, clonal populations of each virus, a combination of both plaque-picking using agarose overlay to obtain virus originating from a single plaque, and a high-throughput method by limiting dilution was successful. Purification was more thorough than standard practice (to plaque purify 3 times), however, it was a necessity as some clones were mixed populations of recombinant and parental virus, as detected by PCR. Carry over of parental virus may highlight a reduced efficacy of $G418^R$ as a dominant selectable marker, relative to what can be achieved (357). Studies by Franke *et al.* (1985) demonstrated maximum inhibition of parental virus when cells were pre-treated for 48 hours in Geneticin®, however this was not feasible in this study as prolonged treatment of cells that would be required (~4-5 days) resulted in cell death.

Isolated clones of vlδA26L.rev, vlδA26L.neo and vlδA26L.EL were negative when screened for the *Eco*GPT gene of the parental primary recombinant virus by PCR, indicating deletion of the gene and removal of parental virus from the culture. In addition, these viruses were positive for the A26L and $G418^R$ genes by PCR, and the sequence integrity of the promoter regions upstream of the engineered A26L gene in each virus was confirmed. Immunoblotting established the production of A26 protein in vlδA26L.rev, vlδA26L.neo and vlδA26L.EL, and its absence in the A26L deletion mutants. For all future studies, the terms vlδA26L.rev refers to clone vlδA26L.rev2.2.3.2, vlδA26L.neo refers to clone vlδA26L.neo3.3.3.3 and vlδA26L.EL refers to clone vlδA26L.EL2.2.1.2.

Although the purity of each clone was verified at the DNA and protein level, previous experience suggests that contaminating parental virus may be present at undetectable levels. For this reason, propagation of recombinant VACV for high titre stocks was always in the presence of 2 mg/ml Geneticin® to prevent amplification of parental virus. For future experiments, it was assumed that the presence of undetectably low quantities of parental virus would not affect the results of the assays used in subsequent studies.

6 Characterisation of Secondary Recombinant VACVs

6.1 Introduction

In addition to the roles of A26 reported by other researchers (134;188;342;351), previous experiments described in Chapter 3 demonstrated a role for A26 in IMV morphogenesis, as first hypothesised by Ulaeto and co-workers (116). Using the panel of recombinants described in Chapters 3 and 5, including two different A26L deletion mutants and a matched revertant control, the function of A26 was investigated further by examining the kinetics of IMV and EV production throughout the infectious cycle using metabolically labelled virus separated through CsCl density gradients. The production of IMV was expected to be reduced throughout the infection when A26L was deleted, with EV production being unaffected. Treatment of cultures with BFA was expected to result in increased EEV production after BFA removal when A26L was deleted, as observed in Chapter 3. This would support the hypothesis that A26 acts as a differentiation switch, causing maturation of virions to switch from EV to IMV. If this were the case, acquisition of A26 on the surface of the virion would serve to negatively regulate EV production as particles could no longer mature as EV. Recent reports provide evidence that the acquisition of A26 by virions is mediated by a direct association of A26 with A27 (134;351) and this might act to prevent the interaction of A27 with Golgi membranes thus preventing EV formation (346). In contrast, when the A26L gene was overexpressed, IMV was expected to be synthesised earlier than normal in the infectious cycle, resulting in increased IMV maturation relative to EV.

6.1.1 Aims of This Study

The revertant vIδA26L.rev and vIδA26L.neo produced in Chapter 5 were used to confirm the role of A26 in maturation of IMV, as demonstrated with vIδA26L in Chapter 3. In addition, these viruses were used to eliminate the possibility that the selection marker gene, *Eco*GPT, had a negative effect on viral replication. These viruses, together with wild-type IHD-J and COP strains, were characterised for their ability to produce IMV and EV *in vitro*. A third recombinant, designed to constitutively express A26L throughout the replicative cycle, was included in this study where the production of IMV was predicted to be increased, reducing the number of virions available for wrapping and thus reducing EV formation. These recombinants may provide further insight into the formation and function of IMV, and modulation of A26 may result in an attenuated phenotype, that may have potential as a safer alternative to current smallpox vaccines.

6.2 Results

6.2.1 Comparative Growth Kinetics of Recombinant VACVs

To compare the ability of IHD-J, vIδA26L, vIδA26L.rev, vIδA26L.neo and vIδA26L.EL to replicate in tissue culture, one-step growth curves were performed in BSC40 cells. This would demonstrate any differences in the growth rates of each of the viruses, and confirm the reduction in titre when A26L is deleted, as observed with vIδA26L in Chapter 3. VACV COP was also included to determine whether there was a difference in growth kinetics to the IHD-J strain, as COP has several lesions in its genome, including a truncation of the A26L gene. The experiment was

performed in triplicate in 24-well tissue culture plates, infecting at MOI 10 to ensure synchronous infections. Cultures were harvested at 6, 12, 16, 24, 30 and 48 hours p.i. and virus quantitated by Reed-Muench limiting dilution analysis (Figure 6.1). The data was $\log_{10}$ transformed and fitted to a one-phase exponential association model to allow statistical analyses (Figure 6.2). Using this model (Y=Ymax(1-exp(-KX))), F-tests with Bonferroni's post-tests were performed to compare the growth rates (K) of each strain of virus. There was no significant difference between the growth rates of all the viruses tested (p=0.3126). Using a two-way ANOVA analysis with Bonferroni's post-tests there was a significant reduction in virus yield in vIδA26L cultures compared to IHD-J (p=0.002), and in vIδA26L.neo cultures compared to vIδA26L.rev (p=0.041).

The results of this experiment confirm the findings of Chapter 3, where deletion of the A26L gene in vIδA26L and vIδA26L.neo resulted in a decrease in total virus yield. This suggests that deletion of A26L may affect the ability of the virus to produce IMV, or possibly the stability or infectivity of IMV, and this was investigated further in this chapter. Importantly, these results indicate it is unlikely that the *Eco*GPT and $G418^R$ genes have a negative effect on viral yields, as similar phenotypes were observed in both vIδA26L and vIδA26L.neo. The wild-type phenotype was restored in the revertant and vIδA26L.EL, where the $G418^R$ gene was also present, confirming that the presence of this gene did not result in reduced viral yields.

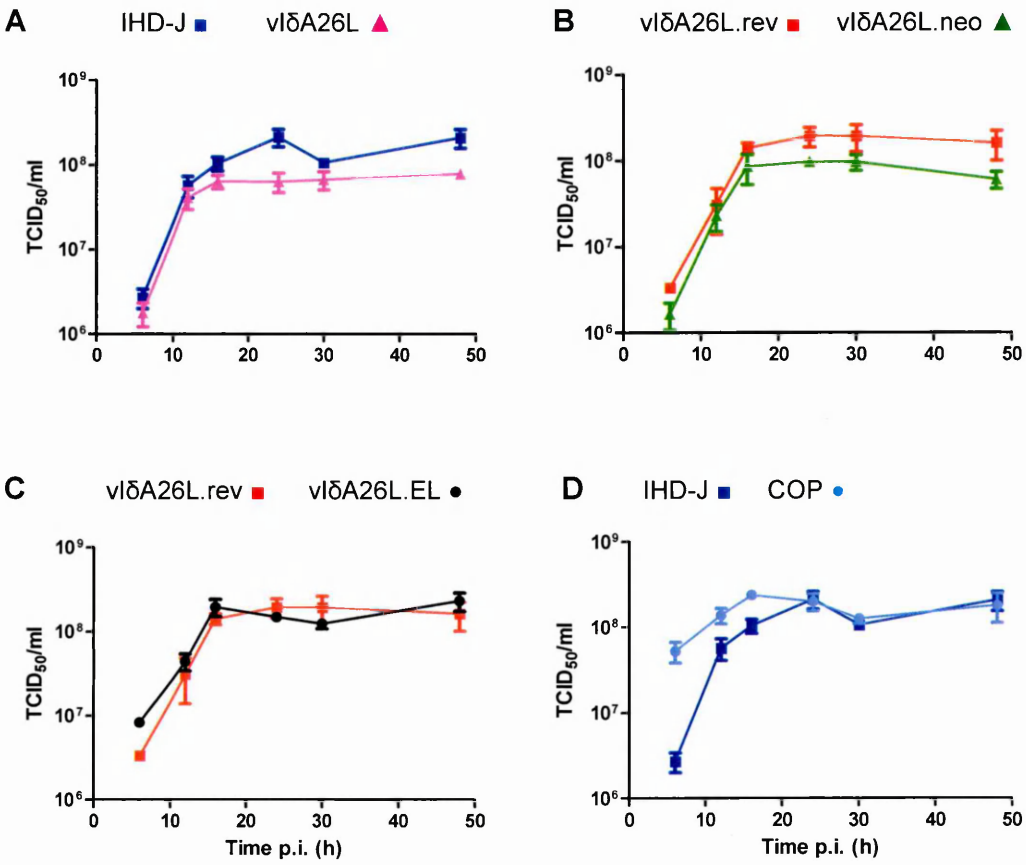

Figure 6.1 One-step Growth Curves for Recombinant VACVs

Freshly confluent monolayers of BSC40 cells in 24-well tissue culture plates were infected at MOI 10 with IHD-J (■) or vIδA26L (▲) **A**; vIδA26L.rev (■) or vIδA26L.neo (▲) **B**; vIδA26L.rev (■) or vIδA26L.EL (●) **C**; IHD-J (■) or COP (●) **D**, in triplicate wells. Cultures were maintained at 37 °C in a 5 % CO_2 humidified atmosphere until the time of harvest. At the appropriate time p.i. replication was halted by freezing the cultures at -80 °C. Virus was liberated by three rounds of freeze-thaw followed by dounce homogenisation, prior to titration by Reed-Muench limiting dilution analysis in RK13 cells. Data is presented as mean $TCID_{50}$/ml and SEM of triplicate cultures.

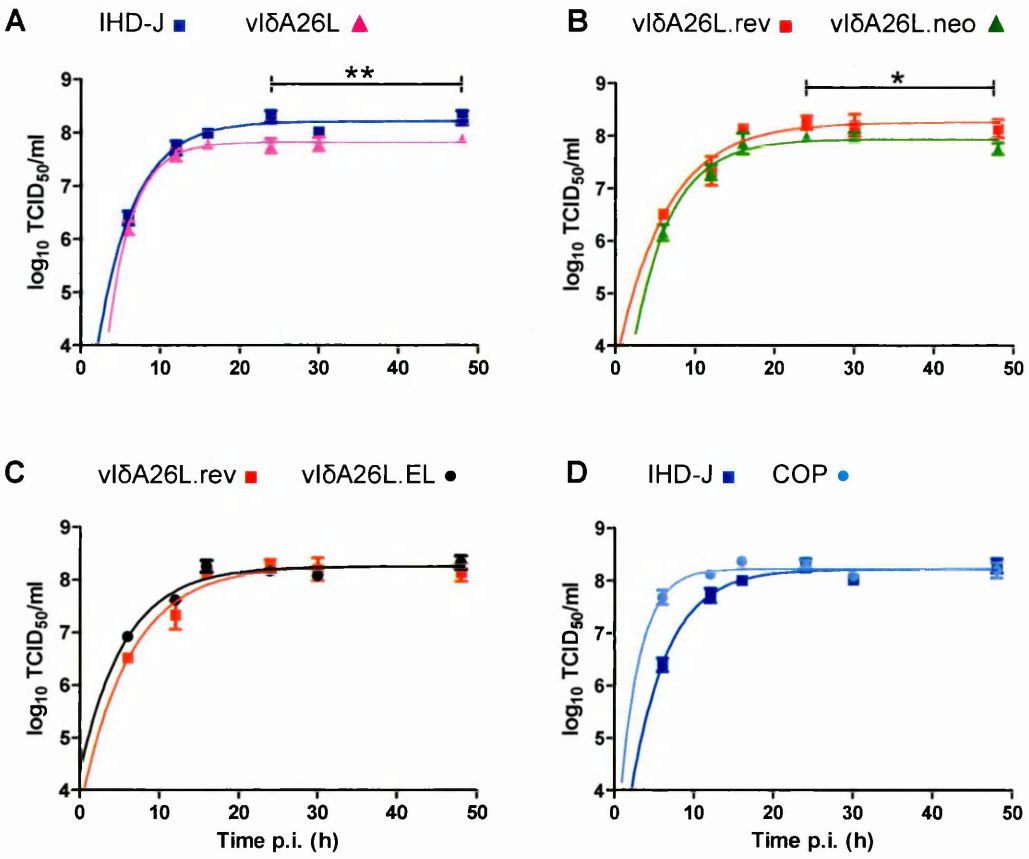

Figure 6.2 Transformation of Data from One-step Growth Curves for Recombinant VACVs

Freshly confluent monolayers of BSC40 cells in 24-well tissue culture plates were infected at MOI 10 IHD-J (■) or vIδA26L (▲) **A**; vIδA26L.rev (■) or vIδA26L.neo (▲) **B**; vIδA26L.rev (■) or vIδA26L.EL (●) **C**; IHD-J (■) or COP (●) **D** in triplicate wells. Cultures were maintained at 37 °C in a 5 % CO_2 humidified atmosphere until the time of harvest. At the appropriate time p.i. replication was halted by freezing the cultures at -80 °C. Virus was liberated by three rounds of freeze-thaw followed by dounce homogenisation, prior to titration by Reed-Muench limiting dilution analysis in RK13 cells. To allow statistical analyses, data was $\log_{10}$ transformed and fitted to a one phase exponential association model (** p=0.002; *p=0.041). Error bars represent SEM of triplicate cultures.

6.2.2 Effect of Deletion of A26L on Maturation of IMV and EV

6.2.2.1 Comet Formation

The production of EEV by each of the recombinant VACV strains and the IHD-J and COP strains was determined by comet formation in RK13 cells (Figure 6.3). Both A26L deletion mutants (Figure 6.3B and 6.3D) produced comets of a similar size to the wild-type IHD-J parent and vIδA26L.rev strains (Figure 6.3A and 6.3C). Although virus was diluted to give approximately 1-10^5 $TCID_{50}$ per well, it would appear that considerably less virus was present when vIδA26L was used (Figure 6.3B). vIδA26L.EL was also able to produce comets suggesting the production of EEV (Figure 6.3E), however as in vIδA26L, less virus appeared to be present in these cultures. This is possibly due to an experimental error where the stock was inadequately mixed before sampling. COP did not produce comets, suggesting the absence of EEV.

6.2.2.2 Kinetics of IMV and EV Production in BSC40 cells

To investigate the role of A26 in maturation of IMV, the production of IMV and EV in IHD-J, vIδA26L, vIδA26L.neo, vIδA26L.rev and COP was examined *in vitro*. This data was intended to build upon that discussed in Chapter 3, to determine the effect of deleting A26L on virus maturation and confirm that deletion of A26L results in a reduction in IMV.

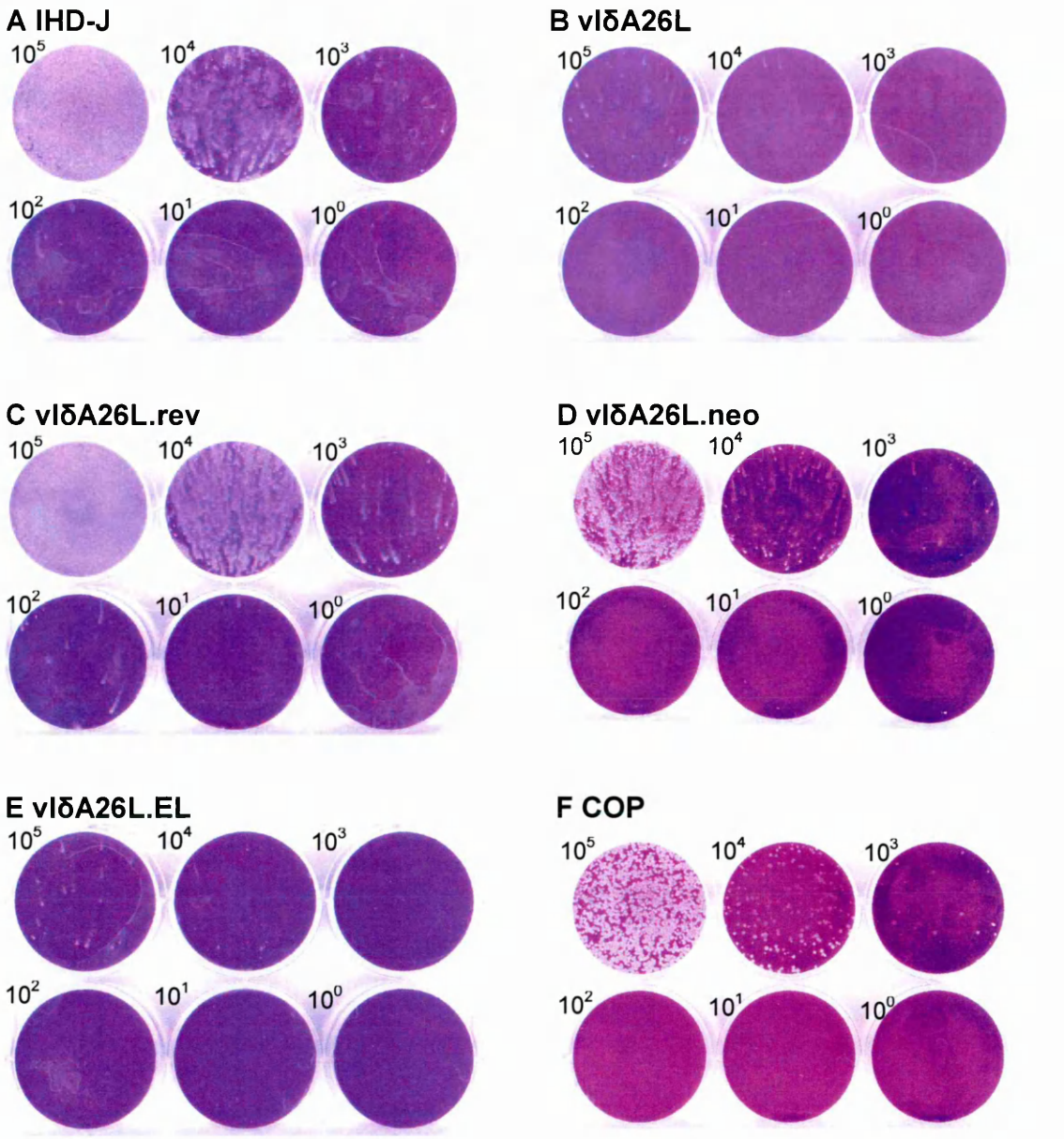

Figure 6.3 Comet Formation in Recombinant VACV Strains

IHD-J (**A**), vIδA26L (**B**), vIδA26L.rev (**C**), vIδA26L.neo (**D**), vIδA26L.EL (**E**) and COP (**F**) were diluted to approximately 1-10^5 $TCID_{50}$ per ml and 1 ml used to infect wells of 6-well tissue culture plates seeded with RK13 cells as indicated. Cultures were maintained at 37 °C in a 5 % CO_2 humidified atmosphere and incubated on a slope to facilitate comet formation in the same direction, for 30 hours. Cultures were fixed and stained with 1 % (v/v) formaldehyde and 1 % (w/v) crystal violet.

BSC40 cells were infected at MOI 10 and incubated for 6, 9, 12, 15 and 24 hours in culture medium supplemented with 10 μCi ^{3}H thymidine. Total progeny virions were separated by ultracentrifugation through CsCl gradients which were then fractionated and subjected to liquid scintillation counting. Interestingly at all of the time points examined, IMV maturation appeared to dominate, even at earlier times p.i. (Figure 6.4) This result differs from previous reports where EV maturation occurs first in the replicative cycle in conjunction with detectable F13, followed by IMV maturation later with detectable A26 synthesis at 15 hours p.i., to become the majority of progeny by 24 hours p.i. (116).

In both A26L deletion mutants, there was a reduction in both IMV and EV at 9 and 12 hours p.i., and a reduction in the ratio of IMV:EV at 12 hours p.i. for both viruses when compared to wild-type IHD-J (Figure 6.4A and B) or vIδA26L.rev (Figure 6.5A and B). In the later stages of the infectious cycle when IMV maturation was expected to dominate, there was a slight reduction in the ratio of IMV:EV at 15 hours p.i., compared to the IHD-J parent (Figure 6.5C) and vIδA26L.rev (Figure 6.4C). At 24 hours p.i., the ratio of IMV:EV was comparable in vIδA26L and IHD-J cultures (Figure 6.4D), however there is a reduction in IMV in vIδA26L.neo compared to vIδA26L.rev, reducing the ratio of IMV:EV (6.5D). The results are starkly different from those in Chapter 3 where a dramatic reduction in IMV was observed at 24 hours p.i. It is possible that there is a difference in the kinetics of virion production when using different cell lines as RK13 cells were used in Chapter 3, therefore the phenotype observed in A26L deletion mutants may be different when cultured in different cell lines.

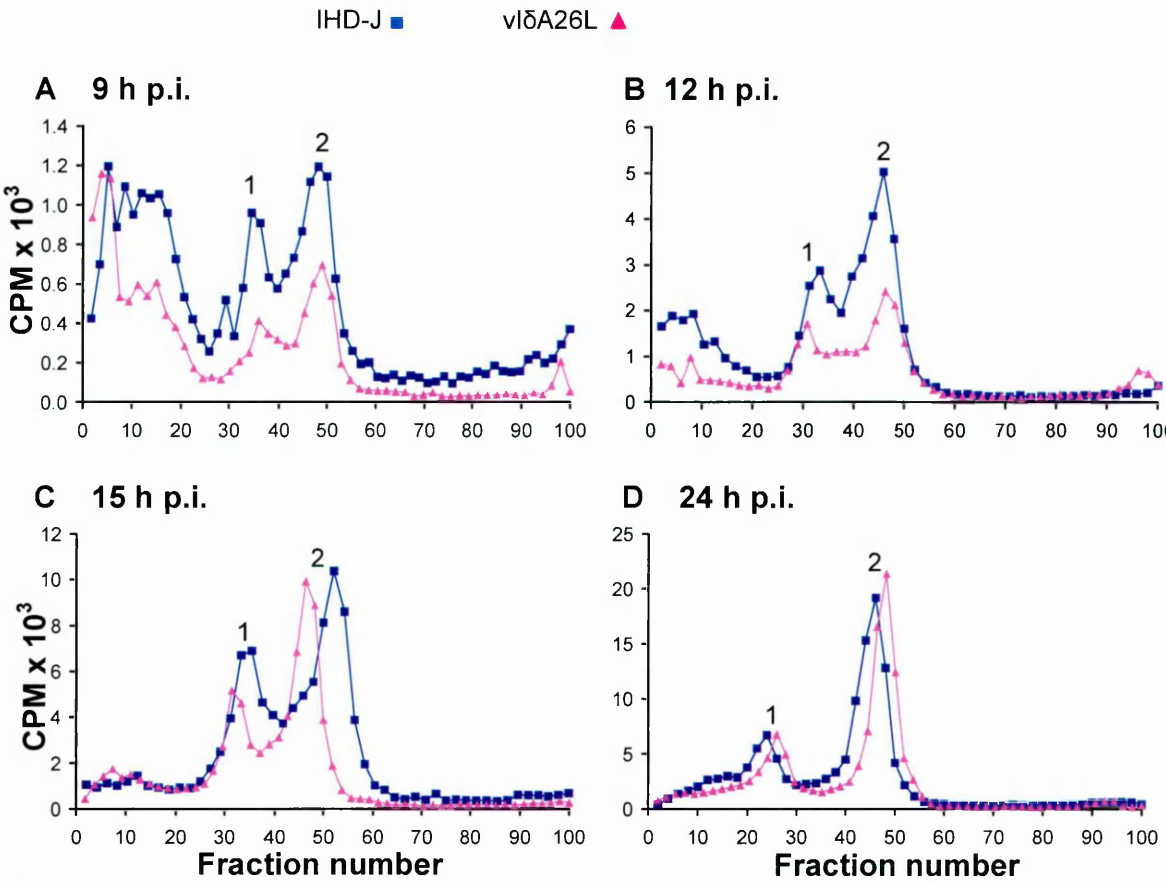

Time p.i. (h)	Ratio IMV:EV	
	IHD-J	vIδA26L
9	1.87	1.75
12	2.23	1.66
15	1.65	1.42
24	2.09	2.17

Figure 6.4 Analysis of IMV and EV by Radioactive Labelling of Virions in IHD-J and vIδA26L Cultures

Liquid scintillation counting of CsCl fractions of ^{3}H thymidine labelled progeny virions from IHD-J (■) and vIδA26L (▲) virus cultured in BSC40 cells. Progeny virus was harvested at 9 (**A**), 12 (**B**), 15 (**C**) and 24 (**D**) hours p.i. and subjected to ultracentrifugation through CsCl gradients. Peaks 1 and 2 represent EV and IMV, respectively. Relative quantities of virus were calculated using the sum of counts (CPM) for peaks corresponding to EV (peak 1) and IMV (peak 2) from each trace. Ratios = sum of IMV counts/sum of EV counts.

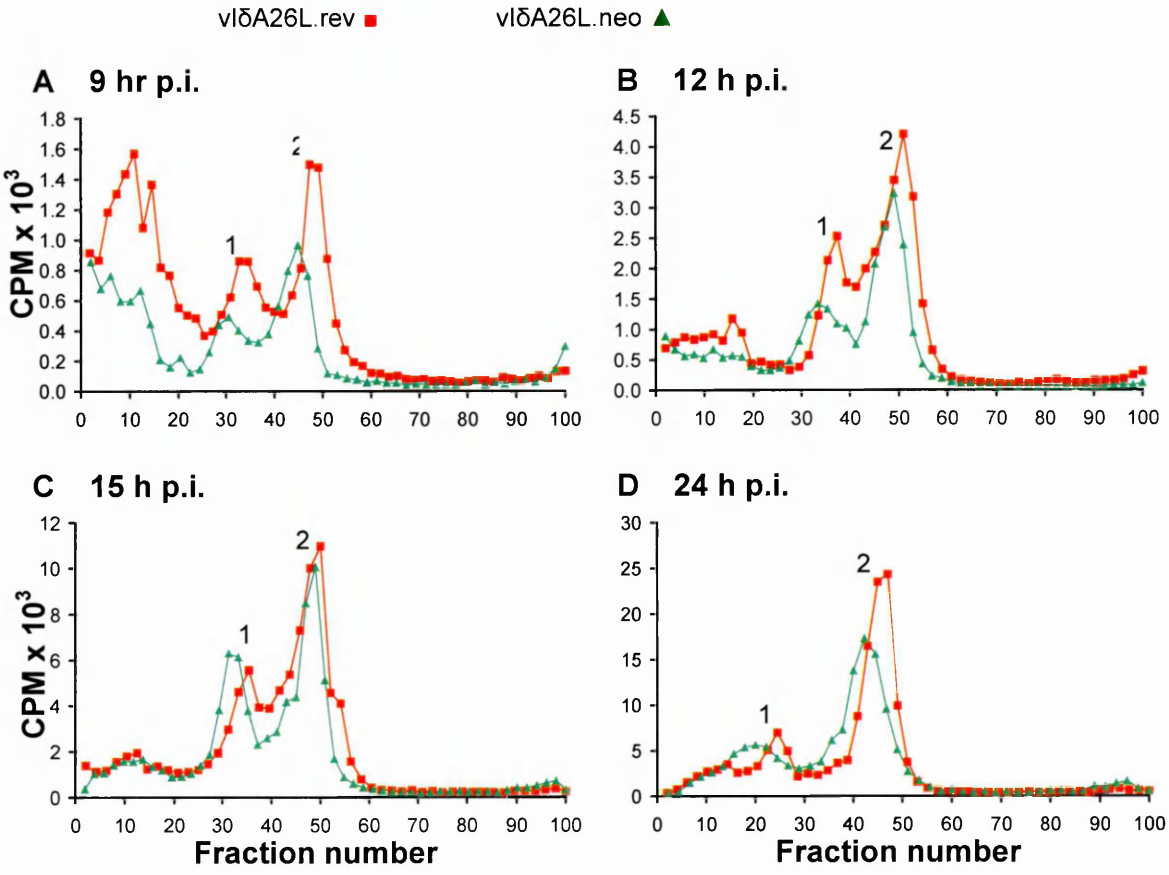

	Ratio IMV:EV	
Time p.i. (h)	vIδA26L.rev	vIδA26L.neo
9	1.25	1.46
12	2.45	1.88
15	2.60	1.97
24	2.69	2.33

Figure 6.5 Analysis of IMV and EV by Radioactive Labelling of Virions in vIδA26L.rev and vIδA26L.neo Cultures

Liquid scintillation counting of CsCl fractions of ^{3}H thymidine labelled progeny virions from vIδA26L.rev (■) and vIδA26L.neo (▲) virus cultured in BSC40 cells. Progeny virus was harvested at 9 (**A**), 12 (**B**), 15 (**C**) and 24 (**D**) hours p.i. and subjected to ultracentrifugation through CsCl gradients. Peaks 1 and 2 represent EV and IMV, respectively. Ratios = sum of IMV counts/sum of EV counts.

In addition to the recombinants generated in this study, the kinetics of IMV and EV production were examined in COP. COP has a truncation of the A26L gene and is thus relevant to this study, although there are several lesions in the COP genome that may alter its maturation phenotype compared to other VACV strains. On comparison of COP to IHD-J, there were greater quantities of progeny virus at 6 and 9 hours p.i in COP cultures (Figures 6.6A and B), and the ratio of IMV:EV in COP was increased at 6 hours p.i. compared to IHD-J. At the later time points, production of IMV and EV in COP were similar to that in IHD-J until 24 hours p.i., where EV was reduced and IMV increased in COP thus resulting in an increased ratio IMV:EV (Figures 6.6C and D).

These results suggest that deletion of A26L expression results in an altered phenotype whereby the relative quantities of IMV and EV are changed. This study also demonstrates that re-insertion of A26L into vIδA26L results in restoration of the wild-type IHD-J phenotype.

6.2.2.3 Kinetics of IMV and EV Production in RK13 cells (I)

As the phenotype observed in both A26L deletion mutants and COP in BSC40 cells differs from that in RK13 cells reported in Chapter 3, the kinetics study was repeated in the RK13 cell line to investigate whether the phenotype observed in Chapter 3 could be repeated. Cells were infected at MOI 10 with IHD-J, vIδA26L.rev, vIδA26L, vIδA26L.neo and COP and cultures supplemented with ^{3}H thymidine. Cultures were harvested at 6, 9, 12, 15, 18, 24 and 30 hours p.i. and

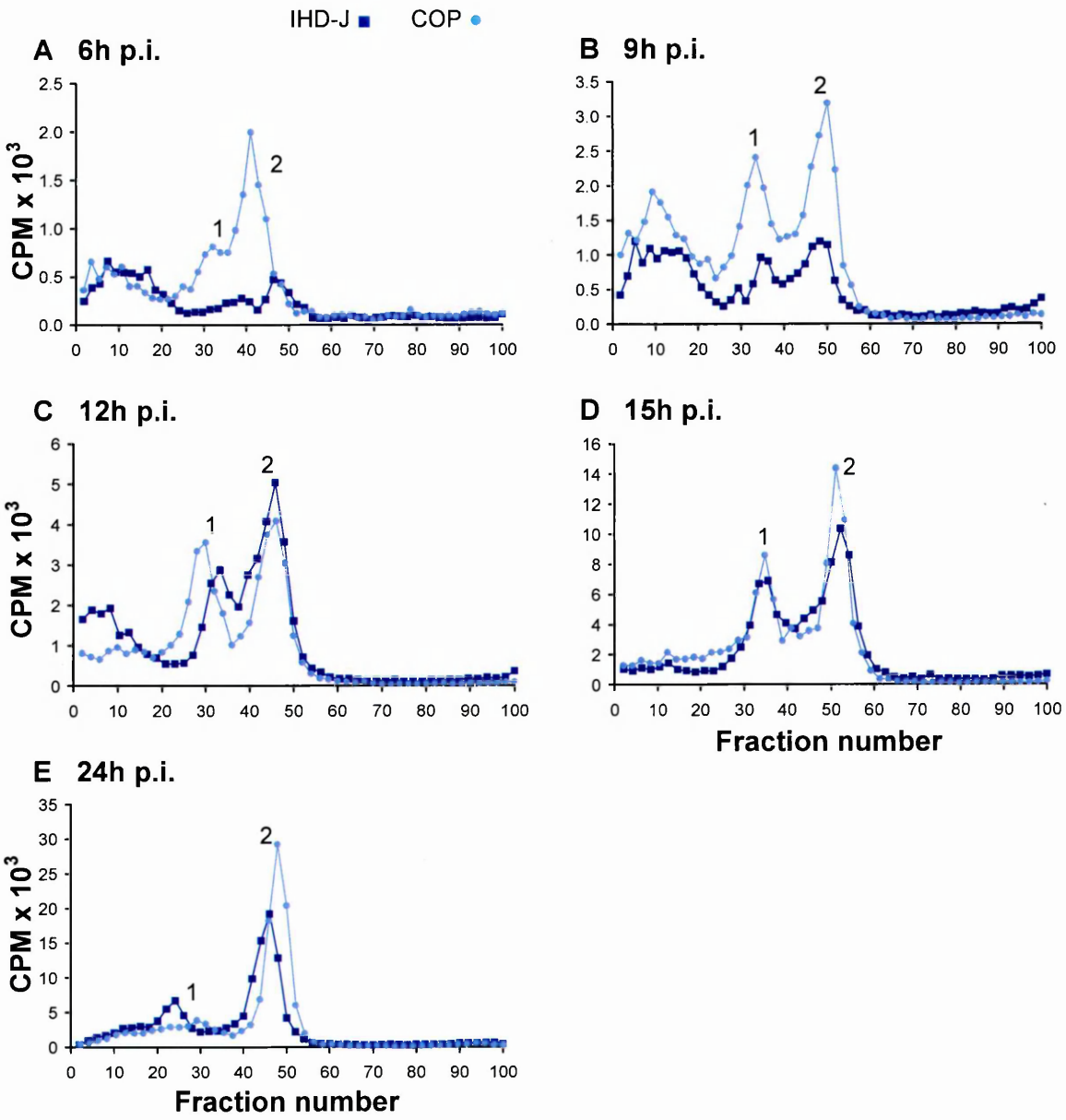

Time p.i. (h)	Ratio IMV:EV	
	IHD-J	COP
6	1.56	3.31
9	1.87	1.39
12	2.23	1.11
15	1.65	1.61
24	2.09	3.52

Figure 6.6 Analysis of IMV and EV by Radioactive Labelling of Virions in IHD-J and COP Cultures

Liquid scintillation counting of CsCl fractions of ^{3}H thymidine labelled progeny virions from IHD-J (■) and COP (○) virus cultured in BSC40 cells. Progeny virus was harvested at 6 (**A**), 9 (**B**), 12 (**C**), 15 (**D**) and 24 (**B**) hours p.i. and subjected to ultracentrifugation through CsCl gradients. Peaks 1 and 2 represent EV and IMV, respectively. Ratios = sum of IMV counts/sum of EV counts.

progeny virions subjected to ultracentrifugation though CsCl gradients to separate IMV and EV, as for previous experiments.

Cultures of vIδA26L produced less progeny particularly in the earlier stages of the infectious cycle (Figure 6.7A-C). As the infection progressed the quantities of IMV increased in vIδA26L cultures, although they were reduced compared to IHD-J (Figure 6.7D-F). EV production was also reduced compared to IHD-J resulting in an increased ratio of IMV:EV between 12 and 24 hours p.i. At 30 hours p.i., EV production was slightly increased compared to that of IHD-J, however, IMV was reduced and consequently the ratio of IMV:EV was reduced (Figure 6.7G).

A similar trend was observed in vIδA26L.neo, where less virus was produced at the earlier time points (Figure 6.8A-C). As the infection progressed, the quantities of IMV increased in vIδA26L.neo cultures, although IMV production was generally reduced compared to vIδA26L.rev (Figures 6.8D and E). At the later stages, EV production appeared to peak by 24 hours p.i., and production of IMV was reduced in vIδA26L.neo, resulting in a decreased ratio of IMV:EV (Figures 6.8F and G).

Characterisation of COP in RK13 cells demonstrated an increase in both IMV and EV in the early stages of infection (Figure 6.9A and B), causing an increase in the ratio of IMV:EV when compared to IHD-J. As the infection progressed, the quantities of EV were reduced and IMV production was equivalent to IHD-J until 18 hours p.i. (Figure 6.9C-E). Production of virus in COP cultures appeared to cease at 24 and 30 hours p.i. resulting in reduced quantities of virus compared to IHD-J at the later time points (Figure 6.9F and G). However, due to a

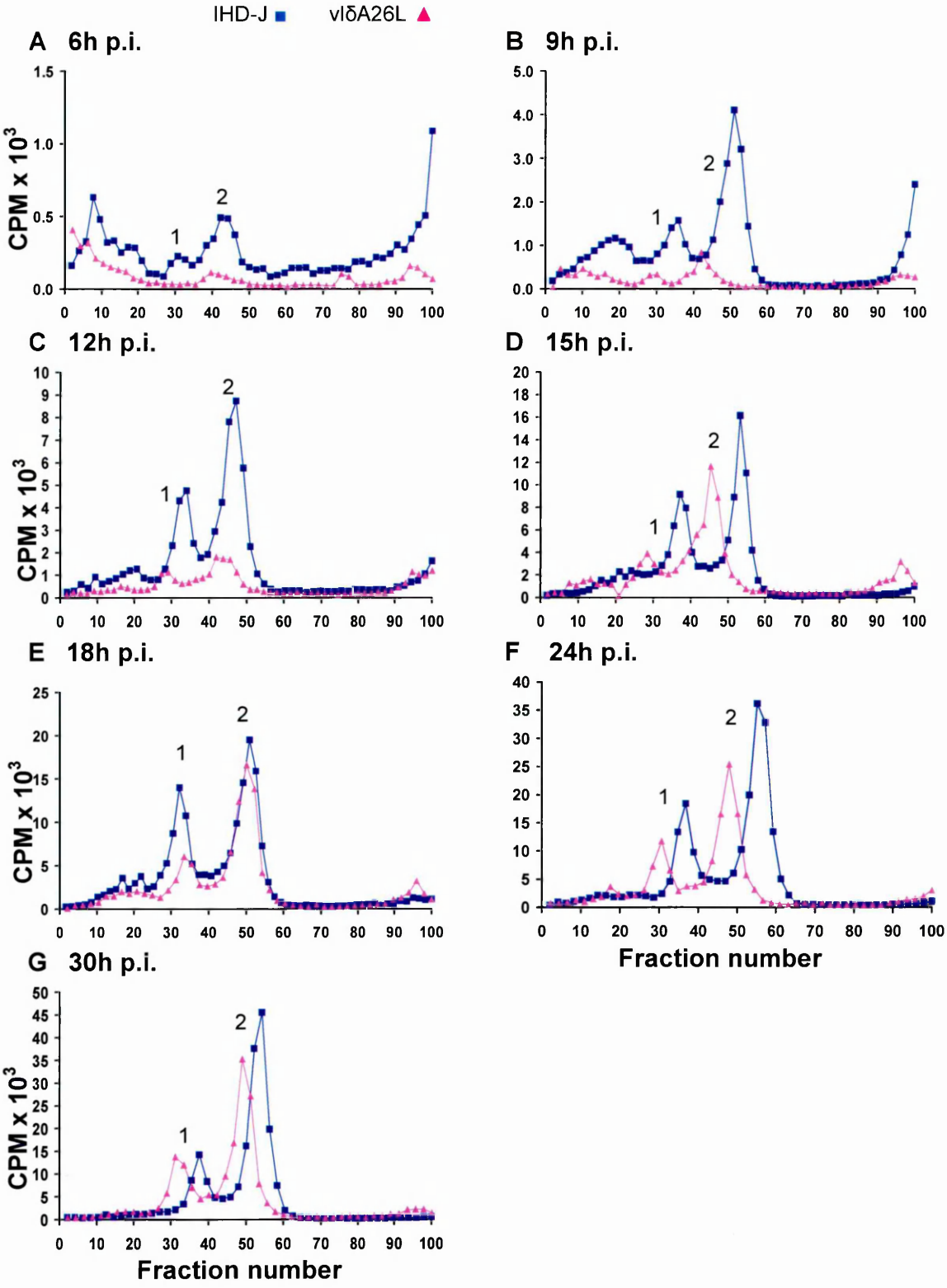
IHD-J ■ vIδA26L ▲
A 6h p.i.
B 9h p.i.
C 12h p.i.
D 15h p.i.
E 18h p.i.
F 24h p.i.
G 30h p.i.
CPM x 10³
Fraction number
1
2

	Ratio IMV:EV	
Time p.i. (h)	IHD-J	vIδA26L
6	3.15	*
9	2.36	2.39
12	2.02	2.62
15	1.37	3.49
18	1.62	3.07
24	2.16	2.41
30	3.06	2.31

Figure 6.7 Analysis of IMV and EV by Radioactive Labelling of Virions in IHD-J and vIδA26L Cultures

Liquid scintillation counting of CsCl fractions of ^{3}H thymidine labelled progeny virions from IHD-J (■) and vIδA26L (▲) virus cultured in RK13 cells. Progeny virus was harvested at 6 (**A**), 9 (**B**), 12 (**C**), 15 (**D**), 18 (**E**), 24 (**F**) and 30 (**G**) hours p.i. and subjected to ultracentrifugation through CsCl gradients. Peaks 1 and 2 represent EV and IMV, respectively. Ratios = sum of IMV counts/sum of EV counts.

* Counts were too low in vIδA26L at 6 hours p.i. to calculate a ratio.

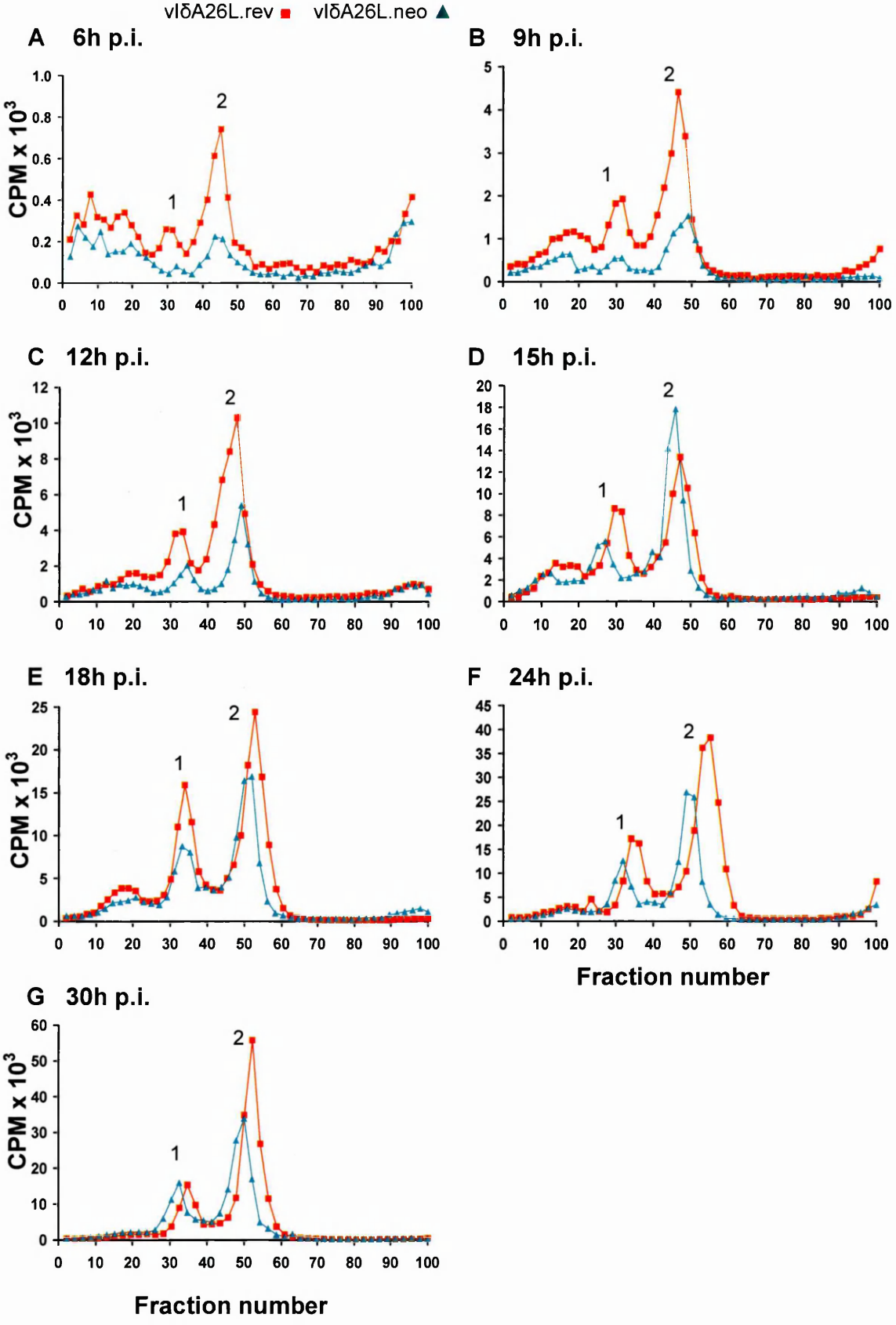
vIδA26L.rev ■ vIδA26L.neo ▲
A 6h p.i.
B 9h p.i.
C 12h p.i.
D 15h p.i.
E 18h p.i.
F 24h p.i.
G 30h p.i.
CPM x 10³
Fraction number

	Ratio IMV:EV	
Time p.i. (h)	vlδA26L.rev	vlδA26L.neo
6	2.82	4.53
9	2.45	3.07
12	2.57	2.19
15	1.46	2.73
18	1.54	2.13
24	2.56	2.34
30	3.58	2.07

Figure 6.8 Analysis of IMV and EV by Radioactive Labelling of Virions in vlδA26L.rev and vlδA26L.neo Cultures

Liquid scintillation counting of CsCl fractions of ^{3}H thymidine labelled progeny virions from vlδA26L.rev (■) and vlδA26L.neo (▲) virus cultured in RK13 cells. Progeny virus was harvested at 6 (**A**), 9 (**B**), 12 (**C**), 15 (**D**), 18 (**E**), 24 (**F**) and 30 (**G**) hours p.i. and subjected to ultracentrifugation through CsCl gradients. Peaks 1 and 2 represent EV and IMV, respectively. Ratios = sum of IMV counts/sum of EV counts.

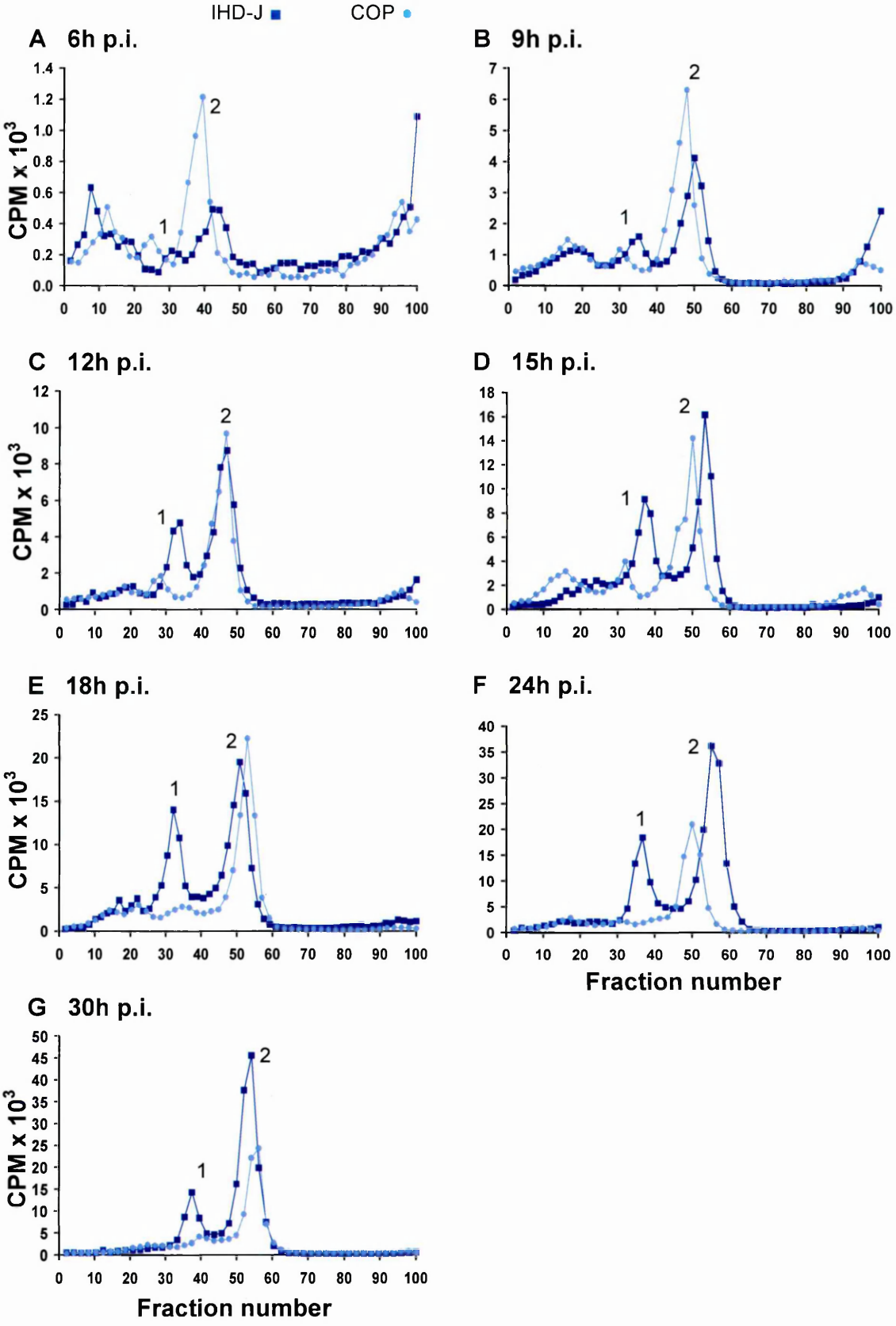
IHD-J
COP
A 6h p.i.
B 9h p.i.
C 12h p.i.
D 15h p.i.
E 18h p.i.
F 24h p.i.
G 30h p.i.
CPM x 10³
Fraction number
1
2

	Ratio IMV:EV	
Time p.i. (h)	IHD-J	COP
6	3.15	3.77
9	2.36	4.65
12	2.02	4.78
15	1.37	3.63
18	1.62	5.28
24	2.16	6.97
30	3.06	4.27

Figure 6.9 Analysis of IMV and EV by Radioactive Labelling of Virions in IHD-J and COP Cultures

Liquid scintillation counting of CsCl fractions of ^{3}H thymidine labelled progeny virions from IHD-J (■) and COP (∘) virus cultured in RK13 cells. Progeny virus was harvested at 6 (**A**), 9 (**B**), 12 (**C**), 15 (**D**), 18 (**E**), 24 (**F**) and 30 (**G**) hours p.i. and subjected to ultracentrifugation through CsCl gradients. Peaks 1 and 2 represent EV and IMV, respectively. Ratios = sum of IMV counts/sum of EV counts.

decrease in EV formation throughout, the ratio of IMV:EV in COP cultures was increased, compared to IHD-J.

The kinetics of IMV and EV maturation in RK13 cells was similar to that in BSC40 cells, where deletion of A26L appeared to perturb the ratio of IMV:EV, even at late times p.i. The vIδA26L.rev behaved in a broadly similar manner to IHD-J, confirming restoration of the wild-type phenotype by re-introducing the A26L gene expressed from its natural promoter into vIδA26L. However, the effect of deletion of A26L was not as profound as the altered phenotype reported in Chapter 3. These results do not convincingly support the hypothesis that A26 modulates the relative quantities of IMV and EV, and do indicate that A26 does not appear to operate as a simple on/off switch of IMV maturation.

6.2.2.4 Kinetics of IMV and EV Production in RK13 cells (II)

The maturation of IMV and EV has been demonstrated to be similar in both BSC40 and RK13 cells, however the experiment was repeated in RK13 cells as confirmation. Cells were infected at MOI 10 with IHD-J, vIδA26L.rev, vIδA26L, vIδA26L.neo and COP, and the cultures were supplemented with ^{3}H thymidine. Cultures were harvested at 6, 9, 12, 15, 18, 24 and 30 hours p.i. Progeny virions were separated by ultracentrifugation through CsCl gradients and the resulting fractions subjected to liquid scintillation counting.

Deletion of the A26L gene in vIδA26L resulted in a reduction in the quantities of progeny produced at earlier times p.i. (Figures 6.10A-C) compared to IHD-J, as observed in previous kinetics experiments in BSC40 and RK13 cells.

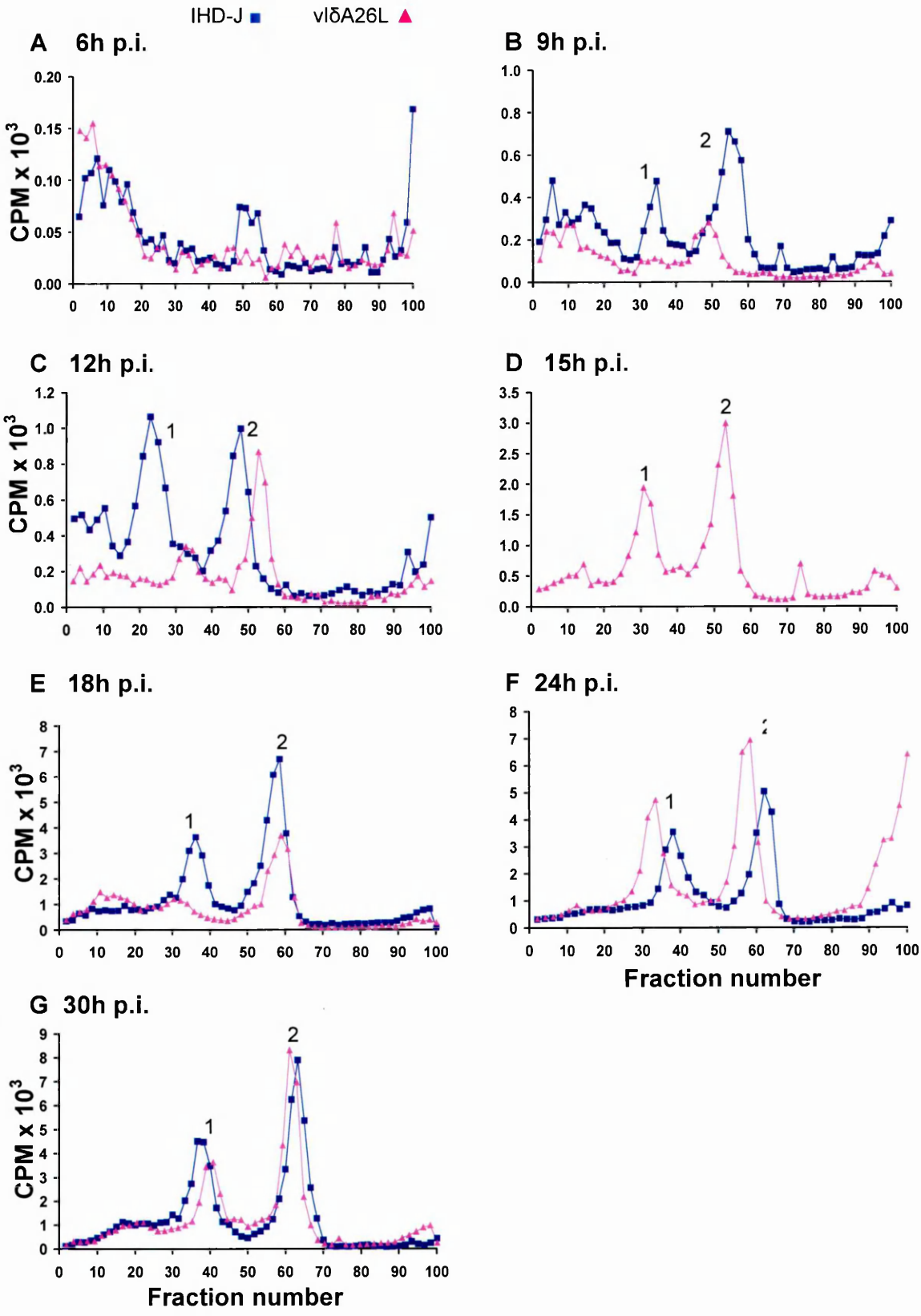
IHD-J ■
vIδA26L ▲
A 6h p.i.
B 9h p.i.
C 12h p.i.
D 15h p.i.
E 18h p.i.
F 24h p.i.
G 30h p.i.
CPM x 10³
Fraction number
1
2

Time p.i. (h)	Ratio IMV:EV	
	IHD-J	vIδA26L
6	*	*
9	1.88	2.90
12	0.75	1.68
15	†	1.40
18	1.47	2.52
24	1.08	1.12
30	1.39	1.53

Figure 6.10 Analysis of IMV and EV by Radioactive Labelling of Virions in IHD-J and vIδA26L Cultures

Liquid scintillation counting of CsCl fractions of ^{3}H thymidine labelled progeny virions from IHD-J (■) and vIδA26L (▲) virus cultured in RK13 cells. Progeny virus was harvested at 6 (**A**), 9 (**B**), 12 (**C**), 15 (**D**), 18 (**E**), 24 (**F**) and 30 (**G**) hours p.i. and subjected to ultracentrifugation through CsCl gradients. Peaks 1 and 2 represent EV and IMV, respectively. Ratios = sum of IMV counts/sum of EV counts.

* Counts too low to determine peaks and therefore to calculate ratio at 6 hours p.i.

† No data for IHD-J at 15 hours p.i. due to a cracked centrifuge tube.

Interestingly, IMV was the dominant particle produced in vIδA26L cultures, whereas EV production dominated in IHD-J cultures, as demonstrated by the increased ratio of IMV:EV compared to IHD-J at 12 hours p.i. As the infection progressed, quantities of IMV exceeded EV in both wild-type IHD-J and vIδA26L cultures, however the quantities of virus produced at 18 hours p.i. were reduced in vIδA26L (Figures 6.10D and E). At 24 hours p.i., the counts for both IMV and EV were greater in vIδA26L cultures than in IHD-J. This was likely due to experimental variation as this does not follow the trend observed in this experiment and previous experiments (Figure 6.10F). At 30 hours p.i. EV was reduced in vIδA26L, resulting in a slightly increased ratio of IMV:EV compared to IHD-J, which has not been observed in previous experiments (Figure 6.10G).

In vIδA26L.neo, a reduction in IMV and EV was observed compared to vIδA26L.rev at 9 hours p.i. (Figure 6.11B). Up to 24 hours p.i., EV production was dominant in both viruses reducing the ratio of IMV:EV to less than 1 (Figures 6.11C -F). The production of IMV and EV were comparable for the two viruses except at 15 hours p.i. where the ratio of IMV:EV in vIδA26L.neo was increased compared to vIδA26L.rev. At 30 hours p.i., equivalent quantities of EV were produced and IMV was slightly reduced in vIδA26L.neo compared to vIδA26L.rev resulting in a reduction in the ratio of IMV:EV in vIδA26L.neo at late times p.i. (Figure 6.11G).

Examining the kinetics of IMV and EV in COP demonstrated that IMV was produced in greater quantity than EV throughout the infectious cycle resulting in an increased ratio of IMV:EV when compared to IHD-J (Figure 6.12). As the infection progressed, the quantities of IMV and EV were reduced compared to IHD-J

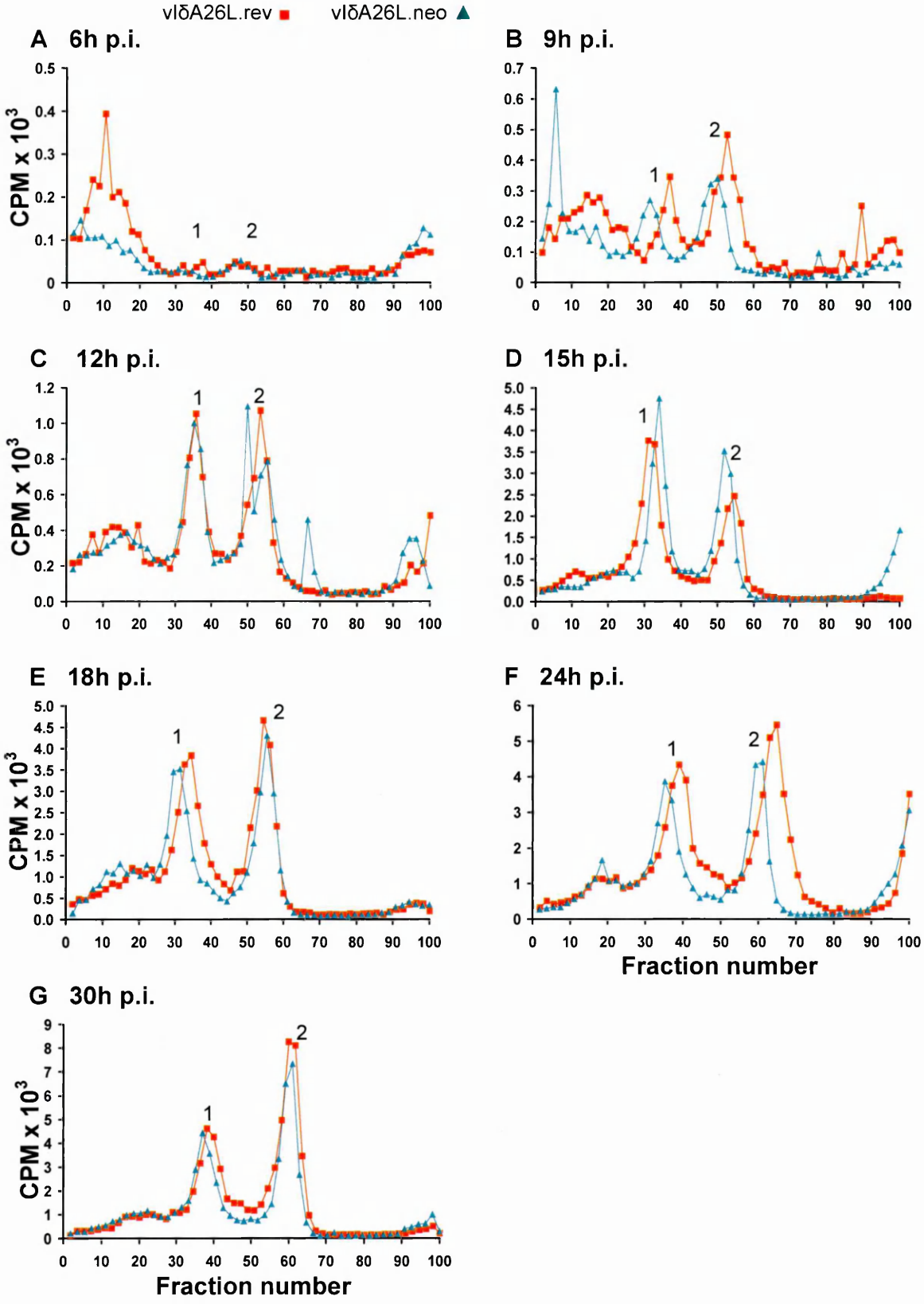
vIδA26L.rev
vIδA26L.neo
A 6h p.i.
B 9h p.i.
C 12h p.i.
D 15h p.i.
E 18h p.i.
F 24h p.i.
G 30h p.i.
CPM x 10³
Fraction number
1
2

	Ratio IMV:EV	
Time p.i. (h)	vlδA26L.rev	vlδA26L.neo
6	1.39	1.14
9	1.66	1.30
12	1.08	1.05
15	0.56	0.88
18	0.95	0.93
24	0.96	0.84
30	1.36	1.10

Figure 6.11 Analysis of IMV and EV by Radioactive Labelling of Virions in vlδA26L.rev and vlδA26L.neo Cultures

Liquid scintillation counting of CsCl fractions of ^{3}H thymidine labelled progeny virions from vlδA26L.rev (■) and vlδA26L.neo (▲) virus cultured in RK13 cells. Progeny virus was harvested at 6 (**A**), 9 (**B**), 12 (**C**), 15 (**D**), 18 (**E**), 24 (**F**) and 30 (**G**) hours p.i. and subjected to ultracentrifugation through CsCl gradients. Peaks 1 and 2 represent EV and IMV, respectively. Ratios = sum of IMV counts/sum of EV counts.

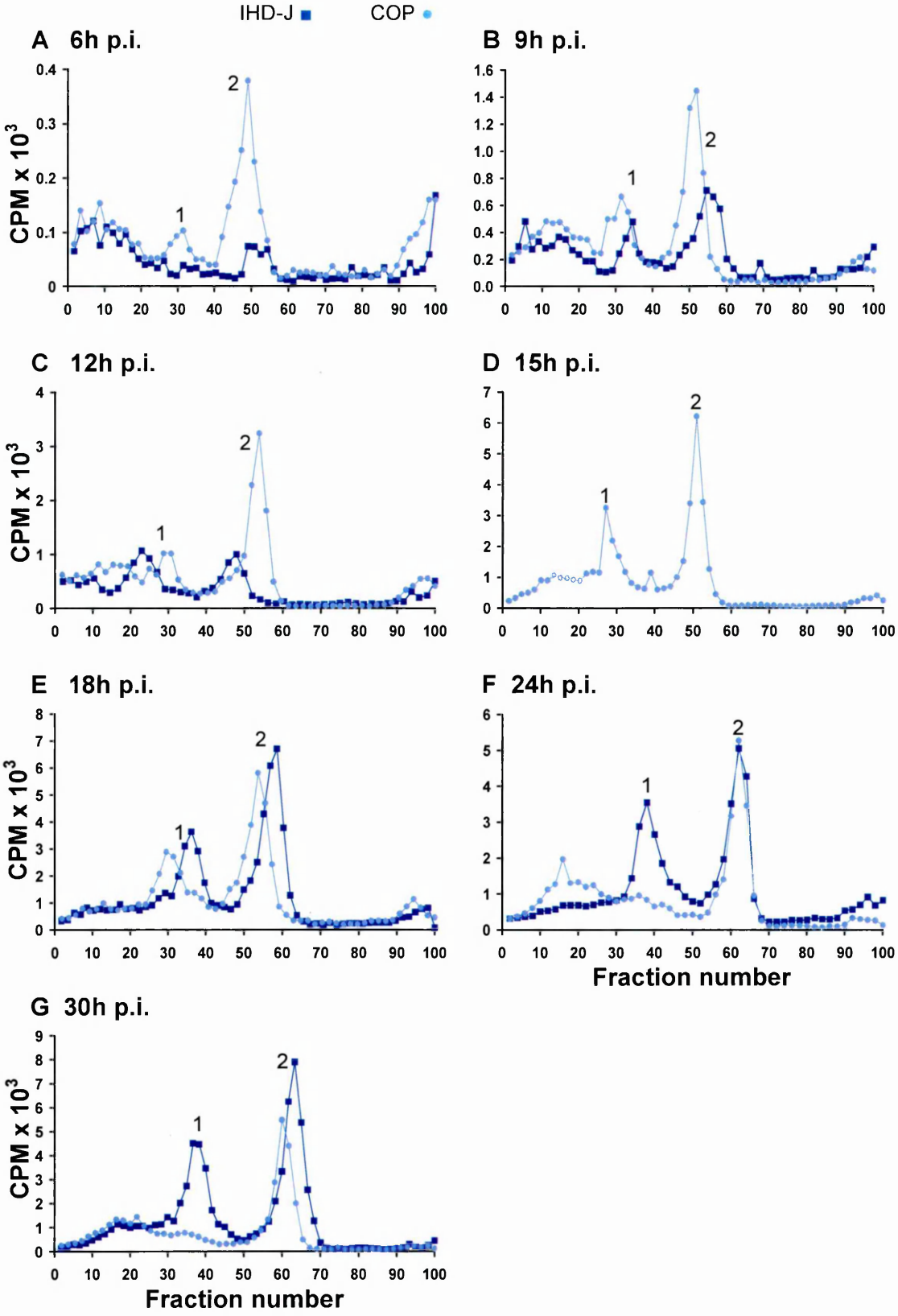
IHD-J
COP
A 6h p.i.
B 9h p.i.
C 12h p.i.
D 15h p.i.
E 18h p.i.
F 24h p.i.
G 30h p.i.
CPM x 10³
Fraction number
1
2

Time p.i. (h)	Ratio IMV:EV	
	IHD-J	COP
6	*	2.69
9	1.88	1.84
12	0.75	2.08
15	†	1.28
18	1.47	1.47
24	1.08	2.43
30	1.39	3.47

Figure 6.12 Analysis of IMV and EV by Radioactive Labelling of Virions in IHD-J and COP Cultures

Liquid scintillation counting of CsCl fractions of ^{3}H thymidine labelled progeny virions from IHD-J (■) and COP (●) virus cultured in RK13 cells. Progeny virus was harvested at 6 (**A**), 9 (**B**), 12 (**C**), 15 (**D**), 18 (**E**), 24 (**F**) and 30 (**G**) hours p.i. and subjected to ultracentrifugation through CsCl gradients. Peaks 1 and 2 represent EV and IMV, respectively. Ratios = sum of IMV counts/sum of EV counts.

* Counts too low to determine peaks and therefore to calculate ratio at 6 hours p.i.

† No data for IHD-J at 15 hours p.i. due to a cracked centrifuge tube.

(Figures 6.12E and F) and by 30 hours p.i. there was a dramatic reduction in EV which resulted in an increased ratio of IMV:EV compared to IHD-J (Figure 6.12G). These findings are similar to those in BSC40 and RK13 cells where the majority of progeny produced by COP was IMV.

Comparison of vIδA26L and vIδA26L.neo demonstrates some differences in their phenotypes although there was a general reduction in virus production in the early stages of replication. One of the major differences observed was the production of IMV in favour of EV in vIδA26L cultures, whereas EV production was favoured in vIδA26L.neo cultures during the early stages of the infectious cycle.

The reasons for this are unclear, as previous experiments in this chapter have demonstrated similar phenotypes for these viruses. It is possible that the cells used for this experiment have introduced some variability resulting in differing maturation kinetics between viruses and also across time points. In addition, where it has been consistently observed that the majority of progeny mature as IMV in this chapter, EV predominated in some cultures. It should also be noted that the CPM for this experiment were reduced compared to the previous two studies suggesting that the metabolic state of the cell cultures may not have been equivalent.

6.2.2.5 Examination of the Kinetics of IMV and EV Production in RK13 cells of Varying Passage History

The differing maturation kinetics observed for the A26L deletion mutants was unclear, therefore to investigate whether this may be due to the passage

history of the cells, the production of IMV and EV was examined in RK13 cells at high and low passage, where high passage represented experiments reported in Chapter 3 and low passage in this chapter. From previously published data, the IHD-J strain should produce ~3-fold greater quantities of IMV than EV by 24 hours p.i. when grown in RK13 cells (181;359).

RK13 cells of low and high passage were infected at MOI 10, and ^{3}H thymidine supplemented cultures incubated for 24 and 30 hours p.i. The experiment was performed three times, resulting in the comparison of cultures at passage 5, 11 and 18 (low) with passages 65, 71 and 78 (high). Progeny virions were separated by ultracentrifugation through CsCl gradients, and the gradients fractionated and subjected to liquid scintillation counting (Figure 6.13). The quantities of IMV and EV were calculated by summing the counts of each peak on the resulting trace (Figure 6.14). At 24 hours p.i., cells at low passage produced more EV than IMV, with the exception of P11 which produced approximately equivalent quantities (Figure 6.14A), and only at P5 was the difference between IMV and EV marked. After 30 hours p.i., EV production still dominated, again except for P11 where the quantities of IMV exceeded EV (Figure 6.14B). Cells at high passage produced greater quantities of EV at both 24 and 30 hours p.i. , although again the difference was only marked at one passage, P65 (Figure 6.14C and D).

The data indicated that different cultures of RK13 cells could give dramatically different IMV:EV ratios, and that this may have little to do with the

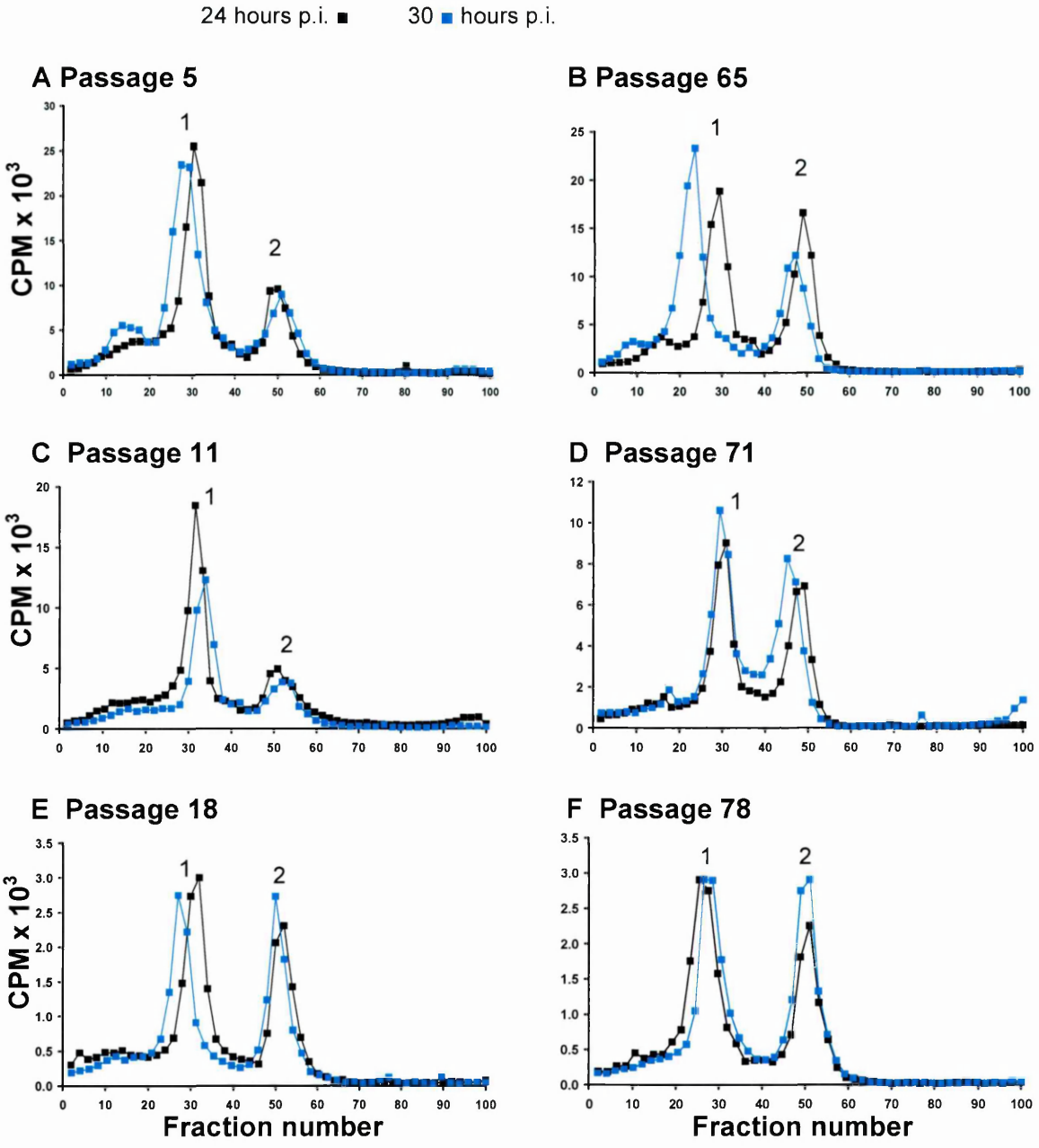

Figure 6.13 Examination of Progeny in RK13 cells of Varying Passage Number

IHD-J was cultured in RK13 cells of various passage numbers (P): **A** – P5; **B** – P65; **C** – P11; **D** – P71; **E** – P18 and **F** – P78, and harvested at 24 (■) and 30 (■) hours p.i. Progeny virions were subjected to ultracentrifugation through CsCl gradients. Peaks 1 and 2 represent EV and IMV, respectively.

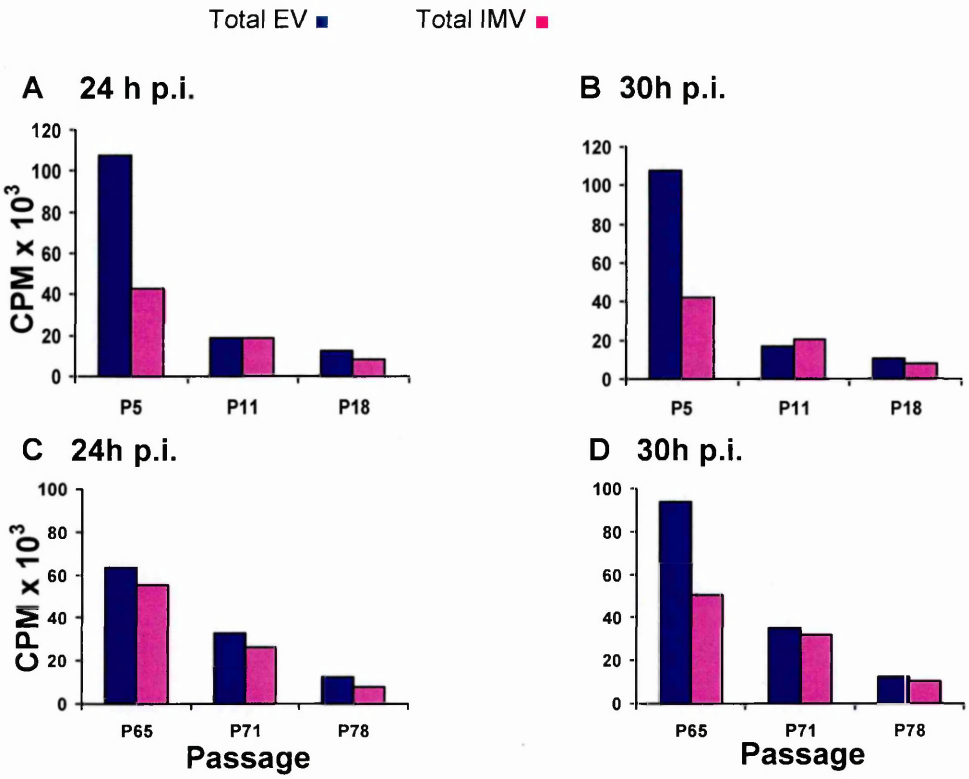

Figure 6.14 Examination of Progeny in RK13 cells of Varying Passage Number

IHD-J was cultured in RK13 cells of various passage numbers (P) at MOI 10 and harvested at 24 (**A** and **C**) and 30 (**B** and **D**) hours p.i. Progeny virions were subjected to ultracentrifugation through CsCl gradients (see Figure 6.13). Data is presented as the sum of counts (CPM) for the EV peak (■) and IMV peak (■) from each trace.

passage history of the cells. This may conceivably be due to alterations in cellular metabolism that leads to a decrease in the rate of the infectious cycle. It is apparent that even when at low passage there is variation in the production of EV and IMV in these cells, and in all of the experiments the total progeny indicated by the total CPM of both EV and IMV also varied considerably. This suggests that there is inter-experimental variation that may not only affect the production of IMV and EV, but also the yield of radiolabelled virus that may not be attributed to the passage history of the cells.

Taking this into consideration, RK13 cells at low passage were used in future kinetics experiments. Prior to the next kinetics study, these cells were examined for their ability to produce IMV and EV (Figure 6.15). At 24 hours p.i. a majority of progeny produced was EV, however IMV was in slight majority in cultures harvested at 30 hours p.i.

6.2.3 Effect of Overexpression of A26L on Maturation of IMV and EV

To test the hypothesis that overexpression of A26L leads to increased IMV and decreased EV production, the ability of vlδA26L.EL to produce each particle was assessed. RK13 cells were synchronously infected at MOI 10 with IHD-J and vlδA26L.EL. Cultures were supplemented with 10 μCi ^{3}H thymidine and virus harvested after 24 hours incubation. Total progeny virions were subjected to ultracentrifugation through CsCl gradients and fractions subjected to liquid scintillation counting (Figure 6.16A).

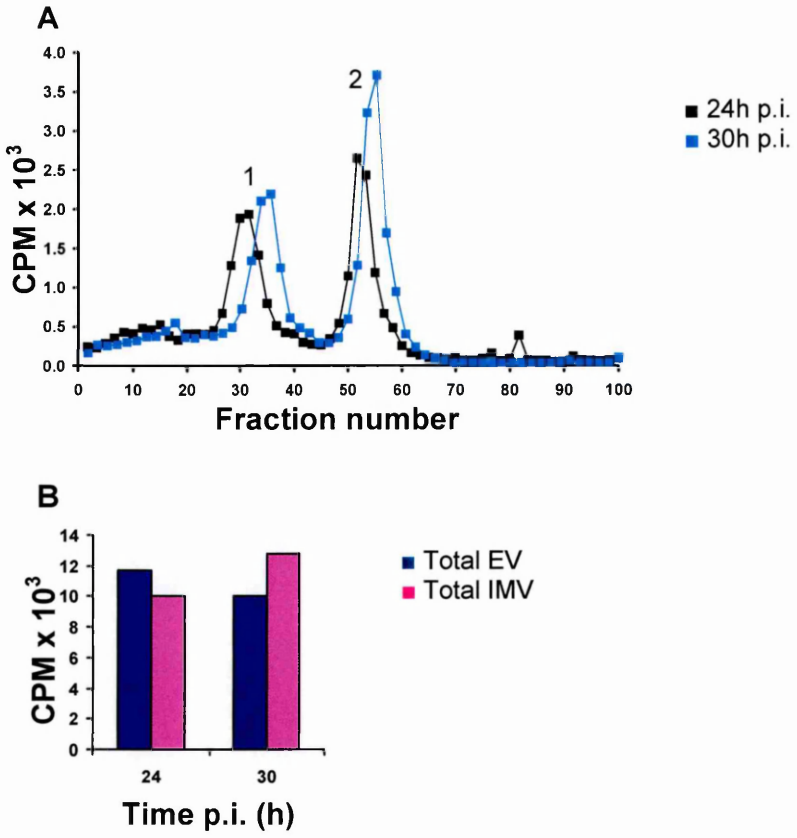

Figure 6.15 Examination of Progeny in RK13 cells at Passage 2

IHD-J was cultured in RK13 cells at MOI. **A** Progeny virions were harvested at 24 (■) and 30 (■) hours p.i. and subjected to ultracentrifugation through CsCl gradients. Peaks 1 and 2 represent EV and IMV, respectively. **B** Data is presented as the sum of counts (CPM) for the EV peak (■) and IMV peak (■) for 24 and 30 hours p.i.

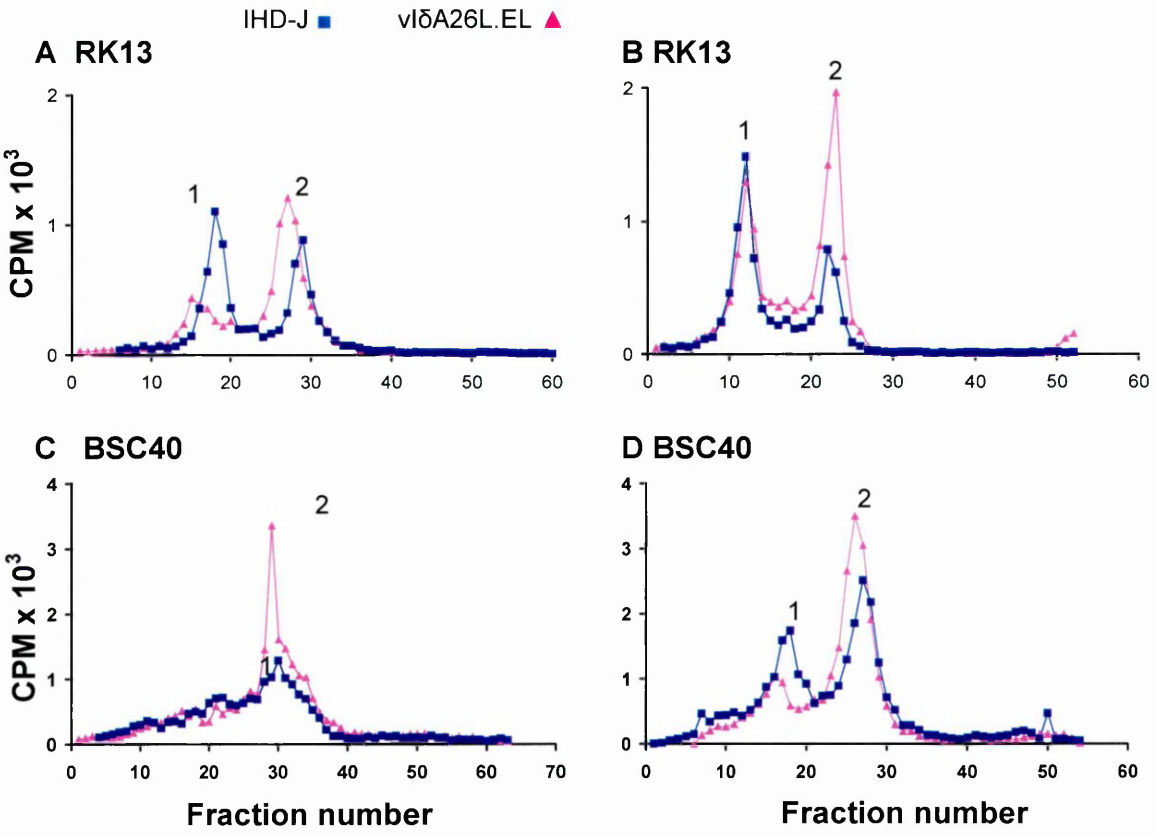

	Ratio IMV:EV	
Culture	IHD-J	vIδA26L.EL
RK13 (A)	0.90	2.36
RK13 (B)	0.50	1.34
BSC40 (C)	2.22	4.67
BSC40 (D)	1.33	3.22

Figure 6.16 Analysis of IMV and EV by Radioactive Labelling of Virions in IHD-J and vIδA26L.EL Cultures

Liquid scintillation counting of CsCl fractions of ^{3}H thymidine labelled progeny virions from IHD-J (■) and vIδA26L.EL (▲) virus cultured in RK13 cells (**A-B**) or in BSC40 cells (**C-D**). Progeny virus was harvested at 24 hours p.i. and subjected to ultracentrifugation through CsCl gradients. Peaks 1 and 2 represent EV and IMV, respectively. Ratios = sum of IMV counts/sum of EV counts.

The results demonstrate an increase in IMV and a decrease in EV in vIδA26L.EL cultures compared to IHD-J, thus increasing the ratio of IMV:EV in vIδA26L.EL. IMV did not constitute the majority of progeny virions in IHD-J cultures and the counts were somewhat low. This demonstrated the variability in these assays, however, vIδA26L.EL was able to produce more IMV suggesting that IMV production was occurring earlier in the infectious cycle. It is possible that the limited production of IMV in the wild-type culture maybe due to limiting ^{3}H thymidine. To try to mitigate this, the experiment was repeated and 20 μCi ^{3}H thymidine was added to the culture medium to increase the availability of ^{3}H thymidine. The production of IMV by IHD-J again was not as great as expected, suggesting that the levels of ^{3}H thymidine available were not limiting in these cultures (Figure 6.16B). These cultures also demonstrated an increase in IMV and a slight decrease in EV in vIδA26L.EL, thus increasing the ratio of IMV:EV relative to IHD-J. Subsequently, the kinetics of IMV and EV production were investigated in BSC40 cells as an alternative model. The experiment was performed twice, both times demonstrating increased IMV production and decreased EV production for vIδA26L.EL compared to IHD-J (Figure 6.16C and D), increasing the ratio of IMV:EV in vIδA26L.EL. In addition, production of IMV exceeded that of EV after 24 hours in IHD-J cultures, demonstrating the expected phenotype at 24 hours p.i.

These results demonstrated that increased levels of IMV are produced in vIδA26L.EL cultures, suggesting that overexpression of A26L results in maturation of IMV at earlier times in the infectious cycle leading to a concomitant reduction in

EV maturation. To investigate this further, the kinetics of IMV and EV maturation were assessed throughout the infectious cycle in BSC40 cells.

6.2.3.1 Kinetics in BSC40 cells

To further assess the phenotype of vIδA26L.EL observed in BSC40 cells and RK13 cells 24 hours p.i., the kinetics of IMV and EV maturation were investigated and compared to vIδA26L.rev, its matched control (Figure 6.17). Although limited progeny virus was produced at 6 and 9 hours p.i., increased amounts of IMV were produced relative to EV in vIδA26L.EL cultures thus increasing the ratio of IMV:EV compared to vIδA26L.rev (Figures 6.17A and B). As the infection progressed, the quantity of virus produced in vIδA26L.EL was reduced compared to vIδA26L.rev at 12 and 15 hours p.i. and the relative quantities of IMV were reduced leading to a reduced ratio of IMV:EV compared to vIδA26L.rev (Figures 6.17C and D). By 24 hours p.i. levels of IMV were increased relative to EV resulting in a markedly increased ratio of IMV:EV in vIδA26L.EL, compared to vIδA26L.rev culture (Figure 6.17E). This suggests that overexpression of A26 by vIδA26L.EL results in a relative increase in IMV and thus increases the ratio of IMV:EV, but only at very late times p.i. This may be due to the kinetics of expression from the synthetic early/late promoter, which was constructed to optimise absolute levels of expression but not the fine kinetics of expression within the early or late stages of the replicative cycle.

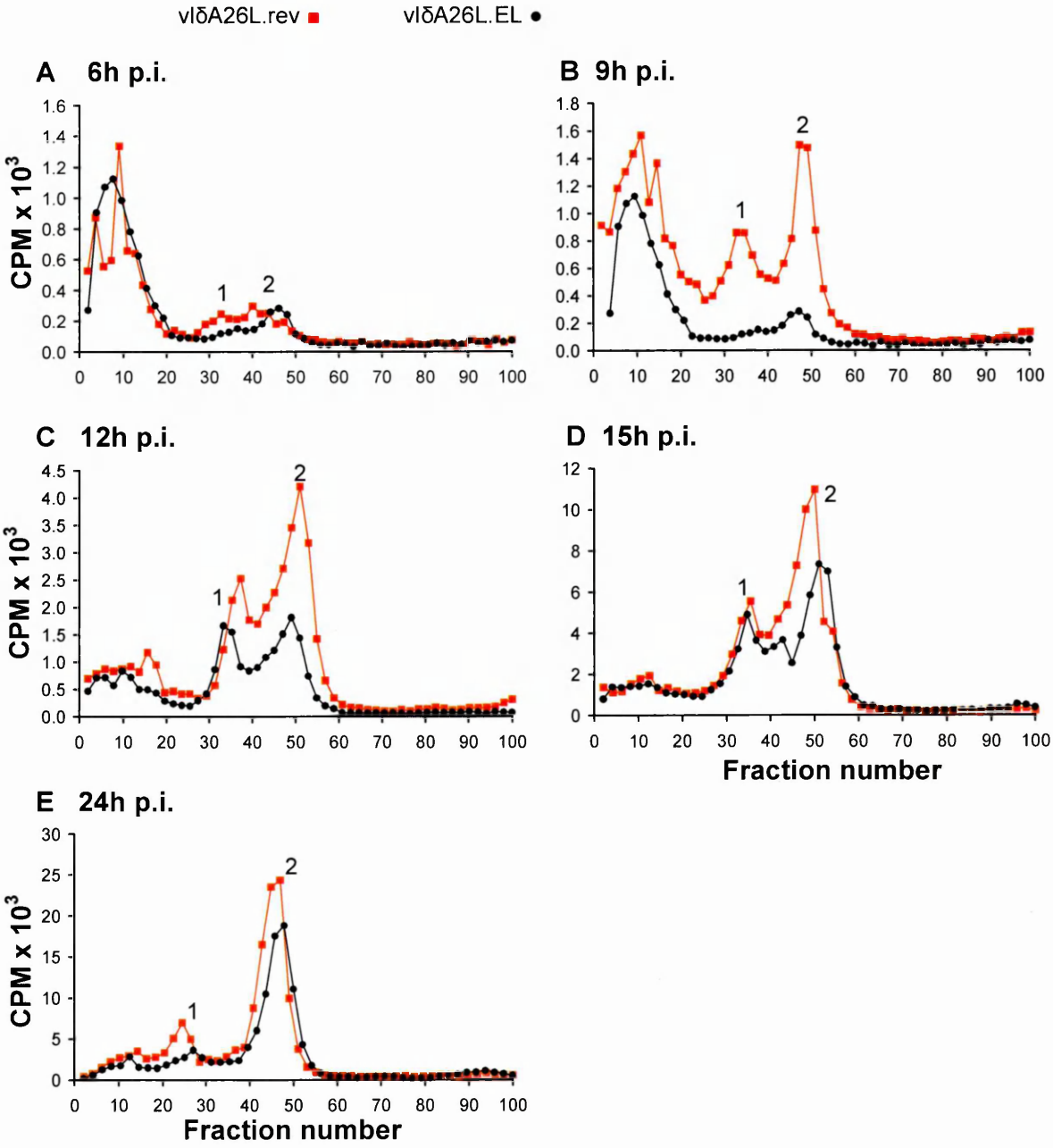

Time p.i. (h)	Ratio IMV:EV	
	vIδA26L.rev	vIδA26L.EL
6	1.32	1.94
9	1.25	1.51
12	2.45	1.37
15	2.60	1.21
24	2.69	4.90

Figure 6.17 Analysis of IMV and EV by Radioactive Labelling of Virions in vIδA26L.rev and vIδA26L.EL Cultures

Liquid scintillation counting of CsCl fractions of ^{3}H thymidine labelled progeny virions from vIδA26L.rev (□) and vIδA26L.EL (●) virus cultured in BSC40 cells. Progeny virus was harvested at 6 (**A**), 9 (**B**), 12 (**C**), 15 (**D**) and 24 (**B**) hours p.i. and subjected to ultracentrifugation through CsCl gradients. Peaks 1 and 2 represent EV and IMV, respectively. Ratios = sum of IMV counts/sum of EV counts.

6.2.3.2 Kinetics in RK13 cells (I)

Due to the difference in phenotype of vIδA26L observed in BSC40 cells (section 6.2.2.2) to that in previous experiments in RK13 cells in Chapter 3, the kinetics of IMV and EV production was examined for vIδA26L.EL also in RK13 cells. Modulation of the A26L gene by vIδA26L.EL resulted in almost identical kinetics to vIδA26L.rev at 6 hours p.i. (Figure 6.18A), however production of IMV at 9 and 12 hours p.i. was reduced while the quantities of EV were unchanged compared to vIδA26L.rev, resulting in a reduction in the ratio of IMV:EV in vIδA26L.EL (Figures 6.18B and C). As the infection progressed, IMV production increased and EV production was reduced in vIδA26L.EL compared to vIδA26L.rev, which was especially apparent at 15, 18 and 24 hours p.i., thus increasing the ratio of IMV:EV (Figures 6.18D-G). This suggests that overexpression of A26L creates an abundance of A26 which leads to increased maturation of progeny as IMV and thus reducing EV maturation. This confirms the findings in BSC40 cells reported earlier in this chapter.

6.2.3.3 Kinetics in RK13 cells (II)

The study of the kinetics of IMV and EV production was repeated in RK13 cells, where overexpression of A26L in vIδA26L.EL resulted in reduced quantities of IMV and EV throughout the infectious cycle (Figure 6.19). A reduction in the ratio of IMV:EV was observed at 9 hours p.i. compared to vIδA26L.rev (Figure 6.19B). At 12 hours p.i., IMV production was equivalent to EV production in both viruses (Figure 6.19C), however, reduced quantities of both forms of virus were produced

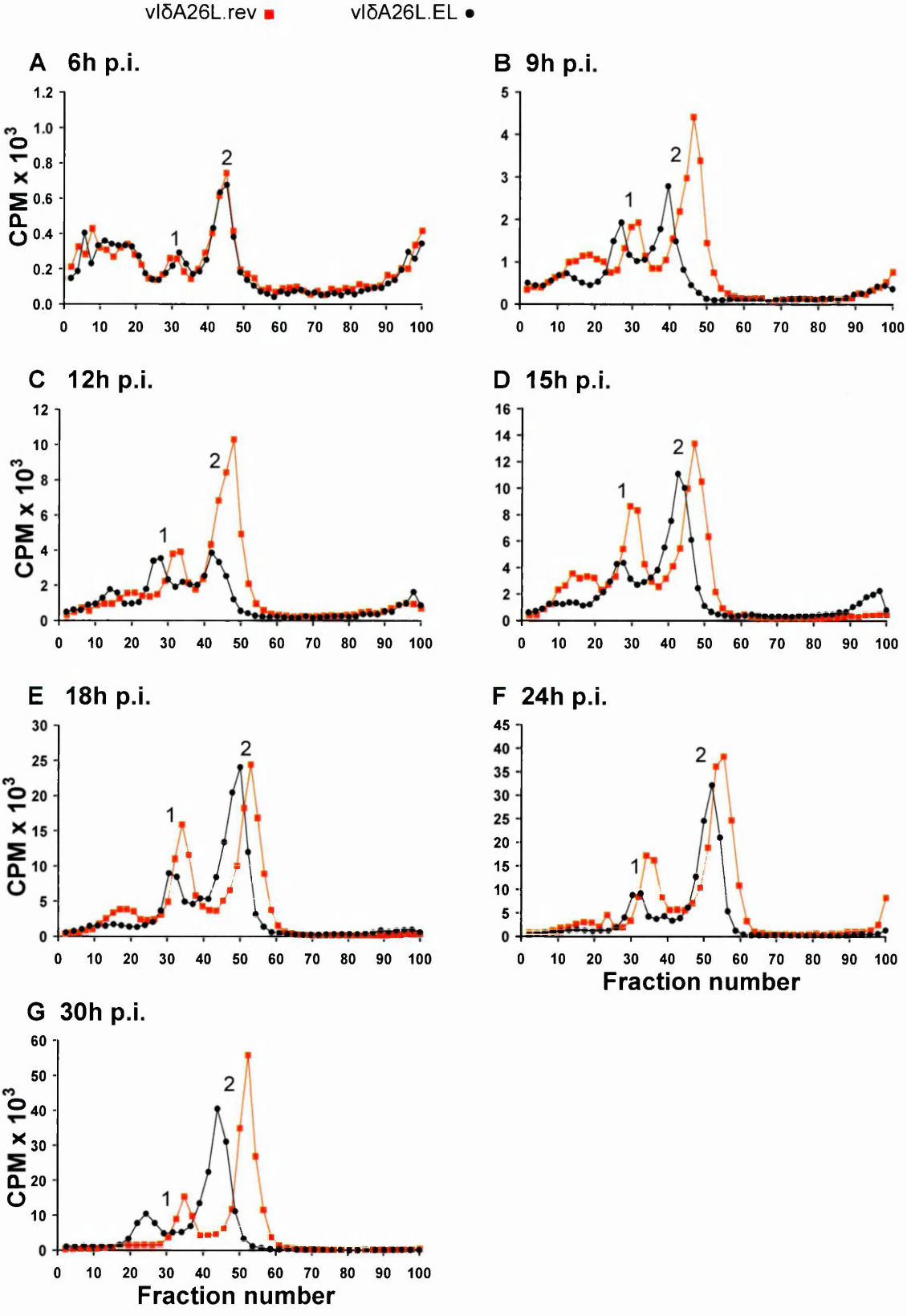
vlδA26L.rev ■
vlδA26L.EL ●
A 6h p.i.
B 9h p.i.
C 12h p.i.
D 15h p.i.
E 18h p.i.
F 24h p.i.
G 30h p.i.
CPM x 10³
Fraction number
1
2

	Ratio IMV:EV	
Time p.i. (h)	vlδA26L.rev	vlδA26L.EL
6	2.82	2.50
9	2.45	1.37
12	2.57	1.20
15	1.46	2.43
18	1.54	2.61
24	2.56	3.77
30	3.58	3.80

Figure 6.18 Analysis of IMV and EV by Radioactive Labelling of Virions in vlδA26L.rev and vlδA26L.EL Cultures

Liquid scintillation counting of CsCl fractions of ^{3}H thymidine labelled progeny virions from vlδA26L.rev (■) and vlδA26L.EL (●) virus cultured in RK13 cells. Progeny virus was harvested at 6 (**A**), 9 (**B**), 12 (**C**), 15 (**D**), 18 (**E**), 24 (**F**) and 30 (**G**) hours p.i. and subjected to ultracentrifugation through CsCl gradients. Peaks 1 and 2 represent EV and IMV, respectively. Ratios = sum of IMV counts/sum of EV counts.

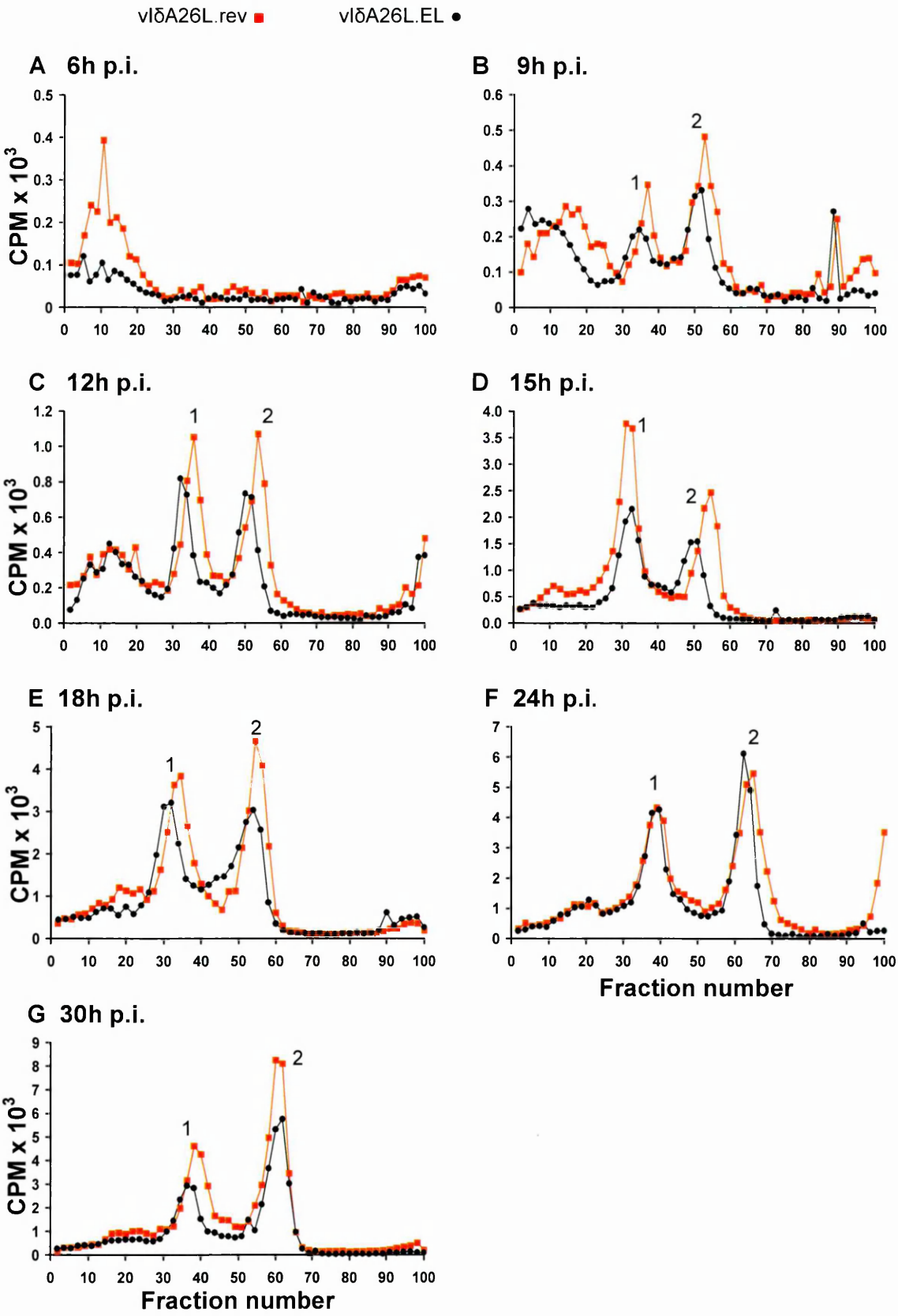
vlδA26L.rev ■
vlδA26L.EL ●
A 6h p.i.
B 9h p.i.
C 12h p.i.
D 15h p.i.
E 18h p.i.
F 24h p.i.
G 30h p.i.
CPM x 10³
Fraction number
1
2

Time p.i. (h)	Ratio IMV:EV	
	vIδA26L.rev	vIδA26L.EL
6	*	*
9	1.66	1.46
12	1.08	1.00
15	0.57	0.69
18	0.95	1.13
24	0.96	0.89
30	1.36	1.45

Figure 6.19 Analysis of IMV and EV by Radioactive Labelling of Virions in vIδA26L.rev and vIδA26L.EL Cultures

Liquid scintillation counting of CsCl fractions of ^{3}H thymidine labelled progeny virions from vIδA26L.rev (■) and vIδA26L.EL (●) virus cultured in RK13 cells. Progeny virus was harvested at 6 (**A**), 9 (**B**), 12 (**C**), 15 (**D**), 18 (**E**), 24 (**F**) and 30 (**G**) hours p.i. and subjected to ultracentrifugation through CsCl gradients. Peaks 1 and 2 represent EV and IMV, respectively. Ratios = sum of IMV counts/sum of EV counts.

* Counts too low to determine peaks and therefore calculate ratio at 6 hours p.i.

by vIδA26L.EL. As the infection progressed, IMV production increased relative to EV, increasing the ratio of IMV:EV at 18 hours p.i. in vIδA26L.EL relative to vIδA26L.rev (Figures 6.19E). At 30 hours p.i., IMV and EV were reduced in vIδA26L.EL compared to vIδA26L.rev, however, as IMV was the majority of progeny in vIδA26L.EL, the ratio of IMV:EV increased slightly compared to vIδA26L.rev (Figure 6.19G). This highlights the variability in the outcomes of these experiments.

6.2.4 Quantification of IMV Produced in VACV Cultures When A26L was Modified

Considering the complexity of the data obtained from CsCl gradients, the data from experiments described in sections 6.2.2 and 6.2.3 was used to determine whether deletion of A26L decreased the proportion of IMV, and if overexpression of A26L increased the proportion of IMV in cultures. The quantity of IMV as a percentage of total progeny virus produced in BSC40 cells at 24 hours p.i. and in RK13 cells at 30 hours p.i. was calculated for IHD-J, vIδA26L, vIδA26L.rev, vIδA26L.neo, COP and vIδA26L.EL cultures (Figure 6.20). There were no significant differences in the proportion of IMV produced in each culture in pairwise comparisons of all viruses using a repeated measures one-way ANOVA (overall $p=0.48$).

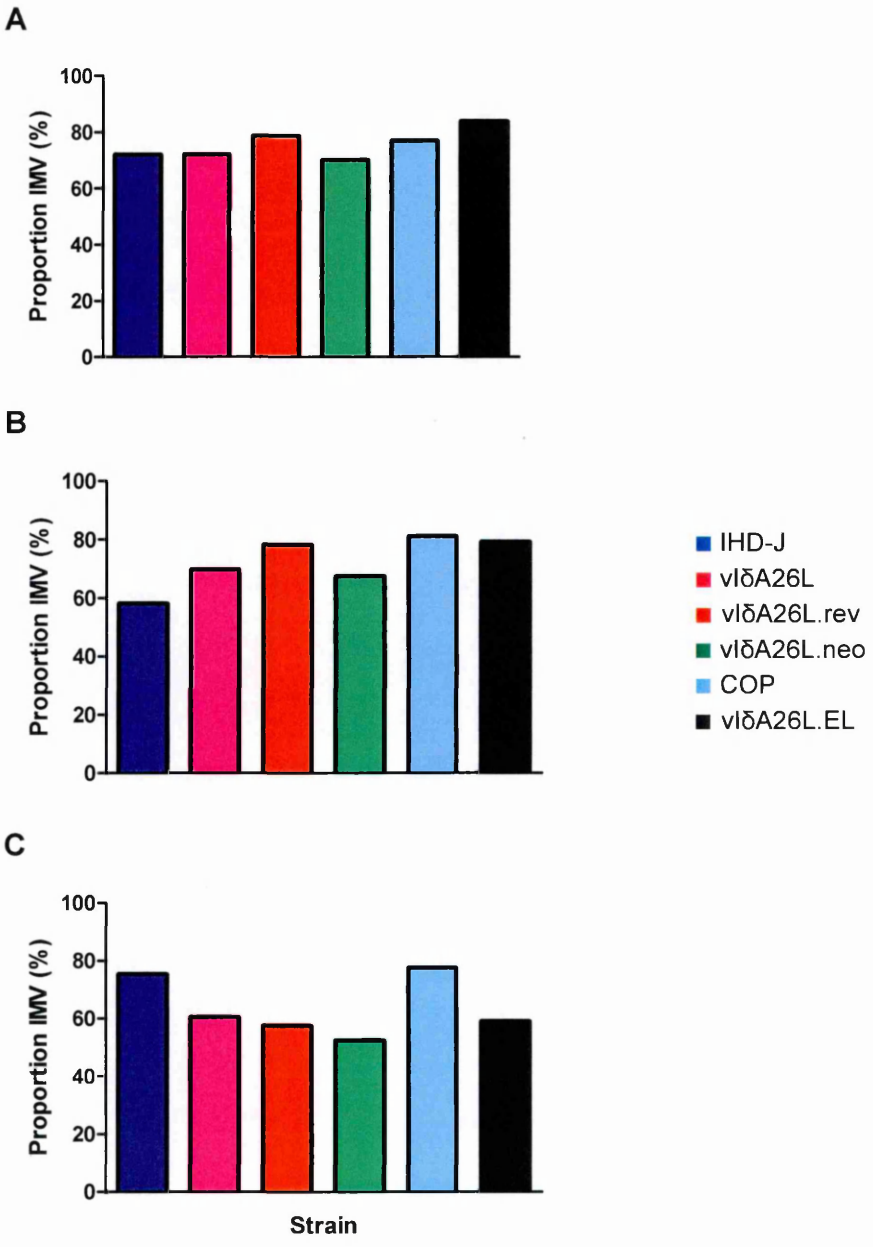

Figure 6.20 Proportion of IMV Produced in Cultures When A26L was Deleted or Overexpressed

IHD-J (■), vIδA26L (■),vIδA26L.rev (■),vIδA26L.neo (■), COP (■) and vIδA26L.EL (■) were cultured in BSC40 cells for 24 hours (**A**) or RK13 cells for 30 hours (**B** and **C**). Data is accumulated from CsCl gradients presented previously in this chapter where the proportion of IMV (%) = sum of counts (CPM) for the IMV peak /total counts (sum of counts (CPM) for IMV and EV peaks) from each trace x 100.

6.2.5 Transmission Electron Microscopy (TEM)

To investigate whether modulation of A26 resulted in a gross defect in virion assembly or morphology that may explain the perturbation of virion maturation in recombinant cultures, viruses were cultured in RK13 cells at MOI 10 for 24 hours and then processed for TEM as described in section 2.5.8. In each of the samples examined, fully mature non-enveloped intracellular virions were observed that were brick-shaped, and contained a dumb-bell shaped core (Figure 6.21). Virions were also observed at the cell surface demonstrating egress of virions from the cells. Other structures characteristic of VACV morphogenesis such as crescents and spherical immature virions were also observed, suggesting normal morphogenesis in the recombinants generated in this study.

6.2.6 Expression Kinetics in VACV Cultures

To examine the kinetics of expression of A26L in the recombinant viruses, TaqMan® assays for the A26L, A27L and F13L genes were designed and optimised by Applied Biosystems (UK) (Table 6.1). Based on the WR genome sequence, the entire coding sequences of both the A27L and F13L genes were used for the assay design. A region of 345 bp (nucleotides 487 to 832) of the A26L gene was targeted on the basis that the target sequence was absent from COP, thus COP was used in these experiments as a negative control for A26L. The eukaryotic 18s rRNA gene was used as an endogenous control in all expression assays to normalise the quantity of template mRNA in each well (32;360). To validate the amplification efficiencies of the TaqMan® assays compared to the

A IHD-J

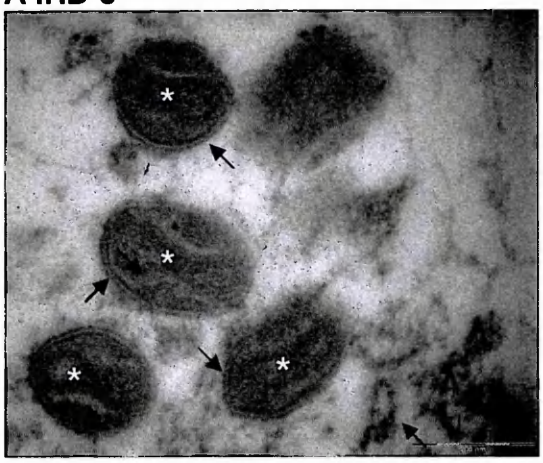

B vIδA26L

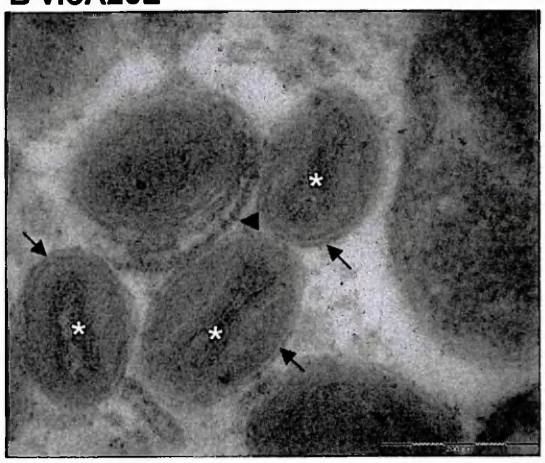

C vIδA26L.rev

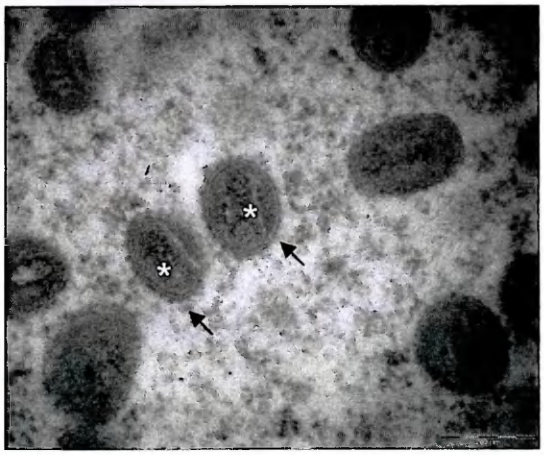

D vIδA26L.neo

E vIδA26L.EL

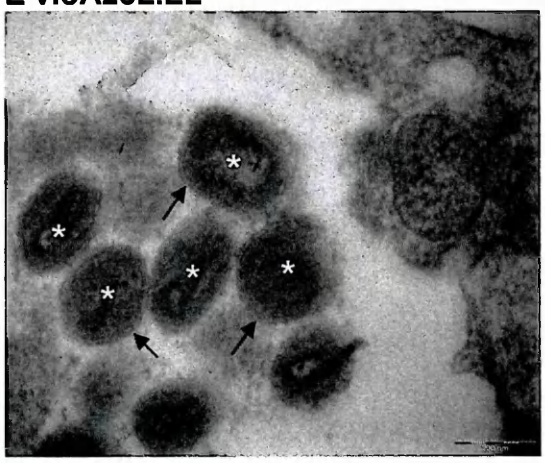

Figure 6.21 Transmission Electron Micrographs of Recombinant VACVs in RK13 cells

RK13 cells were infected at MOI 10 with IHD-J (**A**), or vIδA26L (**B**), vIδA26L.rev (**C**), vIδA26L.neo (**D**) or vIδA26L.EL (**E**) and incubated for 24 hours at 37 °C in a humidified 5 % (v/v) CO_2 atmosphere. Cells were fixed in 500 µl Karnovski fixative for a minimum of 18 hours at 4 °C and processed for TEM as described in section 2.5.8. Arrows indicate the virion membrane. Asterisks indicate dumb-bell shaped cores. The arrow-head in B indicates a putative additional membrane resulting in a partially enveloped virion.

Gene	Forward primer 5'- to 3'-	Reverse primer 5'- to 3'-	Probe 5'- to 3'-
A26L	ACGGATCACAGGTATAT CACGACAT	GTACATAAATGCGTATA GTAGTCTACCTATCTCT	TCGTAATGCC GGTTTTC
A27L	ACGCAACGATGAAGTTC TATTTAGGT	CCAGAGATATCATAGC CGCTCTTAG	CAGCGTGATT TTCC
F13L	CCTTTAATAGCGCAAAA AATTCATGGTT	GCAGTGCTAACTGGCA AACAA	CAAGCCGCAG AGCAT

Table 6.1 Primer and Probe Sequences in TaqMan® Assays

Oligonucleotides sequences were designed by Applied Biosystems (UK) to detect the A26L, A27L and F13L genes using the Applied Biosystems 7000 Real-Time PCR System.

endogenous control, amplification of each target sequence was quantified over a range of dilutions of template mRNA as described in section 2.7 (Figure 6.22). For each gene, the delta cycle threshold (ΔCt) values were similar over a range of 10-fold dilutions of template mRNA, where the absolute value for the gradient of each data set was ~0.1, indicating similar amplification efficiencies for the target genes and the endogenous control. This value was slightly higher for the F13L assay and on consultation with Applied Biosystems (UK), it was considered that this should not affect future experiments.

6.2.6.1 Expression of A26L in vIδA26L.EL Cultures

Constitutive expression of A26L was predicted to increase IMV maturation earlier in the infectious cycle and therefore increase the proportion of IMV produced compared to IHD-J and vIδA26L.rev. This was not observed and therefore quantitative RT-PCR was used to examine whether the A26L gene was expressed earlier than in vIδA26L.rev cultures.

Previous studies suggest that the synthetic early/late promoter used in this study results in at least 2-fold increase in expression compared to the natural 7.5K promoter up to 9 hours p.i. (327). This would suggest that during the early phase of the infectious cycle, A26L transcripts should be more abundant in vIδA26L.EL than in vIδA26L.rev, as indicated by an increased fold change in expression.

RK13 cells were infected at MOI 10 with vIδA26L.EL or vIδA26L.rev and cultured for 1, 2, 3, 6, 12, 15, 18, 24 and 30 hours. Cultures were harvested at 0 hours also to determine a baseline for gene expression. RNA was extracted from

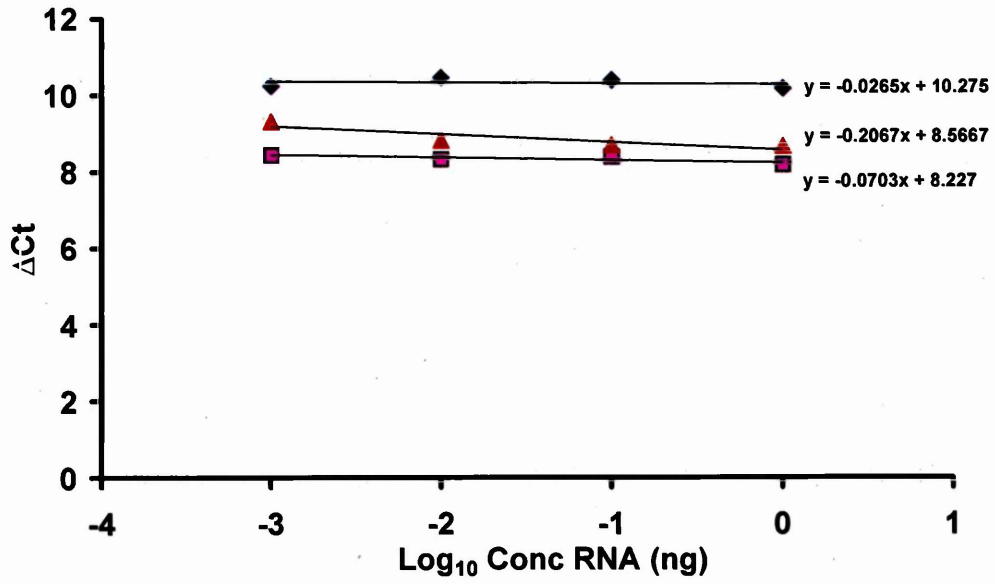

Figure 6.22 Amplification Efficiencies of TaqMan® Assays

Serial dilutions (10-fold) of extracted mRNA from IHD-J infected cultures at 6 hours p.i. were made and expression of the A26L (♦), F13L (▲) and A27L (■) genes determined as relative quantities compared to 18s rRNA (ΔCt). Trendlines were added using the Microsoft Excel® function. Data is representative of triplicate wells.

each culture and transcription of the A26L, A27L and F13L genes was quantified by real-time RT-PCR using the 18s rRNA gene as an endogenous control (section 2.7), as a measure of gene expression (Figure 6.23). Detectable transcription of the A26L gene began at 1 hour p.i., where the quantity steadily increased until 12 hours p.i. and this level of transcription was maintained throughout the infectious cycle (Figure 6.23A). Similar fold changes demonstrated expression of the A26L gene did not occur earlier, or in greater quantities in vIδA26L.EL than vIδA26L.rev in the cultures tested. Similar patterns of expression were also observed for the A27L and F13L genes (Figures 6.23B and C). Using a two-way ANOVA with Bonferroni's post-tests, there were no significant differences in the expression of the genes tested in these viruses (A26L p=0.90; A27L p=0.23; F13L p=0.67).

6.2.6.2 Expression Kinetics of the A26L, A27L and F13L Genes in Recombinant VACV Cultures Throughout Infection in RK13 cells

This study was performed to compare gene expression during the late phase of the infectious cycle in viruses where A26L is deleted or disrupted. It was anticipated that A26L would not be detected in vIδA26L, vIδA26L.neo and COP, and the levels of expression of the A27L and F13L genes would be unaffected. RK13 cells were infected at MOI 10 with IHD-J, vIδA26L.rev, vIδA26L, vIδA26L.neo or COP and cultured for 12, 15, 18, 24 and 30 hours. Cultures were harvested at 0 hours also to determine a baseline for gene expression, and gene transcription was quantified by real-time RT-PCR, as a measure of gene expression (Figure 6.24). Expression of the A26L gene was slightly reduced in

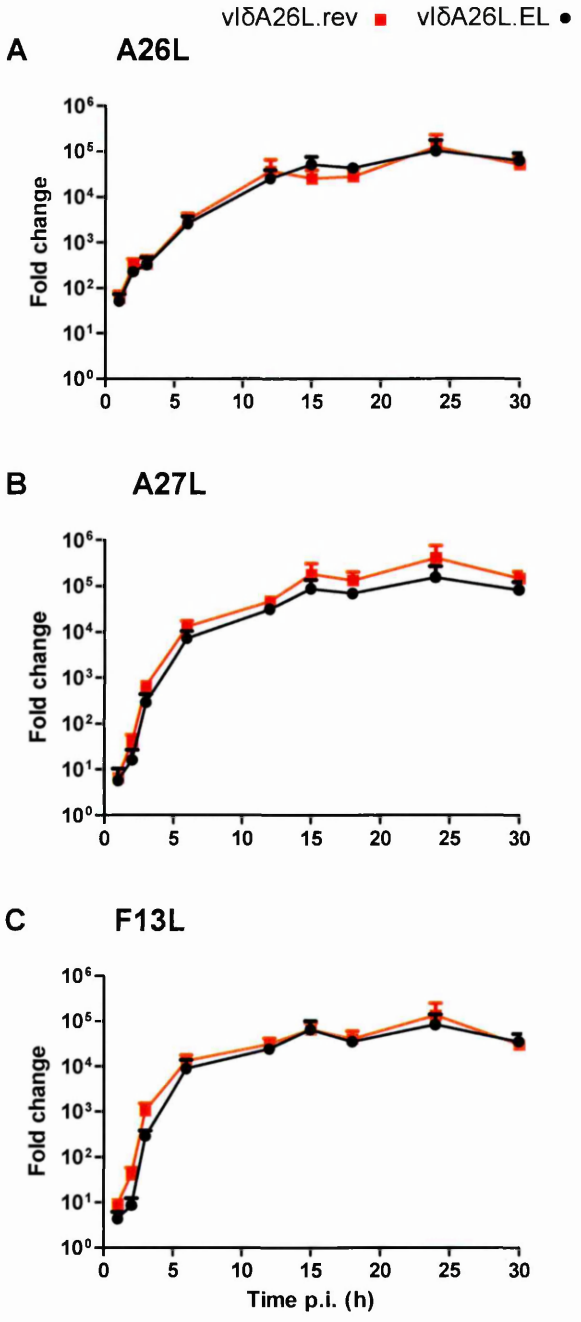

Figure 6.23 Expression Kinetics in vIδA26L.EL Cultures Throughout the Infectious Cycle

RK13 cells were infected at MOI 10 with vIδA26L.rev (■) or vIδA26L.EL (●) and cultures harvested at 0, 1, 2, 3, 6, 12, 15, 18, 24 and 30 hours p.i. RNA was isolated from each culture and expression of the A26L (**A**), A27L (**B**) and F13L (**C**) genes determined using the ΔΔCt method (335). Data is presented as means and SEM of triplicate cultures.

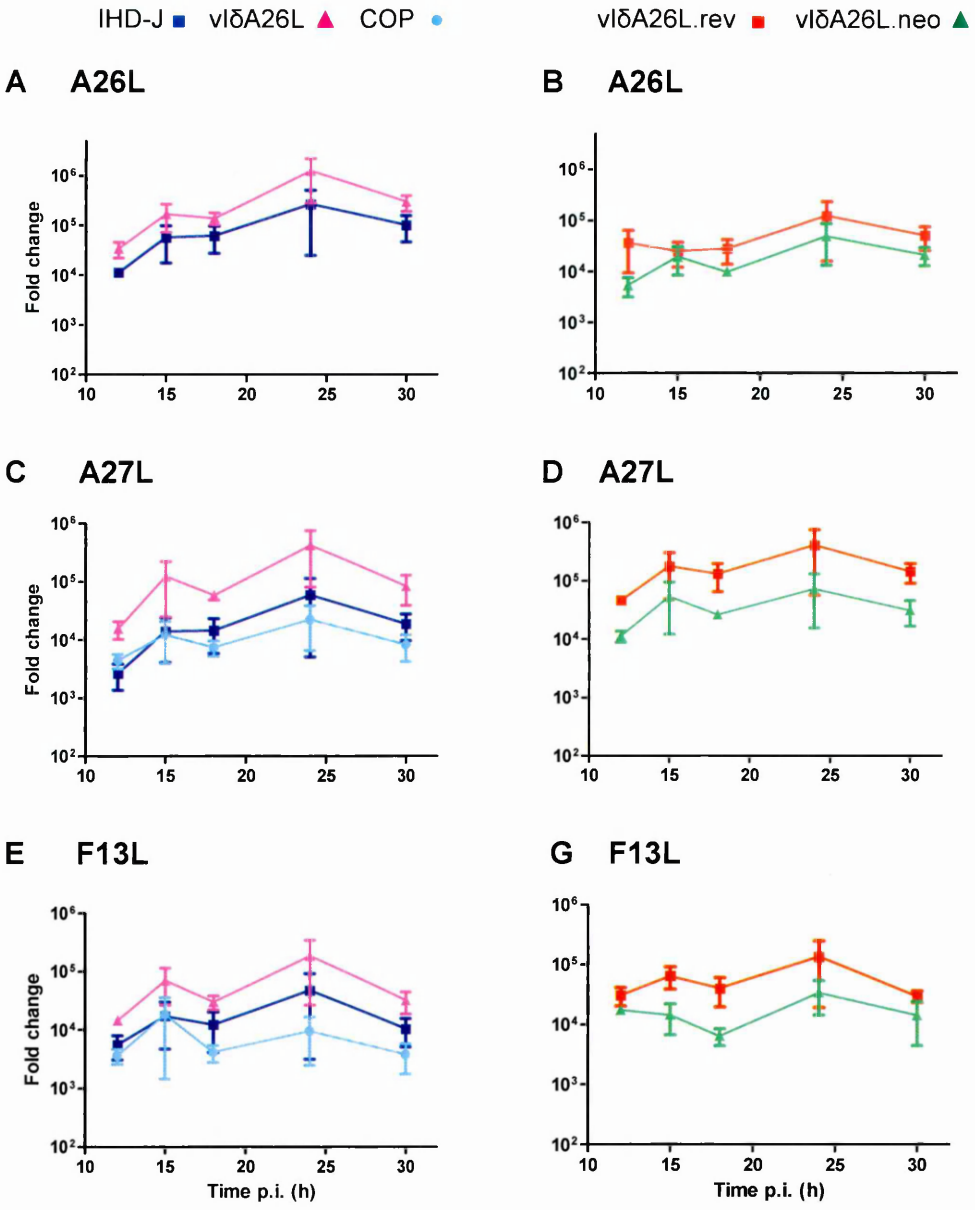

Figure 6.24 Expression Kinetics Throughout the Infectious Cycle in Recombinant VACV Cultures

RK13 cells were infected at MOI 10 with the IHD-J (■),vIδA26L.rev (■),vIδA26L (▲),vIδA26L.neo (▲) or COP (●) and cultures harvested at 0, 12, 15, 18, 24 and 30 hours p.i. RNA was isolated from each culture and expression of the A26L (**A** and **B**), A27L (**C** and **D**) and F13L (**E** and **F**) genes determined using the ΔΔCt method (335). Data is presented as means and SEM of triplicate cultures. A26 transcription was not detected in COP cultures and is therefore absent in A and B.

compared to vIδA26L.rev although this was not statistically significant (p=0.10), and expression was not detected in COP cultures. Unexpectedly, levels of expression were significantly increased in vIδA26L cultures compared to both IHD-J and vIδA26L.rev (p=0.02) (Figure 6.24A). Expression of the A27L and F13L genes increased over time also, peaking at 24 hours p.i., however, the levels of expression appeared to vary between viruses (Figure 6.24C-G). Expression of both the A27L and F13L genes were significantly reduced in vIδA26L.neo compared to vIδA26L.rev (p=0.0075 and p=0.032), and increased in vIδA26L compared to VACV IHD-J (p=0.004 and p=0.043).

On deeper examination of the raw data, this apparent increase in expression of A26L in vIδA26L cultures appears to be an artefact of decreased detection of A26L transcription at t=0, which leads to an increased fold change at all subsequent time points in comparison. The decrease in expression in vIδA26L.neo also appears to be an artefact of increased detection at t=0, which leads to a decrease fold change in comparison. Therefore in an attempt to "normalise" the data, ΔΔCt values were adjusted using IHD-J t=0 and vIδA26L.rev t=0 as baselines for vIδA26L and for vIδA26L.neo, respectively, and the fold change re-calculated (Figure 6.25). This demonstrated similar expression kinetics for all genes tested, suggesting that A26L was detected in vIδA26L and vIδA26L.neo cultures yet levels of expression were no longer statistically different to that of IHD-J and vIδA26L.rev (p>0.05). This also confirmed that expression of A27L had not been disrupted by mutation of the neighbouring locus.

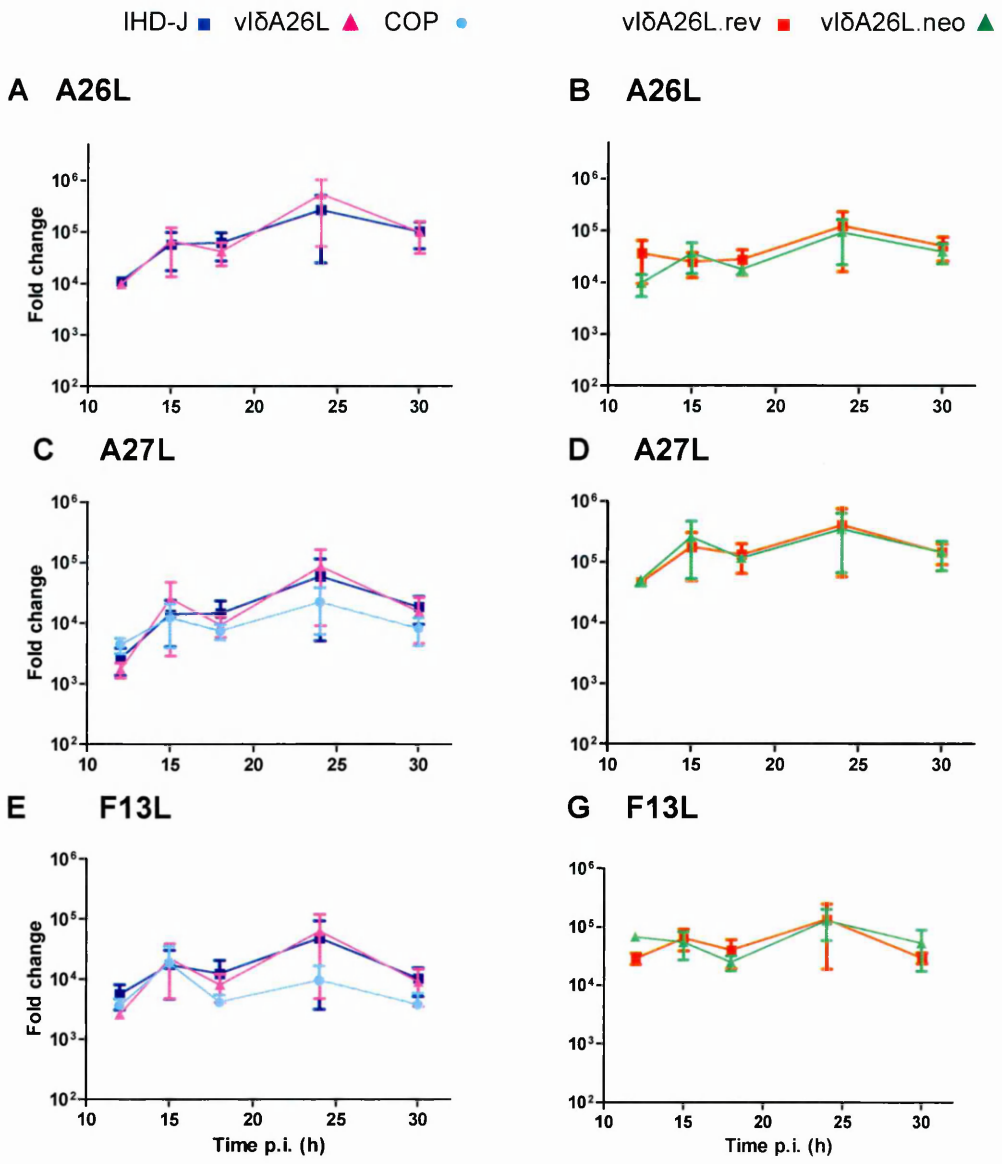

Figure 6.25 Expression Kinetics Throughout the Infectious Cycle in Recombinant VACV Cultures

RK13 cells were infected at MOI 10 with the IHD-J (■),vIδA26L.rev (■),vIδA26L (▲),vIδA26L.neo (▲) or COP (●) and cultures harvested at 0, 12, 15, 18, 24 and 30 hours p.i. RNA was isolated from each culture and expression of the A26L (**A** and **B**), A27L (**C** and **D**) and F13L (**E** and **F**) genes determined using the ΔΔCt method (335). Data is presented as means and SEM of triplicate cultures. A26 transcription was not detected in COP cultures and is therefore absent in A and B.

Note: the ΔΔCt value for vIδA26L and vIδA26L.neo have been calculated using IHD-J or vIδA26L.rev baseline at t=0, respectively, for all genes.

6.3 Discussion

This study was intended to build on previously reported data in Chapter 3, and to address more recent reports to elucidate the role of A26 in virion morphogenesis (1-4;6;27). One-step growth curves demonstrated a reduction in virus yields in both vIδA26L and vIδA26L.neo, and yet their growth rates remain unchanged, when compared to IHD-J and vIδA26L.rev, respectively. This supports the data presented in Chapter 3 for vIδA26L in RK13 cells, suggesting that a reduction in yields was due to deletion of the A26L gene as opposed to the presence of a selection marker gene. The yields in vIδA26L.EL and vIδA26L.rev were equivalent to IHD-J, demonstrating restoration of the wild-type phenotype in vIδA26L.rev, and confirming the null effect of expression of A26L from a synthetic early/late promoter and the presence of selection marker genes. The data also demonstrates similar growth rates for all viruses used in this study, where a difference would have been problematic for the planned kinetic studies. Interestingly, COP was able to replicate as well as the IHD-J strain and reached similar yields. Although COP possesses a truncated A26L gene, it has never been shown whether a truncated protein is assembled into the virion (Dr D. Pickup, personal communication). If the truncate is not incorporated into the virion, this strain may be expected to behave as an A26L deletion mutant and therefore have reduced viral yields. As growth of COP was unaffected, it would appear that the truncated A26L gene in COP is not equivalent to an A26L deletion.

Separation of IMV and EV through CsCl gradients was used to examine the kinetics of IMV and EV production in recombinant cultures, and to monitor the

changes in ratio of IMV:EV throughout the infectious cycle. Using ^{3}H thymidine to metabolically label viral DNA allows quantitation of virions regardless of the particle/pfu ratio, which may differ between IMV and EV (11), and mitigates the effect, if any, on particle aggregation elicited by altering the surface of the virion by deletion of A26. This data was intended to provide further insight into the function of A26, where deletion resulted in a dramatic reduction in IMV as reported in Chapter 3.

Examination of vIδA26L and vIδA26L.neo cultures demonstrated a general reduction in IMV, resulting in a decreased ratio of IMV:EV throughout the infectious cycle when compared to the IHD-J and vIδA26L.rev strains. However, the extent of this reduction varied between the replicates and was not statistically significant; and the reduction was minimal compared to a dramatic reduction in IMV reported in Chapter 3. The reason for this discrepancy is unknown, however the cell type used, metabolic state or the passage history of the cells may contribute to the variability in IMV and EV production observed throughout this study.

If A26 is a differentiation switch and is required for maturation as IMV, then vIδA26L and vIδA26L.neo virions that sediment with the same density as IMV are not true IMV, that is they have not differentiated as EV or IMV, and could be interpreted as a tissue culture artefact resulting from depletion of intracellular membranes that are required for EV wrapping (350). Therefore, it may be hypothesised that vIδA26L and vIδA26L.neo virions that do not either 1) become wrapped or 2) acquire IMV specific proteins such as A26, are less stable. Such an instability could account for the reduction of IMV, and the reduction in viral yields

observed in one-step growth curves. It is difficult to explain the difference between the data reported in Chapter 3 and the data reported here. However, it is possible that minor variation in experimental conditions between Chapter 3 and the experiments described here may have influenced the stability of putative undifferentiated virions.

Interestingly, it is notable that in the experiments presented in this chapter , CsCl gradient analysis demonstrated reduced yields of both IMV and EV when A26L was deleted, suggesting a possible contraindication of deletion of A26L. This reduction in progeny was not the result of slower growth as it was evident in one-step growth curves that the growth rates for both A26L deletion mutants were similar to the wild-type and revertant viruses.

The quantities of EV produced by the deletion mutants were similar to the IHD-J and vIδA26L.rev strains by 24 and 30 hours p.i., suggesting that if deletion of A26L prevents maturation of particles as IMV, this does not result in a concomitant increase in EV. This suggests that if IMV production is controlled independently of EV production, so too EV production is limited by a mechanism independent of IMV production, possibly by the availability of intracellular membranes for wrapping (350).

The deletion of A26 in the WR strain has been reported by others and the effect of deletion on IMV and EEV production investigated (134;351). The results of these studies demonstrate no difference in IMV or EEV production in BSC40, RK13 and HeLa cells, although experiments performed in RK13 and HeLa cells used a low MOI of 0.1. The production of virus from an asynchronous infection will

undoubtedly result in different kinetics of IMV and EEV synthesis, and is unlikely to be the best approach to study this compared to a synchronous infection where one cycle of replication would be observed. These studies also quantified EV in culture supernates and IMV from cell lysates by plaque titration as opposed to CsCl gradient purification of virus used in the current study to separate EV and IMV. The plaque titration method would quantify plaque forming units where the number of virions per plaque forming unit is different for IMV and EV (121) and could plausibly vary if the surface properties are altered by a mutation such as deletion of an IMV-specific protein. Quantification of virions by metabolic labelling of viral genomes has mitigated this in the current study. In addition, quantitation of crude culture extracts can result in false representation of the quantities of virus present as IMV may be found in infected cell culture supernates, and IEV and CEV may be present in the cellular fractions, although this can be mitigated by using IMV- and EV-neutralising antibodies in plaque titrations.

The increased quantities of IMV and reduced quantities of EV observed in COP cultures resulted in an increased ratio of IMV:EV compared to the IHD-J strain. The production of IMV in COP cultures was predicted to be reduced in these cultures as only a truncated version of A26 is synthesised. According to published reports, the final 73 residues of the A26L gene, which are absent in COP, are essential for attachment to the virion via an interaction with A27 (134;342;351). In light of this, the truncated A26 should not be able to bind to virions and therefore IMV would be expected to be reduced if A26 is a maturation marker for IMV. The inability of this strain to occlude IMVs within ATI bodies upon co-infection with

CPXV Brighton Red (an ATI$^+$ strain) further confirms that A26 is not present on the surface of COP IMV particles (188). The high levels of putative IMV produced by COP are at odds with our hypothesis, however it is possible that the apparent IMV produced by COP is in fact nascent, non-differentiated single-membraned virus, and that its abundance is due to an undescribed deficit in wrapping to make EV, or due to the exhaustion of intracellular membranes available for wrapping.

Quantitative RT-PCR suggested that A26L was transcribed in both the A26L deletion mutants. Following normalisation, levels of A26L expression were comparable to IHD-J and vIδA26L.rev. No transcripts were detected in VACV COP cultures across all time points, and so it was surprising that transcripts were detected in the A26L deletion mutants. This may suggest the presence of low quantities of wild-type virus in these cultures. It has been demonstrated in Chapter 4 that wild-type virus can be present in recombinant virus preparations that have undergone multiple rounds of plaque purification. Contaminating wild-type virus was below the limits of detection for the A26L gene by PCR and for A26 by immunoblotting, however it could be amplified using reverse GPT selection when cultured in STO cells in the presence of 6-TG. Although the presence of the IHD-J parent is plausible and may account for detectable A26L transcripts, it is unlikely that enough A26 would be synthesised to complement the mutations in vIδA26L and vIδA26L.neo and indeed the absence of A26 on virions was confirmed in purified virus preparations of both vIδA26L and vIδA26L.neo. Additionally, it is likely that in vIδA26L.neo, the disrupted copy of A26L is transcribed as a result of read-through of the G418^R gene expressed from its synthetic early/late promoter,

as no transcriptional termination sequences were engineered to prevent this occurring during the early phase, and read-through transcription is a well described feature of late stage transcription in poxviruses. The mRNAs generated would be detected by RT-PCR, however due to the frameshift mutation and engineered stop codons throughout the sequence, these transcripts would not be translated. Levels of expression of the A27L and F13L genes in both A26L deletion mutants were also similar to their wild-type counterparts, and expression increased throughout the infectious cycle as expected. The data indicates that deletion of the A26L gene did not affect expression of the neighbouring A27L gene or the F13L gene.

To further confirm the role of A26 in IMV maturation, the ability of vIδA26L and vIδA26L.neo to recover EEV following inhibition of wrapping was assessed. In Chapter 3, vIδA26L was demonstrated to have increased ability to recover EEV when wrapping was inhibited beyond 10 hours p.i. (coinciding with detectable A26 synthesis as reported by Ulaeto *et al.* (116)) using BFA, compared to the IHD-J strain. This suggests that in the absence of A26, virions were able to continue to become enveloped, even at very late times p.i., as the switch from EV to IMV maturation cannot occur. To build on this data, BFA and ST-246 were used to inhibit envelopment until late times p.i. when A26 production should be maximal, and the switch from EV to IMV predominance has occurred. No differences were observed in vIδA26L and vIδA26L.neo cultures when compared to the IHD-J and vIδA26L.rev strains, and recovery of EEV was minimal compared to previous findings in Chapter 3 (data not shown). This assay did not perform as in Chapter 3 as very little recovery of EEV was achieved in BFA- and ST-246-treated cultures.

One possible explanation for this is that the drugs were ineffectively washed out of cultures. Although the original data suggested that A26 was able to negatively regulate maturation of EEV thus acting as a differentiation switch, and that deletion of A26L resulted in increased secretion of EEV when cultures were treated with BFA, conclusions cannot be drawn from these experiments because of the lack of reproducibility reported here.

Increasing expression of A26L and generating increased quantities of A26 to direct maturation of particles to become IMV was intended when constructing vIδA26L.EL. Using CsCl gradients to examine the kinetics of IMV and EV production demonstrated an overall reduction in EV production, thus increasing the ratio of IMV:EV by 24 to 30 hours p.i. However, there was no increase in IMV formation in the early stages of the infectious cycle compared to vIδA26L.rev. Maximal expression from the early/late promoter used in this study may not be optimal to alter the fine kinetics of EV and IMV maturation, and it is possible that the early portion of the promoter was not sufficient to increase the quantities of A26 available in the early stages. It is reported that A26 is attached to the virion via disulfide linkage with A27 (342), and in the absence of this association, A26 is degraded (351), therefore increased quantities of A26 prior to A27 production would not increase maturation as IMV. The late portion of the early/late promoter may not achieve maximal expression at a point that can markedly influence IMV:EV ratios. For example, if maximal A26L expression is only achieved subsequent to maximal expression of F13L (and other EV-associated genes), then EV production may peak or plateau before A26L expression reaches a level where

A26 can effectively compete for attachment to virions. It is also possible in a competitive scenario that increased production of A26 might have to achieve a critical concentration before an increase in IMV maturation would be observed. This may also depend on the relative association constants of A26 with A27, and virions with wrapping membranes, and the ability of the late portion of the synthetic early/late promoter to tilt the competition in favour of A26-A27. This would be expected to result in the phenotype observed in this study.

The ability of A26 to act as a differentiation switch would depend on its attachment to the virion and it has been reported that A26 forms its association with A27 in solution before A27 itself associates with the virion (342;351). Thus a putative competition between IMV and EV maturation may be expected to manifest as a competition between non-differentiated virions and A26, for association with A27. This in turn may be expected to require that A27 and A27-A26 mutually exclude each other from non-differentiated virions upon forming the initial virion association. This is a complex scenario which merits substantial future investigation.

To further characterise the recombinant viruses the levels of transcription of A26L and A27L were examined in vlδA26L.EL and vlδA26L.rev cultures throughout the infectious cycle. It was predicted that A26L transcripts would be detected in the early stages (0-4 hours p.i.) of the replicative cycle compared to expression between 6 and 12 hours p.i. in vlδA26L.rev, and that A27L expression would occur from approximately 4 hours p.i. in both viruses (32). Interestingly, A26L transcription was detected from 1 hour p.i., in both vlδA26L.EL and

vIδA26L.rev, much earlier than predicted. Expression of A27L was comparable in both viruses, indicating that in both viruses, levels of A27 would be sufficient for stability of A26. Expression of F13L was also unaffected in vIδA26L.EL suggesting that the reduction in EV was not due to a reduction in EV-specific proteins. This could suggest that the early portion of the promoter is ineffective and has failed to increase early expression over that seen in vIδA26L.rev, although this promoter is reported to have greater activity than other natural early VACV promoters such as P7.5K (327). However, vIδA26L.rev with which vIδA26L.EL is compared lacks an early termination sequence after the $G418^R$ gene, and transcriptional read-through of the A26L gene may give an apparent level of expression that is comparable to that in vIδA26L.EL, although it is unlikely that this is greater than in wild-type as vIδA26L.rev demonstrates the wild-type phenotype with respect to the kinetics experiments with CsCl gradients, and vIδA26L.EL does not. To further investigate the effects of overexpression of A26L throughout the replicative cycle, increased expression could be examined by engineering other natural VACV promoters or inducible promoters into the VACV genome, by expressing A26L *in trans* using transfected cell lines, or by inserting multiple copies of A26 in the genome.

The altered kinetics of IMV and EV maturation reported in this study for the IHD-J strain requires further investigation. It is apparent that variation in experimental conditions can affect the relative quantities of IMV and EV, where on occasion EV production was dominant even at late times p.i. Various studies have reported the majority of virions are found in the intracellular fraction at the final stages of the infectious cycle in the IHD-J, WR and MVA strains using plaque

titration methods (361;362). Studies by Ulaeto *et al.* (116) have dissected this relationship further by separating virions through CsCl gradients, demonstrating EV is produced first in the replicative cycle, together with detectable F13, followed by a surge in IMV formation accompanied by the production of A26 in the IHD-J strain in RK13 cells. Contrary to this, examination of the different forms of particles associated with the cell by EM demonstrates the majority of virions are IEV and CEV, and IMV is the minority in the IHD-J strain in CEF cells (362) and CsCl gradient density analysis of the WR strain demonstrates the majority of virions are wrapped particles in RK13 cells (361). In addition, Spehner *et al.* (2000) demonstrated the majority of virions mature as EEV by the MVA strain when cultured from low MOI in CEF cells, compared to COP strain that produced very little EEV, by separation through CsCl gradients (363). It would appear that there maybe differences in maturation of VACV when grown from different MOI or in different cell types, and the results may be dependent on the method by which virions are quantified. Using CsCl gradients to separate EV and IMV would appear to be the advantageous method to separate and quantify the different forms compared to plaque titration and EM methodology. Plaque titration of the culture medium and cellular fractions is a crude method particularly when IMV-neutralising antibodies are not used: IMV maybe released into the culture medium as a result of cell lysis at late times p.i., and plaque titration will only quantify plaque forming units as opposed to virus particles. EM methods can be subjective, as results may depend on the number of sections viewed and secreted virions will be lost. CsCl gradient analysis also has its limitations as i) CEV and EEV cannot be

distinguished in culture extracts unless the culture medium and cellular fractions are analysed separately; and ii) the fragility of the EV membrane may affect the number of particles that sediment as EV (339).

It is plausible that the different maturation kinetics of IMV and EV are due to different kinetics of A26 and F13 production of the strains used in these studies. RT-PCR for the IHD-J strain demonstrated F13L expression was maximal at 12 hours p.i. whereas A26L expression was still increasing from 12 hours p.i. and was not maximal until later in the infectious cycle, correlating with previous reports by Ulaeto *et al.* (1996). Transcription of these genes in vlδA26L.rev was observed from as early as 1 hour p.i., although the maximal fold change in F13L expression occurred earlier than the maximal fold change for A26L. For F13L, an exponential increase in transcription occurred between 1 and 6 hours p.i., whereas for A26L the exponential increase in transcription took place between 1 and 12 hours, with a much shallower curve.

The function of A26 has yet to be fully elucidated, however this data has provided further insight into the role of A26 in virion morphogenesis and has shown the variability of the kinetics of IMV and EV production by wild-type virus using CsCl gradients. This study has demonstrated that deletion of A26L in the IHD-J strain negatively affects virus growth. Although the deletion of A26L appears to negatively perturb levels of single-membraned virus, the effect is variable and may be influenced by host cell type, passage history, and possibly metabolic state. It may be suggested that in the absence of A26, single-membraned virus is not IMV and is not a mature, end-stage virion. Rather it is a nascent virion awaiting

envelopment as EV. The differences observed would thus be due to variability in conditions that affect efficiency of wrapping. This bears further examination in the future, including studies to investigate more effective expression of A26L by VACV promoters to better define the role of the A26 protein.

7 Effect of Antimicrobial Peptides on VACV

7.1 Introduction

The main focus of this thesis is to examine the hypothesis that IMV that does not undergo envelopment is a true end-stage product of OPV morphogenesis. It is likely that wrapping of virions to form EV is limited by the availability of required intracellular membranes *in vitro* and possibly *in vivo*, however, this does not preclude the possibility that some single-membraned virions mature in such a way that they cannot be wrapped, even if suitable intracellular membranes are available. The function(s) of IMV and its biological significance during infection and transmission have not fully been determined. As the more robust particle, IMV is likely to be involved in host-to-host transmission, and this would appear even more likely in OPVs such as cowpoxvirus and raccoonpox virus (185;222), that occlude IMVs within A-type inclusions (ATIs), which may protect virus particles in the environment. EV however, is known to promote virus spread both *in vitro* and *in vivo*, and aid virus evasion of antibody and complement (reviewed in (189)).

Antimicrobial peptides (AMPs) such as cathelicidins and defensins are essential components of the innate immune system and have wide-spectrum activity against bacteria, fungi and enveloped viruses, and even cancerous cells (reviewed in ((364)). In addition, AMPs have also been shown to have immunomodulatory functions resulting in activation of the adaptive immune response (reviewed in (365)). They are produced by a range of organisms across the animal kingdoms including mammals, insects, plants and amphibians.

AMPs have been classed according to their structure and amino acid composition. They are generally between 12-50 amino acids in length containing 2 or more positively charged amino acids, usually arginine, lysine or histidine, and a large proportion of hydrophobic residues (366). AMPs are mostly unstructured when free in solution, however, they form secondary structures such as α-helical, linear or disulfide-bonded to give regions of polar and non-polar domains that are required for their activity (reviewed in (364);(366)).

Unlike antibiotics which usually interact with specific target molecules in a bacterial cell, AMPs usually interact specifically with the cell membrane although the mechanisms of action of these peptides are not fully understood. The selectivity of AMPs between prokaryotic and eukaryotic membranes is probably due to variations in the composition of the cell membrane. In the case of eukaryotic cells, the membrane is predominantly neutral in charge and contains cholesterol, which may act to stabilise the membrane. In contrast, bacterial membranes are negatively charged and lack cholesterol. The selectivity of AMPs is due to the cationic nature of AMPs at physiological pH, resulting in an electrostatic attraction with anionic bacterial membranes; AMPs are less likely to associate with zwitterionic mammalian membranes. Once associated with a membrane, their hydrophobic domain and amphipathic structure allows AMPs to disrupt the biological membrane. Two major models of action have been proposed: i) barrel-stave, and ii) the carpet model. In the barrel-stave model, peptides insert into the membrane in an orientation perpendicular to the plane of the lipid bilayer to form "staves" in a barrel-shaped cluster, where the hydrophilic regions of the peptides

face inwards and the hydrophobic regions interact with the bilayer, forming a pore and thus depolarising the membrane. The carpet model suggests peptides aggregate parallel to the surface of the lipid bilayer, coating the membrane with peptide molecules. The activity of peptides in this model is concentration-dependent leading to disruption and disintegration of the membrane when a threshold concentration is reached (reviewed in (364)).

The varying activity of AMPs against prokaryotic and eukaryotic membranes suggests potential therapeutic applications of AMPs against bacterial pathogens, yet some AMPs have activity against enveloped viruses such as HIV-1, HSV types 1 and 2, cytomegalovirus, vesicular stomatitis virus and influenza virus that utilise host-derived membranes (reviewed in (364;367)). It may be therefore assumed that the mechanism of action of AMPs against viruses differs to that observed in bacteria, due to the difference in properties of the mammalian-derived envelope and bacterial outer membranes.

LL-37 of the cathelicidin family of AMPs has recently been shown to have activity against VACV (368), and is thought to cause disruption of the viral membrane as treatment of cell-associated virus demonstrated a loss of integrity of the viral membranes and of the internal structure (368). More recent studies in our laboratory have demonstrated a differential effect on the enveloped and non-enveloped forms of VACV. LL-37 was specifically active against EEV and its activity was enhanced by the addition of the non-ionic detergent Tween-20 (Dean *et al.*, in preparation). In contrast, the *Xenopus*-derived AMP magainin-II had no virucidal activity against either form of VACV, although it acquired significant

virucidal activity against EV in the presence of Tween-20 (Dean *et al.*, in preparation). Interestingly, infectivity of EV could be further decreased using IMV-neutralising antibodies following AMP treatment, suggesting that the envelope had been disrupted to expose antigens on the inner membrane. Treatment of EEV with Tween-20 alone resulted in increased infectivity over a 60 minute incubation period, but when the incubation period was increased to 90 minutes, a significant decrease in infectivity was observed (Dean *et al.*, in preparation).

7.1.1 Aims of This Study

The effect of the AMPs LL-37 and magainin-II, and Tween-20 on viral membranes was investigated in this chapter using CsCl density gradient analysis to allow separation of virions according to their difference in buoyant densities. Removal of the outer membrane of EV would result in an increase in density of treated virions. This chapter will determine if AMPs unwrap EV, and if unwrapped EV is equivalent to IMV. This may also provide evidence for a mechanism for the activity of AMPs against VACV consistent with existing models of action.

7.2 Results

7.2.2 Effect of AMPs on EEV Membrane

The activity of AMPs on VACV has previously been reported, and more recently the activities of LL-37 and magainin-II have been reported to be almost exclusively against enveloped particles (Dean *et al.*, in preparation). To understand this activity further, the effects on the EEV membrane, if any, of these two AMPs

were investigated using CsCl density gradients. Disruption of the viral envelope would result in a change in buoyant density of the virus particle and cause a shift in the density at which the virus particles sediment within the CsCl gradient.

Tritium-labelled EEV-enriched virus preparations were treated with 100 µg/ml LL-37 or magainin-II, or PBS in triplicate for 90 minutes at 37 °C (section 2.5.7). Two out of three of the treated cultures were separated through CsCl density gradients (section 2.5.2 and 2.5.4) and the density was determined by weighing 100 µl of each fraction (Figures 7.1 and 7.2). When EEV preparations were treated with magainin-II, two distinct similarly-sized peaks were seen, one with a density expected for EEV and one with a density expected for IMV. Treatment with LL-37 caused a shift in density of the majority of virus particles, to a higher density similar to that expected of IMV. Interestingly, there was no evidence of particles sedimenting with an intermediate density between the two peaks. The remaining cultures were titrated on RK13 cells (section 2.5.3) in the presence of neutralising-IMV antibodies, as a control to confirm the activity of each of the peptides on the infectivity of EEV (Figure 7.3).

7.2.3 Effect of Detergent on the EEV Membrane

The activity of magainin-II on the EEV membrane has previously been shown to be enhanced in the presence of the non-ionic detergent Tween-20 (Dean *et al.*, in preparation), suggesting a synergy between the two compounds. To dissect the effect of Tween-20 alone on the EEV membrane further, EEV-enriched

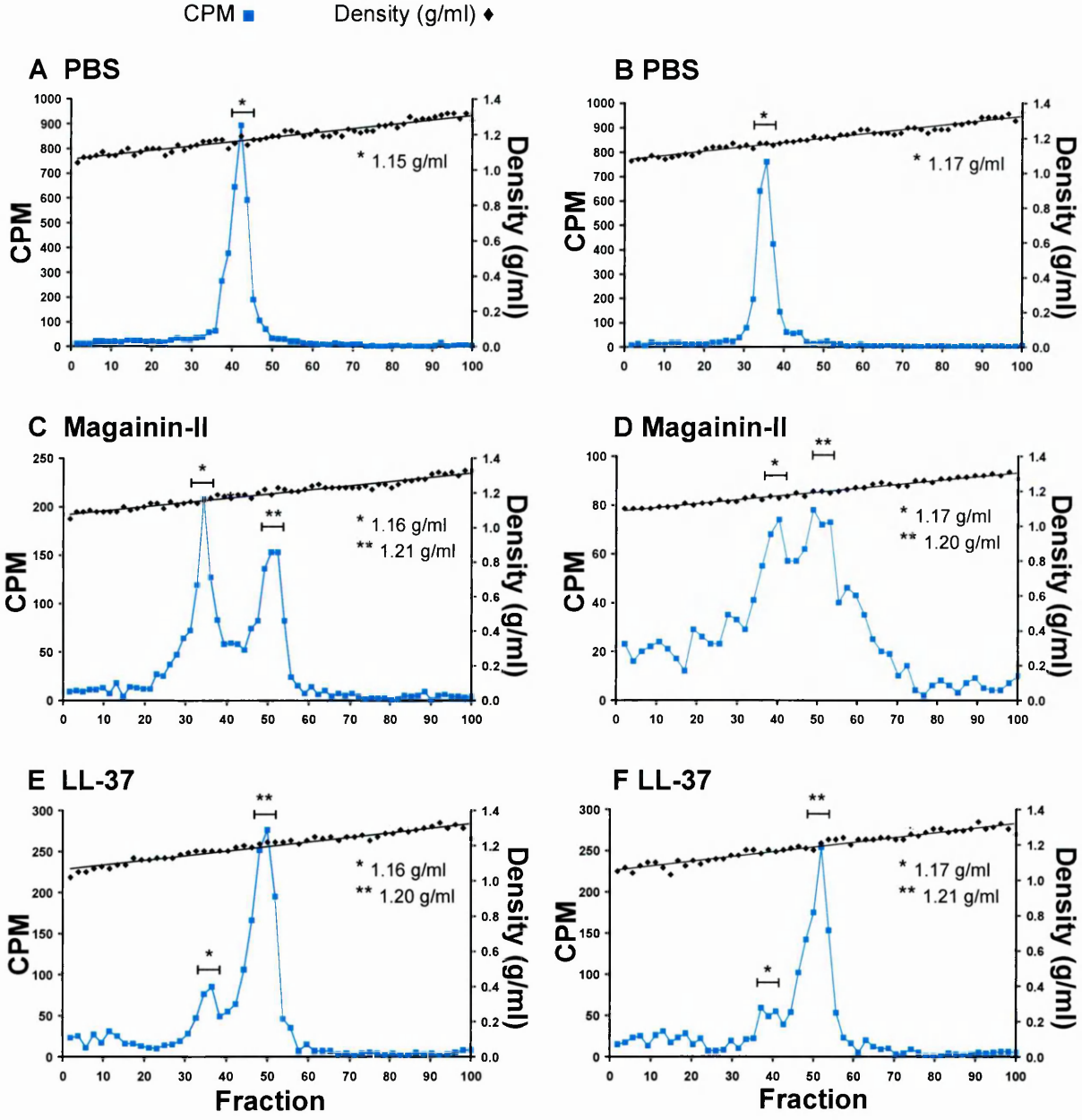

Figure 7.1 Effect of AMPs on the EEV Membrane (I)

Freshly harvested EEV from VACV IHD-J cultures supplemented with ^{3}H thymidine were treated in duplicate with PBS (A and B), magainin-II (C and D) or LL-37 (E and F) for 90 minutes at 37 °C. Virions were separated by ultracentrifugation through CsCl gradients. The density (♦) of each fraction was determined using a fine balance and fractions were subjected to scintillation counting to determine the CPM (■) per fraction. The average densities of each peak were calculated for each trace and are indicated by asterisks.

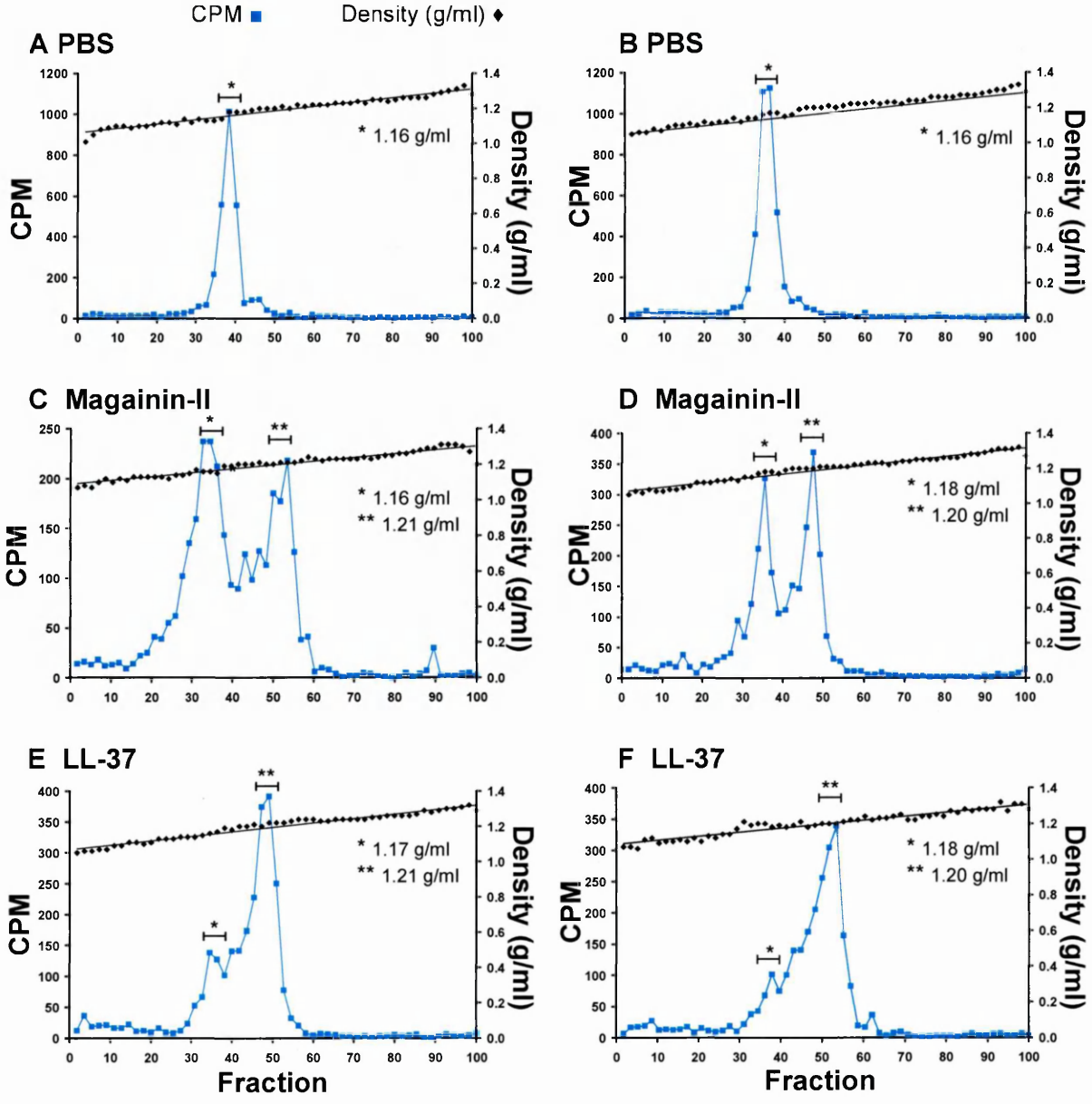

Figure 7.2 Effect of AMPs on the EEV Membrane (II)

Freshly harvested EEV from VACV IHD-J cultures supplemented with ^{3}H thymidine were treated in duplicate with PBS (A and B), magainin-II (C and D) or LL-37 (E and F) for 90 minutes at 37 °C. Virions were separated by ultracentrifugation through CsCl gradients. The density (♦) of each fraction was determined using a fine balance and fractions were subjected to scintillation counting to determine the CPM (■) per fraction. Fractions were normalised to 100. The average densities of each peak were calculated for each trace and are indicated by asterisks.

A

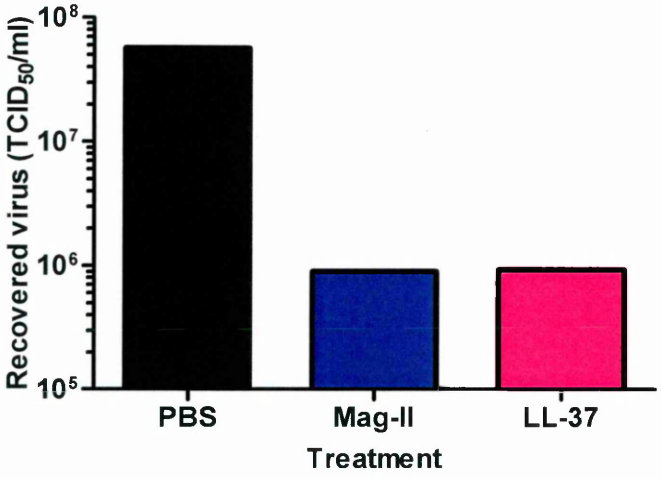

B

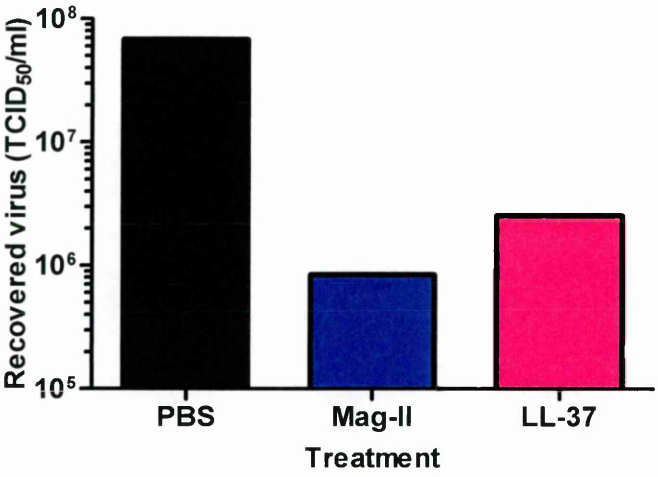

Figure 7.3 Effect of AMPs on EEV-enriched Cultures

Freshly harvested EEV from VACV IHD-J cultures supplemented with ^{3}H thymidine were treated with PBS (■), magainin-II (■) or LL-37 (■), in triplicate, for 90 minutes at 37 °C. The quantity of recovered virus in one replicate was determined by Reed-Muench limiting dilution analysis in the presence of IMV-neutralising antibody. A and B are each representative of two experiments. Virions in the remaining replicates were separated by ultracentrifugation through CsCl gradients where A corresponds with Figure 7.1 and B corresponds with Figure 7.2.

cultures were treated with Tween-20 (0.5 % v/v) for 90 minutes or 180 minutes, or with PBS for 180 minutes in triplicate at 37 °C (section 2.5.7). Two out of three of the treated cultures were separated through CsCl density gradients (section 2.5.2 and 2.5.4) and the density was determined by weighing 100 µl of each fraction (Figures 7.4 and 7.5). Tween-20 treatment resulted in a shift in the density of virus particles, although the peaks were not well defined. Treatment for 90 minutes appeared to show three rather than two peaks and the peaks were not well separated, suggesting that intermediate density particles were present. The putative third peak was of higher density than expected for IMV, and may represent particles where both the inner and outer membranes had been wholly or partially removed. Treatment with Tween-20 for 180 minutes removed most of the lowest density peak observed after 90 minute treatment, and again the remaining peaks were not well separated. The remaining cultures were titrated on RK13 cells (section 2.5.3) in the absence or presence of neutralising-IMV antibodies, as a control to confirm the activity of Tween-20 treatment on the infectivity of EEV (Figure 7.6). Treatment of cultures with Tween-20 resulted in a reduction in virus titre as expected, and this was further reduced in the presence of IMV-neutralising antibodies. A slight reduction in titre was also observed in the PBS treated cultures when quantified in the presence of IMV-neutralising antibodies and this was likely due to a small amount of IMV, as observed in these preparations following CsCl density gradient analysis (Figure 7.6B).

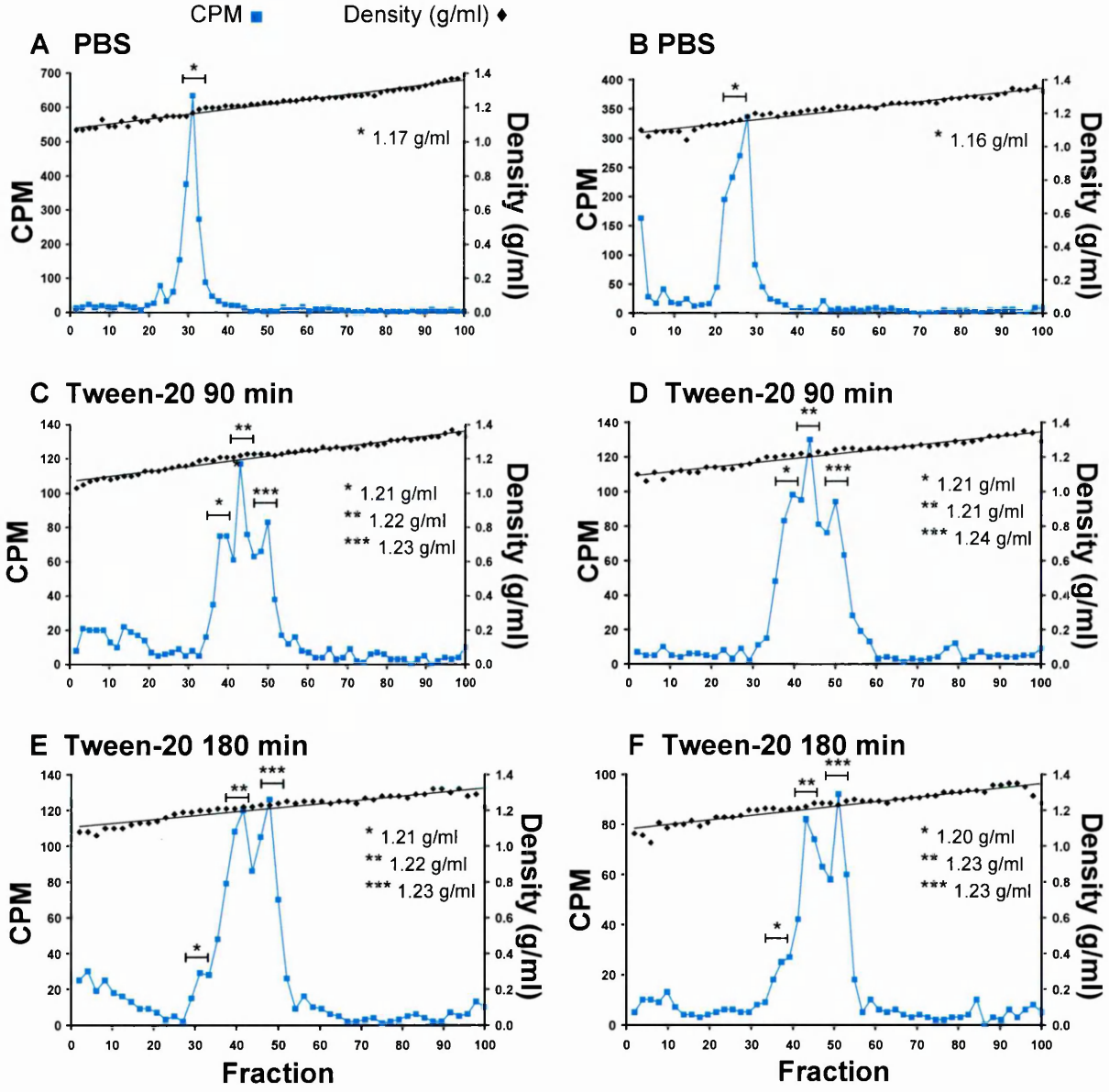

Figure 7.4 Effect of Tween-20 on the EEV Membrane (I)

Freshly harvested EEV from VACV IHD-J cultures supplemented with ^{3}H thymidine were treated with PBS (A and B) or Tween-20 for 90 minutes (C and D) or 180 minutes (E and F) at 37 °C. Virions were separated by ultracentrifugation through CsCl gradients. The density (♦) of each fraction was determined using a fine balance and fractions were subjected to scintillation counting to determine the CPM (■) per fraction. Fractions were normalised to 100. The average density of each peak was calculated for each trace and is indicated by asterisks.

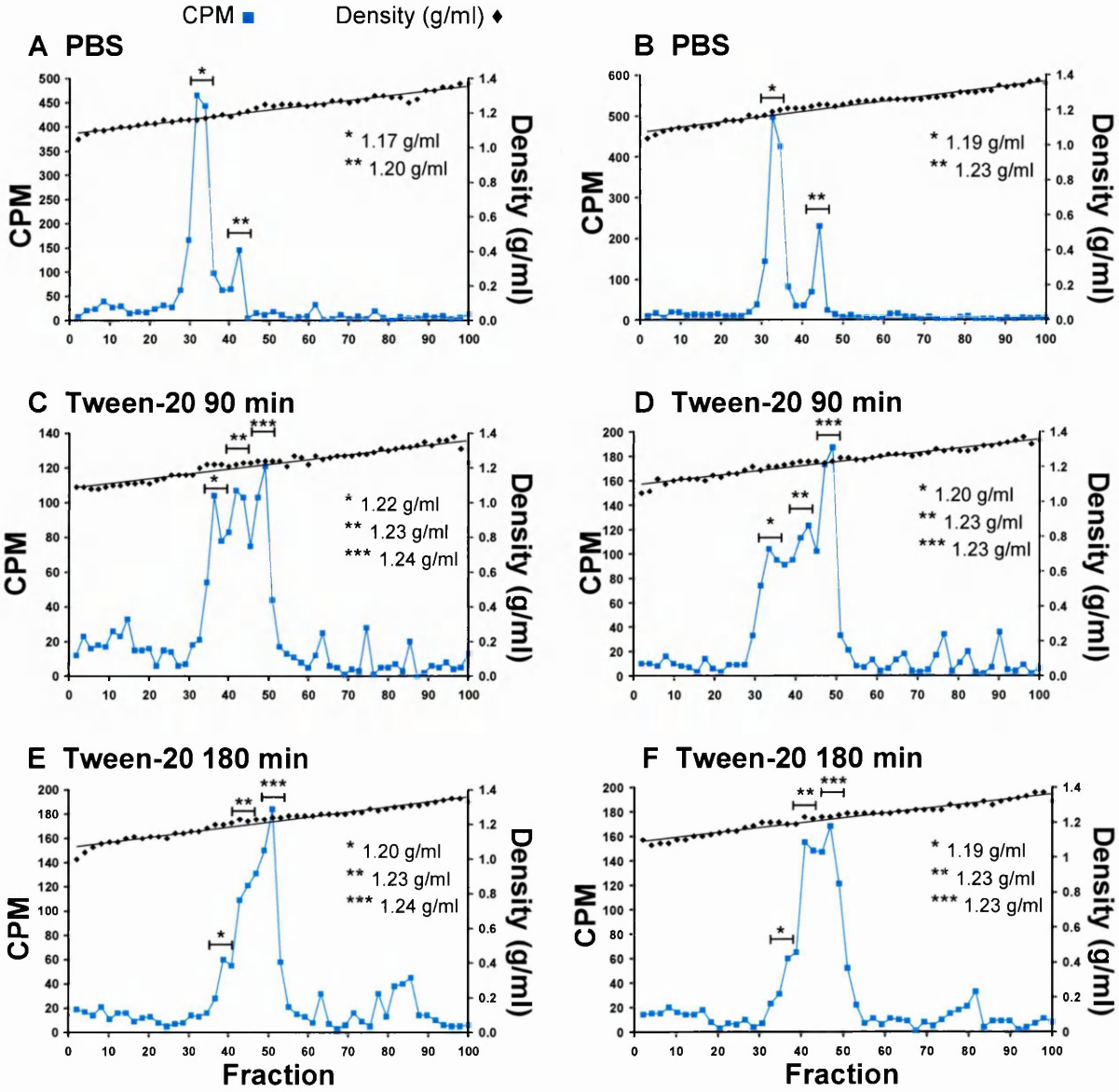

Figure 7.5 Effect of Tween-20 on the EEV Membrane (II)

Freshly harvested EEV from VACV IHD-J cultures supplemented with ^{3}H thymidine were treated with PBS (A and B) or Tween-20 for 90 minutes (C and D) or 180 minutes (E and F) at 37 °C. Virions were separated by ultracentrifugation through CsCl gradients. The density (♦) of each fraction was determined using a fine balance and fractions were subjected to scintillation counting to determine the CPM (■) per fraction. Fractions were normalised to 100. The average density of each peak was calculated for each trace and is indicated by asterisks.

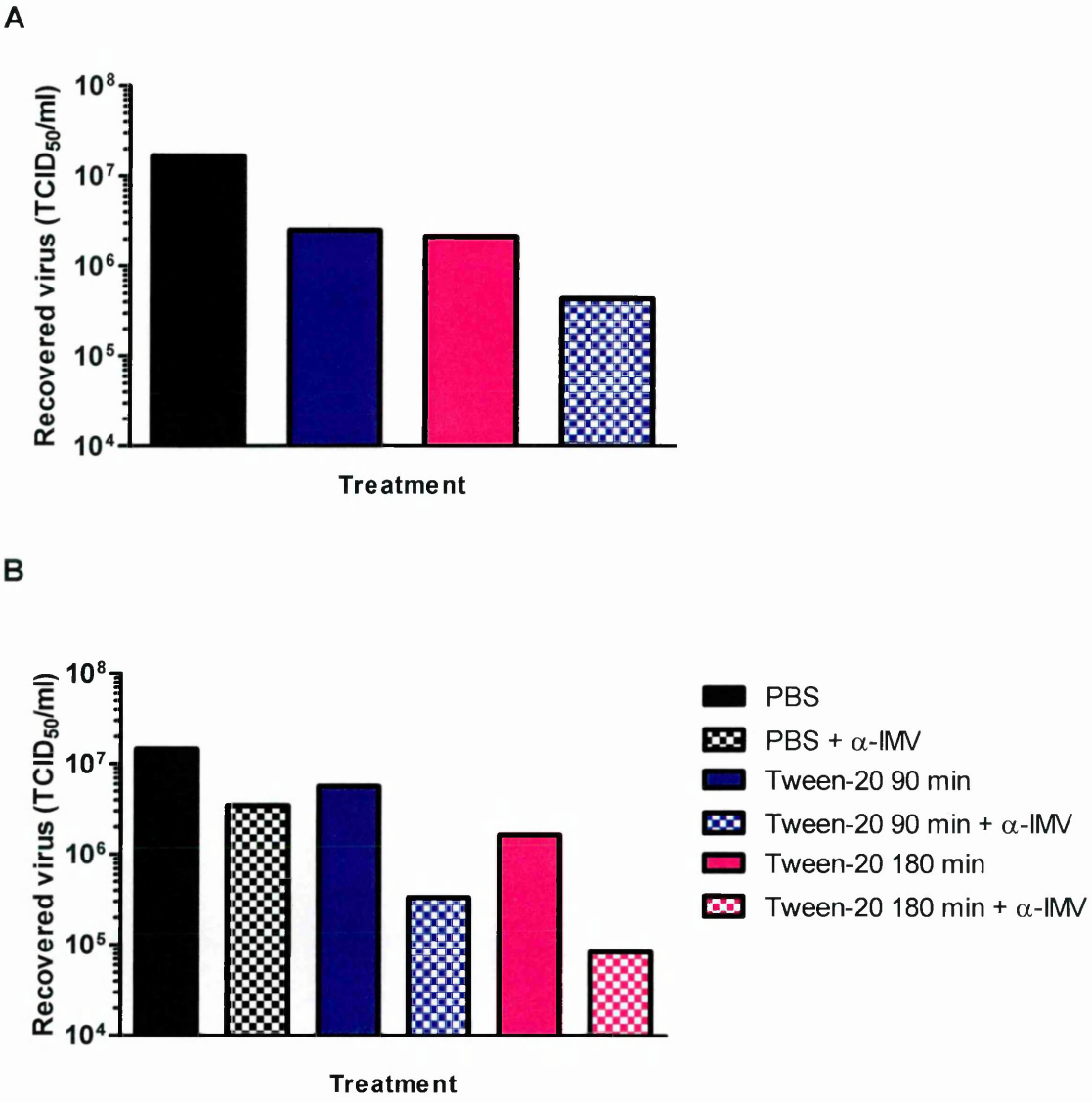

Figure 7.6 Effect of Tween-20 on EEV-enriched Cultures

Freshly harvested EEV from VACV IHD-J cultures supplemented with ^{3}H thymidine were treated with PBS (■), Tween-20 for 90 minutes (■) or 180 minutes (■), in triplicate, at 37 °C. The quantity of virus in one replicate was determined by Reed-Muench limiting dilution analysis in the absence (solid bars) or presence (hatched bars) of IMV-neutralising antibodies. A and B are representative of two experiments. Virions in the remaining replicates were separated by ultracentrifugation through CsCl gradients where A corresponds with Figure 7.4 and B corresponds with Figure 7.5.

7.2.4 Effect of Detergent on the IMV Membrane

LL-37 and magainin-II have been shown to have no effect on infectivity of IMV, although they acquired slight activity in the presence of Tween-20 (Dean *et al.*, in preparation). To investigate the effect of Tween-20 on the IMV membrane further, IMV-enriched cultures were treated with Tween-20 for 90 minutes or 180 minutes, or with PBS for 180 minutes at 37 °C, in triplicate (section 2.5.7). Two out of three of the treated cultures were separated through CsCl density gradients (section 2.5.2 and 2.5.4) and the density was determined by weighing 100 µl of each fraction (Figures 7.7 and 7.8). The majority of particles sedimented with a density expected of IMV following treatment with Tween-20. A lower density peak was observed in PBS treated cultures, with a density lower than that found for EEV in this study. This peak was likely to be IEV, and appeared to be susceptible to Tween-20 treatment resulting in a shift to sediment at a higher density. The remaining cultures were titrated on RK13 cells (section 2.5.3) as a control to determine the activity of Tween-20 treatment on the infectivity of IMV (Figure 7.9). A small reduction in virus titre was observed in cultures treated with Tween-20 and might be due to the inactivation of contaminating IEV in the cultures. It is possible, indeed likely, that single-membraned virus that has not acquired A26 and is destined for envelopment is present in the samples and would be susceptible to inactivation by 90 or 180 minute incubations with Tween-20.

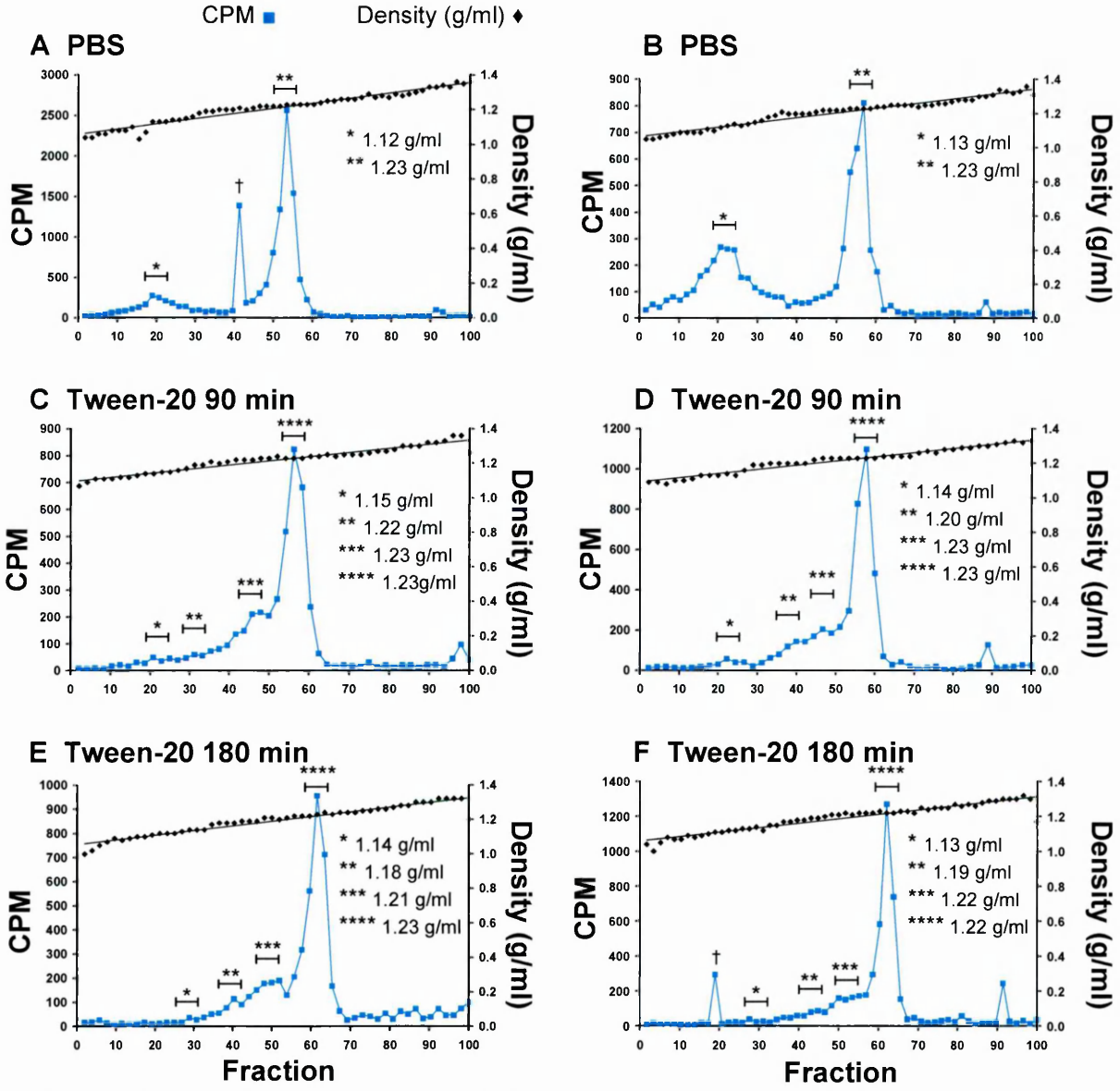

Figure 7.7 Effect of Tween-20 on the IMV Membrane (I)

Freshly harvested IMV from VACV IHD-J cultures supplemented with ^{3}H thymidine were treated with PBS (A and B), Tween-20 for 90 minutes (C and D) or Tween-20 for 180 minutes (E and F) at 37 °C. Virions were separated by ultracentrifugation through CsCl gradients. The density (♦) of each fraction was determined using a fine balance and fractions were subjected to scintillation counting to determine the CPM (■) per fraction. Fractions were normalised to 100. The average density of each peak was calculated for each trace and is indicated by asterisks. Note: † represents "spikes" that are presumed to be due to a fault that occurred during scintillation counting.

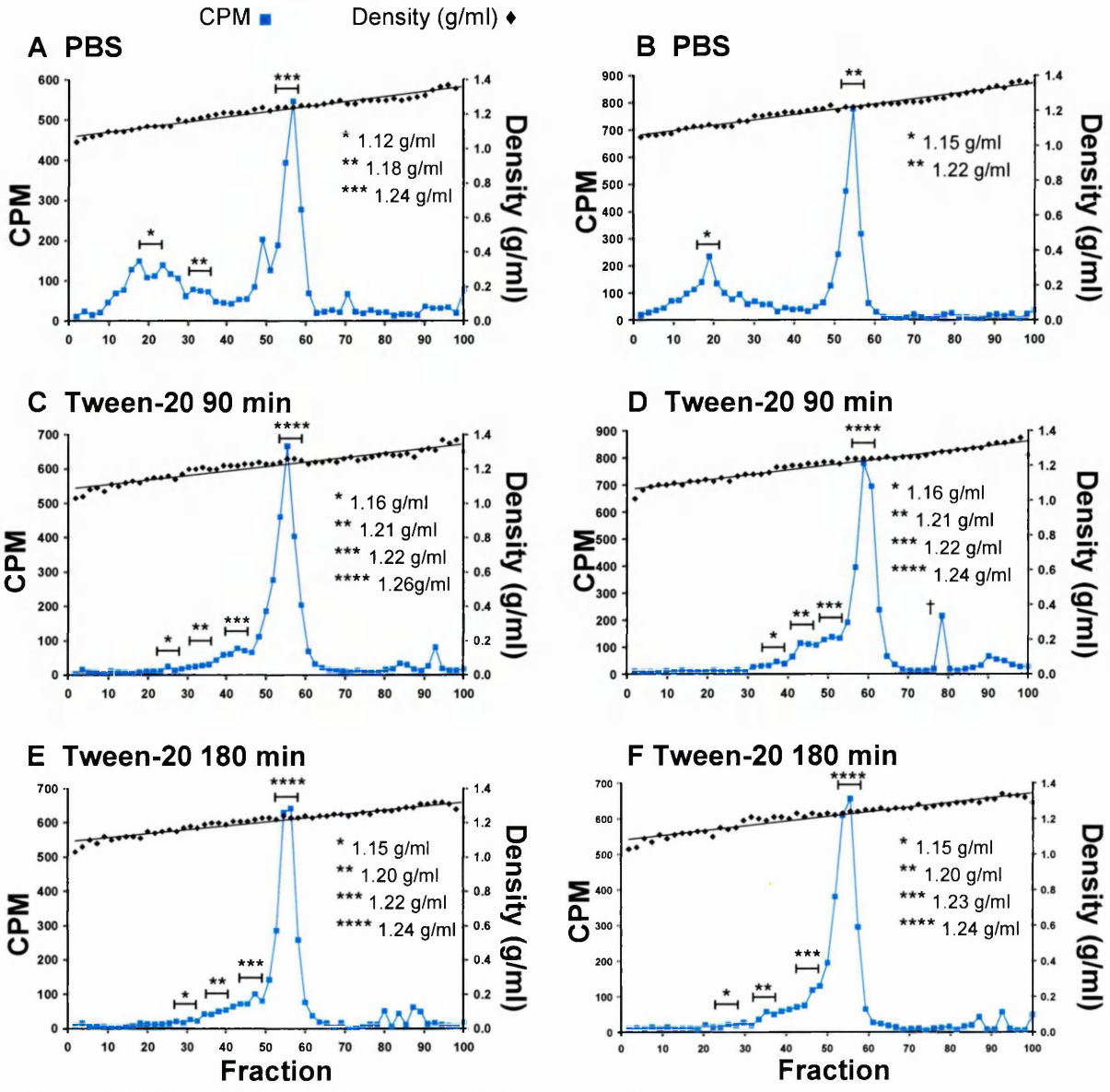

Figure 7.8 Effect of Tween-20 on the IMV Membrane (II)

Freshly harvested IMV from VACV IHD-J cultures supplemented with ^{3}H thymidine were treated with PBS (A and B), Tween-20 for 90 minutes (C and D) or Tween-20 for 180 minutes (E and F) at 37 °C. Virions were separated by ultracentrifugation through CsCl gradients. The density (♦) of each fraction was determined using a fine balance and fractions were subjected to scintillation counting to determine the CPM (■) per fraction. Fractions were normalised to 100. The average density of each peak was calculated for each trace and is indicated by asterisks. Note: † represents "spikes" that are presumed to be due to a fault that occurred during scintillation counting.

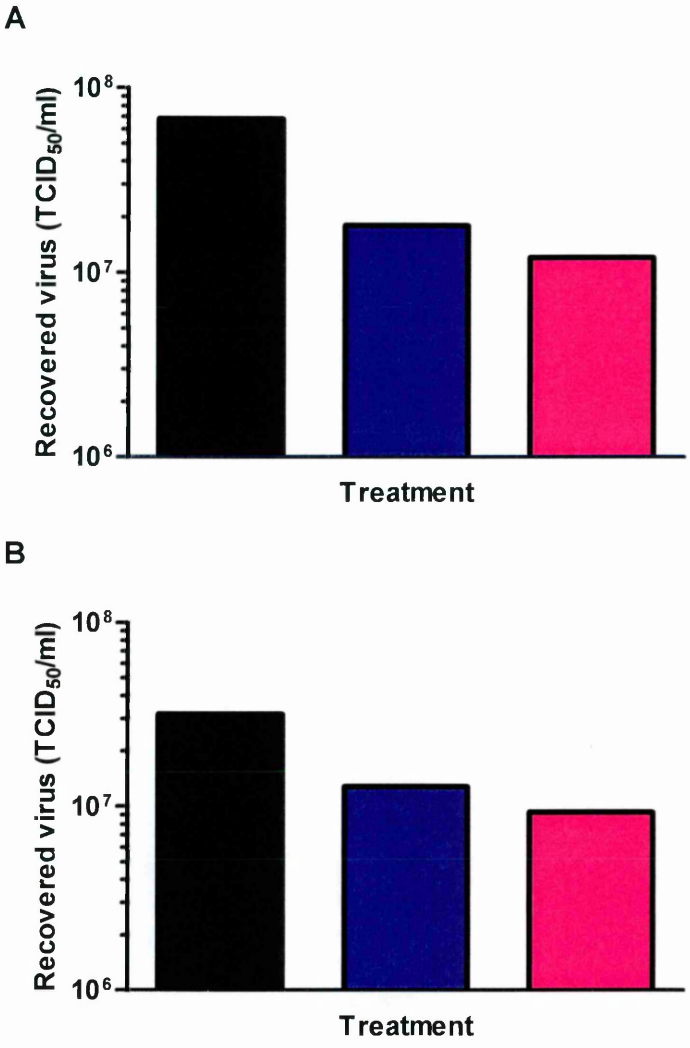

Figure 7.9 Effect of Tween-20 on IMV-enriched Cultures

Freshly harvested IMV from VACV IHD-J cultures supplemented with ^{3}H thymidine were treated with PBS (■), Tween-20 for 90 minutes (■) or 180 minutes (■) in triplicate at 37 °C. The quantity of virus in one replicate was determined by Reed-Muench limiting dilution analysis. A and B are representative of two experiments. Virions in the remaining replicates were separated by ultracentrifugation through CsCl gradients where A corresponds with Figure 7.7 and B corresponds with Figure 7.8.

7.2.5 Stability of VACV When A26 is Deleted

Removal of the outer membrane of EEV using AMPs or detergents appears to have varying effects on infectivity, and can render the virus particle susceptible to neutralisation with IMV-neutralising antibodies. A key difference in the surface properties of EEV that has been stripped of its outer membrane compared to IMV is the absence of IMV-specific proteins such as A26, which may contribute to the increased resistance of IMV to the effects of these compounds. Treatment of IMV-enriched cultures of wild-type VACV IHD-J, vIδA26L.rev, vIδA26L and vIδA26L.neo with Tween-20, Triton X-100, LL-37 or PBS for 180 minutes at 37 °C was investigated to determine the effect of alteration of the surface properties of IMV particles by deletion of A26 (Figure 7.10). Treatment with LL-37 had no discernible effect on infectivity of wild-type or mutant IMV, however an increased reduction in virus titre was observed after treatment with Tween-20 for IMV cultures of vIδA26L when compared to IHD-J ($p<0.01$) and for vIδA26L.neo when compared to vIδA26L.rev ($p<0.05$), using a repeated measures ANOVA with Bonferroni's post-tests. Treatment with Triton X-100 almost completely inactivated virions to less than 100 $TCID_{50}$/ml.

7.3 Discussion

During this study, the activity of both LL-37 and magainin-II has been demonstrated to be restricted to the enveloped form of VACV, where the activity of LL-37 is greater. This differential activity may be due to the reported stability of the α-helical structure of LL-37 in solution which may increase its potency, whereas

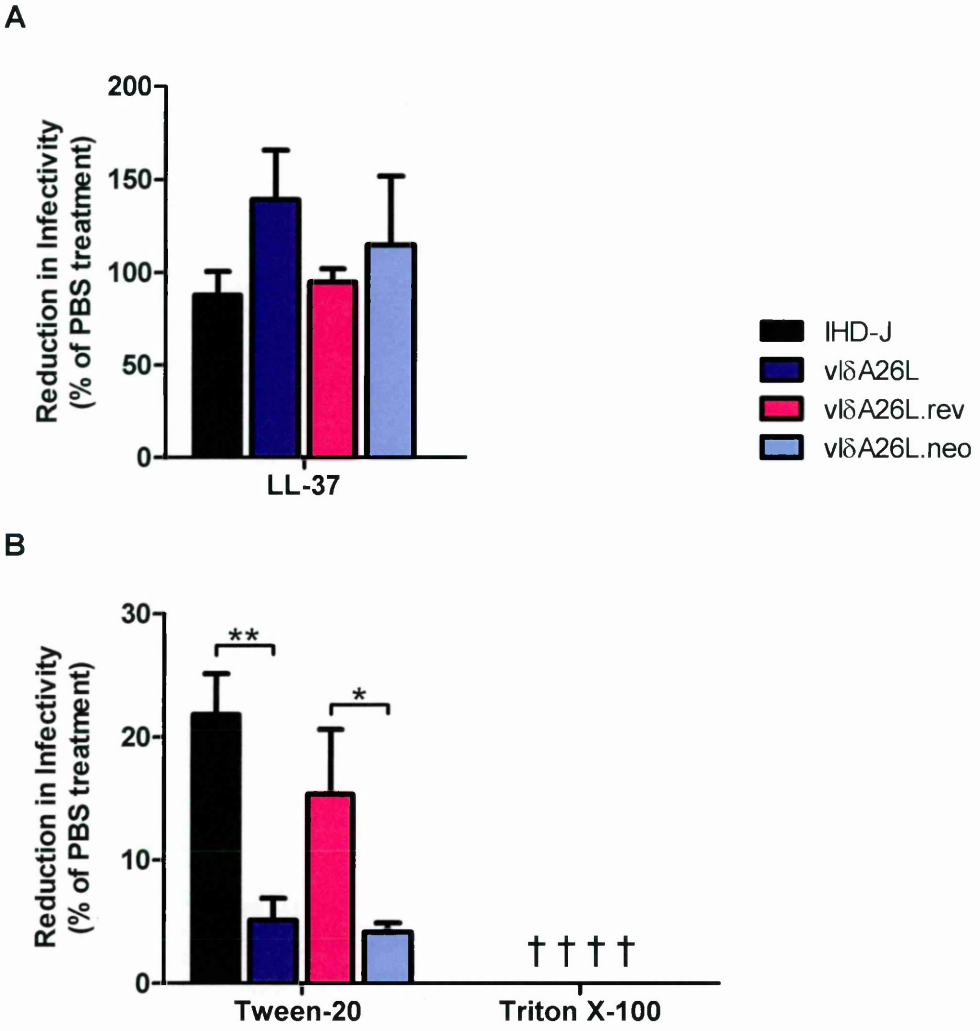

Figure 7.10 Effect of LL-37 and Detergents on Infectivity of IMV-enriched Cultures of Recombinant VACV

IMVs isolated from wild-type IHD-J (■), vIδA26L (■), vIδA26L.rev (■) and v vIδA26L.neo (■) cultures were treated for 180 minutes with LL-37 (A), or the detergents Tween-20 or Triton X-100 (B) then quantitated in RK13 cells as described in section 2.5.3. Data is presented as the mean and SEM of the percentage reduction in infectivity compared to PBS treated cultures. The experiment was performed with duplicate cultures on three separate occasions (n=6) and the combined data for each virus subjected to a two-way ANOVA (** $p<0.001$; * $p<0.05$).

† due to low numbers of virus remaining in these cultures and the limits of detection of the virus titration method numbers of virus was deemed as <100 $TCID_{50}$/ml.

magainin-II is unstructured in solution and has been shown to require the presence of lipids for this conformational change in structure (369); this usually provides the driving force for binding to and disruption of the membrane (370). This would also suggest that interaction of LL-37 with the membrane may have a different energetic basis as it does not undergo a structural change.

Howell *et al.* (2004) reported activity of LL-37 against VACV and suggested that the activity was directed against the IMV form on the basis that their virus was isolated from cell lysates following infection with the Wyeth strain (368). Propagation of the Wyeth strain would be expected to result in retention of EV on the cell surface, as opposed to its release as EEV. This is because the Wyeth strain of VACV, unlike the IHD-J strain, has an A34R gene that is similar to that of the WR strain which has been shown to mediate the over-production of CEV relative to EEV (180). In addition, their virus was prepared from 3-day bulk cultures infected at low multiplicity. With cells at different stages of the infectious cycle it is not possible to be certain that IMV or EV would be the predominant virus form at the time of harvest. It is thus not possible to determine whether the inactivation reported by Howell *et al.* (2004) is of EV or IMV. More recent data (Dean *et al.*, in preparation) indicate clearly that the EV form is the target of AMP activity, and that the IMV form is resistant. The combination of the IHD-J strain and RK13 host cells in high multiplicity synchronous infections used in this study yield dependable quantities of EV in the form of EEV, therefore it is possible to enrich for either EEV or IMV in the culture supernate or cellular fraction, respectively.

Using CsCl density gradient centrifugation to determine the effect of these AMPs on the viral envelope suggests that the membrane is stripped from the virus particle in one event, as treatment of samples resulted in distinct peaks, with no intermediate signal. If the membrane was partially lost in increments a broad peak would be expected where the density of virus particles comprised a continuous range from low-density EV peaks to high-density IMV-like peaks. These results are consistent with the carpet model where the membrane disintegrates when a threshold level of peptide molecules is reached on the membrane surface. In further support of this model, the activity of the non-ionic detergent Tween-20 also demonstrates disruption of the outer membrane when treated EEV particles were separated by CsCl density gradient centrifugation, although stripping of the membranes appears to be consistent with incremental removal of the inner and outer membranes as demonstrated by poorly defined peaks. Neutralisation of stripped virions by IMV-neutralising antibodies following AMP treatment or Tween-20 treatment also confirmed that the outer membrane had been disrupted to reveal neutralising epitopes below.

Treatment of EEV with Tween-20 resulted in a peak that had a greater density than that expected of IMV which suggests that the inner membrane has also been disrupted. This higher density peak was not evident in EEV preparations treated with LL-37 or magainin-II suggesting that both peptides are only able to remove the outer membrane, yet it is unclear why this results in inactivation by LL-37 but not magainin-II. One possible explanation is that LL-37 inactivates unwrapped EEV by disturbing the inner membrane but without removing it,

possibly by perturbing or displacing surface proteins that are essential for infectivity, and that magainin-II is unable to mediate this additional interaction unaided.

The resistance of IMV to LL-37 and magainin-II may be in part due to the presence of IMV-specific surface proteins which may affect the ability of peptides to associate with the virion surface. Previous studies have demonstrated that their activity can be enhanced in the presence of Tween-20, although the possibility that this is due to inactivation of IEV present in the IMV-enriched cultures cannot be excluded (Dean *et al.*, in preparation). In this study, CsCl density gradient analysis demonstrated no effect on the IMV membrane following treatment with Tween-20, although a minimal reduction in infectivity was observed. Resistance of the IMV membrane may be due to the presence of IMV-specific surface proteins, which are not found on EEV that has been stripped of its outer membrane.

To investigate this further, recombinant VACVs were used as a tool where the surface of IMV had been modified by deletion of the A26L ORF. A26 represents 2.8 % of total protein of IMV (240) and has been shown to attach to the surface of the virion via disulphide linkage with A27 (351). Association of A25 (ATI) is mediated by A26 (351), representing a further 3.4 % of total protein of IMV (240). Therefore the surfaces of IMV and stripped EV are distinctly different. Infectivity following LL-37 treatment was unaffected in the mutants indicating that the resistance of IMV to LL-37 was not mediated by A26 or, by extrapolation, by A25. However, treatment with Tween-20 resulted in a significant reduction in infectivity of IMV from both A26 deletion mutants relative to wild-type and revertant viruses.

This demonstrates an observable difference between IMV and unwrapped EEV that is attributable to the presence of the A26 protein on IMV, and is a strong indication that IMV (as defined by the presence of surface A26 and thus the ability to be incorporated into OPV A-type inclusions) is distinct from nascent single-membraned particles destined to be wrapped as EEV.

This study has demonstrated that AMPs are able to strip the outer membrane from EEV particles, but not the inner membrane and that this is sufficient for the human LL-37 AMP to inactivate EEV. This provides a rationale for the future investigation of AMPs as potential therapeutics for OPV infections, in particular for complications of vaccination such as eczema vaccinatum where topical application of therapeutics might significantly affect the course of disease. The presence of two distinct peaks in CsCl gradients representative of enveloped and stripped particles and the absence of intermediate density particles suggests the outer membrane is removed in a single event and is supportive of the carpet model of AMP activity.

Interestingly, AMPs alone appear to have no effect on IMV even when the IMV-specific A26 protein is absent, indicating the peptides are unable to associate effectively with the IMV membrane to cause membrane disruption or reduce infectivity. A26 mediates association of IMV with the only other known IMV-specific protein, the ATI protein A25. Thus by extrapolation, A25 is unlikely to be the mediator of differential susceptibility of IMV and unwrapped EEV to LL-37. Whilst it is possible that additional IMV-specific proteins are yet to be discovered, there are other possible mechanisms for this differential sensitivity, perhaps involving the

association of proteins such as A27 with the EV membrane-associated protein F13. Plausibly, removal of F13 along with the outer membrane of EEV may disrupt the association of a protein such as A27, with the unwrapped particle. Such hypotheses would require further investigation. However, the data presented here provide further evidence that IMV is a true end-stage product of VACV morphogenesis, rather than an EV pre-cursor.

8 Final Discussion

8.1 VACV as a Live Smallpox Vaccine

Although smallpox was eradicated nearly 30 years ago, there are concerns over the safety and efficacy of current vaccines and antiviral therapies that are available in the event of an accidental or deliberate release of VARV, or a fully emergent human MPXV outbreak. The increased understanding of poxvirus biology, in particular from studying the prototypical OPV VACV, paves the way to improving current smallpox vaccines and developing new strategies for antiviral therapies.

Most, if not all, OPVs produce two types of mature virion: EV and IMV. EV is produced first in conjunction with F13 production (116), accounting for up to 25 % of the total virus and is required for dissemination throughout the host (117;118;338). IMV is produced later in the infectious cycle when A26 production is maximal (116), and is the more robust particle. Although the exact role of IMV has not been fully defined, it is likely that the production of each particle type provides some advantages for virus replication. Due to the difference in antigenicity of the enveloped and non-enveloped forms, and the importance that each form of the virus plays in inducing protective immunity (300;302;303;305), a vaccine strain would ideally be required to produce both EV and IMV.

One approach taken elsewhere has been to abrogate EV production by the disruption of genes essential for EV maturation (117-119). This would reduce viral dissemination and hence reduce virulence to create a safer live vaccine (120). Unfortunately, although these EV knockout mutants had an attenuated phenotype,

the production of large quantities of virus was inherently difficult due to the reduced ability to spread in tissue culture.

An alternative strategy would be to increase the quantities of virions that mature as IMV, which would result in reduced EV production as the quantities of virions available for envelopment would be reduced. Directing morphogenesis towards IMV production has the potential to avoid total abrogation of EV production and therefore both forms of the virus could be presented to the immune system. If successful, a significant but not total reduction in the quantities of EV produced might attenuate the virus *in vivo* but still allow an economically acceptable rate of virus propagation in tissue culture-based vaccine production. To achieve this, the mechanism by which maturation of virions switches from EV to IMV during the infectious cycle would need to be understood. This has led to the role of the IMV-specific protein, A26, in IMV morphogenesis being investigated in this study, and the impact of overproduction of A26 on the maturation of EV and IMV examined, as a potential strategy to generate a next generation live smallpox vaccine.

8.2 Role of A26 in IMV Maturation

Prior to this study, the role of A26 in VACV was largely undefined: previous studies had proposed that A26 was a component of surface tubules, although strains that did not have A26 also produced surface tubules (238;239). Another study demonstrated that A26 was an occlusion factor to aid trafficking of IMV into ATI bodies (188). Occlusion of IMVs does not occur in all poxviruses and yet interestingly the A26 ORF, or at least a portion of the ORF, is highly conserved in

OPVs and orthologues are found in other poxviruses (371-374). A26 has also been identified as unique to IMV, where the synthesis of A26 is concurrent with maturation of IMV (116). From this, the hypothesis that A26 acts as a differentiation switch causing maturation to switch from EV to IMV was proposed. More recent studies have demonstrated the association of A26 with A27 (342;351), and this would support the hypothesis where A26 acts to negatively regulate wrapping, as binding of A26 to the virion via A27, could plausibly cause EV maturation to cease and IMV maturation to predominate.

In the study presented here, the A26L deletion mutant strain, vIδA26L, was produced. Initial experiments demonstrated a reduction in virus titres from one-step growth curves that could be attributed to a dramatic reduction in IMV production when examined by CsCl density gradient analysis compared with the IHD-J parent strain. Experiments with a second deletion mutant in the same gene, vIδA26L.neo, demonstrated a similar reduction in virus titres in one-step growth curves compared to a revertant strain, however, the same reduction in IMV was not observed by CsCl density gradient analysis. The reproducibility of the kinetic assays was brought into question in these studies which may have been affected by the host cell type, the passage history and the metabolic state of the cells. Deletion of A26 however, does appear to perturb the production of single-membraned virus, and it could be suggested that single-membraned virions that do not acquire A26 are not a mature end-stage product of virion morphogenesis but are nascent virions awaiting envelopment. This was not observed in other studies that have also used A26L deletion mutant strains to quantify the IMV and EV

produced in culture, although the different quantification methods and culture conditions may contribute to this (134;351). The increased production of IMV in VACV COP does not fit with our hypothesis, and the non-enveloped intracellular virus observed may be in fact nascent virions that cannot be wrapped, for a reason not associated with a lack of A26. The conservation of part of the A26 coding sequence in the COP strain is interesting as the final 73 amino acids are demonstrated to be required for association with A27, and therefore attachment to virions via A27 (342;351): this region is absent in COP. The truncated A26 is not attached to the virion (Dr D. Pickup, personal communication) and the truncated A26 cannot complement occlusion negative strains of CPXV (188). During the course of this study, several researchers reported further roles for A26 in cell attachment by binding IMV to cell surface laminin (134) and the suppression of GAG-mediated cell fusion (342). For these roles, attachment of A26 to the virion surface is likely to be necessary, therefore the function of unbound A26 in COP remains unsolved.

Although the evidence from this study suggests that A26 is not a differentiation switch controlling maturation of IMV, it may still be a marker of fully differentiated, non-enveloped mature virus that can no longer mature as EV.

8.3 IMV as a True End-stage Product of VACV Morphogenesis

It is generally accepted that IMV are precursors of EV where IMV are the kernels that are wrapped to become EV, and that the accumulation of IMV within a cell is a tissue culture artefact that results from limiting quantities of intracellular

membranes used for wrapping. Membrane perturbing agents demonstrated that stripping the outer membrane from EV inactivated the virion but IMV were not inactivated when subjected to the same treatment (Dean *et al.*, in preparation). This suggests that the single-membraned EV pre-cursor and mature IMV are different particles. Modification of the IMV surface by deletion of A26 demonstrated that the intracellular non-enveloped form of the mutant strains had an increased sensitivity to Tween-20, behaving similarly to stripped EV, compared to wild-type intracellular non-enveloped virus. The relative resistance of wild-type IMV to inactivation by Tween-20 might be attributable to the presence of IMV-specific proteins that are not found on stripped EV, such as A26 and by extrapolation, A25 (ATI).

This provides evidence that IMV is a true end-stage product of VACV morphogenesis, and that a mechanism exists by which OPVs actively differentiate particles towards IMV, thus preventing the maturation of a subset of virions as EV. Therefore, it is proposed that in addition to EV and IMV, the term "nascent virus" (NV) be used to describe a third virion form that is non-differentiated but is able to mature as either EV or IMV via two independent maturation pathways (Figure 8.1).

8.4 Active Differentiation of Virions in OPVs

This study presents evidence that IMV is a true-end stage product of OPV morphogenesis, and that OPVs differentiate to produce two mutually non-interchangeable co-existing isoforms of mature infectious virion. Thus OPVs appear to differentiate in a manner that is not known in other virus families.

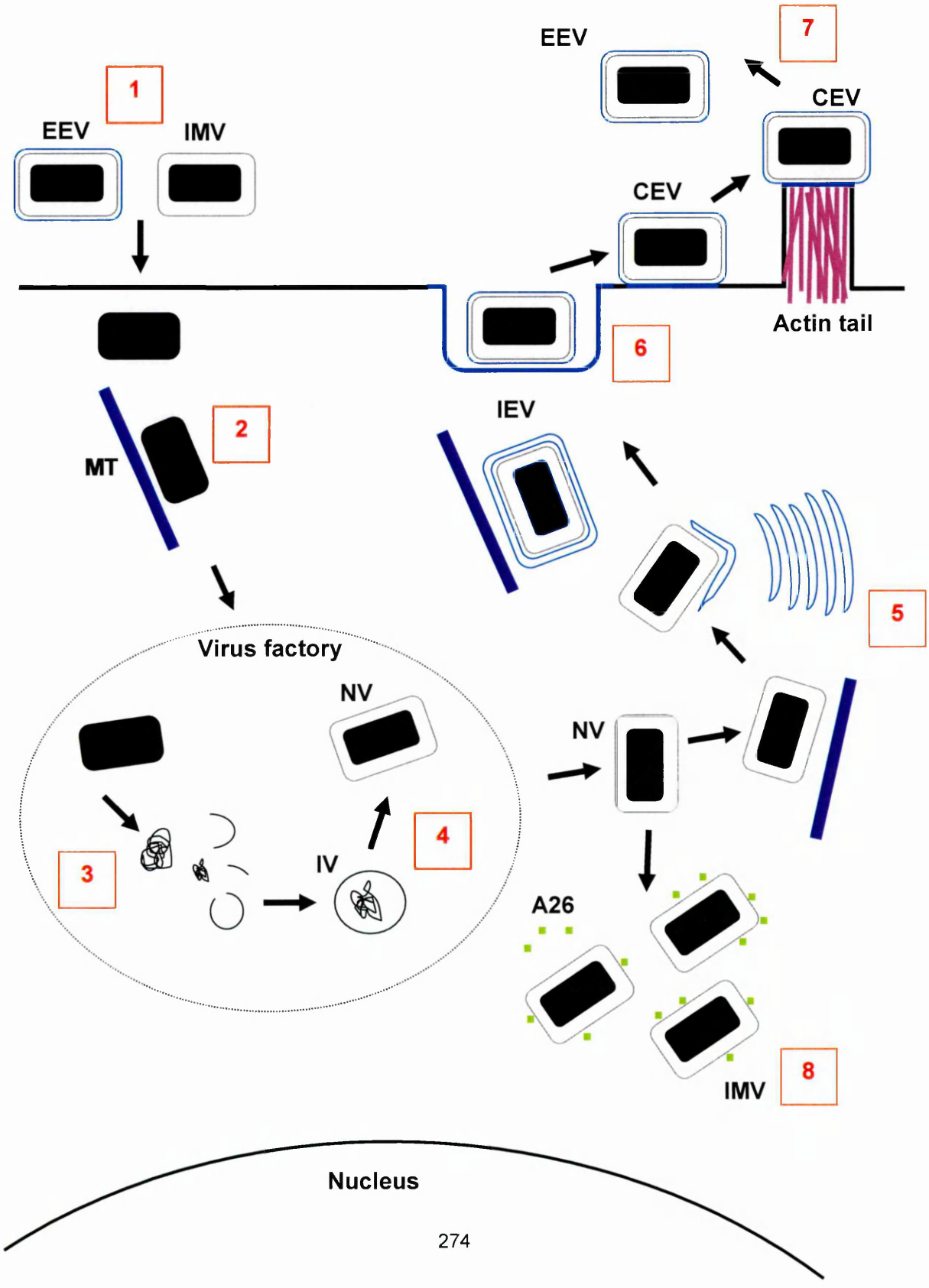
1
EEV
IMV
2
MT
Virus factory
NV
3
4
IV
EEV
7
CEV
CEV
Actin tail
6
IEV
5
NV
A26
IMV
8
Nucleus

Figure 8.1 Proposed VACV Morphogenesis where Two Non-Interchangeable Isoforms of Infectious Virus are Produced

1 EV or IMV bind to the cell and enter following the loss of one or more membranes. The naked viral core is released into the cytoplasm. **2** The core is transported via microtubules (MT) where the formation of viral factories occurs within the cell. **3** Transcription of the early gene leads to core uncoating. DNA replication and viral crescent formation begins. **4** DNA is packaged and immature virions (IV) assemble. Concomitant with proteolytic cleavage of viral core proteins IV are processed to form single-membraned nascent virus (NV). **5** Some virions are transported via microtubules to intracellular membranes for envelopment. **6** NV particles are wrapped by a Golgi or TGN-derived double membrane to form triple-membraned IEV and are then transported to the cell surface via microtubules. **7** To exit the cell, the outer IEV membrane fuses with the cell membrane to expose a CEV at the cell surface. Actin polymerisation beneath the CEV occurs to drive the virus into a neighbouring cell, or the virus is released as an EEV. **8** In the later stages of the infectious cycle, wrapping of virions decreases and some NV acquire A26 and remain within the cell until lysis. These virions cannot become wrapped.

The herpesviruses and papillomaviruses provide examples of viruses whose genomes are able to replicate in non-encapsidated states through manipulation of the host cell and as a result produce two different types of infection: latent and lytic (375;376). Latent infections are an important feature of many viral infections to ensure maintenance of the viral genome within the host indefinitely, where it may be reactivated periodically to produce new progeny and subsequently infect new hosts. During latency, infectious virus is not produced and the virus is maintained as non-encapsidated nucleic acid with only minimal viral gene expression, usually only to prevent apoptosis therefore maintaining viability of the host cell (377-379). The "duality of infection states" exhibited by these viruses is achieved by manipulation of the differentiation state of the host cell to maintain and replicate non-encapsidated viral nucleic acid, and is not indicative of differentiation of the viruses in a manner that is analogous to differentiation in metazoan life-forms.

Bacteriophages are also able to produce either latent or lytic infections in their prokaryotic hosts. Some bacteriophage genomes integrate into the host genome (lysogeny) where the bacteriophage DNA is replicated along with the host chromosome as the bacterial host cell divides (380). This maintains the genetic material in all progeny cells, essentially acting to delay lytic infection until the environmental conditions favour the lytic cycle as the optimal replication strategy. Although bacteriophage lysogeny is analogous to latency in herpesvirus and papillomavirus infections, it cannot be truly be regarded as manipulating the host-cell differentiation state. The "duality of infection states" described for bacteriophages and the eukaryotic viruses aforementioned are examples of viruses

that produce two interchangeable phases of infection that occur sequentially: both infection states cannot co-exist in the same cell and infection produces only one type of viron with one set of functions. This is quite different to what we describe here as OPV differentiation, and is not functionally analogous to differentiation as we understand it in metazoan eukaryotes.

True differentiation is demonstrated in metazoan and some protozoan eukaryotes. In the protozoan *Dictyostelium discoideum*, or cellular slime mould, the organism(s) remain in their single-celled state when nutrients are available. However, when nutrients are depleted, signals are released from the individual cells and they form swarms. The cells join to form a slug-like creature behaving as a multi-cellular organism and the slug migrates towards an open space where a fruiting body develops. The cells differentiate so that some become spores to begin the next generation and others become the basal cells and stalk, sacrificing themselves for the sake of the "organism". The specialist spores will form a new generation, while the specialist basal and stalk cells will not, and the differentiation, once complete, is largely irreversible (381;382).

Eukaryotic differentiation usually begins from a totipotent cell population whose progeny become specialised for their particular task: in metazoans a single zygote is able to differentiate into a complex system of tissues and cell types to construct a complete and viable organism. Cellular differentiation occurs in response to a stimulus and is also controlled at the genetic level. Changes in gene expression usually result from signal molecules such as hormones and growth factors which induce cell-to-cell signalling. This cascade results in the activation of

transcription factors and thus a change in gene expression that will result in cell differentiation (383). Often differentiation is terminal, and cells cannot normally "de-differentiate".

OPVs appear to differentiate in a manner more similar to that of eukaryotic organisms rather than the "duality of infection states" described above for other viruses that can replicate in non-encapsidated states as their host cell divides. Two morphologically distinct forms are produced in OPV infection: EV for virus dissemination in the infected host, and IMV for host-to-host transmission. It is often assumed that the production of EV is limited by the quantities of intracellular membranes that are available for wrapping during the infectious cycle, resulting in an accumulation of IMV by default. However, the presence of the IMV-restricted protein A26, would suggest OPVs actively differentiate particles towards IMV, thus actively preventing the maturation of a subset of virions as EV, resulting in two mutually non-interchangeable co-existing isoforms of mature infectious virion. As an adaptation this would ensure that both forms of virion are produced to perform their individual functions in the virus life-cycle in a manner highly analogous to cellular differentiation in higher eukaryotes. This is the first description of such a process in the virus kingdom.

8.5 Future Work

Examining the kinetics of EV and IMV production has proven to be a difficult task, and a challenge to obtain reproducible results. During the course of these experiments both A26L deletion mutants produced virions that sedimented with the

same density as IMV in wild-type cultures. Although structurally similar to wild-type IMV, these virions do not possess A26 and have increased sensitivity to a non-ionic detergent. Conceivably, if intracellular membranes for virion wrapping are limiting in tissue culture systems, the single-membraned intracellular virus that is produced in wild-type cultures may be a heterogeneous population of virus: a mixture of $A26^+$ (fully differentiated) and $A26^-$ (nascent) virions. It is also conceivable that the quantities of $A26^+$ and $A26^-$ virions in such a situation may differ depending on the cell line used. This could make future studies in this area technically challenging, but might be addressed by limiting virus assembly (e.g. by addition of rifampicin) to a level where wrapping membranes themselves cease to be limiting.

The potential use of a recombinant VACV as a vaccine strain, where the A26L gene was modulated to overproduce A26, was not investigated as set out in the original aims of this project as expression from a synthetic early/late promoter did not appear to increase expression of A26, relative to a revertant. It may be that the early portion of the promoter was not efficient. However, during the course of this project other researchers have found that A26 is not stable in the absence of A27 and is rapidly degraded, which indicates that the approach of controlling A26L with a synthetic early/late promoter could not have achieved the objective. Other approaches could be taken to try to increase the levels of expression of A26 in cultures. This could involve additional transient expression of A26 under a vaccinia promoter in a cultured cell line that was used to propagate VACV, although this would be complicated by the additional production of A26 away from the virus

factories where virions are assembled. Alternatively, different promoters that have been proven to give increased levels of expression such as the T7 bacteriophage promoter system could be engineered into VACV (384), or multiple copies of A26L could be engineered into the VACV genome.

There is no simple explanation for the lack of activity of AMPs on the intracellular virus of the A26L deletion mutant viruses, when the peptides have clear activity against EEV but not against IMV of wild-type IHD-J, and there is a clear difference in susceptibility to Tween-20. Plausibly, there may be additional differences between IMV and unwrapped EV. To try to unravel the reasons for the differential effect of AMPs and Tween-20 on single-membraned intracellular virus from A26L deletion mutants, future analyses could be performed to examine the effect on the virion membrane by CsCl density gradient centrifugation of treated virions, or visualising the effects by electron microscopy.

Ultimately, the goal of this project was to generate a defined VACV strain that could be used as a safer alternative to current licensed smallpox vaccines. This study used the IHD-J strain for proof of principle, as this strain produces increased quantities of EEV when cultured in RK13 cells compared to other laboratory strains such as WR (181). However, such laboratory strains would not be used in the development of a vaccine; a strain with a better safety and efficacy profile such as Lister would be more appropriate. Deletion of A26 in the IHD-J strain in this study resulted in only a mild effect on virus replication, and no effect was observed by other researchers in the WR strain *in vitro* (134;188;342;351). However, the effect *in vivo* has not yet been examined, and as A26 has been

demonstrated to play a role in cell binding and cell-to-cell fusion, it is possible that this protein may yet prove to affect VACV virulence.

CTCTGGCTAA AAAGATTGAT GTTCAGACTG GACGGCGCCC ATATGAGTAA CTTAACTCTT
TTGaattgga tcagcttttt ttttttttt tttggcatat aaataaggtc gacaaaaatt
gaaaaactat tctaatttat tgcacggATG AGCGAAAAAT ACATCGTCAC CTGGGACATG
TTGCAGATCC ATGCACGTAA ACTCGCAAGC CGACTGATGC CTTCTGAACA ATGGAAAGGC
ATTATTGCCG TAAGCCGTGG CGGTCTGGTA CCGGGTGCGT TACTGGCGCG TGAACTGGGT
ATTCGTCATG TCGATACCGT TTGTATTTCC AGCTACGATC ACGACAACCA GCGCGAGCTT
AAAGTGCTGA AACGCGCAGA AGGCGATGGC GAAGGCTTCA TCGTTATTGA TGACCTGGTG
GATACCGGTG GTACTGCGGT TGCGATTCGT GAAATGTATC CAAAAGCGCA CTTTGTCACC
ATCTTCGCAA AACCGGCTGG TCGTCCGCTG GTTGATGACT ATGTTGTTGA TATCCCGCAA
GATACCTGGA TTGAACAGCC GTGGGATATG GGCGTCGTAT TCGTCCCGCC AATCTCCGGT
CGCTAATTAC CCGATTGTAG TTAAGTTTTG AATAAAATTT TTTATAATAA ATGGAGGTCA
CGAACCTTAT TGAAAAATGT ACCAAGCACT CCAAA

Figure A1 vIδA26L Recombination Cassette Sequence

Cassette used to construct vIδA26L virus by replacing A26L with *Eco*GPT (black) expressed from a synthetic early/late promoter (purple). Upstream and downstream flanking regions of A26L are highlighted in red and were included to facilitate homologous recombination.

CTCTGGCTAA AAAGATTGAT GTTCAGACTG GACGGCGCCC ATATGAGTAA CTTAACTCTT
TTGTTAATTA AAAGTATATT CAAAAAATGA GTTATATAAA TGGCGAACAT TATAAATTTA
TGGAACGGAA TTGTACCAAC GGTTCAAGAT GTTAATGTTG CGAGCATTAC TGCGTTTAAA
TCTATGATAG ATGAAACATG GGATAAAAAA ATCGAAGCAA ATACATGCAT CAGTAGAAAA
CATAGAAACA TTATTCACGA AGTTATTAGG GACTTTATGA AAGCCTATCC TAAAATGGAT
GAGAATAAAA AATCTCCATT AGGAGCCCCA ATGCAATGGC TAACACAATA TTATATTTTA
AAGAATGAAT ATCATAAGAC CATGCTAGCG TATGATAATG GATCATTGAA TACAAAATTT
AAAACGTTAA ACATTTATAT GATTACTAAC GTTGGTCAAT ATATTTTATA TATAGTATTT
TGTATAATAT CTGGTAAGAA TCACGATGGT ACTCCTTATA TATACGATTC TGAGATAACG
AGCAATGATA AAAATTTTAT TAATGAGCGT ATCAAGTATG CATGTAAGCA AATATTACAC
GGTCAATTAA CTATAGCTCT GAGAATTAGA AATAAATTCA TGTTTATAGG ATCACCCATG
TATTTATGGT TTAACGTAAA CGGATCACAG GTATATCACG ACATATATGA TCGTAATGCC
GGTTTTCATA ATAAAGAGAT AGGTAGACTA CTATACGCAT TTATGTACTA TCTATCTATA
AGTGGTAGAT TTTTGAATGA TTTCGCACTA TTAAAGTTTA CGTATTTAGG AGAATCCTGG
ACATTTAGTT TGAGTGTCCC TGAATATATA TTATATGGTT TAGGATATTC TGTTTTCGAT
ACTATTGAAA AATTTAGCAA TGATGCTATA CTCGTTTATA TTAGAACAAA CAATAGAAAT
GGATATGATT ATGTAGAGTT TAATAAAAAA GGAATTGCTA AGGTGACAGA AGATAAACCC
GATAACGATA AGCGAATTCA TGCTATAAGA CTCATCAACG ATAGTACTGA TGTTCAACAC
ATACATTTTG GGTTTAGAAA TATGGTAATA ATAGACAATG AATGCGCTAA TATTCAGTCG
AGTGCTGAAA ATGCAACTGA TACAGGACAT CATCAAGATA GCAAAATAAA TATCGAAGTC
GAAGATGATG TCATAGACGA TGATGATTAT AATCCAAAAC CCACTCCGAT ACCGGAGCCT
CACCCTAGAC CACCGTTTCC CAGACATGAA TATCATAAGA GGCCGAAACT TCTTCCTGTA
GAAGAACCTG ATCCTGTCAA AAAAGACGCG GATCGTATAA GACTTGATAA TCATATATTA
AACACATTGG ATCATAATCT TAATTTCATC GGACACTATT GTTGTGATAC AGCGGCAGTT
GATAGGTTAG AACATCACAT CGAAACATTG GGACAATATG CAGTAATACT GGCAAGAAAG
ATAAATATGC AAACATTACT GTTCCCATGG CCATTACCTA CTGTCCATCC ACATGCGATA
GATGGTAGTA TTCCACCACA TGGGAGATCT ACGATTTTAT ATGGAGGTCA CGAACCTTAT
TGAAAAATGT ACCAAGCACT CCAAA

Figure A2 Revertant Construct for Reverse GPT Selection

A26L DNA sequence plus upstream and downstream flanking regions of VACV WR (GenBank Accession Number AY243312, position 138371-140062). The predicted native promoter sequence is highlighted in red; the flanking regions are highlighted in blue.

CTCTGGCTAA AAAGATTGAT GTTCAGACTG GACGGCGCCC ATATGAGTAA CTTAACTCTT
TTGAATTGGA TCAGCTTTTT TTTTTTTTTT TTTGGCATAT AAATAACGTC GACAAAAATT
GAAAAACTAT TCTAATTTAT TGCACGGATG GCGAACATTA TAAATTTATG GAACGGAATT
GTACCAACGG TTCAAGATGT TAATGTTGCG AGCATTACTG CGTTTAAATC TATGATAGAT
GAAACATGGG ATAAAAAAAT CGAAGCAAAT ACATGCATCA GTAGAAAACA TAGAAACATT
ATTCACGAAG TTATTAGGGA CTTTATGAAA GCCTATCCTA AAATGGATGA GAATAAAAAA
TCTCCATTAG GAGCCCCAAT GCAATGGCTA ACACAATATT ATATTTTAAA GAATGAATAT
CATAAGACCA TGCTAGCGTA TGATAATGGA TCATTGAATA CAAAATTTAA AACGTTAAAC
ATTTATATGA TTACTAACGT TGGTCAATAT ATTTTATATA TAGTATTTTG TATAATATCT
GGTAAGAATC ACGATGGTAC TCCTTATATA TACGATTCTG AGATAACGAG CAATGATAAA
AATTTTATTA ATGAGCGTAT CAAGTATGCA TGTAAGCAAA TATTACACGG TCAATTAACT
ATAGCTCTGA GAATTAGAAA TAAATTCATG TTTATAGGAT CACCCATGTA TTTATGGTTT
AACGTAAACG GATCACAGGT ATATCACGAC ATATATGATC GTAATGCCGG TTTTCATAAT
AAAGAGATAG GTAGACTACT ATACGCATTT ATGTACTATC TATCTATAAG TGGTAGATTT
TTGAATGATT TCGCACTATT AAAGTTTACG TATTTAGGAG AATCCTGGAC ATTTAGTTTG
AGTGTCCCTG AATATATATT ATATGGTTTA GGATATTCTG TTTTCGATAC TATTGAAAAA
TTTAGCAATG ATGCTATACT CGTTTATATT AGAACAAACA ATAGAAATGG ATATGATTAT
GTAGAGTTTA ATAAAAAAGG AATTGCTAAG GTGACAGAAG ATAAACCCGA TAACGATAAG
CGAATTCATG CTATAAGACT CATCAACGAT AGTACTGATG TTCAACACAT ACATTTTGGG
TTTAGAAATA TGGTAATAAT AGACAATGAA TGCGCTAATA TTCAGTCGAG TGCTGAAAAT
GCAACTGATA CAGGACATCA TCAAGATAGC AAAATAAATA TCGAAGTCGA AGATGATGTC
ATAGACGATG ATGATTATAA TCCAAAACCC ACTCCGATAC CGGAGCCTCA CCCTAGACCA
CCGTTTCCCA GACATGAATA TCATAAGAGG CCGAAACTTC TTCCTGTAGA AGAACCTGAT
CCTGTCAAAA AAGACGCGGA TCGTATAAGA CTTGATAATC ATATATTAAA CACATTGGAT
CATAATCTTA ATTTCATCGG ACACTATTGT TGTGATACAG CGGCAGTTGA TAGGTTAGAA
CATCACATCG AAACATTGGG ACAATATGCA GTAATACTGG CAAGAAAGAT AAATATGCAA
ACATTACTGT TCCCATGGCC ATTACCTACT GTCCATCCAC ATGCGATAGA TGGTAGTATT
CCACCACATG GGAGATCTAC GATTTTATAA ATGGAGGTCA CGAACCTTAT TGAAAAATGT
ACCAAGCACT CCAAA

Figure A3 EL construct for Reverse GPT Selection

A26L DNA sequence plus upstream and downstream flanking regions of VACV WR (GenBank Accession Number AY243312, position 138371-140062). The synthetic early/late promoter sequence is highlighted in red (327); the flanking regions are highlighted in blue.

CTCTGGCTAA AAAGATTGAT GTTCAGACTG GACGGCGCCC ATATGAGTAA CTTAACTCTT
TGTTACCCGA TTGTAGTTAA GTTTTGAATA AAATTATTTT TTATAATAAA TGGAGGTCAC
GAACC

Figure A4 Null Construct for Reverse GPT Selection

Upstream (blue) and downstream (black) flanking regions of VACV WR A26L sequence (GenBank Accession Number AY243312, position 138371-140062).

CTCTGGCTAA AAAGATTGAT GTTCAGACTG GACGGCGCCC ATATGAGTAA CTTAACTCTT
TTGCAAAAAT TGAAAAACTA TTCTAATTTA TTGCACGGAT GGCGAACATT ATAAATTTAT
GGAACGGAAT TGTACCAACG GTTCAAGATG TTAATGTTGC GAGCATTACT GCGTTTAAAT
CTATGATAGA TGAAACATGG GATAAAAAAA TCGAAGCAAA TACATGCATC AGTAGAAAAC
ATAGAAACAT TATTCACGAA GTTATTAGGG ACTTTATGAA AGCCTATCCT AAAATGGATG
AGAATAAAAA ATCTCCATTA GGAGCCCCAA TGCAATGGCT AACACAATAT TATATTTTAA
AGAATGAATA TCATAAGACC ATGCTAGCGT ATGATAATGG ATCATTGAAT ACAAAATTTA
AAACGTTAAA CATTTATATG ATTACTAACG TTGGTCAATA TATTTTATAT ATAGTATTTT
GTATAATATC TGGTAAGAAT CACGATGGTA CTCCTTATAT ATACGATTCT GAGATAACGA
GCAATGATAA AAATTTTATT AATGAGCGTA TCAAGTATGC ATGTAAGCAA ATATTACACG
GTCAATTAAC TATAGCTCTG AGAATTAGAA ATAAATTCAT GTTTATAGGA TCACCCATGT
ATTTATGGTT TAACGTAAAC GGATCACAGG TATATCACGA CATATATGAT CGTAATGCCG
GTTTTCATAA TAAAGAGATA GGTAGACTAC TATACGCATT TATGTACTAT CTATCTATAA
GTGGTAGATT TTTGAATGAT TTCGCACTAT TAAAGTTTAC GTATTTAGGA GAATCCTGGA
CATTTAGTTT GAGTGTCCCT GAATATATAT TATATGGTTT AGGATATTCT GTTTTCGATA
CTATTGAAAA ATTTAGCAAT GATGCTATAC TCGTTTATAT TAGAACAAAC AATAGAAATG
GATATGATTA TGTAGAGTTT AATAAAAAAG GAATTGCTAA GGTGACAGAA GATAAACCCG
ATAACGATAA GCGAATTCAT GCTATAAGAC TCATCAACGA TAGTACTGAT GTTCAACACA
TACATTTTGG GTTTAGAAAT ATGGTAATAA TAGACAATGA ATGCGCTAAT ATTCAGTCGA
GTGCTGAAAA TGCAACTGAT ACAGGACATC ATCAAGATAG CAAAATAAAT ATCGAAGTCG
AAGATGATGT CATAGACGAT GATGATTATA ATCCAAAACC CACTCCGATA CCGGAGCCTC
ACCCTAGACC ACCGTTTCCC AGACATGAAT ATCATAAGAG GCCGAAACTT CTTCCTGTAG
AAGAACCTGA TCCTGTCAAA AAAGACGCGG ATCGTATAAG ACTTGATAAT CATATATTAA
ACACATTGGA TCATAATCTT AATTTCATCG GACACTATTG TTGTGATACA GCGGCAGTTG
ATAGGTTAGA ACATCACATC GAAACATTGG GACAATATGC AGTAATACTG GCAAGAAAGA
TAAATATGCA AACATTACTG TTCCCATGGC CATTACCTAC TGTCCATCCA CATGCGATAG
ATGGTAGTAT TCCACCACAT GGGAGATCTA CGATTTTATA AATGGAGGTC ACGAACCTTA
TTGAAAAATG TACCAAGCAC TCCAAA

Figure A5 Early Construct for Reverse GPT Selection

A26L DNA sequence plus upstream and downstream flanking regions of VACV WR (GenBank Accession Number AY243312, position 138371-140062). The early promoter sequence is highlighted in red (327); the flanking regions are highlighted in blue.

CTCTGGCTAA AAAGATTGAT GTTCAGACTG GACGGCGCCC ATATGAGTAA CTTAACTCTT
TTGATTTGGA TCAGCTTTTT TTTTTTTTTT TTTGGCATAT AAATGGCGAA CATTATAAAT
TTATGGAACG GAATTGTACC AACGGTTCAA GATGTTAATG TTGCGAGCAT TACTGCGTTT
AAATCTATGA TAGATGAAAC ATGGGATAAA AAAATCGAAG CAAATACATG CATCAGTAGA
AAACATAGAA ACATTATTCA CGAAGTTATT AGGGACTTTA TGAAAGCCTA TCCTAAAATG
GATGAGAATA AAAAATCTCC ATTAGGAGCC CCAATGCAAT GGCTAACACA ATATTATATT
TTAAAGAATG AATATCATAA GACCATGCTA GCGTATGATA ATGGATCATT GAATACAAAA
TTTAAAACGT TAAACATTTA TATGATTACT AACGTTGGTC AATATATTTT ATATATAGTA
TTTTGTATAA TATCTGGTAA GAATCACGAT GGTACTCCTT ATATATACGA TTCTGAGATA
ACGAGCAATG ATAAAAATTT TATTAATGAG CGTATCAAGT ATGCATGTAA GCAAATATTA
CACGGTCAAT TAACTATAGC TCTGAGAATT AGAAATAAAT TCATGTTTAT AGGATCACCC
ATGTATTTAT GGTTTAACGT AAACGGATCA CAGGTATATC ACGACATATA TGATCGTAAT
GCCGGTTTTC ATAATAAAGA GATAGGTAGA CTACTATACG CATTTATGTA CTATCTATCT
ATAAGTGGTA GATTTTTGAA TGATTTCGCA CTATTAAAGT TTACGTATTT AGGAGAATCC
TGGACATTTA GTTTGAGTGT CCCTGAATAT ATATTATATG GTTTAGGATA TTCTGTTTTC
GATACTATTG AAAAATTTAG CAATGATGCT ATACTCGTTT ATATTAGAAC AAACAATAGA
AATGGATATG ATTATGTAGA GTTTAATAAA AAAGGAATTG CTAAGGTGAC AGAAGATAAA
CCCGATAACG ATAAGCGAAT TCATGCTATA AGACTCATCA ACGATAGTAC TGATGTTCAA
CACATACATT TTGGGTTTAG AAATATGGTA ATAATAGACA ATGAATGCGC TAATATTCAG
TCGAGTGCTG AAAATGCAAC TGATACAGGA CATCATCAAG ATAGCAAAAT AAATATCGAA
GTCGAAGATG ATGTCATAGA CGATGATGAT TATAATCCAA AACCCACTCC GATACCGGAG
CCTCACCCTA GACCACCGTT TCCCAGACAT GAATATCATA AGAGGCCGAA ACTTCTTCCT
GTAGAAGAAC CTGATCCTGT CAAAAAAGAC GCGGATCGTA TAAGACTTGA TAATCATATA
TTAAACACAT TGGATCATAA TCTTAATTTC ATCGGACACT ATTGTTGTGA TACAGCGGCA
GTTGATAGGT TAGAACATCA CATCGAAACA TTGGGACAAT ATGCAGTAAT ACTGGCAAGA
AAGATAAATA TGCAAACATT ACTGTTCCCA TGGCCATTAC CTACTGTCCA TCCACATGCG
ATAGATGGTA GTATTCCACC ACATGGGAGA TCTACGATTT TATAAATGGA GGTCACGAAC
CTTATTGAAA AATGTACCAA GCACTCCAAA

Figure A6 Late Construct for Reverse GPT Selection

A26L DNA sequence plus upstream and downstream flanking regions of VACV WR (GenBank Accession Number AY243312, position 138371-140062). The late promoter sequence is highlighted in red (327); the flanking regions are highlighted in blue.

CTCTGGCTAA AAAGATTGAT GTTCAGACTG GACGGCGCCC ATATGAGTAA CTTAACTCTT
TTGGGATGTA TAAGTTTTTA TGTTAACTAA ATGGCGAACA TTATAAATTT ATGGAACGGA
ATTGTACCAA CGGTTCAAGA TGTTAATGTT GCGAGCATTA CTGCGTTTAA ATCTATGATA
GATGAAACAT GGGATAAAAA AATCGAAGCA AATACATGCA TCAGTAGAAA ACATAGAAAC
ATTATTCACG AAGTTATTAG GGACTTTATG AAAGCCTATC CTAAAATGGA TGAGAATAAA
AAATCTCCAT TAGGAGCCCC AATGCAATGG CTAACACAAT ATTATATTTT AAAGAATGAA
TATCATAAGA CCATGCTAGC GTATGATAAT GGATCATTGA ATACAAAATT TAAAACGTTA
AACATTTATA TGATTACTAA CGTTGGTCAA TATATTTTAT ATATAGTATT TTGTATAATA
TCTGGTAAGA ATCACGATGG TACTCCTTAT ATATACGATT CTGAGATAAC GAGCAATGAT
AAAAATTTTA TTAATGAGCG TATCAAGTAT GCATGTAAGC AAATATTACA CGGTCAATTA
ACTATAGCTC TGAGAATTAG AAATAAATTC ATGTTTATAG GATCACCCAT GTATTTATGG
TTTAACGTAA ACGGATCACA GGTATATCAC GACATATATG ATCGTAATGC CGGTTTTCAT
AATAAAGAGA TAGGTAGACT ACTATACGCA TTTATGTACT ATCTATCTAT AAGTGGTAGA
TTTTTGAATG ATTTCGCACT ATTAAAGTTT ACGTATTTAG GAGAATCCTG GACATTTAGT
TTGAGTGTCC CTGAATATAT ATTATATGGT TTAGGATATT CTGTTTTCGA TACTATTGAA
AAATTTAGCA ATGATGCTAT ACTCGTTTAT ATTAGAACAA ACAATAGAAA TGGATATGAT
TATGTAGAGT TTAATAAAAA AGGAATTGCT AAGGTGACAG AAGATAAACC CGATAACGAT
AAGCGAATTC ATGCTATAAG ACTCATCAAC GATAGTACTG ATGTTCAACA CATACATTTT
GGGTTTAGAA ATATGGTAAT AATAGACAAT GAATGCGCTA ATATTCAGTC GAGTGCTGAA
AATGCAACTG ATACAGGACA TCATCAAGAT AGCAAAATAA ATATCGAAGT CGAAGATGAT
GTCATAGACG ATGATGATTA TAATCCAAAA CCCACTCCGA TACCGGAGCC TCACCCTAGA
CCACCGTTTC CCAGACATGA ATATCATAAG AGGCCGAAAC TTCTTCCTGT AGAAGAACCT
GATCCTGTCA AAAAAGACGC GGATCGTATA AGACTTGATA ATCATATATT AAACACATTG
GATCATAATC TTAATTTCAT CGGACACTAT TGTTGTGATA CAGCGGCAGT TGATAGGTTA
GAACATCACA TCGAAACATT GGGACAATAT GCAGTAATAC TGGCAAGAAA GATAAATATG
CAAACATTAC TGTTCCCATG GCCATTACCT ACTGTCCATC CACATGCGAT AGATGGTAGT
ATTCCACCAC ATGGGAGATC TACGATTTTA TAAATGGAGG TCACGAACCT TATTGAAAAA
TGTACCAAGC ACTCCAAA

Figure A7 F13L Construct for Reverse GPT Selection

A26L DNA sequence plus upstream and downstream flanking regions of VACV WR (GenBank Accession Number AY243312, position 138371-140062). The predicted F13L promoter sequence is highlighted in red; the flanking regions are highlighted in blue.

CCCGGGatga gcgaaaaata catcgtcacc tgggacatgt tgcagatcca tgcacGCGGC
CGCaattgga tcagcttttt ttttttttt tttggcatat aaataaggtc gacaaaaatt
gaaaaactat tctaatttat tgcacggATG ATCGAGCAGG ACGGCCTGCA CGCCGGCTCC
CCCGCCGCCT GGGTGGAGCG CCTGTTCGGC TACGACTGGG CCCAGCAGAC CATCGGCTGC
TCCGACGCCG CCGTGTTCCG CCTGTCCGCC CAGGGCCGCC CCGTGCTGTT CGTGAAGACC
GACCTGTCCG GCGCCCTGAA CGAGCTGCAG GACGAGGCCG CCCGCCTGTC CTGGCTGGCC
ACCACCGGCG TGCCCTGCGC CGCCGTGCTG GACGTGGTGA CCGAGGCCGG CCGCGACTGG
CTGCTGCTGG GCGAGGTGCC CGGCCAGGAC CTGCTGTCCT CCCACCTGGC CCCCGCCGAG
AAGGTGTCCA TCATGGCCGA CGCCATGCGC CGCCTGCACA CCCTGGACCC CGCCACCTGC
CCCTTCGACC ACCAGGCCAA GCACCGCATC GAGCGCGCCC GCACCCGCAT GGAGGCCGGC
CTGGTGGACC AGGACGACCT GGACGAGGAG CACCAGGGCC TGGCCCCCGC CGAGCTGTTC
GCCCGCCTGA AGGCCCGCAT GCCCGACGGC GAGGACCTGG TGGTGACCCA CGGCGACGCC
TGCCTGCCCA ACATCATGGT GGAGAACGGC CGCTTCTCCG GCTTCATCGA CTGCGGCCGC
CTGGGCGTGG CCGACCGCTA CCAGGACATC GCCCTGGCCA CCCGCGACAT CGCCGAGGAG
CTGGGCGGCG AGTGGGCCGA CCGCTTCCTG GTGCTGTACG GCATCGCCGC CCCCGACTCC
CAGCGCATCG CCTTCTACCG CCTGCTGGAC GAGTTCTTCT AAtaacttaa ctcttttgtt
aattaaaagt atattcaaaa aatgagttat ataaATGGCG AACATTATAA ATTTATGGAA
CGGAATTGTA CCAACGGTTC AAGATGTTAA TGTTGCGAGC ATTACTGCGT TTAAATCTAT
GATAGATGAA ACATGGGATA AAAAAATCGA AGCAAATACA TGCATCAGTA GAAAACATAG
AAACATTATT CACGAAGTTA TTAGGGACTT TATGAAAGCC TATCCTAAAA TGGATGAGAA
TAAAAAATCT CCATTAGGAG CCCCAATGCA ATGGCTAACA CAATATTATA TTTTAAAGAA
TGAATATCAT AAGACCATGC TAGCGTATGA TAATGGATCA TTGAATACAA AATTTAAAAC
GTTAAACATT TATATGATTA CTAACGTTGG TCAATATATT TTATATATAG TATTTTGTAT
AATATCTGGT AAGAATCACG ATGGTACTCC TTATATATAC GATTCTGAGA TAACGAGCAA
TGATAAAAAT TTTATTAATG AGCGTATCAA GTATGCATGT AAGCAAATAT TACACGGTCA
ATTAACTATA GCTCTGAGAA TTAGAAATAA ATTCATGTTT ATAGGATCAC CCATGTATTT
ATGGTTTAAC GTAAACGGAT CACAGGTATA TCACGACATA TATGATCGTA ATGCCGGTTT
TCATAATAAA GAGATAGGTA GACTACTATA CGCATTTATG TACTATCTAT CTATAAGTGG
TAGATTTTTG AATGATTTCG CACTATTAAA GTTTACGTAT TTAGGAGAAT CCTGGACATT
TAGTTTGAGT GTCCCTGAAT ATATATTATA TGGTTTAGGA TATTCTGTTT TCGATACTAT
TGAAAAATTT AGCAATGATG CTATACTCGT TTATATTAGA ACAAACAATA GAAATGGATA
TGATTATGTA GAGTTTAATA AAAAAGGAAT TGCTAAGGTG ACAGAAGATA AACCCGATAA
CGATAAGCGA ATTCATGCTA TAAGACTCAT CAACGATAGT ACTGATGTTC AACACATACA
TTTTGGGTTT AGAAATATGG TAATAATAGA CAATGAATGC GCTAATATTC AGTCGAGTGC
TGAAAATGCA ACTGATACAG GACATCATCA AGATAGCAAA ATAAATATCG AAGTCGAAGA
TGATGTCATA GACGATGATG ATTATAATCC AAAACCCACT CCGATACCGG AGCCTCACCC
TAGACCACCG TTTCCCAGAC ATGAATATCA TAAGAGGCCG AAACTTCTTC CTGTAGAAGA
ACCTGATCCT GTCAAAAAAG ACGCGGATCG TATAAGACTT GATAATCATA TATTAAACAC
ATTGGATCAT AATCTTAATT TCATCGGACA CTATTGTTGT GATACAGCGG CAGTTGATAG
GTTAGAACAT CACATCGAAA CATTGGGACA ATATGCAGTA ATACTGGCAA GAAAGATAAA
TATGCAAACA TTACTGTTCC CATGGCCATT ACCTACTGTC CATCCACATG CGATAGATGG
TAGTATTCCA CCACATGGGA GATCTACGAT TTTATAAagc cgtgggatat gggcgtcgta
ttcgtcccgc caatctccgg tcgctaaCCC GGG

Figure A8 Revertant Recombination Cassette Sequence

Cassette used to construct vIδA26L.rev the revertant virus by replacing *Eco*GPT (green) with G148^{R} (black) expressed from a synthetic early/late promoter (purple), followed by A26L (blue) expressed from its predicted natural promoter (red). Cassette contains *Sma*I restriction sites at each end of the construct to allow excision from plasmid vector. *Not*I restriction sites were included to allow inactivation of G418^{R} at a later stage if preferred.

CCCGGGatga gcgaaaaata catcgtcacc tgggacatgt tgcagatcca tgcacGCGGC
CGCaattgga tcagcttttt ttttttttt tttggcatat aaataaggtc gacaaaaatt
gaaaaactat tctaatttat tgcacggATG ATCGAGCAGG ACGGCCTGCA CGCCGGCTCC
CCCGCCGCCT GGGTGGAGCG CCTGTTCGGC TACGACTGGG CCCAGCAGAC CATCGGCTGC
TCCGACGCCG CCGTGTTCCG CCTGTCCGCC CAGGGCCGCC CCGTGCTGTT CGTGAAGACC
GACCTGTCCG GCGCCCTGAA CGAGCTGCAG GACGAGGCCG CCCGCCTGTC CTGGCTGGCC
ACCACCGGCG TGCCCTGCGC CGCCGTGCTG GACGTGGTGA CCGAGGCCGG CCGCGACTGG
CTGCTGCTGG GCGAGGTGCC CGGCCAGGAC CTGCTGTCCT CCCACCTGGC CCCCGCCGAG
AAGGTGTCCA TCATGGCCGA CGCCATGCGC CGCCTGCACA CCCTGGACCC CGCCACCTGC
CCCTTCGACC ACCAGGCCAA GCACCGCATC GAGCGCGCCC GCACCCGCAT GGAGGCCGGC
CTGGTGGACC AGGACGACCT GGACGAGGAG CACCAGGGCC TGGCCCCCGC CGAGCTGTTC
GCCCGCCTGA AGGCCCGCAT GCCCGACGGC GAGGACCTGG TGGTGACCCA CGGCGACGCC
TGCCTGCCCA ACATCATGGT GGAGAACGGC CGCTTCTCCG GCTTCATCGA CTGCGGCCGC
CTGGGCGTGG CCGACCGCTA CCAGGACATC GCCCTGGCCA CCCGCGACAT CGCCGAGGAG
CTGGGCGGCG AGTGGGCCGA CCGCTTCCTG GTGCTGTACG GCATCGCCGC CCCCGACTCC
CAGCGCATCG CCTTCTACCG CCTGCTGGAC GAGTTCTTCT atGcgaacat tataaattta
tggaacggaa ttgtaccaac ggttcaagat gttaatgttg cgagcattac tgcgtttaaa
tctatgatag atgaaacatg ggataaaaaa atcgaagcaa atacatgcat cagtagaaaa
catagaaaca ttattcacga agttattagg gactttatga aagcctatcc taaaatggat
gagaataaaa aatctccatt aggaTAAcca atgcaatggc taacacaata ttatatttta
aagaatgaat atcataagac catgctagcg tatgataatg gatcattgaa tacaaaattt
aaaacgttaa acatttatat gattactaac gttggtcaat atattttata tatagtattt
tgtataatat ctggtaagaa tcacgatggt actccttata tatacgattc tgagataacg
agcaatgata aaaattttat taatgagcgt atcaagtatg caTAAaagca aatattacac
ggtcaattaa ctatagctct gagaattaga aataaattca tgtttatagg atcacccatg
tatttatggt ttaacgtaaa cggatcacag gtatatcacg acatatatga tcgtaatgcc
ggttttcata ataaagagat aggtagacta ctatacgcat ttatgtacta tctatctata
agtggtagat ttttgaatga tttcgcacta ttaaagttta cgtatttagg agaatcctgg
acatttagtt tgagtgtccc tgaatatata ttatatggtt taggatattc tgttttcgat
actattgaaa aatttagcaa tgatgctata TAAgtttata ttagaacaaa caatagaaat
ggatatgatt atgtagagtt taataaaaaa ggaattgcta aggtgacaga agataaaccc
gataacgata agcgaattca tgctataaga ctcatcaacg atagtactga tgttcaacac
atacattttg ggtttagaaa tatggtaata atagacaatg aatgcgctaa tattcagtcg
agtgctgaaa atgcaactga tacaggaTAA catcaagata gcaaaataaa tatcgaagtc
gaagatgatg tcatagacga tgatgattat aatccaaaac ccactccgat accggagcct
caccctagac caccgtttcc cagacatgaa tatcataaga ggccgaaact tcttcctgta
gaagaacctg atcctgtcaa aaaagacgcg gatcgtataa gacttgataa tcatatatta
aacacattgg atcataatct taatttcatc ggacactatt gtTAAgatac agcggcagtt
gataggttag aacatcacat cgaaacattg ggacaatatg cagtaatact ggcaagaaag
ataaatatgc aaacattact gttcccatgg ccattaccta ctgtccatcc acatgcgata
gatggtagta ttccaccaca tgggagatct acgattttat aaAGCCGTGG GATATGGGCG
TCGTATTCGT CCCGCCAATC TCCGGTCGCT AAcccggg

Figure A9 vIδA26L.neo Recombination Cassette Sequence

Cassette used to construct vIδA26L.neo virus by replacing *Eco*GPT (green) with G148^{R} (black) expressed from a synthetic early/late promoter (purple), followed by a non-functional A26L (blue). Mutations within A26L are highlighted as block capitals. Cassette contains *Sma*I restriction sites at each end of the construct to allow excision from plasmid vector. *Not*I restriction sites were included to allow inactivation of G418^{R} at a later stage if preferred.

CCCGGGatga gcgaaaaata catcgtcacc tgggacatgt tgcagatcca tgcacGCGGC
CGCaattgga tcagcttttt ttttttttt tttggcatat aaataaggtc gacaaaaatt
gaaaaactat tctaatttat tgcacggATG ATCGAGCAGG ACGGCCTGCA CGCCGGCTCC
CCCGCCGCCT GGGTGGAGCG CCTGTTCGGC TACGACTGGG CCCAGCAGAC CATCGGCTGC
TCCGACGCCG CCGTGTTCCG CCTGTCCGCC CAGGGCCGCC CCGTGCTGTT CGTGAAGACC
GACCTGTCCG GCGCCCTGAA CGAGCTGCAG GACGAGGCCG CCCGCCTGTC CTGGCTGGCC
ACCACCGGCG TGCCCTGCGC CGCCGTGCTG GACGTGGTGA CCGAGGCCGG CCGCGACTGG
CTGCTGCTGG GCGAGGTGCC CGGCCAGGAC CTGCTGTCCT CCCACCTGGC CCCCGCCGAG
AAGGTGTCCA TCATGGCCGA CGCCATGCGC CGCCTGCACA CCCTGGACCC CGCCACCTGC
CCCTTCGACC ACCAGGCCAA GCACCGCATC GAGCGCGCCC GCACCCGCAT GGAGGCCGGC
CTGGTGGACC AGGACGACCT GGACGAGGAG CACCAGGGCC TGGCCCCCGC CGAGCTGTTC
GCCCGCCTGA AGGCCCGCAT GCCCGACGGC GAGGACCTGG TGGTGACCCA CGGCGACGCC
TGCCTGCCCA ACATCATGGT GGAGAACGGC CGCTTCTCCG GCTTCATCGA CTGCGGCCGC
CTGGGCGTGG CCGACCGCTA CCAGGACATC GCCCTGGCCA CCCGCGACAT CGCCGAGGAG
CTGGGCGGCG AGTGGGCCGA CCGCTTCCTG GTGCTGTACG GCATCGCCGC CCCCGACTCC
CAGCGCATCG CCTTCTACCG CCTGCTGGAC GAGTTCTTCT AAaattggat cagcttttt
ttttttttt ttggcatata aataaggtcg acaaaaattg aaaaactatt ctaatttatt
gcacggATGG CGAACATTAT AAATTTATGG AACGGAATTG TACCAACGGT TCAAGATGTT
AATGTTGCGA GCATTACTGC GTTTAAATCT ATGATAGATG AAACATGGGA TAAAAAAATC
GAAGCAAATA CATGCATCAG TAGAAAACAT AGAAACATTA TTCACGAAGT TATTAGGGAC
TTTATGAAAG CCTATCCTAA AATGGATGAG AATAAAAAAT CTCCATTAGG AGCCCCAATG
CAATGGCTAA CACAATATTA TATTTTAAAG AATGAATATC ATAAGACCAT GCTAGCGTAT
GATAATGGAT CATTGAATAC AAAATTTAAA ACGTTAAACA TTTATATGAT TACTAACGTT
GGTCAATATA TTTTATATAT AGTATTTTGT ATAATATCTG GTAAGAATCA CGATGGTACT
CCTTATATAT ACGATTCTGA GATAACGAGC AATGATAAAA ATTTTATTAA TGAGCGTATC
AAGTATGCAT GTAAGCAAAT ATTACACGGT CAATTAACTA TAGCTCTGAG AATTAGAAAT
AAATTCATGT TTATAGGATC ACCCATGTAT TTATGGTTTA ACGTAAACGG ATCACAGGTA
TATCACGACA TATATGATCG TAATGCCGGT TTTCATAATA AAGAGATAGG TAGACTACTA
TACGCATTTA TGTACTATCT ATCTATAAGT GGTAGATTTT TGAATGATTT CGCACTATTA
AAGTTTACGT ATTTAGGAGA ATCCTGGACA TTTAGTTTGA GTGTCCCTGA ATATATATTA
TATGGTTTAG GATATTCTGT TTTCGATACT ATTGAAAAAT TTAGCAATGA TGCTATACTC
GTTTATATTA GAACAAACAA TAGAAATGGA TATGATTATG TAGAGTTTAA TAAAAAAGGA
ATTGCTAAGG TGACAGAAGA TAAACCCGAT AACGATAAGC GAATTCATGC TATAAGACTC
ATCAACGATA GTACTGATGT TCAACACATA CATTTTGGGT TTAGAAATAT GGTAATAATA
GACAATGAAT GCGCTAATAT TCAGTCGAGT GCTGAAAATG CAACTGATAC AGGACATCAT
CAAGATAGCA AAATAAATAT CGAAGTCGAA GATGATGTCA TAGACGATGA TGATTATAAT
CCAAAACCCA CTCCGATACC GGAGCCTCAC CCTAGACCAC CGTTTCCCAG ACATGAATAT
CATAAGAGGC CGAAACTTCT TCCTGTAGAA GAACCTGATC CTGTCAAAAA AGACGCGGAT
CGTATAAGAC TTGATAATCA TATATTAAAC ACATTGGATC ATAATCTTAA TTTCATCGGA
CACTATTGTT GTGATACAGC GGCAGTTGAT AGGTTAGAAC ATCACATCGA AACATTGGGA
CAATATGCAG TAATACTGGC AAGAAAGATA AATATGCAAA CATTACTGTT CCCATGGCCA
TTACCTACTG TCCATCCACA TGCGATAGAT GGTAGTATTC CACCACATGG GAGATCTACG
ATTTTATAAa gccgtgggat atgggcgtcg tattcgtccc gccaatctcc ggtcgctaaC
CCGGG

Figure A10 vIδA26L.EL Recombination Cassette Sequence

Cassette used to construct vIδA26L.EL by replacing *Eco*GPT (green) with G148^{R} (black) expressed from a synthetic early/late promoter (purple), followed by A26L (blue) expressed from a synthetic early/late promoter (purple). Cassette contains *Sma*I restriction sites at each end of the construct to allow excision from plasmid vector. *Not*I restriction sites were included to allow inactivation of G418^{R} at a later stage if preferred.

Reference List

(1) Barquet N, Domingo P. Smallpox: The Triumph over the Most Terrible of the Ministers of Death. Ann Intern Med 1997; 127(8 Part 1):635-642.

(2) Behbehani AM. The smallpox story: life and death of an old disease. Microbiol Rev 1983; 47(4):455-509.

(3) Fenner F, Henderson D, Arita I, Ježek Z, Ladnyi I. Smallpox and Its Eradication. Switzerland: World Health Organization; 1988.

(4) Dixon CW. Smallpox. London: Churchill; 1962.

(5) Moss B. *Poxviridae*: The Viruses and Their Replication. In: Fields BN, Knipe DM, Howley PM, editors. Fields Virology. 3rd ed. Philadelphia: Lippincott-Raven Publishers; 1996. 2637-2671.

(6) Griffiths G, Wepf R, Wendt T, Locker JK, Cyrklaff M, Roos N. Structure and assembly of intracellular mature vaccinia virus: isolated-particle analysis. J Virol 2001; 75(22):11034-11055.

(7) Roos N, Cyrklaff M, Cudmore S, Blasco R, Krijnse-Locker J, Griffiths G. A novel immunogold cryoelectron microscopic approach to investigate the structure of the intracellular and extracellular forms of vaccinia virus. EMBO J 1996; 15(10):2343-2355.

(8) Sodeik B, Krijnse-Locker J. Assembly of vaccinia virus revisited: *de novo* membrane synthesis or acquisition from the host? Trends Microbiol 2002; 10(1):15-24.

(9) Malkin AJ, McPherson A, Gershon PD. Structure of intracellular mature vaccinia virus visualized by in situ atomic force microscopy. J Virol 2003; 77(11):6332-6340.

(10) Cyrklaff M, Risco C, Fernyez JJ, Jiménez MV, Estéban M, Baumeister W et al. Cryo-electron tomography of vaccinia virus. Proc Natl Acad Sci U S A 2005; 102(8):2772-2777.

(11) Dubochet J, Adrian M, Richter K, Garces J, Wittek R. Structure of intracellular mature vaccinia virus observed by cryoelectron microscopy. J Virol 1994; 68(3):1935-1941.

(12) WESTWOOD JC, HARRIS WJ, ZWARTOUW HT, TITMUSS DH, PPLEYARD G. STUDIES ON THE STRUCTURE OF VACCINIA VIRUS. J Gen Microbiol 1964; 34:67-78.

(13) Heuser J. Deep-etch EM reveals that the early poxvirus envelope is a single membrane bilayer stabilized by a geodetic "honeycomb" surface coat. J Cell Biol 2005; 169(2):269-283.

(14) Medzon EL, Bauer H. Structural features of vaccinia virus revealed by negative staining, sectioning, and freeze-etching. Virology 1970; 40(4):860-867.

(15) Wilton S, Mohandas AR, Dales S. Organization of the vaccinia envelope and relationship to the structure of intracellular mature virions. Virology 1995; 214(2):503-511.

(16) Peters D, Mueller G. The Fine Structure of the DNA-Containing Core of Vaccinia Virus. Virology 1963; 21:267-269.

(17) ZWARTOUW HT. THE CHEMICAL COMPOSITION OF VACCINIA VIRUS. J Gen Microbiol 1964; 34:115-123.

(18) Hiller G, Eibl H, Weber K. Acyl bis(monoacylglycero)phosphate, assumed to be a marker for lysosomes, is a major phospholipid of vaccinia virions. Virology 1981; 113(2):761-764.

(19) Stern W, Dales S. Biogenesis of vaccinia: concerning the origin of the envelope phospholipids. Virology 1974; 62(2):293-306.

(20) Lanzer W, Holowczak JA. Polyamines in vaccinia virions and polypeptides released from viral cores by acid extraction. J Virol 1975; 16(5):1254-1264.

(21) Shchelkunov SN, Resenchuk SM, Totmenin AV, Blinov VM, Marennikova SS, Sandakhchiev LS. Comparison of the genetic maps of variola and vaccinia viruses. FEBS Lett 1993; 327(3):321-324.

(22) Goebel SJ, Johnson GP, Perkus ME, Davis SW, Winslow JP, Paoletti E. The complete DNA sequence of vaccinia virus. Virology 1990; 179(1):247-66, 517.

(23) Massung RF, Liu LI, Qi J, Knight JC, Yuran TE, Kerlavage AR et al. Analysis of the complete genome of smallpox variola major virus strain Bangladesh-1975. Virology 1994; 201(2):215-240.

(24) Holowczak JA, Thomas VI, Flores L. Isolation and characterization of vaccinia virus "nucleoids". Virology 1975; 67(2):506-519.

(25) Soloski M, Holowczak JA. Preparation of subviral particles from vaccinia virions irradiated with ultraviolet light. J Virol Methods 1980; 1(4):185-195.

(26) Soloski MJ, Holowczak JA. Characterization of supercoiled nucleoprotein complexes released from detergent-treated vaccinia virions. J Virol 1981; 37(2):770-783.

(27) Soloski MJ, Cabrera CV, Esteban M, Holowczak JA. Studies concerning the structure and organization of the vaccinia virus nucleoid. I. Isolation and characterization of subviral particles prepared by treating virions with guanidine-HCL, nonidet-P40, and 2-mercaptoethanol. Virology 1979; 99(2):209-217.

(28) Broyles SS. Vaccinia virus transcription. J Gen Virol 2003; 84(Pt 9):2293-2303.

(29) Baroudy BM, Moss B. Purification and characterization of a DNA-dependent RNA polymerase from vaccinia virions. J Biol Chem 1980; 255(9):4372-4380.

(30) Spencer E, Shuman S, Hurwitz J. Purification and properties of vaccinia virus DNA-dependent RNA polymerase. J Biol Chem 1980; 255(11):5388-5395.

(31) Oda KI, Joklik WK. Hybridization and sedimentation studies on "early" and "late" vaccinia messenger RNA. J Mol Biol 1967; 27(3):395-419.

(32) Assarsson E, Greenbaum JA, Sundström M, Schaffer L, Hammond JA, Pasquetto V et al. Kinetic analysis of a complete poxvirus transcriptome reveals an immediate-early class of genes. Proc Natl Acad Sci U S A 2008; 105(6):2140-2145.

(33) Smith GL, Chan YS, Kerr SM. Transcriptional mapping and nucleotide sequence of a vaccinia virus gene encoding a polypeptide with extensive homology to DNA ligases. Nucleic Acids Res 1989; 17(22):9051-9062.

(34) Lee-Chen GJ, Niles EG. Transcription and translation mapping of the 13 genes in the vaccinia virus HindIII D fragment. Virology 1988; 163(1):52-63.

(35) Jones EV, Moss B. Mapping of the vaccinia virus DNA polymerase gene by marker rescue and cell-free translation of selected RNA. J Virol 1984; 49(1):72-77.

(36) Smith GL, de Carlos A, Chan YS. Vaccinia virus encodes a thymidylate kinase gene: sequence and transcriptional mapping. Nucleic Acids Res 1989; 17(19):7581-7590.

(37) Hruby DE, Ball LA. Mapping and identification of the vaccinia virus thymidine kinase gene. J Virol 1982; 43(2):403-409.

(38) Ahn BY, Gershon PD, Jones EV, Moss B. Identification of rpo30, a vaccinia virus RNA polymerase gene with structural similarity to a eucaryotic transcription elongation factor. Mol Cell Biol 1990; 10(10):5433-5441.

(39) Kotwal GJ, Hügin AW, Moss B. Mapping and insertional mutagenesis of a vaccinia virus gene encoding a 13,800-Da secreted protein. Virology 1989; 171(2):579-587.

(40) Moore JB, Smith GL. Steroid hormone synthesis by a vaccinia enzyme: a new type of virus virulence factor. EMBO J 1992; 11(9):-3490.

(41) Davison AJ, Moss B. Structure of vaccinia virus early promoters. J Mol Biol 1989; 210(4):749-769.

(42) Broyles SS, Moss B. DNA-dependent ATPase activity associated with vaccinia virus early transcription factor. J Biol Chem 1988; 263(22):10761-10765.

(43) Ahn BY, Moss B. RNA polymerase-associated transcription specificity factor encoded by vaccinia virus. Proc Natl Acad Sci U S A 1992; 89(8):3536-3540.

(44) Deng L, Shuman S. A role for the H4 subunit of vaccinia RNA polymerase in transcription initiation at a viral early promoter. J Biol Chem 1994; 269(19):14323-14328.

(45) Broyles SS, Li J, Moss B. Promoter DNA contacts made by the vaccinia virus early transcription factor. J Biol Chem 1991; 266(23):15539-15544.

(46) Gershon PD, Moss B. Early transcription factor subunits are encoded by vaccinia virus late genes. Proc Natl Acad Sci U S A 1990; 87(11):4401-4405.

(47) Cassetti MA, Moss B. Interaction of the 82-kDa subunit of the vaccinia virus early transcription factor heterodimer with the promoter core sequence directs downstream DNA binding of the 70-kDa subunit. Proc Natl Acad Sci U S A 1996; 93(15):7540-7545.

(48) Ahn BY, Gershon PD, Moss B. RNA polymerase-associated protein Rap94 confers promoter specificity for initiating transcription of vaccinia virus early stage genes. J Biol Chem 1994; 269(10):7552-7557.

(49) Zhang Y, Ahn BY, Moss B. Targeting of a multicomponent transcription apparatus into assembling vaccinia virus particles requires RAP94, an RNA polymerase-associated protein. J Virol 1994; 68(3):1360-1370.

(50) Yuen L, Moss B. Oligonucleotide sequence signaling transcriptional termination of vaccinia virus early genes. Proc Natl Acad Sci U S A 1987; 84(18):6417-6421.

(51) Deng L, Shuman S. Elongation properties of vaccinia virus RNA polymerase: pausing, slippage, 3' end addition, and termination site choice. Biochemistry 1997; 36(50):15892-15899.

(52) Christen LM, Sanders M, Wiler C, Niles EG. Vaccinia virus nucleoside triphosphate phosphohydrolase I is an essential viral early gene transcription termination factor. Virology 1998; 245(2):360-371.

(53) Deng L, Shuman S. Vaccinia NPH-I, a DExH-box ATPase, is the energy coupling factor for mRNA transcription termination. Genes Dev 1998; 12(4):538-546.

(54) Vos JC, Stunnenberg HG. Derepression of a novel class of vaccinia virus genes upon DNA replication. EMBO J 1988; 7(11):3487-3492.

(55) Baldick CJ, Jr., Keck JG, Moss B. Mutational analysis of the core, spacer, and initiator regions of vaccinia virus intermediate-class promoters. J Virol 1992; 66(8):4710-4719.

(56) Broyles SS, Liu X, Zhu M, Kremer M. Transcription factor YY1 is a vaccinia virus late promoter activator. J Biol Chem 1999; 274(50):35662-35667.

(57) Vos JC, Sasker M, Stunnenberg HG. Promoter melting by a stage-specific vaccinia virus transcription factor is independent of the presence of RNA polymerase. Cell 1991; 65(1):105-113.

(58) Vos JC, Sasker M, Stunnenberg HG. Vaccinia virus capping enzyme is a transcription initiation factor. EMBO J 1991; 10(9):2553-2558.

(59) Rosales R, Harris N, Ahn BY, Moss B. Purification and identification of a vaccinia virus-encoded intermediate stage promoter-specific transcription factor that has homology to eukaryotic transcription factor SII (TFIIS) and an additional role as a viral RNA polymerase subunit. J Biol Chem 1994; 269(19):14260-14267.

(60) Rosales R, Sutter G, Moss B. A cellular factor is required for transcription of vaccinia viral intermediate-stage genes. Proc Natl Acad Sci U S A 1994; 91(9):3794-3798.

(61) Sanz P, Moss B. Identification of a transcription factor, encoded by two vaccinia virus early genes, that regulates the intermediate stage of viral gene expression. Proc Natl Acad Sci U S A 1999; 96(6):2692-2697.

(62) Baldick CJ, Jr., Moss B. Characterization and temporal regulation of mRNAs encoded by vaccinia virus intermediate-stage genes. J Virol 1993; 67(6):3515-3527.

(63) Broyles SS, Fesler BS. Vaccinia virus gene encoding a component of the viral early transcription factor. J Virol 1990; 64(4):1523-1529.

(64) Davison AJ, Moss B. Structure of vaccinia virus late promoters. J Mol Biol 1989; 210(4):771-784.

(65) Ahn BY, Moss B. Capped poly(A) leaders of variable lengths at the 5' ends of vaccinia virus late mRNAs. J Virol 1989; 63(1):226-232.

(66) Schwer B, Visca P, Vos JC, Stunnenberg HG. Discontinuous transcription or RNA processing of vaccinia virus late messengers results in a 5' poly(A) leader. Cell 1987; 50(2):163-169.

(67) Wright CF, Moss B. *In vitro* synthesis of vaccinia virus late mRNA containing a 5' poly(A) leader sequence. Proc Natl Acad Sci U S A 1987; 84(24):8883-8887.

(68) Keck JG, Baldick Jr CJ, Moss B. Role of DNA replication in vaccinia virus gene expression: a naked template is required for transcription of three late trans-activator genes. Cell 1990; 61(5):801-809.

(69) Kovacs GR, Moss B. The vaccinia virus H5R gene encodes late gene transcription factor 4: purification, cloning, and overexpression. J Virol 1996; 70(10):6796-6802.

(70) Wright CF, Oswald BW, Dellis S. Vaccinia virus late transcription is activated *in vitro* by cellular heterogeneous nuclear ribonucleoproteins. J Biol Chem 2001; 276(44):40680-40686.

(71) Gunasinghe SK, Hubbs AE, Wright CF. A vaccinia virus late transcription factor with biochemical and molecular identity to a human cellular protein. J Biol Chem 1998; 273(42):27524-27530.

(72) Xiang Y, Latner DR, Niles EG, Condit RC. Transcription elongation activity of the vaccinia virus J3 protein in vivo is independent of poly(A) polymerase stimulation. Virology 2000; 269(2):356-369.

(73) Black EP, Condit RC. Phenotypic characterization of mutants in vaccinia virus gene G2R, a putative transcription elongation factor. J Virol 1996; 70(1):47-54.

(74) Latner DR, Xiang Y, Lewis JI, Condit J, Condit RC. The vaccinia virus bifunctional gene J3 (nucleoside-2'-O-)-methyltransferase and poly(A) polymerase stimulatory factor is implicated as a positive transcription elongation factor by two genetic approaches. Virology 2000; 269(2):345-355.

(75) Xiang Y, Simpson DA, Spiegel J, Zhou A, Silverman RH, Condit RC. The vaccinia virus A18R DNA helicase is a postreplicative negative transcription elongation factor. J Virol 1998; 72(9):7012-7023.

(76) Antczak JB, Patel DD, Ray CA, Ink BS, Pickup DJ. Site-specific RNA cleavage generates the 3' end of a poxvirus late mRNA. Proc Natl Acad Sci U S A 1992; 89(24):12033-12037.

(77) Amegadzie BY, Sisler JR, Moss B. Frame-shift mutations within the vaccinia virus A-type inclusion protein gene. Virology 1992; 186(2):777-782.

(78) D'Costa SM, Antczak JB, Pickup DJ, Condit RC. Post-transcription cleavage generates the 3' end of F17R transcripts in vaccinia virus. Virology 2004; 319(1):1-11.

(79) Balassu TC, Robinson AJ. Orf virus replication in bovine testis cells: kinetics of viral DNA, polypeptide, and infectious virus production and analysis of virion polypeptides. Arch Virol 1987; 97(3-4):267-281.

(80) Prideaux CT, Boyle DB. Fowlpox virus polypeptides: sequential appearance and virion associated polypeptides. Arch Virol 1987; 96(3-4):185-199.

(81) Joklik WK, Becker Y. The replication and coating of vaccinia DNA. J Mol Biol 1964; 10:452-474.

(82) SALZMAN NP. The rate of formation of vaccinia deoxyribonucleic acid and vaccinia virus. Virology 1960; 10:150-152.

(83) Traktman P. Poxviruses: an emerging portrait of biological strategy. Cell 1990; 62(4):621-626.

(84) Pennington TH, Follett EA. Vaccinia virus replication in enucleate BSC-1 cells: particle production and synthesis of viral DNA and proteins. J Virol 1974; 13(2):488-493.

(85) Prescott DM, Kates J, Kirkpatrick JB. Replication of vaccinia virus DNA in enucleated L-cells. J Mol Biol 1971; 59(3):505-508.

(86) Broyles SS. Vaccinia virus encodes a functional dUTPase. Virology 1993; 195(2):863-865.

(87) DUBBS DR, KIT S. ISOLATION AND PROPERTIES OF VACCINIA MUTANTS DEFICIENT IN THYMIDINE KINASE-INDUCING ACTIVITY. Virology 1964; 22:214-225.

(88) Weir JP, Bajszy G, Moss B. Mapping of the vaccinia virus thymidine kinase gene by marker rescue and by cell-free translation of selected mRNA. Proc Natl Acad Sci U S A 1982; 79(4):1210-1214.

(89) Slabaugh M, Roseman N, Davis R, Mathews C. Vaccinia virus-encoded ribonucleotide reductase: sequence conservation of the gene for the small subunit and its amplification in hydroxyurea-resistant mutants. J Virol 1988; 62(2):519-527.

(90) Tengelsen LA, Slabaugh MB, Bibler JK, Hruby DE. Nucleotide sequence and molecular genetic analysis of the large subunit of ribonucleotide reductase encoded by vaccinia virus. Virology 1988; 164(1):121-131.

(91) Child SJ, Palumbo GJ, Buller RM, Hruby DE. Insertional inactivation of the large subunit of ribonucleotide reductase encoded by vaccinia virus is associated with reduced virulence *in vivo*. Virology 1990; 174(2):625-629.

(92) Buller RM, Smith GL, Cremer K, Notkins AL, Moss B. Decreased virulence of recombinant vaccinia virus expression vectors is associated with a thymidine kinase-negative phenotype. Nature 1985; 317(6040):813-815.

(93) Challberg MD, Englund PT. Purification and properties of the deoxyribonucleic acid polymerase induced by vaccinia virus. J Biol Chem 1979; 254(16):7812-7819.

(94) Ishii K, Moss B. Role of vaccinia virus A20R protein in DNA replication: construction and characterization of temperature-sensitive mutants. J Virol 2001; 75(4):1656-1663.

(95) Rochester SC, Traktman P. Characterization of the single-stranded DNA binding protein encoded by the vaccinia virus I3 gene. J Virol 1998; 72(4):2917-2926.

(96) Shaffer R, Traktman P. Vaccinia virus encapsidates a novel topoisomerase with the properties of a eucaryotic type I enzyme. J Biol Chem 1987; 262(19):9309-9315.

(97) Shuman S, Moss B. Identification of a vaccinia virus gene encoding a type I DNA topoisomerase. Proc Natl Acad Sci U S A 1987; 84(21):7478-7482.

(98) Millns AK, Carpenter MS, DeLange AM. The vaccinia virus-encoded uracil DNA glycosylase has an essential role in viral DNA replication. Virology 1994; 198(2):504-513.

(99) Evans E, Traktman P. Molecular genetic analysis of a vaccinia virus gene with an essential role in DNA replication. J Virol 1987; 61(10):3152-3162.

(100) Roseman NA, Hruby DE. Nucleotide sequence and transcript organization of a region of the vaccinia virus genome which encodes a constitutively expressed gene required for DNA replication. J Virol 1987; 61(5):1398-1406.

(101) Rempel RE, Anderson MK, Evans E, Traktman P. Temperature-sensitive vaccinia virus mutants identify a gene with an essential role in viral replication. J Virol 1990; 64(2):574-583.

(102) Garcia AD, Aravind L, Koonin EV, Moss B. Bacterial-type DNA holliday junction resolvases in eukaryotic viruses. Proc Natl Acad Sci U S A 2000; 97(16):8926-8931.

(103) Du S, Traktman P. Vaccinia virus DNA replication: two hundred base pairs of telomeric sequence confer optimal replication efficiency on minichromosome templates. Proc Natl Acad Sci U S A 1996; 93(18):9693-9698.

(104) DeLange AM. Identification of temperature-sensitive mutants of vaccinia virus that are defective in conversion of concatemeric replicative intermediates to the mature linear DNA genome. J Virol 1989; 63(6):2437-2444.

(105) Merchlinsky M, Moss B. Resolution of vaccinia virus DNA concatemer junctions requires late-gene expression. J Virol 1989; 63(4):1595-1603.

(106) Palaniyar N, Fisher C, Parks R, Evans DH. SFV topoisomerase: sequence specificity in a genetically mapped interval. Virology 1996; 221(2):351-354.

(107) Sekiguchi J, Seeman NC, Shuman S. Resolution of Holliday junctions by eukaryotic DNA topoisomerase I. Proc Natl Acad Sci U S A 1996; 93(2):785-789.

(108) Fenner F. The biological characters of several strains of vaccinia, cowpox and rabbitpox viruses. Virology 1958; 5(3):502-529.

(109) Merchlinsky M. Intramolecular homologous recombination in cells infected with temperature-sensitive mutants of vaccinia virus. J Virol 1989; 63(5):2030-2035.

(110) Odom MR, Hendrickson RC, Lefkowitz EJ. Poxvirus protein evolution: family wide assessment of possible horizontal gene transfer events. Virus Res 2009; 144(1-2):233-249.

(111) Strayer DS, Sell S. Immunohistology of malignant rabbit fibroma virus--a comparative study with rabbit myxoma virus. J Natl Cancer Inst 1983; 71(1):105-116.

(112) Strayer DS, Cabirac G, Sell S, Leibowitz JL. Malignant rabbit fibroma virus: observations on the culture and histopathologic characteristics of a new virus-induced rabbit tumor. J Natl Cancer Inst 1983; 71(1):91-104.

(113) Upton C, McFadden G. Tumorigenic poxviruses: analysis of viral DNA sequences implicated in the tumorigenicity of Shope fibroma virus and malignant rabbit virus. Virology 1986; 152(2):308-321.

(114) Nakano E, Panicali D, Paoletti E. Molecular genetics of vaccinia virus: demonstration of marker rescue. Proc Natl Acad Sci U S A 1982; 79(5):1593-1596.

(115) Moss B. Vaccinia virus: a tool for research and vaccine development. Science 1991; 252(5013):1662-1667.

(116) Ulaeto D, Grosenbach D, Hruby DE. The vaccinia virus 4c and A-type inclusion proteins are specific markers for the intracellular mature virus particle. J Virol 1996; 70(6):3372-3377.

(117) Blasco R, Moss B. Extracellular vaccinia virus formation and cell-to-cell virus transmission are prevented by deletion of the gene encoding the 37,000-Dalton outer envelope protein. J Virol 1991; 65(11):5910-5920.

(118) Engelstad M, Smith GL. The vaccinia virus 42-kDa envelope protein is required for the envelopment and egress of extracellular virus and for virus virulence. Virology 1993; 194(2):627-637.

(119) Wolffe EJ, Isaacs SN, Moss B. Deletion of the vaccinia virus B5R gene encoding a 42-kilodalton membrane glycoprotein inhibits extracellular virus envelope formation and dissemination. J Virol 1993; 67(8):4732-4741.

(120) Payne LG. Significance of extracellular enveloped virus in the *in vitro* and *in vivo* dissemination of vaccinia. J Gen Virol 1980; 50(1):89-100.

(121) Vanderplasschen A, Smith GL. A novel virus binding assay using confocal microscopy: demonstration that the intracellular and extracellular vaccinia virions bind to different cellular receptors. J Virol 1997; 71(5):4032-4041.

(122) Senkevich TG, Moss B. Vaccinia virus H2 protein is an essential component of a complex involved in virus entry and cell-cell fusion. J Virol 2005; 79(8):4744-4754.

(123) Law M, Carter GC, Roberts KL, Hollinshead M, Smith GL. Ligand-induced and nonfusogenic dissolution of a viral membrane. Proc Natl Acad Sci U S A 2006; 103(15):5989-5994.

(124) Senkevich TG, Ward BM, Moss B. Vaccinia virus entry into cells is dependent on a virion surface protein encoded by the A28L gene. J Virol 2004; 78(5):2357-2366.

(125) Carter GC, Law M, Hollinshead M, Smith GL. Entry of the vaccinia virus intracellular mature virion and its interactions with glycosaminoglycans. J Gen Virol 2005; 86(Pt 5):1279-1290.

(126) Townsley AC, Weisberg AS, Wagenaar TR, Moss B. Vaccinia virus entry into cells via a low-pH-dependent endosomal pathway. J Virol 2006; 80(18):8899-8908.

(127) Townsley AC, Moss B. Two distinct low-pH steps promote entry of vaccinia virus. J Virol 2007; 81(16):8613-8620.

(128) Bengali Z, Townsley AC, Moss B. Vaccinia virus strain differences in cell attachment and entry. Virology 2009; 389(1-2):132-140.

(129) Mercer J, Helenius A. Vaccinia virus uses macropinocytosis and apoptotic mimicry to enter host cells. Science 2008; 320(5875):531-535.

(130) Chung CS, Hsiao JC, Chang YS, Chang W. A27L protein mediates vaccinia virus interaction with cell surface heparan sulfate. J Virol 1998; 72(2):1577-1585.

(131) Hsiao JC, Chung CS, Chang W. Cell surface proteoglycans are necessary for A27L protein-mediated cell fusion: identification of the N-terminal region of A27L protein as the glycosaminoglycan-binding domain. J Virol 1998; 72(10):8374-8379.

(132) Hsiao JC, Chung CS, Chang W. Vaccinia virus envelope D8L protein binds to cell surface chondroitin sulfate and mediates the adsorption of intracellular mature virions to cells. J Virol 1999; 73(10):8750-8761.

(133) Lin CL, Chung CS, Heine HG, Chang W. Vaccinia virus envelope H3L protein binds to cell surface heparan sulfate and is important for intracellular mature virion morphogenesis and virus infection *in vitro* and *in vivo*. J Virol 2000; 74(7):3353-3365.

(134) Chiu WL, Lin CL, Yang MH, Tzou DL, Chang W. Vaccinia virus 4c (A26L) protein on intracellular mature virus binds to the extracellular cellular matrix laminin. J Virol 2007; 81(5):2149-2157.

(135) Foo CH, Lou H, Whitbeck JC, Ponce-de-León M, Atanasiu D, Eisenberg RJ et al. Vaccinia virus L1 binds to cell surfaces and blocks virus entry independently of glycosaminoglycans. Virology 2009; 385(2):368-382.

(136) McIntosh AA, Smith GL. Vaccinia virus glycoprotein A34R is required for infectivity of extracellular enveloped virus. J Virol 1996; 70(1):272-281.

(137) Bisht H, Weisberg AS, Moss B. Vaccinia virus I1 protein is required for cell entry and membrane fusion. J Virol 2008; 82(17):8687-8694.

(138) Brown E, Senkevich TG, Moss B. Vaccinia virus F9 virion membrane protein is required for entry but not virus assembly, in contrast to the related L1 protein. J Virol 2006; 80(19):9455-9464.

(139) Izmailyan RA, Huang CY, Mohammad S, Isaacs SN, Chang W. The envelope G3L protein is essential for entry of vaccinia virus into host cells. J Virol 2006; 80(17):8402-8410.

(140) Nichols RJ, Stanitsa E, Unger B, Traktman P. The vaccinia virus gene I2L encodes a membrane protein with an essential role in virion entry. J Virol 2008; 82(20):10247-10261.

(141) Ojeda S, Domi A, Moss B. Vaccinia virus G9 protein is an essential component of the poxvirus entry-fusion complex. J Virol 2006; 80(19):9822-9830.

(142) Ojeda S, Senkevich TG, Moss B. Entry of vaccinia virus and cell-cell fusion require a highly conserved cysteine-rich membrane protein encoded by the A16L gene. J Virol 2006; 80(1):51-61.

(143) Satheshkumar PS, Moss B. Characterization of a newly identified 35-amino-acid component of the vaccinia virus entry/fusion complex conserved in all chordopoxviruses. J Virol 2009; 83(24):12822-12832.

(144) Townsley AC, Senkevich TG, Moss B. Vaccinia virus A21 virion membrane protein is required for cell entry and fusion. J Virol 2005; 79(15):9458-9469.

(145) Townsley AC, Senkevich TG, Moss B. The product of the vaccinia virus L5R gene is a fourth membrane protein encoded by all poxviruses that is required for cell entry and cell-cell fusion. J Virol 2005; 79(17):10988-10998.

(146) Senkevich TG, Ojeda S, Townsley A, Nelson GE, Moss B. Poxvirus multiprotein entry-fusion complex. Proc Natl Acad Sci U S A 2005; 102(51):18572-18577.

(147) Upton C, Slack S, Hunter AL, Ehlers A, Roper RL. Poxvirus orthologous clusters: toward defining the minimum essential poxvirus genome. J Virol 2003; 77(13):7590-7600.

(148) Wagenaar TR, Moss B. Association of vaccinia virus fusion regulatory proteins with the multicomponent entry/fusion complex. J Virol 2007; 81(12):6286-6293.

(149) Wagenaar TR, Ojeda S, Moss B. Vaccinia virus A56/K2 fusion regulatory protein interacts with the A16 and G9 subunits of the entry fusion complex. J Virol 2008; 82(11):5153-5160.

(150) Tolonen N, Doglio L, Schleich S, Krijnse LJ. Vaccinia virus DNA replication occurs in endoplasmic reticulum-enclosed cytoplasmic mini-nuclei. Mol Biol Cell 2001; 12(7):2031-2046.

(151) Moss B. Regulation of vaccinia virus transcription. Annu Rev Biochem 1990; 59:661-688.

(152) Dales S, Mosbach EH. Vaccinia as a model for membrane biogenesis. Virology 1968; 35(4):564-583.

(153) Hollinshead M, Vanderplasschen A, Smith GL, Vaux DJ. Vaccinia virus intracellular mature virions contain only one lipid membrane. J Virol 1999; 73(2):1503-1517.

(154) Sodeik B, Doms RW, Ericsson M, Hiller G, Machamer CE, van 't Hof W et al. Assembly of vaccinia virus: role of the intermediate compartment between the endoplasmic reticulum and the Golgi stacks. J Cell Biol 1993; 121(3):521-541.

(155) Rodriguez D, Byena M, Möbius W, Schleich S, Esteban M, Geerts WJ et al. A vaccinia virus lacking A10L: viral core proteins accumulate on structures derived from the endoplasmic reticulum. Cell Microbiol 2006; 8(3):427-437.

(156) Grimley PM, Rosenblum EN, Mims SJ, Moss B. Interruption by Rifampin of an early stage in vaccinia virus morphogenesis: accumulation of membranes which are precursors of virus envelopes. J Virol 1970; 6(4):519-533.

(157) da Fonseca FG, Weisberg AS, Caeiro MF, Moss B. Vaccinia virus mutants with alanine substitutions in the conserved G5R gene fail to initiate morphogenesis at the nonpermissive temperature. J Virol 2004; 78(19):10238-10248.

(158) DeMasi J, Traktman P. Clustered charge-to-alanine mutagenesis of the vaccinia virus H5 gene: isolation of a dominant, temperature-sensitive mutant with a profound defect in morphogenesis. J Virol 2000; 74(5):2393-2405.

(159) Resch W, Weisberg AS, Moss B. Vaccinia virus nonstructural protein encoded by the A11R gene is required for formation of the virion membrane. J Virol 2005; 79(11):6598-6609.

(160) Traktman P, Caligiuri A, Jesty SA, Liu K, Sankar U. Temperature-sensitive mutants with lesions in the vaccinia virus F10 kinase undergo arrest at the earliest stage of virion morphogenesis. J Virol 1995; 69(10):6581-6587.

(161) Wang S, Shuman S. Vaccinia virus morphogenesis is blocked by temperature-sensitive mutations in the F10 gene, which encodes protein kinase 2. J Virol 1995; 69(10):6376-6388.

(162) Black EP, Moussatche N, Condit RC. Characterization of the interactions among vaccinia virus transcription factors G2R, A18R, and H5R. Virology 1998; 245(2):313-322.

(163) Ishii K, Moss B. Mapping interaction sites of the A20R protein component of the vaccinia virus DNA replication complex. Virology 2002; 303(2):232-239.

(164) McCraith S, Holtzman T, Moss B, Fields S. Genome-wide analysis of vaccinia virus protein-protein interactions. Proc Natl Acad Sci U S A 2000; 97(9):4879-4884.

(165) Beaud G, Beaud R, Leader DP. Vaccinia virus gene H5R encodes a protein that is phosphorylated by the multisubstrate vaccinia virus B1R protein kinase. J Virol 1995; 69(3):1819-1826.

(166) Beaud G, Beaud R. Temperature-dependent phosphorylation state of the H5R protein synthesised at the early stage of infection in cells infected with vaccinia virus ts mutants of the B1R and F10L protein kinases. Intervirology 2000; 43(1):67-70.

(167) Brown NG, Nick MD, Beaud G, Hardie G, Leader DP. Identification of sites phosphorylated by the vaccinia virus B1R kinase in viral protein H5R. BMC Biochem 2000; 1:-2.

(168) Lin S, Broyles SS. Vaccinia protein kinase 2: a second essential serine/threonine protein kinase encoded by vaccinia virus. Proc Natl Acad Sci U S A 1994; 91(16):7653-7657.

(169) Krijnse-Locker J, Schleich S, Rodriguez D, Goud B, Snijder EJ, Griffiths G. The role of a 21-kDa viral membrane protein in the assembly of vaccinia virus from the intermediate compartment. J Biol Chem 1996; 271(25):14950-14958.

(170) Rodriguez D, Rodriguez JR, Esteban M. The vaccinia virus 14-kilodalton fusion protein forms a stable complex with the processed protein encoded by the vaccinia virus A17L gene. J Virol 1993; 67(6):3435-3440.

(171) Salmons T, Kuhn A, Wylie F, Schleich S, Rodriguez JR, Rodriguez D et al. Vaccinia virus membrane proteins p8 and p16 are cotranslationally inserted into the rough endoplasmic reticulum and retained in the intermediate compartment. J Virol 1997; 71(10):7404-7420.

(172) Wolffe EJ, Moore DM, Peters PJ, Moss B. Vaccinia virus A17L open reading frame encodes an essential component of nascent viral membranes that is required to initiate morphogenesis. J Virol 1996; 70(5):2797-2808.

(173) Traktman P, Liu K, DeMasi J, Rollins R, Jesty S, Unger B. Elucidating the essential role of the A14 phosphoprotein in vaccinia virus morphogenesis: construction and characterization of a tetracycline-inducible recombinant. J Virol 2000; 74(8):3682-3695.

(174) Rodriguez JR, Risco C, Carrascosa JL, Esteban M, Rodriguez D. Characterization of early stages in vaccinia virus membrane biogenesis: implications of the 21-kilodalton protein and a newly identified 15-kilodalton envelope protein. J Virol 1997; 71(3):1821-1833.

(175) Rodriguez JR, Risco C, Carrascosa JL, Esteban M, Rodriguez D. Vaccinia virus 15-kilodalton (A14L) protein is essential for assembly and attachment of viral crescents to virosomes. J Virol 1998; 72(2):1287-1296.

(176) Rodriguez D, Esteban M, Rodriguez JR. Vaccinia virus A17L gene product is essential for an early step in virion morphogenesis. J Virol 1995; 69(8):4640-4648.

(177) Rodriguez D, Risco C, Rodriguez JR, Carrascosa JL, Esteban M. Inducible expression of the vaccinia virus A17L gene provides a synchronized system to monitor sorting of viral proteins during morphogenesis. J Virol 1996; 70(11):7641-7653.

(178) Betakova T, Wolffe EJ, Moss B. Membrane topology of the vaccinia virus A17L envelope protein. Virology 1999; 261(2):347-356.

(179) Mercer J, Traktman P. Investigation of structural and functional motifs within the vaccinia virus A14 phosphoprotein, an essential component of the virion membrane. J Virol 2003; 77(16):8857-8871.

(180) Blasco R, Sisler JR, Moss B. Dissociation of progeny vaccinia virus from the cell membrane is regulated by a viral envelope glycoprotein: effect of a point mutation in the lectin homology domain of the A34R gene. J Virol 1993; 67(6):3319-3325.

(181) Payne LG. Identification of the vaccinia hemagglutinin polypeptide from a cell system yielding large amounts of extracellular enveloped virus. J Virol 1979; 31(1):147-155.

(182) Meiser A, Sancho C, Krijnse LJ. Plasma membrane budding as an alternative release mechanism of the extracellular enveloped form of vaccinia virus from HeLa cells. J Virol 2003; 77(18):9931-9942.

(183) Boulanger D, Smith T, Skinner MA. Morphogenesis and release of fowlpox virus. J Gen Virol 2000; 81(Pt 3):675-687.

(184) Ichihashi Y, Matsumoto S. Studies on the nature of Marchal bodies (A-type inclusion) during ectromelia virus infection. Virology 1966; 29(2):264-275.

(185) Patel DD, Pickup DJ, Joklik WK. Isolation of cowpox virus A-type inclusions and characterization of their major protein component. Virology 1986; 149(2):174-189.

(186) Sadasiv EC, Chang PW, Gulka G. Morphogenesis of canary poxvirus and its entrance into inclusion bodies. Am J Vet Res 1985; 46(2):529-535.

(187) RANDALL CC, GAFFORD LG. Histochemical andbiochemical studies of isolated viral inclusions. Am J Pathol 1962; 40:51-62.

(188) McKelvey TA, Andrews SC, Miller SE, Ray CA, Pickup DJ. Identification of the Orthopoxvirus p4c Gene, Which Encodes a Structural Protein That Directs Intracellular Mature Virus Particles into A-Type Inclusions. J Virol 2002; 76(22):11216-11225.

(189) Smith GL, Vanderplasschen A, Law M. The formation and function of extracellular enveloped vaccinia virus. J Gen Virol 2002; 83(Pt 12):2915-2931.

(190) Payne L. Polypeptide composition of extracellular enveloped vaccinia virus. J Virol 1978; 27(1):28-37.

(191) Duncan SA, Smith GL. Identification and characterization of an extracellular envelope glycoprotein affecting vaccinia virus egress. J Virol 1992; 66(3):1610-1621.

(192) Engelstad M, Howard ST, Smith GL. A constitutively expressed vaccinia gene encodes a 42-kDa glycoprotein related to complement control factors that forms part of the extracellular virus envelope. Virology 1992; 188(2):801-810.

(193) Hirt P, Hiller G, Wittek R. Localization and fine structure of a vaccinia virus gene encoding an envelope antigen. J Virol 1986; 58(3):757-764.

(194) Isaacs SN, Kotwal GJ, Moss B. Vaccinia virus complement-control protein prevents antibody-dependent complement-enhanced neutralization of infectivity and contributes to virulence. Proc Natl Acad Sci U S A 1992; 89(2):628-632.

(195) Payne LG. Characterization of vaccinia virus glycoproteins by monoclonal antibody precipitation. Virology 1992; 187(1):251-260.

(196) Roper RL, Payne LG, Moss B. Extracellular vaccinia virus envelope glycoprotein encoded by the A33R gene. J Virol 1996; 70(6):3753-3762.

(197) Shida H. Nucleotide sequence of the vaccinia virus hemagglutinin gene. Virology 1986; 150(2):451-462.

(198) van Eijl H, Hollinshead M, Rodger G, Zhang WH, Smith GL. The vaccinia virus F12L protein is associated with intracellular enveloped virus particles and is required for their egress to the cell surface. J Gen Virol 2002; 83(Pt 1):195-207.

(199) Zhang WH, Wilcock D, Smith GL. Vaccinia virus F12L protein is required for actin tail formation, normal plaque size, and virulence. J Virol 2000; 74(24):11654-11662.

(200) Parkinson JE, Smith GL. Vaccinia virus gene A36R encodes a M(r) 43-50 K protein on the surface of extracellular enveloped virus. Virology 1994; 204(1):376-390.

(201) van Eijl H, Hollinshead M, Smith GL. The vaccinia virus A36R protein is a type Ib membrane protein present on intracellular but not extracellular enveloped virus particles. Virology 2000; 271(1):26-36.

(202) Grosenbach DW, Hansen SG, Hruby DE. Identification and analysis of vaccinia virus palmitylproteins. Virology 2000; 275(1):193-206.

(203) Koonin EV. A duplicated catalytic motif in a new superfamily of phosphohydrolases and phospholipid synthases that includes poxvirus envelope proteins. Trends Biochem Sci 1996; 21(7):242-243.

(204) Ponting CP, Kerr ID. A novel family of phospholipase D homologues that includes phospholipid synthases and putative endonucleases: identification of duplicated repeats and potential active site residues. Protein Sci 1996; 5(5):914-922.

(205) Sung TC, Roper RL, Zhang Y, Rudge SA, Temel R, Hammond SM et al. Mutagenesis of phospholipase D defines a superfamily including a trans-Golgi viral protein required for poxvirus pathogenicity. EMBO J 1997; 16(15):4519-4530.

(206) Baek SH, Kwak JY, Lee SH, Lee T, Ryu SH, Uhlinger DJ et al. Lipase activities of p37, the major envelope protein of vaccinia virus. J Biol Chem 1997; 272(51):32042-32049.

(207) Bednarek SY, Orci L, Schekman R. Traffic COPs and the formation of vesicle coats. Trends Cell Biol 1996; 6(12):468-473.

(208) Colley WC, Sung TC, Roll R, Jenco J, Hammond SM, Altshuller Y et al. Phospholipase D2, a distinct phospholipase D isoform with novel regulatory properties that provokes cytoskeletal reorganization. Curr Biol 1997; 7(3):191-201.

(209) Husain M, Moss B. Vaccinia virus F13L protein with a conserved phospholipase catalytic motif induces colocalization of the B5R envelope glycoprotein in post-Golgi vesicles. J Virol 2001; 75(16):7528-7542.

(210) Schmutz C, Wittek R. Release of extracellular particles by recombinant vaccinia virus over-expressing the major envelope protein p37K. J Gen Virol 1995; 76 (Pt 12):2963-2968.

(211) Isaacs SN, Wolffe EJ, Payne LG, Moss B. Characterization of a vaccinia virus-encoded 42-kilodalton class I membrane glycoprotein component of the extracellular virus envelope. J Virol 1992; 66(12):7217-7224.

(212) Martinez-Pomares L, Stern RJ, Moyer RW. The ps/hr gene (B5R open reading frame homolog) of rabbitpox virus controls pock color, is a component of extracellular enveloped virus, and is secreted into the medium. J Virol 1993; 67(9):5450-5462.

(213) Röttger S, Frischknecht F, Reckmann I, Smith GL, Way M. Interactions between vaccinia virus IEV membrane proteins and their roles in IEV assembly and actin tail formation. J Virol 1999; 73(4):2863-2875.

(214) Perdiguero B, Blasco R. Interaction between vaccinia virus extracellular virus envelope A33 and B5 glycoproteins. J Virol 2006; 80(17):8763-8777.

(215) Hollinshead M, Rodger G, van Eijl H, Law M, Hollinshead R, Vaux DJ et al. Vaccinia virus utilizes microtubules for movement to the cell surface. J Cell Biol 2001; 154(2):389-402.

(216) Katz E, Wolffe EJ, Moss B. The cytoplasmic and transmembrane domains of the vaccinia virus B5R protein target a chimeric human immunodeficiency virus type 1 glycoprotein to the outer envelope of nascent vaccinia virions. J Virol 1997; 71(4):3178-3187.

(217) Ward BM, Moss B. Golgi network targeting and plasma membrane internalization signals in vaccinia virus B5R envelope protein. J Virol 2000; 74(8):3771-3780.

(218) Takahashi-Nishimaki F, Funahashi S, Miki K, Hashizume S, Sugimoto M. Regulation of plaque size and host range by a vaccinia virus gene related to complement system proteins. Virology 1991; 181(1):158-164.

(219) Aldaz-Carroll L, Whitbeck JC, Ponce de LM, Lou H, Hirao L, Isaacs SN et al. Epitope-mapping studies define two major neutralization sites on the vaccinia virus extracellular enveloped virus glycoprotein B5R. J Virol 2005; 79(10):6260-6271.

(220) Johnston SC, Ward BM. Vaccinia virus protein F12 associates with intracellular enveloped virions through an interaction with A36. J Virol 2009; 83(4):1708-1717.

(221) Dodding MP, Newsome TP, Collinson LM, Edwards C, Way M. An E2-F12 complex is required for IEV morphogenesis during vaccinia infection. Cell Microbiol 2009; 11(5):808-824.

(222) Ichihashi Y, Matsumoto S, Dales S. Biogenesis of poxviruses: role of A-type inclusions and host cell membranes in virus dissemination. Virology 1971; 46(3):507-532.

(223) Rietdorf J, Ploubidou A, Reckmann I, Holmström A, Frischknecht F, Zettl M et al. Kinesin-dependent movement on microtubules precedes actin-based motility of vaccinia virus. Nat Cell Biol 2001; 3(11):992-1000.

(224) Roper RL, Wolffe EJ, Weisberg A, Moss B. The envelope protein encoded by the A33R gene is required for formation of actin-containing microvilli and efficient cell-to-cell spread of vaccinia virus. J Virol 1998; 72(5):4192-4204.

(225) Wolffe EJ, Weisberg AS, Moss B. The vaccinia virus A33R protein provides a chaperone function for viral membrane localization and tyrosine phosphorylation of the A36R protein. J Virol 2001; 75(1):303-310.

(226) Sanderson CM, Frischknecht F, Way M, Hollinshead M, Smith GL. Roles of vaccinia virus EEV-specific proteins in intracellular actin tail formation and low pH-induced cell-cell fusion. J Gen Virol 1998; 79 (Pt 6):1415-1425.

(227) Ichihashi Y, Dales S. Biogenesis of poxviruses: interrelationship between hemagglutinin production and polykaryocytosis. Virology 1971; 46(3):533-543.

(228) Turner PC, Moyer RW. The cowpox virus fusion regulator proteins SPI-3 and hemagglutinin interact in infected and uninfected cells. Virology 2006; 347(1):88-99.

(229) Wagenaar TR, Moss B. Expression of the A56 and K2 proteins is sufficient to inhibit vaccinia virus entry and cell fusion. J Virol 2009; 83(4):1546-1554.

(230) Turner PC, Moyer RW. The vaccinia virus fusion inhibitor proteins SPI-3 (K2) and HA (A56) expressed by infected cells reduce the entry of superinfecting virus. Virology 2008; 380(2):226-233.

(231) Arif BM. Recent advances in the molecular biology of entomopoxviruses. J Gen Virol 1995; 76 (Pt 1):1-13.

(232) Rohrmann GF, National Center for Biotechnology Information (. Baculovirus molecular biology [electronic resource] / G.F. Rohrmann.

(233) Butler-Cole C, Wagner MJ, Da SM, Brown GD, Burke RD, Upton C. An ectromelia virus profilin homolog interacts with cellular tropomyosin and viral A-type inclusion protein. Virol J 2007; 4:-76.

(234) Willer DO, McFadden G, Evans DH. The complete genome sequence of shope (rabbit) fibroma virus. Virology 1999; 264(2):319-343.

(235) Lee HJ, Essani K, Smith GL. The genome sequence of Yaba-like disease virus, a yatapoxvirus. Virology 2001; 281(2):170-192.

(236) Stern W, Dales S. Biogenesis of vaccinia: isolation and characterization of a surface component that elicits antibody suppressing infectivity and cell-cell fusion. Virology 1976; 75(1):232-241.

(237) Stern W, Dales S. Biogenesis of vaccinia: relationship of the envelope to virus assembly. Virology 1976; 75(1):242-255.

(238) Ichihashi Y, Oie M. Adsorption and penetration of the trypsinized vaccinia virion. Virology 1980; 101(1):50-60.

(239) Ichihashi Y, Tsuruhara T, Oie M. The effect of proteolytic enzymes on the infectivity of vaccinia virus. Virology 1982; 122(2):279-289.

(240) Chung CS, Chen CH, Ho MY, Huang CY, Liao CL, Chang W. Vaccinia virus proteome: identification of proteins in vaccinia virus intracellular mature virion particles. J Virol 2006; 80(5):2127-2140.

(241) Jensen ON, Houthaeve T, Shevchenko A, Cudmore S, Ashford T, Mann M et al. Identification of the major membrane and core proteins of vaccinia virus by two-dimensional electrophoresis. J Virol 1996; 70(11):7485-7497.

(242) Saarloos MN, Sullivan BL, Czerniewski MA, Parameswar KD, Spear GT. Detection of HLA-DR associated with monocytotropic, primary, and plasma isolates of human immunodeficiency virus type 1. J Virol 1997; 71(2):1640-1643.

(243) Saifuddin M, Parker CJ, Peeples ME, Gorny MK, Zolla-Pazner S, Ghassemi M et al. Role of virion-associated glycosylphosphatidylinositol-linked proteins CD55 and CD59 in complement resistance of cell line-derived and primary isolates of HIV-1. J Exp Med 1995; 182(2):501-509.

(244) Saifuddin M, Hedayati T, Atkinson JP, Holguin MH, Parker CJ, Spear GT. Human immunodeficiency virus type 1 incorporates both glycosyl phosphatidylinositol-anchored CD55 and CD59 and integral membrane CD46 at levels that protect from complement-mediated destruction. J Gen Virol 1997; 78 (Pt 8):1907-1911.

(245) Spear GT, Lurain NS, Parker CJ, Ghassemi M, Payne GH, Saifuddin M. Host cell-derived complement control proteins CD55 and CD59 are incorporated into the virions of two unrelated enveloped viruses. Human T cell leukemia/lymphoma virus

type I (HTLV-I) and human cytomegalovirus (HCMV). J Immunol 1995; 155(9):4376-4381.

(246) Krauss O, Hollinshead R, Hollinshead M, Smith GL. An investigation of incorporation of cellular antigens into vaccinia virus particles. J Gen Virol 2002; 83(Pt 10):2347-2359.

(247) Vanderplasschen A, Mathew E, Hollinshead M, Sim RB, Smith GL. Extracellular enveloped vaccinia virus is resistant to complement because of incorporation of host complement control proteins into its envelope. Proc Natl Acad Sci U S A 1998; 95(13):7544-7549.

(248) Castro AP, Carvalho TM, Moussatché N, Damaso CR. Redistribution of cyclophilin A to viral factories during vaccinia virus infection and its incorporation into mature particles. J Virol 2003; 77(16):9052-9068.

(249) Webb JH, Mayer RJ, Dixon LK. A lipid modified ubiquitin is packaged into particles of several enveloped viruses. FEBS Lett 1999; 444(1):136-139.

(250) Franke CA, Hruby DE. Association of non-viral proteins with recombinant vaccinia virus virions. Arch Virol 1987; 94(3-4):347-351.

(251) Johnston JB, McFadden G. Poxvirus immunomodulatory strategies: current perspectives. J Virol 2003; 77(11):6093-6100.

(252) Guerin JL, Gelfi J, Boullier S, Delverdier M, Bellanger FA, Bertagnoli S et al. Myxoma virus leukemia-associated protein is responsible for major histocompatibility complex class I and Fas-CD95 down-regulation and defines scrapins, a new group of surface cellular receptor abductor proteins. J Virol 2002; 76(6):2912-2923.

(253) Früh K, Bartee E, Gouveia K, Mansouri M. Immune evasion by a novel family of viral PHD/LAP-finger proteins of gamma-2 herpesviruses and poxviruses. Virus Res 2002; 88(1-2):55-69.

(254) Smith CA, Davis T, Wignall JM, Din WS, Farrah T, Upton C et al. T2 open reading frame from the Shope fibroma virus encodes a soluble form of the TNF receptor. Biochem Biophys Res Commun 1991; 176(1):335-342.

(255) Upton C, Macen JL, Schreiber M, McFadden G. Myxoma virus expresses a secreted protein with homology to the tumor necrosis factor receptor gene family that contributes to viral virulence. Virology 1991; 184(1):370-382.

(256) Smith GL, Chan YS. Two vaccinia virus proteins structurally related to the interleukin-1 receptor and the immunoglobulin superfamily. J Gen Virol 1991; 72 (Pt 3):511-518.

(257) Paez E, Esteban M. Resistance of vaccinia virus to interferon is related to an interference phenomenon between the virus and the interferon system. Virology 1984; 134(1):12-28.

(258) Kotwal GJ, Moss B. Vaccinia virus encodes a secretory polypeptide structurally related to complement control proteins. Nature 1988; 335(6186):176-178.

(259) Chang HW, Watson JC, Jacobs BL. The E3L gene of vaccinia virus encodes an inhibitor of the interferon-induced, double-stranded RNA-dependent protein kinase. Proc Natl Acad Sci U S A 1992; 89(11):4825-4829.

(260) Davies MV, Chang HW, Jacobs BL, Kaufman RJ. The E3L and K3L vaccinia virus gene products stimulate translation through inhibition of the double-stranded RNA-dependent protein kinase by different mechanisms. J Virol 1993; 67(3):1688-1692.

(261) Arness MK, Eckart RE, Love SS, Atwood JE, Wells TS, Engler RJ et al. Myopericarditis following smallpox vaccination. Am J Epidemiol 2004; 160(7):642-651.

(262) Update: cardiac-related events during the civilian smallpox vaccination program--United States, 2003. MMWR Morb Mortal Wkly Rep 2003; 52(21):492-496.

(263) Cardiac adverse events following smallpox vaccination--United States, 2003. MMWR Morb Mortal Wkly Rep 2003; 52(12):248-250.

(264) Artenstein AW, Johnson C, Marbury TC, Morrison D, Blum PS, Kemp T et al. A novel, cell culture-derived smallpox vaccine in vaccinia-naive adults. Vaccine 2005; 23(25):3301-3309.

(265) Monath TP, Caldwell JR, Mundt W, Fusco J, Johnson CS, Buller M et al. ACAM2000 clonal Vero cell culture vaccinia virus (New York City Board of Health strain)--a second-generation smallpox vaccine for biological defense. Int J Infect Dis 2004; 8 Suppl 2:S31-S44.

(266) Greenberg RN, Kennedy JS, Clanton DJ, Plummer EA, Hague L, Cruz J et al. Safety and immunogenicity of new cell-cultured smallpox vaccine compared with calf-lymph derived vaccine: a blind, single-centre, randomised controlled trial. Lancet 2005; 365(9457):398-409.

(267) Poland GA, Grabenstein JD, Neff JM. The US smallpox vaccination program: a review of a large modern era smallpox vaccination implementation program. Vaccine 2005; 23(17-18):2078-2081.

(268) Hashizume S, Yoshizawa H, Morita M, Suzuki K. Properties of attenuated mutant of vaccinia virus, LC16m8, derived from Lister strain. In: Quinnan GV, editor. Vaccinia Virus as Vectors for Vaccine Antigens. Amsterdam, New York & Oxford: Elsevier; 1985. 87-99.

(269) Saito T, Fujii T, Kanatani Y, Saijo M, Morikawa S, Yokote H et al. Clinical and immunological response to attenuated tissue-cultured smallpox vaccine LC16m8. JAMA 2009; 301(10):1025-1033.

(270) Morikawa S, Sakiyama T, Hasegawa H, Saijo M, Maeda A, Kurane I et al. An attenuated LC16m8 smallpox vaccine: analysis of full-genome sequence and induction of immune protection. J Virol 2005; 79(18):11873-11891.

(271) Saijo M, Ami Y, Suzaki Y, Nagata N, Iwata N, Hasegawa H et al. LC16m8, a highly attenuated vaccinia virus vaccine lacking expression of the membrane protein B5R, protects monkeys from monkeypox. J Virol 2006; 80(11):5179-5188.

(272) Meseda CA, Mayer AE, Kumar A, Garcia AD, Campbell J, Listrani P et al. Comparative evaluation of the immune responses and protection engendered by LC16m8 and

Dryvax smallpox vaccines in a mouse model. Clin Vaccine Immunol 2009; 16(9):1261-1271.

(273) Empig C, Kenner JR, Perret-Gentil M, Youree BE, Bell E, Chen A et al. Highly attenuated smallpox vaccine protects rabbits and mice against pathogenic orthopoxvirus challenge. Vaccine 2006; 24(17):3686-3694.

(274) Bell E, Shamim M, Whitbeck JC, Sfyroera G, Lambris JD, Isaacs SN. Antibodies against the extracellular enveloped virus B5R protein are mainly responsible for the EEV neutralizing capacity of vaccinia immune globulin. Virology 2004; 325(2):425-431.

(275) Pütz MM, Midgley CM, Law M, Smith GL. Quantification of antibody responses against multiple antigens of the two infectious forms of Vaccinia virus provides a benchmark for smallpox vaccination. Nat Med 2006; 12(11):1310-1315.

(276) Jones-Trower A, Garcia A, Meseda CA, He Y, Weiss C, Kumar A et al. Identification and preliminary characterization of vaccinia virus (Dryvax) antigens recognized by vaccinia immune globulin. Virology 2005; 343(1):128-140.

(277) Lawrence SJ, Lottenbach KR, Newman FK, Buller RM, Bellone CJ, Chen JJ et al. Antibody responses to vaccinia membrane proteins after smallpox vaccination. J Infect Dis 2007; 196(2):220-229.

(278) Mayr A, Hochstein-Mintzel V, Stickl H. Abstammung, Eigenschaften und Verwendung des attenuierten Vaccinia-Stammes MVA. Infection 1975; 3:6-14.

(279) Drexler I, Heller K, Wahren B, Erfle V, Sutter G. Highly attenuated modified vaccinia virus Ankara replicates in baby hamster kidney cells, a potential host for virus propagation, but not in various human transformed and primary cells. J Gen Virol 1998; 79 (Pt 2):347-352.

(280) Vollmar J, Arndtz N, Eckl KM, Thomsen T, Petzold B, Mateo L et al. Safety and immunogenicity of IMVAMUNE, a promising candidate as a third generation smallpox vaccine. Vaccine 2006; 24(12):2065-2070.

(281) Coulibaly S, Brühl P, Mayrhofer J, Schmid K, Gerencer M, Falkner FG. The nonreplicating smallpox candidate vaccines defective vaccinia Lister (dVV-L) and modified vaccinia Ankara (MVA) elicit robust long-term protection. Virology 2005; 341(1):-101.

(282) Earl PL, Americo JL, Wyatt LS, Eller LA, Whitbeck JC, Cohen GH et al. Immunogenicity of a highly attenuated MVA smallpox vaccine and protection against monkeypox. Nature 2004; 428(6979):182-185.

(283) Belyakov IM, Earl P, Dzutsev A, Kuznetsov VA, Lemon M, Wyatt LS et al. Shared modes of protection against poxvirus infection by attenuated and conventional smallpox vaccine viruses. Proc Natl Acad Sci U S A 2003; 100(16):9458-9463.

(284) Phelps AL, Gates AJ, Hillier M, Eastaugh L, Ulaeto DO. Comparative efficacy of modified vaccinia Ankara (MVA) as a potential replacement smallpox vaccine. Vaccine 2007; 25(1):34-42.

(285) Staib C, Suezer Y, Kisling S, Kalinke U, Sutter G. Short-term, but not post-exposure, protection against lethal orthopoxvirus challenge after immunization with modified vaccinia virus Ankara. J Gen Virol 2006; 87(Pt 10):2917-2921.

(286) Parrino J, McCurdy LH, Larkin BD, Gordon IJ, Rucker SE, Enama ME et al. Safety, immunogenicity and efficacy of modified vaccinia Ankara (MVA) against Dryvax challenge in vaccinia-naÃ¯ve and vaccinia-immune individuals. Vaccine 2007; 25(8):1513-1525.

(287) Gherardi MM, Esteban M. Recombinant poxviruses as mucosal vaccine vectors. J Gen Virol 2005; 86(Pt 11):2925-2936.

(288) Moss B, Carroll MW, Wyatt LS, Bennink JR, Hirsch VM, Goldstein S et al. Host range restricted, non-replicating vaccinia virus vectors as vaccine candidates. Adv Exp Med Biol 1996; 397:7-13.

(289) Moorthy VS, Pinder M, Reece WH, Watkins K, Atabani S, Hannan C et al. Safety and immunogenicity of DNA/modified vaccinia virus ankara malaria vaccination in African adults. J Infect Dis 2003; 188(8):1239-1244.

(290) Moorthy VS, McConkey S, Roberts M, Gothard P, Arulanantham N, Degano P et al. Safety of DNA and modified vaccinia virus Ankara vaccines against liver-stage *P. falciparum* malaria in non-immune volunteers. Vaccine 2003; 21(17-18):1995-2002.

(291) Kreijtz JH, Suezer Y, de MG, van den Brand JM, van AG, Schnierle BS et al. Preclinical evaluation of a modified vaccinia virus Ankara (MVA)-based vaccine against influenza A/H5N1 viruses. Vaccine 2009; 27(45):6296-6299.

(292) Kreijtz JH, Suezer Y, de Mutsert G, van den Brand JM, van Amerongen G, Schnierle BS et al. Recombinant modified vaccinia virus Ankara expressing the hemagglutinin gene confers protection against homologous and heterologous H5N1 influenza virus infections in macaques. J Infect Dis 2009; 199(3):405-413.

(293) Tchilian EZ, Desel C, Forbes EK, Bandermann S, Sander CR, Hill AV et al. Immunogenicity and protective efficacy of prime-boost regimens with recombinant (delta)ureC hly+ *Mycobacterium bovis* BCG and modified vaccinia virus ankara expressing *M. tuberculosis* antigen 85A against murine tuberculosis. Infect Immun 2009; 77(2):622-631.

(294) Earl PL, Cotter C, Moss B, VanCott T, Currier J, Eller LA et al. Design and evaluation of multi-gene, multi-clade HIV-1 MVA vaccines. Vaccine 2009; 27(42):5885-5895.

(295) Esteban M. Attenuated poxvirus vectors MVA and NYVAC as promising vaccine candidates against HIV/AIDS. Hum Vaccin 2009; 5(12).

(296) Rodriguez AM, Turk G, Pascutti MF, Ferrer F, Najera JL, Mónaco D et al. Characterization of DNA and MVA vectors expressing Nef from HIV-1 CRF12_BF revealed high immune specificity with low cross-reactivity against subtype B. Virus Res 2009; 146(1-2):1-12.

(297) Amato RJ, Shingler W, Goonewardena M, deBelin J, Naylor S, Jac J et al. Vaccination of renal cell cancer patients with modified vaccinia Ankara delivering the tumor antigen 5T4 (TroVax) alone or administered in combination with interferon-alpha (IFN-alpha): a phase 2 trial. J Immunother 2009; 32(7):765-772.

(298) Hodge JW, Higgins J, Schlom J. Harnessing the unique local immunostimulatory properties of modified vaccinia Ankara (MVA) virus to generate superior tumor-specific immune responses and antitumor activity in a diversified prime and boost vaccine regimen. Vaccine 2009; 27(33):4475-4482.

(299) Kaufman HL, Taback B, Sherman W, Kim DW, Shingler WH, Moroziewicz D et al. Phase II trial of Modified Vaccinia Ankara (MVA) virus expressing 5T4 and high dose Interleukin-2 (IL-2) in patients with metastatic renal cell carcinoma. J Transl Med 2009; 7:-2.

(300) Pulford DJ, Gates A, Bridge SH, Robinson JH, Ulaeto D. Differential efficacy of vaccinia virus envelope proteins administered by DNA immunisation in protection of BALB/c mice from a lethal intranasal poxvirus challenge. Vaccine 2004; 22(25-26):3358-3366.

(301) Lai CF, Gong SC, Esteban M. The purified 14-kilodalton envelope protein of vaccinia virus produced in Escherichia coli induces virus immunity in animals. J Virol 1991; 65(10):5631-5635.

(302) Hooper JW, Custer DM, Schmaljohn CS, Schmaljohn AL. DNA vaccination with vaccinia virus L1R and A33R genes protects mice against a lethal poxvirus challenge. Virology 2000; 266(2):329-339.

(303) Hooper JW, Custer DM, Thompson E. Four-gene-combination DNA vaccine protects mice against a lethal vaccinia virus challenge and elicits appropriate antibody responses in nonhuman primates. Virology 2003; 306(1):181-195.

(304) Hooper JW, Thompson E, Wilhelmsen C, Zimmerman M, Ichou MA, Steffen SE et al. Smallpox DNA vaccine protects nonhuman primates against lethal monkeypox. J Virol 2004; 78(9):4433-4443.

(305) Fogg C, Lustig S, Whitbeck JC, Eisenberg RJ, Cohen GH, Moss B. Protective immunity to vaccinia virus induced by vaccination with multiple recombinant outer membrane proteins of intracellular and extracellular virions. J Virol 2004; 78(19):10230-10237.

(306) Davies DH, McCausland MM, Valdez C, Huynh D, Hernandez JE, Mu Y et al. Vaccinia virus H3L envelope protein is a major target of neutralizing antibodies in humans and elicits protection against lethal challenge in mice. J Virol 2005; 79(18):11724-11733.

(307) Parker S, Handley L, Buller RM. Therapeutic and prophylactic drugs to treat orthopoxvirus infections. Future Virol 2008; 3(6):595-612.

(308) Magee WC, Hostetler KY, Evans DH. Mechanism of inhibition of vaccinia virus DNA polymerase by cidofovir diphosphate. Antimicrob Agents Chemother 2005; 49(8):3153-3162.

(309) Magee WC, Aldern KA, Hostetler KY, Evans DH. Cidofovir and (S)-9-[3-hydroxy-(2-phosphonomethoxy)propyl]adenine are highly effective inhibitors of vaccinia virus DNA polymerase when incorporated into the template strand. Antimicrob Agents Chemother 2008; 52(2):586-597.

(310) De CE, Sakuma T, Baba M, Pauwels R, Balzarini J, Rosenberg I et al. Antiviral activity of phosphonylmethoxyalkyl derivatives of purine and pyrimidines. Antiviral Res 1987; 8(5-6):261-272.

(311) Painter GR, Hostetler KY. Design and development of oral drugs for the prophylaxis and treatment of smallpox infection. Trends Biotechnol 2004; 22(8):423-427.

(312) Hostetler KY. Synthesis and evaluation of broad spectrum, orally active analogs of cidofovir and other acylic nucleoside phosphonates. In: De Clercq E, editor. Advances in Antiviral Drug Design. 5th ed. USA: Elsevier; 2007. 167-184.

(313) Hostetler KY. Alkoxyalkyl prodrugs of acyclic nucleoside phosphonates enhance oral antiviral activity and reduce toxicity: current state of the art. Antiviral Res 2009; 82(2):A84-A98.

(314) Kornbluth RS, Smee DF, Sidwell RW, Snarsky V, Evans DH, Hostetler KY. Mutations in the E9L polymerase gene of cidofovir-resistant vaccinia virus strain WR are associated with the drug resistance phenotype. Antimicrob Agents Chemother 2006; 50(12):4038-4043.

(315) Yang G, Pevear DC, Davies MH, Collett MS, Bailey T, Rippen S et al. An orally bioavailable antipoxvirus compound (ST-246) inhibits extracellular virus formation and protects mice from lethal orthopoxvirus Challenge. J Virol 2005; 79(20):13139-13149.

(316) Sbrana E, Jordan R, Hruby DE, Mateo RI, Xiao SY, Siirin M et al. Efficacy of the antipoxvirus compound ST-246 for treatment of severe orthopoxvirus infection. Am J Trop Med Hyg 2007; 76(4):768-773.

(317) Duraffour S, Vigne S, Vermeire K, Garcel A, Vanstreels E, Daelemans D et al. Specific targeting of the F13L protein by ST-246 affects orthopoxvirus production differently. Antivir Ther 2008; 13(8):977-990.

(318) Reeves PM, Bommarius B, Lebeis S, McNulty S, Christensen J, Swimm A et al. Disabling poxvirus pathogenesis by inhibition of Abl-family tyrosine kinases. Nat Med 2005; 11(7):731-739.

(319) De CE, Sakuma T, Baba M, Pauwels R, Balzarini J, Rosenberg I et al. Antiviral activity of phosphonylmethoxyalkyl derivatives of purine and pyrimidines. Antiviral Res 1987; 8(5-6):261-272.

(320) De CE, Montgomery J. John Montgomery's legacy: carbocyclic adenosine analogues as SAH hydrolase inhibitors with broad-spectrum antiviral activity. Nucleosides Nucleotides Nucleic Acids 2005; 24(10-12):1395-1415.

(321) Smee DF, Bray M, Huggins JW. Antiviral activity and mode of action studies of ribavirin and mycophenolic acid against orthopoxviruses *in vitro*. Antivir Chem Chemother 2001; 12(6):327-335.

(322) Smee DF, Bailey KW, Sidwell RW. Treatment of cowpox virus respiratory infections in mice with ribavirin as a single agent or followed sequentially by cidofovir. Antivir Chem Chemother 2000; 11(4):303-309.

(323) Ikeda S, Yazawa M, Nishimura C. Antiviral activity and inhibition of topoisomerase by ofloxacin, a new quinolone derivative. Antiviral Res 1987; 8(3):103-113.

(324) Sekiguchi J, Stivers JT, Mildvan AS, Shuman S. Mechanism of inhibition of vaccinia DNA topoisomerase by novobiocin and coumermycin. J Biol Chem 1996; 271(4):2313-2322.

(325) Tse-Dinh YC. Exploring DNA topoisomerases as targets of novel therapeutic agents in the treatment of infectious diseases. Infect Disord Drug Targets 2007; 7(1):3-9.

(326) Bennett AM, Slomka MJ, Brown DW, Lloyd G, Mackett M. Protection against herpes B virus infection in rabbits with a recombinant vaccinia virus expressing glycoprotein D. J Med Virol 1999; 57(1):47-56.

(327) Hammond JM, Oke PG, Coupar BE. A synthetic vaccinia virus promoter with enhanced early and late activity. J Virol Methods 1997; 66(1):135-138.

(328) Vogelstein B, Gillespie D. Preparative and analytical purification of DNA from agarose. Proc Natl Acad Sci U S A 1979; 76(2):615-619.

(329) Birnboim HC, Doly J. A rapid alkaline extraction procedure for screening recombinant plasmid DNA. Nucleic Acids Res 1979; 7(6):1513-1523.

(330) Reed LJ, Muench H. A simple method of estimating fifty percent endpoints. Am J Hyg 1938; 27:493-497.

(331) Ulaeto D, Grosenbach D, Hruby DE. Brefeldin A inhibits vaccinia virus envelopment but does not prevent normal processing and localization of the putative envelopment receptor P37. J Gen Virol 1995; 76 (Pt 1):103-111.

(332) Chomczynski P, Sacchi N. Single-step method of RNA isolation by acid guanidinium thiocyanate-phenol-chloroform extraction. Anal Biochem 1987; 162(1):156-159.

(333) Boom R, Sol CJ, Salimans MM, Jansen CL, Wertheim-van Dillen PM, van der Noordaa J. Rapid and simple method for purification of nucleic acids. J Clin Microbiol 1990; 28(3):495-503.

(334) Marko MA, Chipperfield R, Birnboim HC. A procedure for the large-scale isolation of highly purified plasmid DNA using alkaline extraction and binding to glass powder. Anal Biochem 1982; 121(2):382-387.

(335) Livak KJ, Schmittgen TD. Analysis of relative gene expression data using real-time quantitative PCR and the 2(-Delta Delta C(T)) Method. Methods 2001; 25(4):402-408.

(336) Appleyard G, Hapel AJ, Boulter EA. An antigenic difference between intracellular and extracellular rabbitpox virus. J Gen Virol 1971; 13(1):9-17.

(337) Boulter EA. Protection against poxviruses. Proc R Soc Med 1969; 62(3):295-297.

(338) Payne LG, Kristensson K. Extracellular release of enveloped vaccinia virus from mouse nasal epithelial cells in vivo. J Gen Virol 1985; 66 (Pt 3):643-646.

(339) Ichihashi Y. Extracellular enveloped vaccinia virus escapes neutralization. Virology 1996; 217(2):478-485.

(340) Vanderplasschen A, Hollinshead M, Smith GL. Antibodies against vaccinia virus do not neutralize extracellular enveloped virus but prevent virus release from infected cells and comet formation. J Gen Virol 1997; 78 (Pt 8):2041-2048.

(341) Sarov I, Joklik WK. Studies on the nature and location of the capsid polypeptides of vaccinia virions. Virology 1972; 50(2):579-592.

(342) Ching YC, Chung CS, Huang CY, Hsia Y, Tang YL, Chang W. Disulfide bond formation at the C-termini of vaccinia A26 and A27 proteins does not require viral redox enzymes and suppresses glycosaminoglycan-mediated cell fusion. J Virol 2009; 83(13):6464-6476.

(343) Doms RW, Blumenthal R, Moss B. Fusion of intra- and extracellular forms of vaccinia virus with the cell membrane. J Virol 1990; 64(10):4884-4892.

(344) Rodriguez JF, Janeczko R, Esteban M. Isolation and characterization of neutralizing monoclonal antibodies to vaccinia virus. J Virol 1985; 56(2):482-488.

(345) Gong SC, Lai CF, Esteban M. Vaccinia virus induces cell fusion at acid pH and this activity is mediated by the N-terminus of the 14-kDa virus envelope protein. Virology 1990; 178(1):81-91.

(346) Rodriguez JF, Smith GL. IPTG-dependent vaccinia virus: identification of a virus protein enabling virion envelopment by Golgi membrane and egress. Nucleic Acids Res 1990; 18(18):5347-5351.

(347) Boyle DB, Coupar BE. A dominant selectable marker for the construction of recombinant poxviruses. Gene 1988; 65(1):123-128.

(348) Falkner FG, Moss B. *Escherichia coli gpt* gene provides dominant selection for vaccinia virus open reading frame expression vectors. J Virol 1988; 62(6):1849-1854.

(349) Isaacs SN, Kotwal GJ, Moss B. Reverse guanine phosphoribosyltransferase selection of recombinant vaccinia viruses. Virology 1990; 178(2):626-630.

(350) Payne LG, Kristenson K. Mechanism of vaccinia virus release and its specific inhibition by N1-isonicotinoyl-N2-3-methyl-4-chlorobenzoylhydrazine. J Virol 1979; 32(2):614-622.

(351) Howard AR, Senkevich TG, Moss B. Vaccinia virus A26 and A27 proteins form a stable complex tethered to mature virions by association with the A17 transmembrane protein. J Virol 2008; 82(24):12384-12391.

(352) Mackett M, Smith GL, Moss B. General method for production and selection of infectious vaccinia virus recombinants expressing foreign genes. J Virol 1984; 49(3):857-864.

(353) Lee MS, Roos JM, McGuigan LC, Smith KA, Cormier N, Cohen LK et al. Molecular attenuation of vaccinia virus: mutant generation and animal characterization. J Virol 1992; 66(5):2617-2630.

(354) Fuerst TR, Fernandez MP, Moss B. Transfer of the inducible *lac* repressor/operator system from *Escherichia coli* to a vaccinia virus expression vector. Proc Natl Acad Sci U S A 1989; 86(8):2549-2553.

(355) Rodriguez JF, Smith GL. Inducible gene expression from vaccinia virus vectors. Virology 1990; 177(1):239-250.

(356) Davies J, Jimenez A. A new selective agent for eukaryotic cloning vectors. Am J Trop Med Hyg 1980; 29(5 Suppl):1089-1092.

(357) Frank CA, Rice CM, Strauss JM, Hruby DE. Neomycin resistance as a dominant selectable marker for selection and isolation of vaccinia virus recombinants. Mol Cell Biol 1985; 5(8):1918-1924.

(358) Mackett M, Smith GL, Moss B. Vaccinia virus: a selectable eukaryotic cloning and expression vector. Proc Natl Acad Sci U S A 1982; 79(23):7415-7419.

(359) Blasco R, Moss B. Role of cell-associated enveloped vaccinia virus in cell-to-cell spread. J Virol 1992; 66(7):4170-4179.

(360) Sundstrom M, Chatterji U, Schaffer L, de Rozières S., Elder JH. Feline immunodeficiency virus OrfA alters gene expression of splicing factors and proteasome-ubiquitination proteins. Virology 2008; 371(2):394-404.

(361) Katz E, Ward BM, Weisberg AS, Moss B. Mutations in the vaccinia virus A33R and B5R envelope proteins that enhance release of extracellular virions and eliminate formation of actin-containing microvilli without preventing tyrosine phosphorylation of the A36R protein. J Virol 2003; 77(22):12266-12275.

(362) Meiser A, Boulanger D, Sutter G, Krijnse LJ. Comparison of virus production in chicken embryo fibroblasts infected with the WR, IHD-J and MVA strains of vaccinia virus: IHD-J is most efficient in trans-Golgi network wrapping and extracellular enveloped virus release. J Gen Virol 2003; 84(Pt 6):1383-1392.

(363) Spehner D, Drillien R, Proamer F, Houssais-Pêcheur C, Zanta MA, Geist M et al. Enveloped virus is the major virus form produced during productive infection with the modified vaccinia virus Ankara strain. Virology 2000; 273(1):9-15.

(364) Jenssen H, Hamill P, Hancock RE. Peptide antimicrobial agents. Clin Microbiol Rev 2006; 19(3):491-511.

(365) Scott MG, Hancock RE. Cationic antimicrobial peptides and their multifunctional role in the immune system. Crit Rev Immunol 2000; 20(5):407-431.

(366) Wang Z, Wang G. APD: the Antimicrobial Peptide Database. Nucleic Acids Res 2004; 32(Database issue):D590-D592.

(367) Daher KA, Selsted ME, Lehrer RI. Direct inactivation of viruses by human granulocyte defensins. J Virol 1986; 60(3):1068-1074.

(368) Howell MD, Jones JF, Kisich KO, Streib JE, Gallo RL, Leung DY. Selective killing of vaccinia virus by LL-37: implications for eczema vaccinatum. J Immunol 2004; 172(3):1763-1767.

(369) Ramamoorthy A, Thennarasu S, Lee DK, Tan A, Maloy L. Solid-state NMR investigation of the membrane-disrupting mechanism of antimicrobial peptides MSI-78 and MSI-594 derived from magainin 2 and melittin. Biophys J 2006; 91(1):206-216.

(370) Wieprecht T, Apostolov O, Beyermann M, Seelig J. Thermodynamics of the alpha-helix-coil transition of amphipathic peptides in a membrane environment: implications for the peptide-membrane binding equilibrium. J Mol Biol 1999; 294(3):785-794.

(371) Gubser C, Hué S, Kellam P, Smith GL. Poxvirus genomes: a phylogenetic analysis. J Gen Virol 2004; 85(Pt 1):105-117.

(372) Shchelkunov SN, Totmenin AV, Babkin IV, Safronov PF, Ryazankina OI, Petrov NA et al. Human monkeypox and smallpox viruses: genomic comparison. FEBS Lett 2001; 509(1):66-70.

(373) Shchelkunov SN, Totmenin AV, Loparev VN, Safronov PF, Gutorov VV, Chizhikov VE et al. Alastrim smallpox variola minor virus genome DNA sequences. Virology 2000; 266(2):361-386.

(374) Massung RF, Esposito JJ, Liu LI, Qi J, Utterback TR, Knight JC et al. Potential virulence determinants in terminal regions of variola smallpox virus genome. Nature 1993; 366(6457):748-751.

(375) Howley PM. *Papillomavirinae*: The viruses and their replication. In: Fields BN, Knipe DM, Howley PM, editors. Fields Virology. 3rd ed. Philadelphia: Lippincott-Raven Publishers; 1996. 2045-2076.

(376) Roizman B. *Herpesviridae*. In: Fields BN, Knipe DM, Howley PM, editors. Fields Virology. 3rd ed. Philadelphia: Lippincott-Raven Publishers; 1996. 2221-2230.

(377) Garcia-Blanco MA, Cullen BR. Molecular basis of latency in pathogenic human viruses. Science 1991; 254(5033):815-820.

(378) Leopardi R, Van Sant C, Roizman B. The herpes simplex virus 1 protein kinase US3 is required for protection from apoptosis induced by the virus. Proc Natl Acad Sci U S A 1997; 94(15):7891-7896.

(379) Ciacci-Zanella J, Stone M, Henderson G, Jones C. The latency-related gene of bovine herpesvirus 1 inhibits programmed cell death. J Virol 1999; 73(12):9734-9740.

(380) Campbell A. Bacteriophages. In: Fields BN, Knipe DM, Howley PM, editors. Fields Virology. 3rd ed. Philadelphia: Lippincott-Raven Publisher; 1996. 587-607.

(381) Newell PC. The development of the cellular slime mould *Dictyostelium discoideum*: a model system for the study of cellular differentiation. Essays Biochem 1971; 7:87-126.

(382) Gerisch G. Cell aggregation and differentiation in *Dictyostelium*. Curr Top Dev Biol 1968; 3:157-197.

(383) Jeong Y, Mangelsdorf DJ. Nuclear receptor regulation of stemness and stem cell differentiation. Exp Mol Med 2009; 41(8):525-537.

(384) Mohamed MR, Niles EG. Transient and inducible expression of vaccinia/T7 recombinant viruses. Methods Mol Biol 2004; 269:41-50.